Nuclear Operating Company

South Texas Project Electric Generating Station P.O. Box 289 Wadsworth, Texas 77483

October 20, 2016
NOC-AE-16003401
10CFR50.12
10CFR50.90

U. S. Nuclear Regulatory Commission
Attention: Document Control Desk
Washington, DC 20555-0001

South Texas Project
Units 1 and 2
Docket Nos. STN 50-498 and STN 50-499
Supplement 3 to Revised STP Pilot Submittal and Requests for Exemptions and License Amendment for a Risk-Informed Approach to Address Generic Safety Issue (GSI)-191 and Respond to Generic Letter (GL) 2004-02
(TAC NOS. MF2400 - MF2409)

References:

1. Letter, G. T. Powell, STPNOC, to NRC Document Control Desk, "Supplement 2 to Revised STP Pilot Submittal and Requests for Exemptions and License Amendment for a Risk-Informed Approach to Resolving Generic Safety Issue (GSI)-191", August 20, 2015, NOC-AE-16003241, ML15246A126 – A129

This submittal updates portions of the previous supplement to the STP Risk-Informed GSI-191 application (Reference 1) with resolution of NRC staff comments on the STP Risk over Deterministic (RoverD) methodology and RAI responses. Unaffected parts of Reference 1 are generally not included in this submittal.

The current draft of 10CFR50.46c rule change and associated draft RG 1.229 requires that the risk contribution from the effects of debris be small for the debris effects not to be considered in the analysis. The STP piloted risk-informed approach to resolving GSI-191 shows that the risk associated with debris from pipe breaks that generate quantities of debris that are not bounded by plant-specific prototypical testing is very small, in accordance with the acceptance criteria of RG 1.174. The changes in this supplement had no significant effect on the risk quantifications in Reference 1 and STPNOC's conclusions are unchanged. Attachment 1-3 includes the risk quantification.

Attachment 1 provides updates to the technical bases for the licensing application. Specifically, Attachment 1-1 is an introduction overview, Attachment 1-2 makes a minor update to the deterministic element, Attachment 1-3 updates the RoverD methodology for the proposed risk-informed approach to addressing the GSI-191 issue as described in GL 2004-02, consistent with RG 1.174 guidance, and Attachment 1-4 clarifies responses to RAIs. Changes to the RoverD description in Attachment 1-3 include incorporation of small breaks in the Reactor Coolant System (RCS) cold leg into the section showing that there is insufficient debris to affect long-term core cooling, resolution of staff comments regarding erosion of small fibrous debris, conservatively assigning all RCS hot leg breaks larger than 16 inches to the risk-informed element, and resolution of staff comments on break sizes. The changes with respect to the erosion and the 16-inch breaks

A002
NRR

resulted in an insignificant increase in the calculated ΔCDF and ΔLERF, which are summarized in the attachment.

Attachment 2 summarizes the proposed exemptions from certain regulatory requirements in accordance with the provisions of 10CFR50.12. Except for changing the 10CFR50.46(d) exemption to be to 10CFR50.46(a)(1) (see ML16111B204), there are no changes to the proposed exemptions described in Reference 1 and they are not repeated in this supplement.

Attachment 3 provides the License Amendment Request (LAR), pursuant to 10CFR50.90, for approval of the proposed changes to the STP Units 1 and 2 licensing basis including page markups for the affected Technical Specification (TS) pages and Updated Final Safety Analysis Report (UFSAR) pages. The primary changes are to revise the basis for the TS completion time and to correct the ECCS TS end state for the debris-related action. The technical basis is revised to be based on configuration management instead of a risk-informed basis, and STPNOC added a section in the UFSAR to govern the requirements for change control and monitoring and reporting changes to risk contribution from debris. The ECCS end state is corrected to be HOT SHUTDOWN instead of COLD SHUTDOWN to maintain consistency with the existing TS MODE applicability for ECCS. The LAR includes technical and regulatory evaluations for the proposed change, a no significant hazards consideration determination pursuant to 10CFR50.92, and an environmental considerations review. The no significant hazards considerations determination and environmental considerations review are unchanged from the previous supplement. The Plant Operations Review Committee has approved the proposed change. In accordance with 10CFR50.91(b), STPNOC has notified the State of Texas by transmitting a copy of this letter and enclosure to the State of Texas Official. Changes to the STP Technical Specifications and UFSAR are to be implemented pursuant to NRC approval of LAR.

A 90-day implementation period is requested to provide time to revise the applicable STP licensing documents and implement the Technical Specification changes. There are no other commitments in this letter.

If there are questions regarding this submittal, please contact Mike Murray at 361-972-8146, or me at 361-972-7344.

I declare under penalty of perjury that the foregoing is true and correct.

Executed on 10/20/16

James Connolly
Site Vice President

awh

Attachments:

1. STP Piloted Risk-Informed Approach to Closure for GSI-191
   - 1-1 Introduction
   - 1-2 Deterministic Basis
   - 1-3 Risk-Informed Basis
   - 1-4 Resolution of NRC Comments on Responses to Round 3 and 4 RAIs
2. Requests for Exemptions for STP Piloted Risk-Informed Approach to Closure for GSI-191
3. License Amendment Request for STP Piloted Risk-informed Approach to Closure for GSI-191
   - 3-1 Technical Specification Page Markups
   - 3-2 "Clean" Technical Specification Pages
   - 3-3 Technical Specifications Bases Page Markups
   - 3-4 UFSAR Markups
4. List of Commitments
5. Definitions and Acronyms

cc:

(paper copy)
Regional Administrator, Region IV
U. S. Nuclear Regulatory Commission
1600 East Lamar Boulevard
Arlington, TX 76011-4511

Lisa M. Regner
Senior Project Manager
U.S. Nuclear Regulatory Commission
One White Flint North (O8H04)
11555 Rockville Pike
Rockville, MD 20852

NRC Resident Inspector
U. S. Nuclear Regulatory Commission
P. O. Box 289, Mail Code: MN116
Wadsworth, TX 77483

(electronic copy)
Morgan, Lewis & Bockius LLP
Steven P. Frantz, Esquire

U. S. Nuclear Regulatory Commission
Lisa M. Regner

NRG South Texas LP
Chris O'Hara
Jim von Suskil
Skip Zahn

CPS Energy
Kevin Pollo
Cris Eugster
L. D. Blaylock

City of Austin
Elaina Ball
John Wester

Texas Dept of State Health Services
Helen Watkins
Robert Free

Attachment 1

STP Piloted Risk-Informed Approach to Closure for GSI-191

1-1 Introduction

This attachment provides the STPNOC methodology for a risk-informed approach to addressing Generic Safety Issue (GSI)-191 issues and responding to GL 2004-02, as discussed in SECY Paper, "Closure Options for Generic Safety Issue - 191, Assessment of Debris Accumulation on Pressurized-Water Reactor Sump Performance". The STP risk-informed approach is intended to be applied to STP Units 1 and 2 as pilot plants.

In the STP Risk over Deterministic (RoverD) methodology, the effects of debris that are bounded by the plant-specific testing are deterministically mitigated in accordance with NRC-accepted methodology for resolution of GL 2004-02. Breaks that are not bounded by the plant-specific testing are conservatively assumed to result in core damage. RoverD addresses the effects on long-term cooling due to debris accumulation on Emergency Core Cooling System (ECCS) and Containment Spray System (CSS) sump strainers in recirculation mode, as well as core flow blockage due to in-vessel effects of debris that bypasses the strainers. A full spectrum of postulated LOCAs is analyzed, including double-ended guillotine breaks (DEGBs) for all pipe sizes up to the largest pipe in the reactor coolant system. The changes to CDF and LERF associated with GSI-191 concerns are quantified by applying the LOCA frequencies published in NUREG-1829, and then compared to RG 1.174 acceptance guidelines. The results quantified in Section 4.5 of Attachment 1-3, in combination with the defense-in-depth and safety margin described in Attachment 1-4 of Reference 1 to the cover letter, meet the criteria of RG 1.174 for considering the risk from effects of LOCA debris to be in Region III (very small) and that no additional plant modification is required to close GL 2004-02 for STP.

The regulations require a deterministic analysis. Implementation of the licensing basis requires justification in accordance with 10CFR50.12 of exemptions to the relevant regulations; i.e. 10CFR50.46(a)(1), GDC 35, GDC 38 and GDC 41. The exemptions are complemented by proposed amendments to the STP Unit 1 and Unit 2 operating licenses to allow for the change in analysis methodology per 10CFR50.59 and to change ECCS and CSS Technical Specifications.

The basis for the proposed 10CFR50.46c rule change allows the effects of debris to be excluded from the 10CFR50.46 long-term cooling analysis and from the analyses associated with GDC 35, 38 and 41 if the risk contribution from the debris effects is small. The STPNOC Licensing Basis with regard to effects of debris is that there is a high probability that the effects of LOCA debris will be mitigated based on successful plant-specific prototypical testing using deterministic assumptions, and analyses show that the risk from breaks that could generate debris that is not bounded by the testing is very small in accordance with the criteria of RG 1.174.

The conclusions above and implementation actions described in this application allow GL2004-02 to be closed for STP Units 1 and 2.

1-2 Deterministic Basis

1-2 Deterministic Basis

The deterministic basis was addressed in Attachment 1-2 of Reference 1 to the cover letter using the NRC's content guide. There are no changes.

In the July 28, 2016, meeting with the NRC staff, the staff suggested that a statement in the STPNOC response to RAI 52 should be revised. The revised response to RAI 52 is provided below.

J. Chemical Effects

RAI #52

The licensee performed integrated head loss testing in a flume by adding chemical precipitates after other non-chemical debris. The NRC staff questions the transport of the calcium phosphate precipitate during the test since the plant's trisodium phosphate basket location relative to the sump strainers varies and in some cases may be less than the distance from the precipitate introduction point to the strainer section in the test flume. The staff also questions if fibrous debris settlement within the narrow cross section of the test flume may create a pile of fiber that filters the calcium phosphate precipitate in a non-conservative manner since this precipitate settles more rapidly than the aluminum based precipitate. Given this concern, please justify why the head loss testing was appropriate in terms of calcium phosphate precipitate transport to the test strainer.

Revised Response to RAI #52

This RAI response has been written to support the applicability of the July 2008 STP strainer head loss testing (52.2) to the RoverD methodology.

Based on the PCI / AREVA NP test protocol (52.1), the chemical debris surrogates are introduced into the test flume through the surface of the water at the upstream section of the test flume (see Figure 52-1 below). From visual observation, the chemical debris was observed to be transported to the strainer module. This was based on the gradual change in opacity of the water after the chemical debris was introduced into the test flume. After all of the chemical debris was added, the opacity of the flume water stabilized and remained constant during the remainder of the test. See Figure 52-2 and Figure 52-3 for chemical debris that was suspended in the water column within the test flume all the way up to the location of the test strainer module.

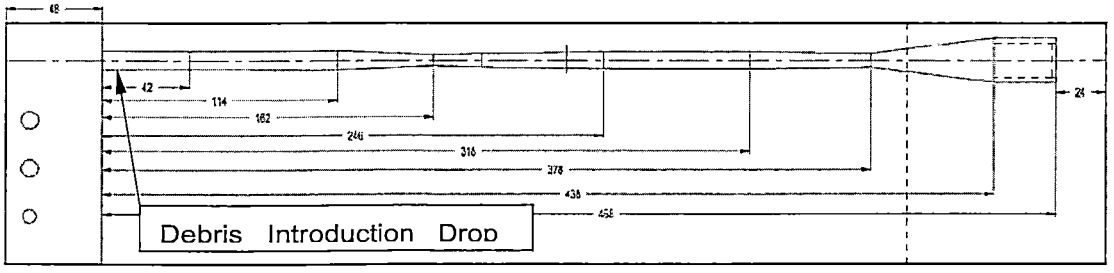

Figure 52-1: Debris Introduction Drop Zone for Non-Chemical and Chemical Debris

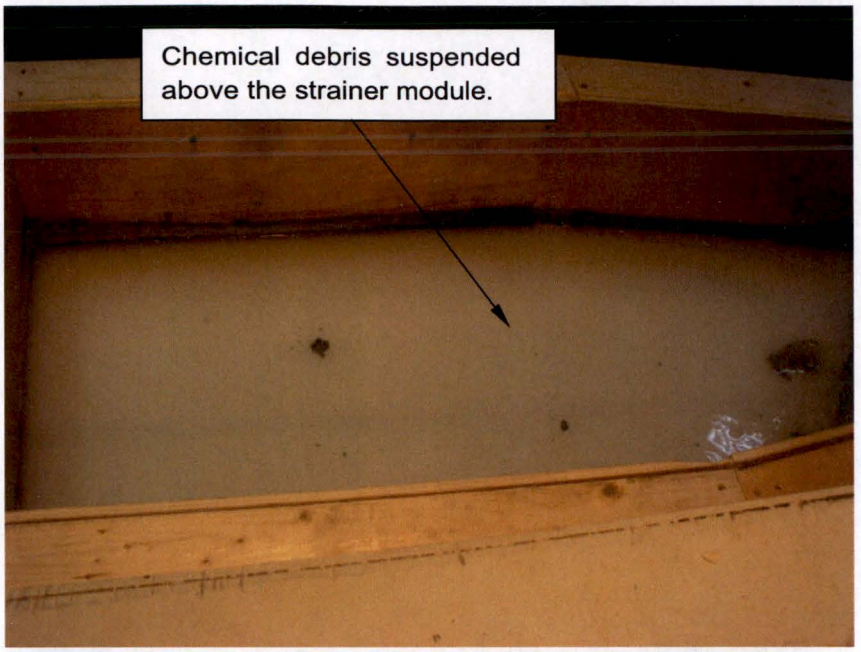

Figure 52-2: Area above the Strainer Prior to Drain Down

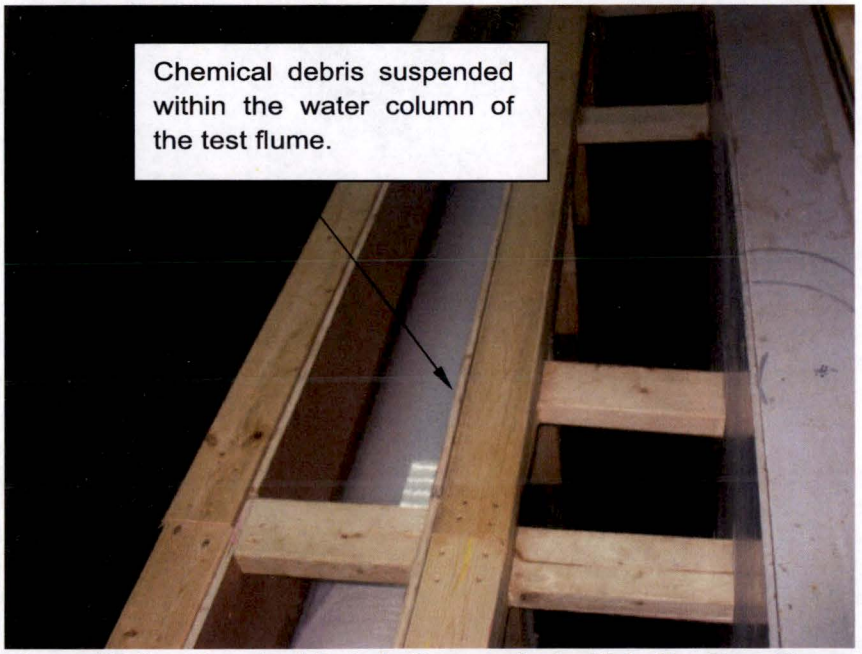

Figure 52-3: Chemical Debris Suspended within the Test Flume

Both aluminum oxyhydroxide and calcium phosphate were generated for the STP design basis test in accordance with the acceptance criteria presented in WCAP-16530-NP (52.3). Though Figure 52-2 and Figure 52-3 show the chemical precipitate in suspension, it is difficult to visually distinguish between aluminum oxyhydroxide and calcium phosphate since both have a similar indistinguishable 'milky-white' color.

A closer look at STP post-LOCA operational activities and the various properties of calcium phosphate precipitates are needed in order to assess calcium phosphate transport during STP strainer qualification testing. During the start of ECCS recirculation, it is expected that a large amount of tri-sodium phosphate (TSP) located in the TSP baskets will dissolve at high temperatures and distribute throughout containment due to a combination of ECCS recirculation and containment spray.

Figure 52-4 shows the locations of the TSP baskets located in STP containment. One TSP basket is located in close proximity to the ECCS sumps. This has caused concern with the NRC Staff, regarding the non-conservatism associated with the introduction zone of chemical debris (i.e., calcium phosphate) relative to the location of the test strainer. Since chemical precipitates are expected to form during the recirculation phase, it is expected that most of the chemical precipitates would be dispersed throughout the containment (greater than the distance of the debris introduction zone relative to the strainer in the STP test flume configuration). This is based on the dissolution of the TSP during the initial high temperature post-LOCA period and subsequent flow into the strainers and ECCS. The combination of the ECCS and CSS would serve to both mix and distribute the dissolved TSP throughout the STP containment and prevent significant concentration in the immediate area of the strainers. Therefore, only a small portion of the total quantity of chemical precipitates is expected to form in the proximity of the ECCS strainers. The calculated total amount of calcium phosphate precipitant was then introduced into the test flume upstream of the strainer. Theoretically, even if some of the calcium phosphate precipitant were to settle or be artificially filtered out by the non-chemical debris upstream of the strainer, it is expected that the amount that reached the test strainer was greater than or equal to that of expected for the actual plant strainers. Under this basis, the STP test flume configuration is considered to be prototypical of the STP containment and the TSP basket locations are not a concern due to the mixing and distribution of the dissolved TSP by the combined ECCS and CSS.

The calcium phosphate transport was appropriately tested for STP head loss testing since calcium phosphate precipitate was generated per WCAP-16530 (52.3) guidance and sequenced in such a manner to prevent over concentration in the test flume, thus minimizing settling of the precipitate. Based on the total volume in the test flume and piping, one flume turnover is approximately 5 – 6 minutes. As seen in Figure 52-1, the distance between the drop zone and the front surface of the strainer module consists of a smaller volume of water compared to the total flume volume. Based on the volume between the debris drop zone and the front surface of the strainer module, it would take debris approximately 2 minutes to travel to the strainer once introduced into the test flume. Based on the STP Test Plan, there was one flume turnover between chemical introductions of aluminum oxyhydroxide and calcium phosphate, and two flume turnovers between consecutive batches of calcium phosphate. Thus, sufficient time was allowed between all batches of chemical precipitate to allow the precipitate to transport to the strainer prior to the next chemical introduction.

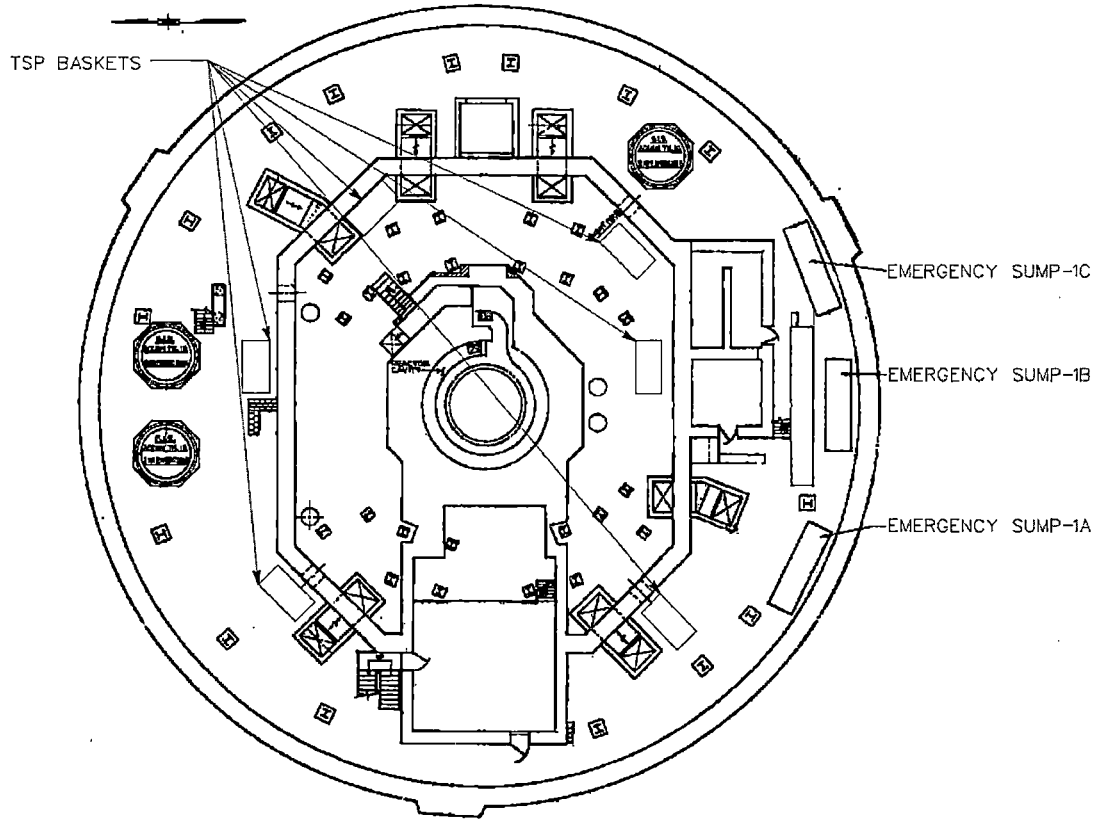

Figure 52-4: Location of TSP Baskets Located in STP Containment

REFERENCES:

52.1 AREVA NP Document 63-9086408-001, "South Texas Project Test Plan for ECCS Strainer Performance Testing", August 2008

52.2 66-9088089-000, South Texas Project Test Report for ECCS Strainer Testing, Revision 0. AREVA, August 2008.

52.3 WCAP-16530-NP, Rev. 0 "Evaluation of Post-Accident Chemical Effects in Containment Sump Fluids to Support GSI-191", February 2006

1-3 Risk-Informed Basis

RoverD:
Use of Test Data in GSI-191 Risk Assessment

List of contributors and affiliation
Edition date, time - Wednesday 19th October, 2016, 16:41

Contributor(s)	Affiliation	Contribution
Steve Blossom	STPNOC	Project Manager, STP GSI-191 project
Ernie Kee	STPNOC	Author & RoverD concept, STPNOC technical lead
Zahra Mohaghegh	University of Illinois at Urbana-Champaign	Oversight review
Seyed Reihani	University of Illinois at Urbana-Champaign	Oversight review, FIDOE and RUFF independent validation and verification
Alex Zolan and John Hasenbein	the University of Texas at Austin	LOCA frequency, strainer penetration review and analysis
Don Wakefield	ABS Consulting	LOCA Frequency, PRA development
Wayne Harrison and Drew Richards	STPNOC	Regulatory compliance review
Rodolfo Vaghetto	Texas A&M University	RCS Thermal-Hydraulics
Fatma Yilmaz	STPNOC	LOCA Frequency review
Phil Grissom	Southern Nuclear Co.	RoverD impact on Option 2b plants
David Imbaratto	Pacific Gas & Electric	RoverD impact on Option 2b plants
Bruce Letellier and Jeremy Tejada	Alion Science and Technology	CASA Grande results for real size and location
Dominic Munoz	Alion Science and Technology	CASA Debris Generation & Transport description
Vera Moisetytseva	YK.risk, LLC	Oversight review

Executive summary

The objective of the work described in this evaluation is to supplement defense in depth and safety margin analyses that support the STP[1] design for long term core cooling given the concerns raised in GSI-191[2]. Results are developed and presented in Section 4.5 for frequencies of ΔCDF[3], CDF[4], ΔLERF[5], and LERF[6] that show that the STP design will support the long term core cooling function with high probability.

The risk assessment includes design basis and beyond design basis scenarios to provide a comprehensive picture of the probability for successful long term cooling. Risk is assessed for all Class I weld locations in the STP RCB against test conditions that are intended to create the maximum head loss on the ECCS[7] strainers with additional (biased to higher head loss) uncertainty. Risk is assessed using different methods of estimate aggregation. The risk evaluated (mean values) assuming the STP geometric mean and continuum break aggregation estimates meets the RG 1.174 Region III guidance for high probability of success (that is, 'very small' risk).

Assessments show that very small amounts of fiber will accumulate on the fuel assemblies in CLB[8] scenarios. The small amount of fiber assessed to accumulate would produce negligible pressure drop in the core and would therefore be unable to impede cooling flow. Fiber accumulation in the core fuel assemblies during CLB is also assessed to be so small that dilution flows would continue such that boric acid concentration would remain below precipitation limits as assessed in the plant design calculations.

Thermal-hydraulic analyses of HLBs[9] smaller than approximately 16 inches with the BB[10], cold leg-to-hot leg, baffle former-to-FAs[11], and core FA thimble tubes completely blocked following SSO[12] are performed. These analyses show that, with these limiting assumptions, the core is provided sufficient flow such that long term cooling is not challenged up to the theoretical maximum blockage.

[1] South Texas Project
[2] Generic Safety Issue 191 - the NRC Generic Safety Issue number 191
[3] Change in core damage frequency above a baseline level
[4] Core Damage Frequency
[5] Change in large early release frequency above a baseline level
[6] Large Early Release Frequency
[7] Emergency Core Cooling System
[8] Cold Leg Break
[9] Hot Leg Breaks
[10] Core Barrel Bypass
[11] Fuel Assembly. Several fuel assemblies are loaded in the reactor vessel to form the reactor cores
[12] Sump Switch Over

Change summary August, 2015

Several changes have been made to the methodology first described in documents (Harrison, 2015), (STPNOC, 2015), and (Powell, 2015b, Attachment 7) sent to the NRC since late 2014 regarding a new approach to addressing concerns raised in GSI-191 using a risk-informed method, now referred to as RoverD. The most recent document (Powell, 2015b) included the white paper, 'RoverD: USE OF TEST DATA IN GSI-191 RISK ASSESSMENT' has been significantly revised in here. The primary changes are summarized as enumerated in the following:

1. A more detailed description specific to the elements of CASA used in the RoverD methodology is added that the analysis can be evaluated without reference to other documents. See Section 3, page 14.

2. The FIDOE sensitivity analyses to include sensitivities on core flow versus ECCS flows are revised. Sensitivities are added to investigate expected and beyond design basis core fiber loadings for CLBs. Particular interest is focused on two-train operation. See Section 3.5, page 26.

3. Detailed descriptions of FIDOE and RUFF that included the fiber mass conservation and frequency calculation tools (code listings and input decks) are removed and only the methodology descriptions are retained. The details removed are in technical papers cited (Hasenbein et al., 2015; Zolan et al., 2016). See Section 3.3, page 23 and Section 4.1, page 28.

4. The ΔLERF calculation is changed to include a more detailed analysis compared to the simple method presented in the earlier documents. See Section 4.3.

5. The thermal-hydraulic analysis is changed to add details specific to the RoverD methodology so that the thermal-hydraulic analysis can be evaluated without reference to other documents. See Section 5, page 38. Detailed descriptions have been previously provided by Powell (2015c, NRC ADAMS reference number ML14009A307).

6. The core cooling section (Section 6.1, page 39) is changed to make clear reliance on the thermal-hydraulics analysis for HLB. Success of HLBs relied on the thermal hydraulic analysis in the previous revision but now, the reliance is now explicitly stated.

7. The analysis of the effect of boric acid precipitation is modified to an evaluation of the fiber that might be transported to the core in CLBs. See Section 6.2, page 39.

8. The results of the RoverD analysis for individual weld locations now include IOZ amounts for a 10D ZOI to verify no additional risk due to the ZOI change to 10D. See Section 7, page 41.

9. In several sections, editorial changes are made.

Change summary September, 2016

Changes have been made to the RoverD methodology described in ML15246A126 (Powell, 2015a, Attachment 1-3, ML15246A127). A vertical bar in the margin indicates where something is changed. A small square in the margin indicates where something is deleted. Figure numbering is changed in most of the document although the figures themselves have not been changed; vertical bars in the margin by figures only indicate a changed figure number. Some references have changed; they are identified in the text (vertical bars) but not in the References section. The primary changes are summarized as enumerated in the following:

1. The ΔCDF and ΔLERF values are slightly higher due to changes in the break size determination.

   (a) The amount of fiber fines arriving on the strainer has been conservatively increased to include fines assumed to be eroded from smalls transported to the RCB pool. Tables 13 and 15 reflect break size changes resulting from the erosion assumption. Transport of fiber is modified to include 7% erosion to fines of all fiber smalls that transport to the RCB pool (Table 3 values reflect new assumptions).

   (b) HLBs larger than 16 inches are assigned to the risk-informed category, which results in adding 8 risk-informed RV nozzle locations. Break scenarios at each added location would have less than 191.78 lbm of fiber fines transported to the RCB pool at DEGB size.

2. Small CLBs are now evaluated using FIDOE bounding fiber amounts.

3. Thermal-hydraulic analyses are moved to the STPNOC Appendix B program in a set of four Engineering Calculations (Howard, 2015), one of which is the certification of the input, the other three, simulations of HLB scenarios. As a consequence, the section discussing thermal-hydraulics (Section 5) is greatly condensed.

4. The IOZ contribution to debris is no longer included in Table 14 as that contribution has been shown to be bounded (Connolly, 2016b, Attachment 2, SSIB 3-4).

5. The method for DEGB break frequency is changed to the method described by Zolan et al. (2016).

Contents

List of Figures

List of Tables

Listings

1 Introduction

RoverD is a method that follows the guidance of Regulatory Guide 1.174 (NRC, 2011) to assess the risk associated with concerns raised in GSI-191. RoverD uses test data and NRC (2011) guidance to evaluate the magnitude of LOCAs required to exceed a performance threshold that is established by testing for effects associated with concerns raised in GSI-191. The performance threshold is set low, set to underestimate the true level where functionality may be lost, so that risk for strainer failure is overestimated. Even when adopting a low threshold for failure , the risk is shown to be very small (NRC, 2011, pages 16–19).

RoverD evaluates two categories of scenarios designated as 'deterministic' and 'risk-informed' as illustrated in Figure 1. The deterministic scenarios are those in which the LDFG fiber fines estimated to arrive in the ECCS sump following LOCA are equal to, or less than, the amount of fines used in deterministic strainer testing; alternatively, a break size may be assigned at a location or locations to for example, reduce or simplify the scope of review or bound uncertainties.

The limit is set using testing methods intended to determine the maximum ECCS strainer head loss for the tested condition. For example, single failure criteria are adopted in combination with conditions known to overestimate head loss such as chemical quantities and morphology, strainer flow rate, and fiber fine amounts that include mechanical processing of fiber. If the strainer performance test shows a LOCA scenario will not cause any strainer performance requirements to be exceeded, then that scenario will not result in failure and is categorized as deterministic as shown in Figure 1.

Scenarios are the result of exhaustive sampling for break sizes and orientations at weld locations (described in Section 7, Page 41) to identify the smallest break size that would exceed the tested amount of fine fiber. Although some scenarios at a weld location with one or more scenarios in the risk-informed category may be successful, in RoverD, the frequency assigned at any risk-informed weld is the frequency associated with the smallest break size for that weld. As a consequence, some scenarios at weld locations may have break sizes larger than the smallest size, but do not produce more fines than the tested amount. That is, some scenarios for any particular non-DEGB risk-informed weld may be successful (in fact, many may be successful). The nature of this kind of behavior is shown in Figure 2.

The term 'deterministic' refers to test conditions that would not be expected in an actual accident unless all the uncertainties assumed in the design basis event as stated above were to be realized. Such tests can be used to establish a bounding envelope of performance (low threshold of failure) for the realistic scenarios realized or hypothesized. Using test data that include unrealizable circumstances may result in scenarios that would fall outside the bounding envelope defined by such test data. The risk for any such scenarios is required to meet a 'very small' threshold as shown in Figure 3.

In the following, the various analyses required to complete a RoverD assessment are summarized. The steps required to complete a RoverD analysis are summarized in Section 2.

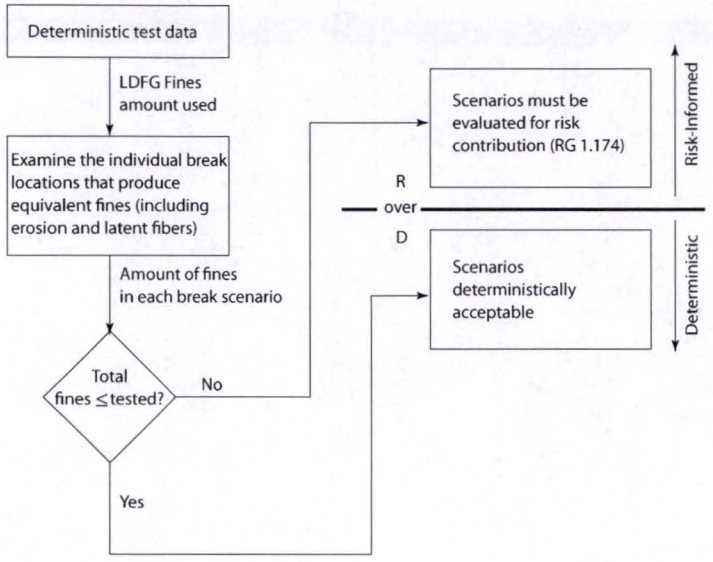

Figure 1: RoverD separates those scenarios that go to success deterministically from those that are assumed to go to failure and require risk-informed analysis

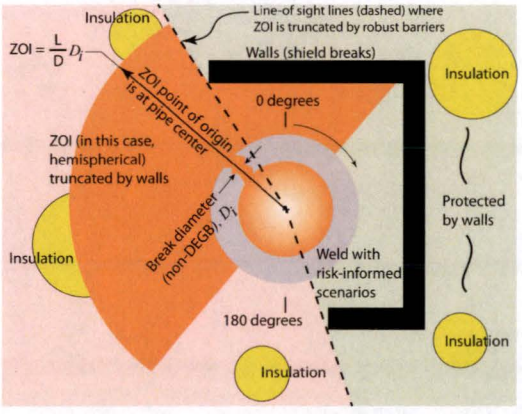

(a) Conceptual illustration of a break with diameter D_i where robust barriers truncate the ZOI such that breaks larger than the smallest break exceeding the tested amount of fines result in less amounts of fines.

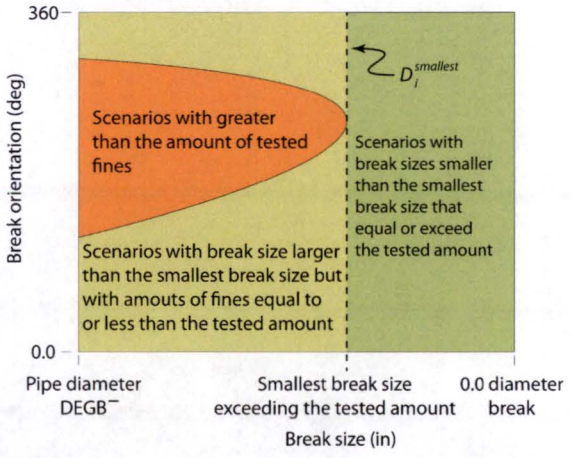

(b) Depiction on the {angle of orientation,break size} phase plane of the smallest break size and the resulting amount of fines. Some areas on the phase plane at break sizes larger than the smallest have less than the tested amount of fines.

Figure 2: Hypothetical break and the fines production for different break sizes and orientations showing how some break sizes larger than the smallest break size in a risk-informed weld location can have less fines produced.

Section 3 summarizes the way RoverD fiber generation, transport, erosion, and latent fiber quantity are established. Section 4 summarizes the LOCA frequency determination for scenarios in the risk-informed category. The basic approach uses top-down frequency partitioning. In-vessel analyses are briefly summarized in Section 5. Core performance metrics must be met in addition to strainer performance. Section 6 summarizes evaluation of core performance metrics.

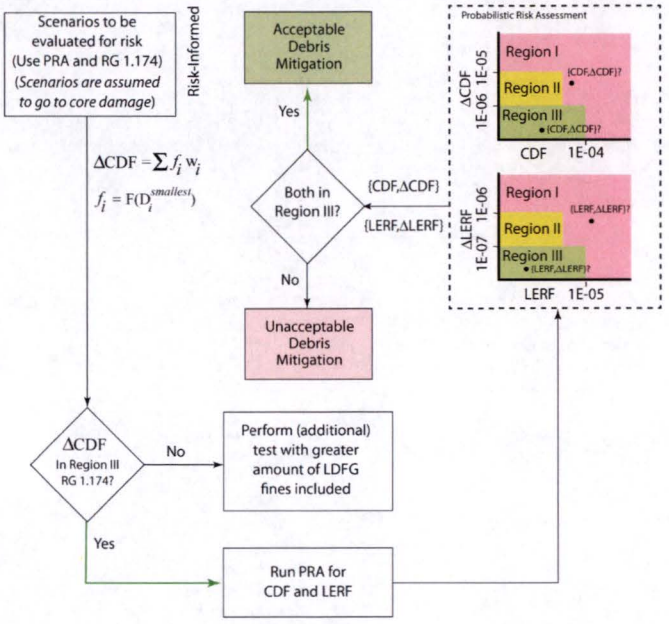

Figure 3: Flow chart showing the RoverD evaluation process following categorization of scenarios to determine risk acceptability. In this depiction, the frequency, f_i, of break at any location is evaluated based on its diameter using NUREG 1829.

2 RoverD methodology summary

RoverD involves the following steps to assess the risk associated with the concerns raised in GSI-191:

1. Perform a test that has some margin to failure following accepted protocols (see AREVA, 2008)

   Note the amount of fiber fines tested (in this case, 191.78 lbm) as well as the configuration (in this case, two ECCS trains). The plant configuration is important to ensure whether the test bounds other plant states. Fine fiber is used because it is the transportable form of the LDFG created in the break scenario (NEI, 2004, page 4-5).

Note that the test results must be applied to strainer performance criteria to ensure they are met using deterministic analysis requirements (for example, vortexing, structural margin, flashing, and so forth)

2. In-vessel performance criteria (core cooling, including fiber effects, boric acid precipitation) must be met under the conditions tested

3. Run CASA (Alion Science & Technology, 2015) to itemize all break locations, break sizes, and amount of LDFG fines in the sump (including erosion and latent fiber); include any additional locations if added for other reasons.

4. Compare the amount of fiber fines in each break scenario to the tested amount (AREVA, 2008)

   If the amount is equal to or less than the tested amount, categorize the scenario 'deterministic'

   If the amount exceeds (that is, 'over') the tested amount,or is added for other reasons, categorize the scenario 'risk-informed'

5. Evaluate the risk contribution (including in-vessel) of scenarios in the risk-informed category against the Regulatory Guide 1.174 quantitative criteria for {CDF,ΔCDF}, {LERF,ΔLERF}

   Assign change in core damage frequency to the frequency from (4)

   Check {CDF,ΔCDF} against the quantitative requirement of Regulatory Guide 1.174, Region III

   Check {LERF,ΔLERF} against the quantitative requirement of Regulatory Guide 1.174, Region III

   Verify other requirements (for example, safety margin, defense in depth) of Regulatory Guide 1.174 are met

6. If all requirements are met for the risk-informed category, the performance is acceptable

3 Reactor containment building debris generation and transport

NEI (2004) documented an acceptable methodology for determining the amount of debris generated in a LOCA of any particular size by defining a ZOI. Within the ZOI, specific size distributions of LDFG particles can be estimated using acceptable methods (Figure 4a). The amount and type of each debris species transported to the ECCS sump is governed by logic trees (see Figure 6, Page 21) developed to estimate the amounts captured and

sequestered, and the amounts that would continue to transport (for example see NEI, 2004, ppg 3-45, 3-53).

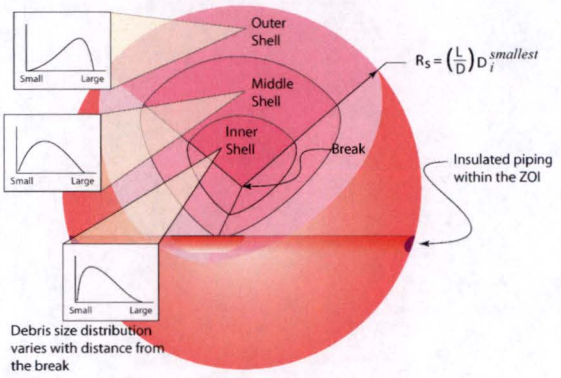

(a) Conceptual illustration of three zones of destruction potential within the ZOI showing how the debris distribution shifts towards larger sizes further from the break.

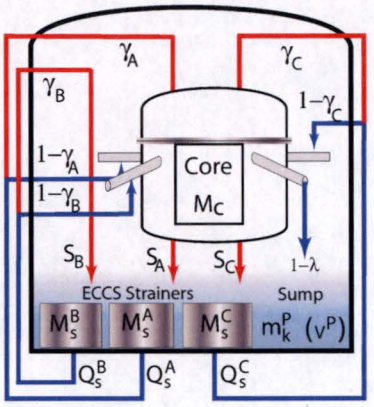

(b) Fiber flow paths for a three–train plant (trains A, B, and C) in containment after ECCS recirculation showing flow splits, γ, between total strainer flow and CSS flow.

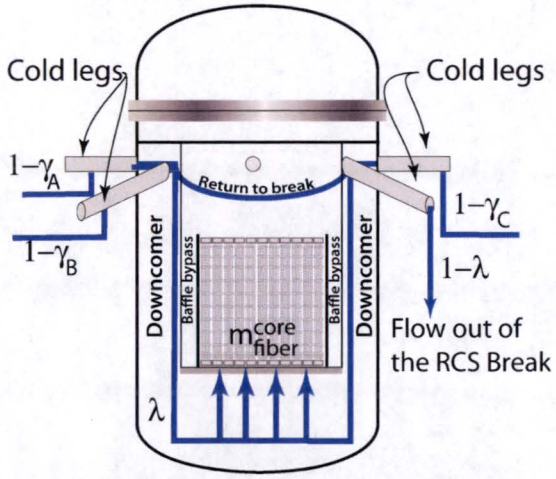

(c) Fiber flow paths through the reactor vessel following ECCS recirculation showing the additional flow split (λ) to the core and the break.

Figure 4: Conceptual illustration of fiber distribution within the ZOI and the transport paths through the RCB and RCS.

The flow paths through the RCB with the water flowing out of the breach in the RCS as well as with water from sources such as ECCS and CSS during the recirculation phase are shown in Figures 4b and 4c. Although different size particles are created from partially destroyed fiberglass insulation strands within the ZOI (fig. 4a), the smallest particles that transport readily through the RCB are 'fines'. Larger and partially destroyed LDFG insulation either do not transport or quickly sink to the containment floor and remain there. Over time, water flowing through the RCB tends to erode some of the larger particles captured outside of the ECCS sump into fine particles. Besides LDFG either destroyed or eroded into fine particles, fine particles from latent dust and dirt need to be taken into account.

A break size and location define a scenario from which is derived the amount of LDFG fines that arrive in the ECCS sumps. The methodology for examining many thousands of possible break sizes, orientations, truncation of ZOIs, transport of fines, and erosion of LDFG requires a computational framework implemented on a computer.

3.1 Computer implementation of debris generation & transport

As stated previously, generation, transport and erosion of LDFG fines requires a computational framework implemented on a computer. Alion Science & Technology (2015) has developed a generalized computer implementation inside CASA that uses a STP plant-specific CAD model of the RCB. The methodology used to obtain the amount of LDFG fines generated and transported to the STP RCB recirculation pool for each postulated break is described in the following sections. The overall steps used to calculate debris generation, particularly fiber fines and IOZ particles, with CASA can be summarized as enumerated below:

1. Importing CAD geometry,
2. Line of sight grouping of voxels that can be seen by each weld location that are not shadowed by robust structures, and
3. Insulation debris generation for each weld location based on scenario specific break size.

3.1.1 Import of CAD geometry

There are three types of geometry files that are imported into a CASA simulation for use in the insulation debris generation routines:

1. pipe extract insulation data files,
2. equipment insulation text files, and
3. robust barriers STL files.

These three types of geometry files and descriptions of how they are imported and used in the CASA debris generation routines are described below.

Pipe extract insulation data Pipe data are extracted from the piping assembly in the 3D containment CAD model using a proprietary AutoDesk Inventor add-in (created by AutoDesk for Alion). The data include all information about piping and piping insulation needed to rebuild the piping insulation geometry numerically inside of CASA. Specifically, pipe extract insulation data includes pipe segment lengths, pipe names, pipe insulation types, Cartesian coordinates of extracted points on pipe centerlines (Work-Point), bend radii of extracted Work-Points, inner and outer diameters of insulation shells, and Work-Point types (that is, valve, hangar, weld, and so forth). An example of a pipe segment in a pipe extract insulation input file is Table 1.

Table 1: Pipe Extract insulation data file example. The data include three header records and pipe work point data in columns: Inventor Ipart (.ipt Name), work point ID (Point), Cartesian coordinates (X, Y, and Z), bend radii (Rad), inner insulation shell diameter (ID), outer insulation shell diameter (OD), and work point type (WP).

extracted data

12-11-26 South Texas Plant.iam
Number of Points = 26. Number of Straights = 9. Unit of Length = Inches.

.ipt Name	Point	X	Y	Z	Rad	ID	OD	WP
30MS-1002-GA2 [NUKON]:1	0	-137.14	369.14	1404.88	0	32.75	38.75	
30MS-1002-GA2 [NUKON]:1	1	-137.14	369.14	1441.89	0	32.75	38.75	WELD
30MS-1002-GA2 [NUKON]:1	2	-137.14	369.14	1496.75	49.12	32.75	38.75	
30MS-1002-GA2 [NUKON]:1	3	-193.84	367.73	1496.75	0	32.75	38.75	FW0060
30MS-1002-GA2 [NUKON]:1	4	-301.05	365.07	1496.75	49.12	32.75	38.75	
30MS-1002-GA2 [NUKON]:1	5	-301.05	365.07	1420.97	0	32.75	38.75	WELD1
30MS-1002-GA2 [NUKON]:1	6	-301.05	365.07	1271.75	0	32.75	38.75	FW0002
30MS-1002-GA2 [NUKON]:1	7	-301.05	365.07	1202.25	0	32.75	38.75	HL5016
30MS-1002-GA2 [NUKON]:1	8	-301.05	365.07	1173.99	0	32.75	38.75	HL5015
30MS-1002-GA2 [NUKON]:1	9	-301.05	365.07	1148.88	0	32.75	38.75	HL5009
30MS-1002-GA2 [NUKON]:1	10	-301.05	365.07	1047	49.12	32.75	38.75	
30MS-1002-GA2 [NUKON]:1	11	-343.48	407.5	1047	0	32.75	38.75	HL5008
30MS-1002-GA2 [NUKON]:1	12	-386.54	450.55	1047	0	32.75	38.75	WELD2
30MS-1002-GA2 [NUKON]:1	13	-417.99	482.01	1047	49.12	32.75	38.75	
30MS-1002-GA2 [NUKON]:1	14	-461.28	438.72	1047	0	32.75	38.75	WELD3
30MS-1002-GA2 [NUKON]:1	15	-489.05	410.95	1047	0	32.75	38.75	HL5006
30MS-1002-GA2 [NUKON]:1	16	-613.41	286.59	1047	0	32.75	38.75	FW0004
30MS-1002-GA2 [NUKON]:1	17	-660	240	1047	49.12	32.75	38.75	
30MS-1002-GA2 [NUKON]:1	18	-660	120	1047	49.12	32.75	38.75	
30MS-1002-GA2 [NUKON]:1	19	-660	120	986.02	0	32.75	38.75	HL5001
30MS-1002-GA2 [NUKON]:1	20	-660	120	964.3	0	32.75	38.75	HL5002
30MS-1002-GA2 [NUKON]:1	21	-660	120	801	49.12	32.75	38.75	
30MS-1002-GA2 [NUKON]:1	22	-721.12	120	801	0	32.75	38.75	FW005A
30MS-1002-GA2 [NUKON]:1	23	-834.94	120	801	0	32.75	38.75	FW0006
30MS-1002-GA2 [NUKON]:1	24	-849.94	120	801	0	32.75	38.75	
30MS-1002-GA2 [NUKON]:1	25	-957.94	120	801	0	32.75	38.75	

Point to Point Length: 1748.53

The data from each pipe segment in the Pipe Extract insulation file are read into CASA and used to create a numerical reconstruction of the piping insulation with volume elements called voxels; where each voxel's volume is modeled to reside at its center point. The user can specify the numerical resolution of the piping insulation reconstruction (with voxels) in the CASA simulation by defining linear resolution and number of azimuthal bins in the simulation input deck (Listing 1).

Listing 1: Example of an input for defining piping insulation discretization

```
% ------------------------------------------------------------------------
''Spatial Resolution for Discretizing Insulation''
% ------------------------------------------------------------------------
% (must repeat weld target sort if these are changed)
% (delete all master files and rerun with new delL and Nangbin)

% Linear Resolution (inches)
6

% Azimuthal Bins in 2 Pi Radians on Pipes
12

\% ------------------------------------------------------------------------
```

An example of how the piping discretization works for a straight pipe is illustrated in Figure 5. The illustration shows how the insulation is discretized on the pipe. Also shown is the way the ZOI interacts with the voxels defined by azimuthal and linear parameters. The pipe actually appears transparent in the ZOI (spherical or hemispherical) and if the center-point of the voxel is within the ZOI the entire insulation volume within the voxel is assumed destroyed.

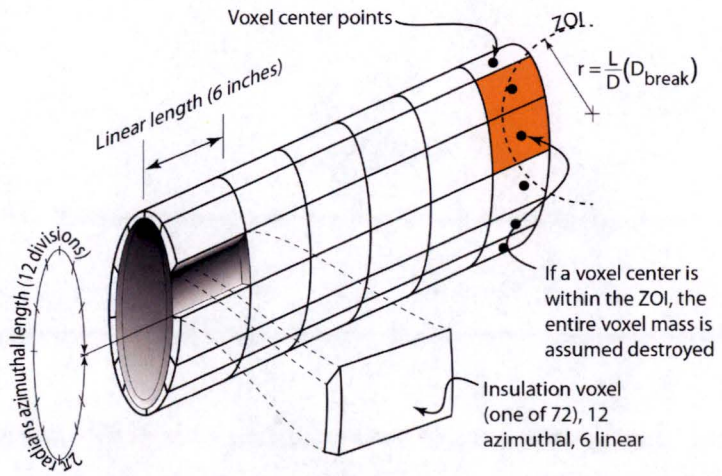

Figure 5: Illustration of insulation discretization on piping. The discretization is defined in input as shown in the input fragment in Table 1

Equipment extract data Equipment insulation voxels are defined differently than the piping because equipment shapes may be fairly arbitrary as compared to pipes. Therefore, equipment voxels are defined in files with X, Y, Z coordinates defining the center of a voxel having volume, V, and insulation type (as appropriate).

The simplicity of the equipment insulation definition files allows them to be created in a text file or spreadsheet. The STP equipment definitions were created from high-resolution STL exports of equipment insulation from the CAD software. The STL files were pre-processed to supply the necessary Cartesian coordinate data.

Robust barriers STL file The robust barriers input file is a STL data file containing all CAD-defined plant robust barriers' structure geometry and is used to represent robust barriers (insulation shielding) in the insulation destruction computations. The STL data file is interpreted as a collection of surface triangle faces (facets) and respective unit surface normal direction vectors in three-space such that the line-of-sight can be defined from the ZOI point of origin. The CAD generated STL files resolve detailed features such as door casings and cylindrical pipe penetrations. All surfaces defined as robust barriers in the 'robust barriers' input file are used to truncate ZOIs centered on weld locations. Insulation shielding by large equipment such as the steam generators and RCPs is not credited in the STP CASA debris generation calculation.

3.1.2 Line of sight calculations

Before debris generation is calculated for varying break sizes at each weld location, a line of sight grouping of insulation not shadowed by robust barriers is performed. These computations analyze each weld location and save the insulation voxels that are not shadowed by robust barriers along with their associated spatial location and volume information in a voxel packet specific to each weld. This step organizes visible (non-shadowed) voxels into weld specific voxel packets that make ZOI calculations of destroyed insulation faster during simulations over all weld locations in containment

3.1.3 Weld location based debris generation

After CAD geometry is imported and line of sight voxel computations are performed, weld location-based insulation debris generation can be calculated for scenario specific break sizes. Each scenario specific break is numerically represented by either a spherical ZOI for double-ended guillotine breaks (DEGB) or by a hemispherical ZOI for partial breaks. For both spherical and hemispherical breaks, the individual voxel center point locations from the voxel packet (Section 3.1.2) for the scenario-specific weld location are compared to the spherical or hemispherical ZOI centered on the current weld location for interference. Any insulation voxel with a centerpoint voxel from the weld specific voxel packet that is inside the ZOI is counted as destroyed, and all destroyed voxels are summed for each insulation debris type to yield total insulation generation for the analyzed break scenario. User-defined ZOI sizes for each insulation type are properly applied during the debris generation process.

3.2 Fine fiber debris sources

The sources of fine fiber debris that must be considered for each break scenario modeled for STP are: Nukon®, Thermal-Wrap®, and latent fiber (Alion Science & Technology, 2008). Note that the fixed amount of latent fiber specified as input for the plant is applied to every break scenario and that Nukon® and Thermal-Wrap® generation is scenario specific. The ZOI sizes and insulation debris size distributions used for the CASA computations of each modeled fiber type at STP are described in this section.

Insulation specific ZOIs Each of the insulation types, in Section 3.2 analyzed for fiber fine destruction in the STP RoverD methodology, have individually defined ZOIs based on jet testing. The maximum ZOIs used for each of the STP fiber-producing insulation types are summarized below in Table 2 and are based on the standard deterministic approach promulgated by NEI (2004, Volume 1 and 2).

Table 2: Summary of the ZOIs for fiber-producing insulation

Insulation Type	ZOI $\left(\frac{\text{radius}}{\text{break diameter}}\right)$	Reference
Nukon®	17.0	(NEI, 2004)
Thermal-Wrap®	17.0	(NEI, 2004)

In the way previously illustrated in Figure 4a, the ZOIs for Nukon® and Thermal-Wrap® insulation are shells with different percentages of debris sizes created within each shell. Along with fiber fines produced, debris sizes are calculated from each shell for small pieces, large pieces, and intact blankets (Alion Science & Technology, 2009).

Latent debris fiber sources The bounding latent debris mass of 200 lbm as suggested by NEI (2004, Volume 1), was used as the latent debris source for the STP evaluation. Fifteen percent (30 lbm) of the 200 lbm latent debris was introduced as fiber fines based on the NRC safety evaluation report NEI (2004, Volume 2) (15% fiber and 85% particulate by mass).

Destroyed volume mass All destroyed insulation volume was converted to mass using the manufactured densities:

- Nukon® $2.4\,\frac{lbm}{ft^3}$ (NEI, 2004, Volume 1)
- Thermal-Wrap® $2.4\,\frac{lbm}{ft^3}$ (NEI, 2004, Volume 1)
- Microtherm® $15\,\frac{lbm}{ft^3}$ (Alion Science & Technology, 2008, Table 5-2, Page 34 of 82)

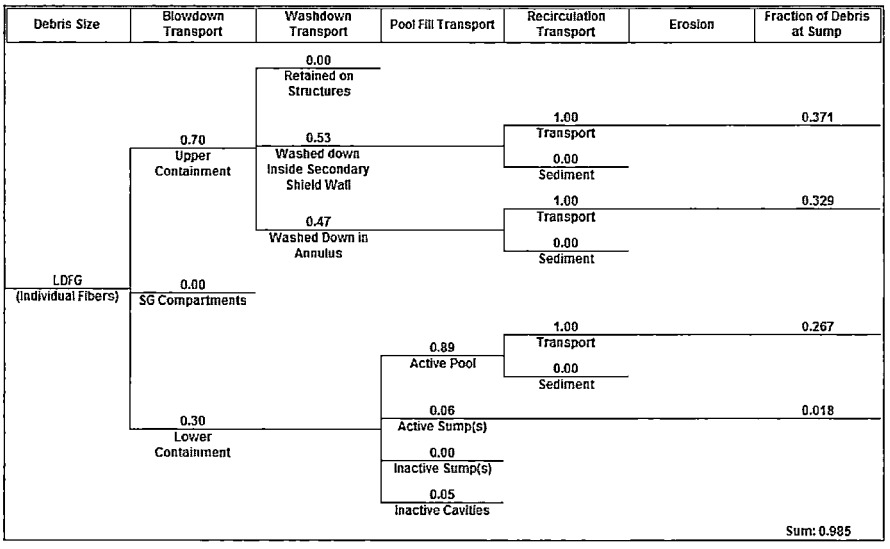

Figure 6: Example of a transport logic tree that can be used to obtain the mass of fiber fines transported to the containment pool.

3.2.1 Fiber fines debris transport

Once the amounts and distributions of fiber types are known, a transport logic tree, Figure 6, is used to arrive at the amount of fiber distributed to various areas of the RCB. Only fiber fines generated from the break are analyzed this way, the other two sources of fiber fines, latent fiber and eroded fiber, are transported directly to the sump. The transport fractions are representative of a break in the Steam Generator compartment, which bound transport fractions that would represent other possible break locations in the RCB.

Fiber fines from the ZOI The majority of fiber fines (98.5%) destroyed from insulation in the ZOI are transported to the containment pool. The other 1.5% of debris not transported to the RCB sump is trapped in inactive cavities during pool fill. The transport modes and their contributing fractions to the containment pool for ZOI-generated fiber fines are described below.

Blowdown Fiber fines were initially calculated to be blown to upper and lower containment at 30% and 70%, respectively (Alion Science & Technology, 2014). The percentages blown to upper and lower containment were calculated as volume fractions taken as ratios of the open containment volume in upper containment and lower containment compared to the total open containment volume. This proportion of fibrous fines transport was assumed (Alion Science & Technology, 2014) to be reasonable because fine debris generated by the LOCA jet would be easily entrained

and carried with blow down flow.

Wash Down All (100%) of the fiber fines blown to upper containment is washed down and homogenized in the containment pool. Note that wash down fractions from upper containment were split between the "Inside Secondary Shield Wall" and "Annulus" compartments; because both of these compartments are at the pool level, and because fine debris is assumed homogenized, these fractions are inconsequential except for their combined total which is 100%.

Pool Fill 5% of the fiber fines transported to lower containment during blow down is trapped in inactive cavities. This pool fill transport fraction of 5% is less than the NEI (2004) SER suggested maximum inactive cavity pool fill transport fraction of 15%.

Recirculation All fiber fines were assigned a conservative recirculation transport fraction of 100%. CFD calculations were not used to predict the amount of fines that may settle on the pool floor. One hundred percent transportability exceeds the fine fiber introduced to the containment pool for each analyzed break scenario and the amount of fine fiber introduced by AREVA (2008) in the flume test. Credit for realistic settling is an inherent part of the test conditions.

Eroded fines Three types of erosion were considered for small and large pieces of fibrous debris held up on containment structures:

1. CSS spray flow
2. Break flow
3. Pool recirculation (Alion Science & Technology, 2014)

The percentage of small and large fibrous insulation pieces eroded into fines as a result of CSS flow is assigned the maximum value of 1% as found by Rao et al. (1998). The percentage of small and large pieces eroded into fines by break flow is negligible in the STP RCB since debris is blown away from the break location. The eroded percentage of settled small and large pieces in the pool is set to 7% based on testing (Alion Science & Technology, 2011). The erosion testing found a 30-day recirculation erosion fraction value of 7% that bounds STP postulated pool conditions. Total fractions of small and large fibrous debris held up on containment structures, their corresponding erosion fractions, and resulting total fiber fines transport fractions homogenized in the containment pool have been provided in Table 3.

Table 3: Erosion modes and erosion percentage summary of smalls and large pieces eroded to fines.

Insulation Size	Erosion Mode	Held Up Fraction	Erosion Fraction	Total Fines from Pieces
Small Pieces	Spray	36.5%	1.0%	0.4%
	Recirculation	63.5%	7.0%	4.4%
Large Pieces	Sprayed	100.0%	1.0%	1.0%
	Recirculation	0.0%	7.0%	0.0%

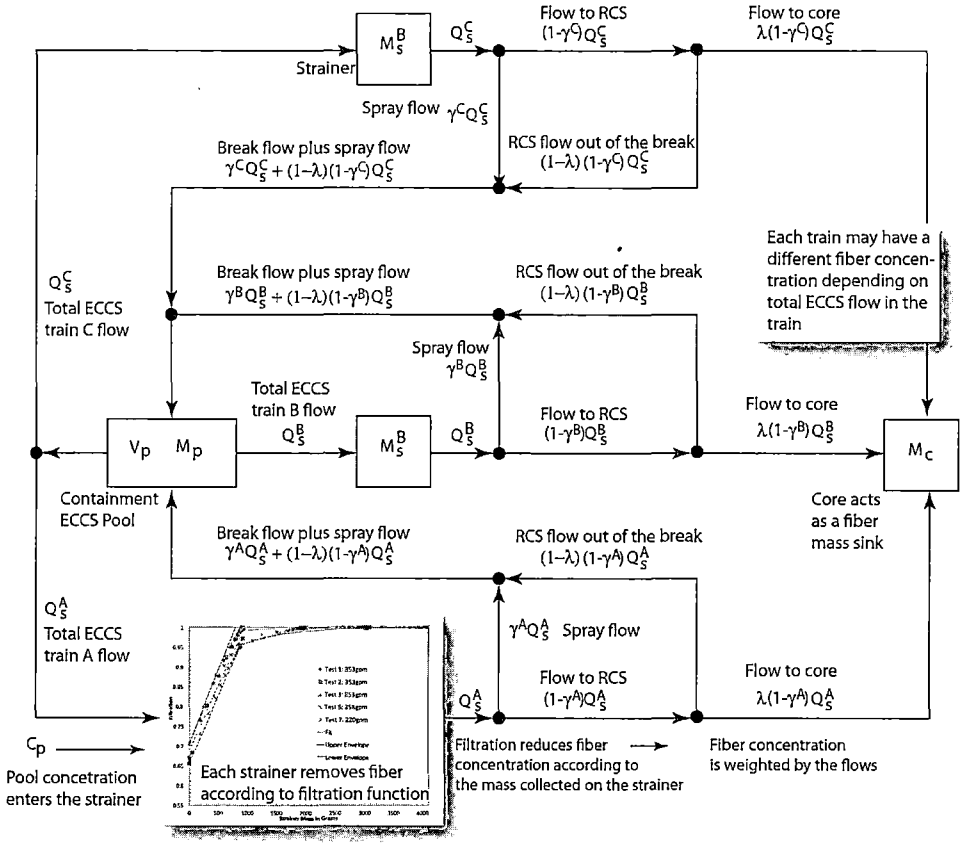

Figure 7: Flow network for the three STP ECCS and CSS trains showing the three places debris is caught: the pool, the strainer, and the core during a CLB scenario. Shown as well are the various flow splits that take place between the places debris is caught. The flow split λ is defined by the amount of flow demanded by the core to remove decay heat.

3.3 Mass conservation

A flow network that approximates the transport and capture of debris in containment in a CLB is shown in Figure 7. The primitive data for this system are: (1) time-dependent

Table 4: Example of the first few flows that would result from a decay heat load in a 40K MWd/MTU exposure assuming 3853 MW operation history. Note that the time is not shifted to account for delay to start of recirculation following a LLOCA.

Hour	Flow (gpm)	Hour	Flow (gpm)	Hour	Flow (gpm)
0	2141.1	0.0075	1718.6	0.015	1401.1
0.0025	2141.1	0.01	1564.8	0.0175	1352.5
0.005	1964.3	0.0125	1467.4	0.02	1314.1

flows $Q_s(\cdot)$ and $Q_c(\cdot)$, (2) scalars V_p, $M_p(0)$, and γ. The flows are time-dependent due to the influence of Q_c on λ. Q_c as a function of time is obtained from a table and is governed by the decay heat level. Table 4 lists the first few entries in an example of the table. Given these model primitives, an analysis of the time-dependent accumulation of debris on the strainer, core, and in the pool can be performed. These functions are governed by a set of non-linear differential equations. The non-linearity arises due to the *filtration function*, as shall become apparent in the following.

The transportable debris from the hypothesized LOCA moves down into the containment annulus forming a pool of water (Figure 8). The initial concentration of debris in the containment water pool is $C_p(0) = \frac{M_p(0)}{V_p}$. At the start of the ECCS recirculation phase, we assume all the transportable debris is in the pool. Hence, there is none on the strainer or the core ($M_s(0) = 0$ and $M_c(0) = 0$). The rate of accumulation of the debris on the strainer and the core is almost entirely governed by the amount of fiber that penetrates the strainer and is subsequently transported to the core as a result of the core flow rate. The governing conservation equations are:

$$\frac{d}{dt}M_s^k(t) = Q_s^k(t)C_p(t)f(M_s^k(t)), \tag{1a}$$

$$\frac{d}{dt}M_c(t) = Q_c(t)C_p(t)\frac{\sum_k \left[\left(1 - f(M_s^k(t))\right)\left(1-\gamma^k\right)Q_s^k(t)\right]}{\sum_k \left[(1-\gamma^k)Q_s^k(t)\right]}, \tag{1b}$$

$$0 = \frac{d}{dt}M_p(t) + \frac{d}{dt}\sum_k M_s^k(t) + \frac{d}{dt}M_c(t), \tag{1c}$$

where k is the strainer index. Wherever k appears the index is taken over all the values in $\{A, B, C\}$, that is, the three strainers. The model assumptions are:

1. $f(M_s)$ is a fraction between 0 and 1 (Figure 9), dependent on the amount of mass on the strainer (Ogden et al., 2013, Figure 13)[13],

[13]Ogden et al. (2013) used test data from measurements performed on one spare module (20 strainer modules are installed) in each STP ECCS train. As a consequence, the data must be scaled to the full

2. $Q_s(\cdot)$ should be treated generally as a function of time to model pumps turning on and off (discrete tabular function),
3. $Q_c(\cdot)$ is a known function of time (discrete tabular function based on decay heat demand),
4. V_p is a given constant value for any particular scenario,
5. The initial mass on the core is $M_c(0) = 0$,
6. The initial mass in the pool, $M_p(0)$, is given,
7. And $C_p(t) = M_p(t)/V_p$.

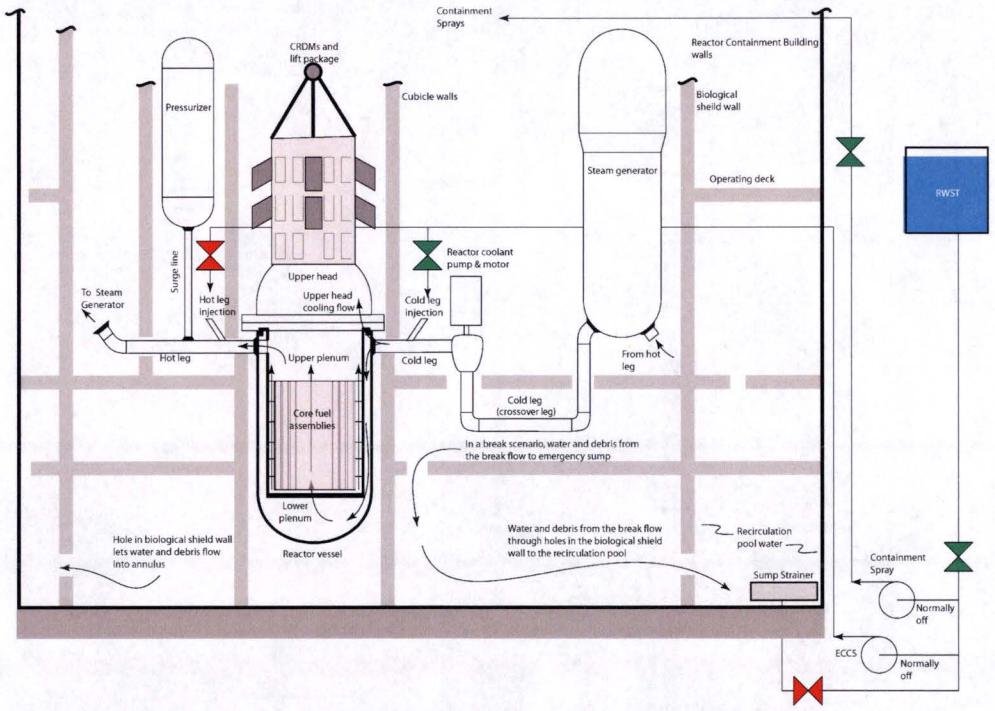

Figure 8: Simplified arrangement of the reactor system, ECCS and CSS with flow directions shown during normal operation for the intact plant and flows in the emergency systems when demanded. The arrangement has been distorted so the flows and equipment can be seen. Shown as well are flow paths from hypothesized breaks out to the ECCS sump strainers.

strainer area (scaled by a factor of 20) when applied to the full plant.

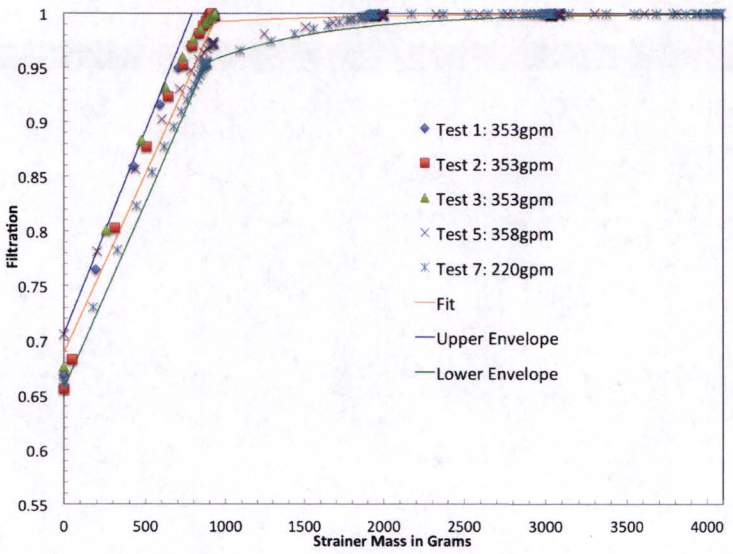

Figure 9: Filtration efficiency fits as a function of mass compared to measured data for the STP ECCS strainer modules. Efficiency fits obtained for the upper, central, and lower limits of the measurements are compared to the measured data.

3.4 Results

(1a) to (1c) are integrated in an application called FIDOE designed by Hasenbein et al. (2015) to provide solutions for different initial conditions and boundary conditions supplied in simple text files. Sensitivities are performed (for CLB) to ensure that the fiber limit of 15 gm/FA for core cooling is not exceeded when the tested amount of fine fiber is present in the containment pool. Sensitivities are performed for expected and design basis (two-train) operation.

Analysis has shown that the maximum fiber accumulation is realized when the core flow is approximately the same as the ECCS flow. For example, when $\lambda = 1.0$, all fiber entering the RCS is accumulated on the core, simulating a HLB. Results for cases over large ECCS flow variations for normal and two–train operation are presented in Table 5.

3.5 Fiber sensitivity analysis

The amount of fiber bypassed to the core is primarily dependent on the initial sump pool concentration, $C_p(t = 0)$, the filtration efficiency, $f(\cdot)$, and the decay heat demand, $Q_c(t)$ assumed to be a fixed function of time. The pool concentration is defined by the amount of LDFG arriving in the ECCS sump pool for each D_i^{small} and the pool volume. The filtration efficiency is based on data with uncertainty (Figure 9). Sensitivity to the coefficients and initial conditions in equations (1) is investigated in Powell (2015b, Attachment 7,

page 9). However, further study for cases at and around the design basis case (two trains of ECCS and CSS) helps in understanding margins to core fiber accumulation in the RoverD methodology.

3.5.1 Inputs

Based on exhaustive sampling for the smallest break sizes (D_i^{small}), all STP scenarios in the risk-informed category are LLOCA. With the exception of the location 16-RC-1412-NSS-8 (Table 13, page 42) that, due to an artifact of the break model, exceeds 192 lbm by a small margin (that is, its smallest diameter is DEGB at approximately 12.8 in), all breaks produce very nearly 192 lbm of fines. The most important parameters for core fiber accumulation are the ECCS flow and number of strainers in operation. Therefore, FIDOE (Hasenbein et al., 2015) sensitivity analyses for two-train operation are focused on various ECCS design basis and beyond design basis pump configuration scenarios with approximately 500,000 gal of water and roughly 87,000 gm of fiber in the containment pool. The analyses use ECCS flow rates of 2,800 gpm for a LHSI pump, 1600 gpm for a HHSI pump, and 2350 gpm for a CSS pump unless specified otherwise. The core flow rate is the same as in previous analyses (STPNOC, 2015, Attachment 7, Page 63 for example).

3.5.2 Sensitivities

The design basis pump configuration is 2 trains of LHSI, HHSI, and CSS with the six pumps operating in two trains (the third train has no pumps operating). FIDOE sensitivity studies indicate that the design basis pump configuration produces the minimum core fiber accumulation compared to the beyond design basis cases. With intuition gained from FIDOE calculations, one may realize that the design basis case is not limiting for core fiber buildup.

Notice the italicized case in Table 5, a case within the design basis (that is, at least two full trains of ECCS and CSS are operating). As can be inferred from the FIDOE sensitivity cases, the most limiting cases for core fiber accumulation are those with as many as possible ECCS strainers in operation, each with the lowest possible flow. The italicized case represents one that, from an ECCS flow perspective, exceeds the design basis configuration but results in more core fiber accumulation than the design basis case.

Finally, as may be expected, CSS flow reduces the amount of fiber that gets downstream due to recirculation through the strainer (refer to Figure 7, page 23). The CSS effect is seen by comparing the '2 LHSI 2 HHSI' case with the '2 CSS 2 LHSI 2 HHSI' case in Table 5. Further studies related to fiber accumulation are summarized in Sections 6.1 to 6.3, starting on page 39.

Table 5: Sensitivity of core fiber buildup to total ECCS flow. The "Plant state" column represents the nominal plant configuration for the flows in the column "Total ECCS flow". The Plant state '2 CSS 2 LHSI 2 HHSI' (bold typeface) most closely approximates a two-train design configuration. All cases use 'center' values for the STP ECCS strainer data fit.

Plant state (approx.)	Total ECCS flow	Core fiber (gm)	Core fiber (gm/FA)
Half HHSI flow	800	2,400	12.4
0 LHSI 1 HHSI	1,600	1,344.5	7.0
1 LHSI 0 HHSI	2,800	799.5	4.1
0 LHSI 2 HHSI	3,200	1327.3	6.9
1 LHSI 1 HHSI	4,400	982.1	5.1
2 LHSI 0 HHSI	5,600	791.7	4.1
2 LHSI 1 HHSI	7,200	618.8	3.2
2 LHSI 2 HHSI	8,800	511.3	2.6
2 CSS 2 LHSI 3 HHSI	*10,400*	*424*	*2.2*
2 CSS 2 LHSI 2 HHSI[a]	8,800	339.8	**1.8**

[a] This case is conservatively calculated assuming the two remaining ECCS trains inject into intact RCS loops. The design basis assumes that one of the trains is pumping out of the break which would recirculate that flow back to the strainer.

4 LOCA frequencies

In general, the ECCS strainer may operate under several different plant states. Most of the plant states tested will be congruent with deterministic assumptions on train availability (plant states). In the risk-informed category of RoverD, scenarios associated with plant states not tested would be relegated to failure, or could be assessed for risk based on their risk contribution in a way similar to the states tested. Because different plant states may need to be evaluated, depending on details associated with the test used in the RoverD assessment, an additional step may need to be taken to account for plant states not tested. Based on the STP ECCS/CSS design, two evaluations for break size determination are performed, one for design basis cases (Table 13, Page 42 corresponding to two or more ECCS trains operating) and (Table 15, Page 57 corresponding to single train ECCS operation).

As shown in Table 13, all breaks in the risk-informed category fall into the PRA LLOCA category (the smallest break size is greater than 7 in.) Therefore, only the upper two elicited intervals (7 in.–14 in., 14 in.–31 in.) are required for frequency analyses. The pipe sizes involved in the risk-informed category are 16 in. (nominal pipe size) and larger.

4.1 ΔCDF method development

A fundamental goal of the RoverD approach is to determine the total frequency of breaks that fall into the risk-informed category. In a preprocessing step known as RoverD's *fetch*

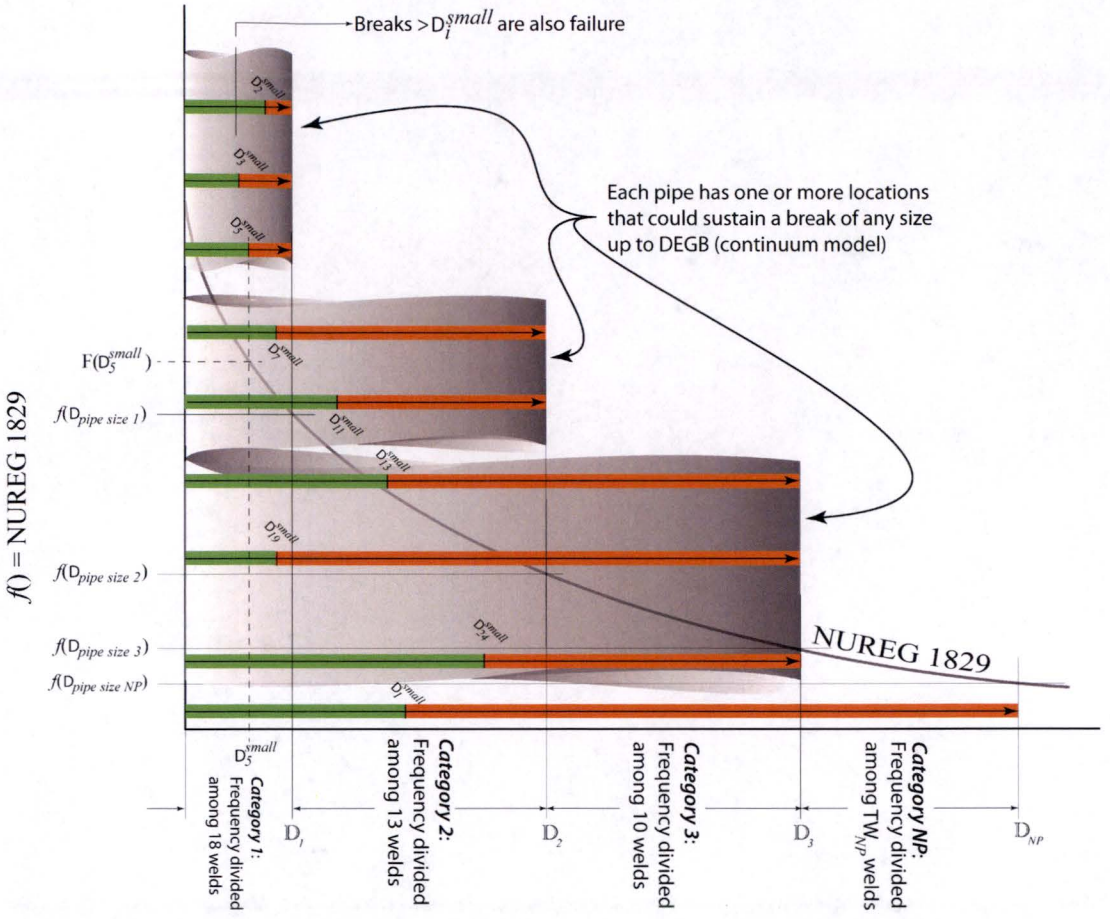

Figure 10: The top-down approach assigns equally-weighted frequency in intervals between pipe diameter extents. As D_i^{small} becomes larger, the total number of welds (Table 12, Page 41) in successive categories decreases.

stage, CASA runs are performed to identify all weld locations, with corresponding break sizes, which produce more than the allowable amount of fiber fines.

With fetch completed, the RoverD approach has data that can be thought of as ordered pairs consisting of a weld index and a break size. For now, assume that I weld locations are in the risk-informed category and these locations are indexed by $i = 1, \ldots, I$. Each weld location i then has a corresponding break size D_i^{small} which caused it to be placed in the risk-informed category. It is possible that for a single weld, multiple break scenarios caused it to be put in this category. If so, define D_i^{small} to be the smallest such break size. That is, there is no break size smaller that can produce more fines than the D_i^{small} at the

corresponding weld.

Now, recall that the goal is to determine the overall frequency of events that generate too many fiber fines. Two primary principles are adhered to in order to obtain the top-down frequency:

1. In the limiting case for which every weld and every break above x is considered "bad" (that is, at that break size, more fines come to the sump than were tested), the overall frequency, Φ, should equal to $f(x)$, the NUREG 1829 exceedence frequency at x (for any given quantile or mean),

2. In the top-down method, Φ should depend on the number of welds in the RoverD fetch file, for any (fixed) plant. In particular, Φ should increase if welds are added to the set of "bad" welds.

For each weld i in the risk-informed category the goal is to determine the frequency of breaks that exceed D_i^{small}. This is called $F(D_i^{small})$ and is the frequency of unacceptable events caused by that particular weld. Then, the overall frequency of unacceptable events caused by breaks in the risk-informed category is simply the sum of these frequencies:

$$\Phi = \sum_{i=1}^{I} F(D_i^{small}).$$

In general, as shown in Figure 10, interpolation is required to obtain frequencies at break sizes (that is, D_i^{small}) and at pipe diameters other than those in Table 6. From inspection (for example, Table 6), Tregoning et al. (2008) exceedence frequencies decrease rapidly (at larger diameters, they decrease roughly logarithmically) with increasing pipe size.

Linear-linear interpolation is used to estimate a frequency ϕ_x falling between known exceedance frequencies ϕ_a and ϕ_b:

$$\phi_x = \phi_a + (\phi_b - \phi_a)\frac{(x-a)}{(b-a)}. \tag{2}$$

Log-linear and log-log interpolation methods were also considered. However, as shown in Hasenbein (2015), these latter two methods always produce lower interpolated values than linear-linear interpolation for the Tregoning et al. exceedence data.

Based on its interpolation behavior, the linear-linear method is used for the ΔCDF determination of the scenarios in the risk category.

To explain the calculations, we first focus on a particular weld from Figure 10. In particular, in a pipe of category 1, which is denoted by $\mathbb{D}_1$, we examine Weld 5. To determine $F(D_5^{small})$, the goal is to be consistent with NUREG-1829. Any particular quantile value in Table 6 may be used as the basis. For example, the PRA LOCA initiating event frequencies are based on the mean value. Let $f(D_5^{small})$ be the exceedance frequency for a break of size

Table 6: NUREG-1829 (Tregoning et al., 2008, Table 7.19) and NUREG-1829 (Tregoning et al., 2008, Table 7.13) for the geometric (GM) and arithmetic averaged (AM) mean, median, 5th percentile, and 95th percentile exceedence frequency values for current-day estimates STP PRA break sizes for small, medium and large LOCA are: less than 2 in (small), 2 in to 6 in (medium), greater than 6 in (large).

NUREG-1829 Values, Table 7.19				
Break Size (in)	**5th**	**Median**	**Mean**	**95th**
$\frac{1}{2}$	6.8E-05	6.3E-04	1.9E-03	7.1E-03
$1\frac{5}{8}$	5.0E-06	8.9E-05	4.2E-04	1.6E-03
3	2.1E-07	3.4E-06	1.6E-05	6.1E-05
7	1.4E-08	3.1E-07	1.6E-06	6.1E-06
14	4.1E-10	1.2E-08	2.0E-07	5.8E-07
31	3.5E-11	1.2E-09	2.9E-08	8.1E-08
NUREG-1829 Values, Table 7.13				
Break Size (in)	**5th**	**Median**	**Mean**	**95th**
$\frac{1}{2}$	8.1E-04	4.8E-03	1.0E-02	3.6E-02
$1\frac{5}{8}$	4.2E-05	7.0E-04	3.0E-03	1.2E-02
3	1.3E-06	1.9E-05	7.3E-05	2.9E-04
7	6.9E-08	1.3E-06	9.4E-06	3.0E-05
14	9.9E-09	2.6E-07	2.4E-06	7.2E-06
31	5.9E-09	1.5E-07	1.5E-06	5.2E-06

D_5^{small} as implied by a selected quantile value in Table 6. In general, such a quantity must be interpolated from the values in the NUREG-1829 categories.

Plant-wide, the frequency of breaks of size D_5^{small} and larger is

$$f(D_5^{small}).$$

Shown along the bottom of Figure 10 are categories defined by increasing pipe sizes. We define $Cat(D_i^{small})$ as $0 < \mathbb{D}_1 < D_2 < \ldots < \mathbb{D}_{j-1} < D_i^{small} < \mathbb{D}_j \ldots < \mathbb{D}_{n-1} < \mathbb{D}_n$, $Cat(D_i^{small}) = j$. Every weld that can experience a break of size D_5^{small} or larger contributes to the overall frequency. Referring to Figure 10, D_5^{small} falls into Category 1. Hence, it is deduced that:

$$F(D_5^{small}) = \frac{f(D_5^{small})}{TW_1},$$

where TW_n for Category n is the total number of welds in pipes of this category or larger (Table 12, 41).

For a pipe in category 2, the calculation is similar. However, it should be noted that the denominator in the equation above depends only on the size of the break and not the

category of pipe in which the weld resides. So, for Weld 7 in pipe category 2, D_7^{small} is smaller than $\mathbb{D}_1$. In this case, the frequency of a break of size D_7^{small} is

$$F(D_7^{small}) = \frac{f(D_7^{small})}{TW_1}.$$

For Weld 11, it is

$$F(D_{11}^{small}) = \frac{f(D_{11}^{small})}{TW_2}.$$

Now for any weld i in pipe category n with a smallest break size D_i^{small} a general formula can be written:

$$F(D_i^{small}) = \frac{f(D_i^{small})}{TW_{Cat(D_i^{small})}}. \tag{3}$$

$Cat(D_i^{small})$ is the pipe category corresponding to D_i^{small}. For example, if Category 1 is 1-inch pipes and Category 2 is 2-inch pipes, then for a break of 1.75in, $Cat(1.75in) = 2$.

Now, let R_n be the set of all welds which are in the risk-informed category and are associated with pipes of category n. Then, the frequency of unacceptable events due to weld breaks in pipes of category n can be written as:

$$\sum_{i \in R_n} F(D_i^{small}).$$

Finally, (referring to Figure 10 showing the count of the Categories as NP), the overall frequency of events in the risk-informed category is given by:

$$\Phi = \sum_{n=1}^{NP} \sum_{i \in R_n}^{I} F(D_i^{small}). \tag{4}$$

Zolan et al. (2016) implemented (4) in an application, RUFF, that takes as input the appropriate table from Tregoning et al. (2008), the plant weld inside diameters, and the D_i^{small} for each risk-informed scenario and provides Φ evaluated for the quantiles and mean frequencies from Tregoning et al. (2008) data supplied.

4.2 Plant states not tested

The ECCS debris screen testing considers two trains operating, one train idle, to be consistent with deterministic design assumptions that is, one train is assumed failed. The more likely case (not tested) would be three trains in operation in which case the debris would be spread over three ECCS strainers. It is clear that the three train case is bounded (in terms of debris loading) by the two-train case.

The limiting single ECCS/CSS train operation is when all pumps are operating on one ECCS strainer. For example, if one LHSI is operating on one strainer and one HHSI is operating on a different strainer, the maximum loading on each strainer would be less than if both pumps operated on the same ECCS strainer. If the CSS were to be operating on the third strainer, approximately one third of the debris would load on the that (third) strainer without passing to the RCS. However, in a risk-based assessment, single train operation is possible and for certain scenarios, single train operation is assessed to go to success in the PRA. In the STP ECCS design, single train operation would result in twice the debris load on the operating strainer. Therefore, the breaks that could be tolerated would be those with one half the tested (two-train operation) debris load.

The break frequency description above would apply in the same way to the single train operation, but would clearly result in higher frequencies due to the increased debris load. To account for the increased risk, (4) could be assessed for the cases where two or three trains are operating (cases either tested or bounded by the test) and assessed again for the untested case (single train operation) with the higher frequency. For example, if f_2 is the success frequency for two or more trains operating and f_1 is the success frequency for single train operation, (4) can be rewritten to accommodate the total frequency, $\hat{\Phi}$, for both operating states:

$$w_j = \frac{f_j}{\sum_j f_j};\ j = 1, 2, \tag{5a}$$

$$\Phi_j = w_j \sum_{n=1}^{NP} \sum_{i \in R_n}^{I} F(D_i^{small}), \tag{5b}$$

$$\hat{\Phi} = \sum_j \Phi_j. \tag{5c}$$

In Section 7 it is shown that pipe break sizes exceeding the amount of fines tested fall only within the large break LOCA range of sizes; that is, greater than the equivalent 6 inches in diameter. In referring to the number of trains of ECCS pumps operating following a LLOCA, it is important to consider all the applicable pump types; that is HHSI, LHSI, and containment spray pumps. Since the spray pumps are eventually shut down after swap over to recirculation and the HHSI pumps are of much lower capacity, the frequencies of ECCS trains operating is evaluated on the status of the LHSI pumps only. Therefore f_1 (for single train operation) is computed as the sum of all pump state frequencies in which exactly one LHSI pump is operating, regardless of the status of the HHSI or containment spray pumps. Similarly, f_2 (that is for two or more trains in operation) is based on the sum of all pump states in which 2 or 3 trains of LHSI pumps are operating, again, regardless of the number of HHSI pumps or containment spray pumps operating. For both computations, only those pump states in which the large break LOCA is successfully mitigated in the

absence of GSI-191 phenomena are tracked. There are no success sequences in which zero LHSI pumps operate. The results for f_1 and f_2 are provided below in Table 7 (Johnson, 2015, Page 5).

Table 7: Summary of success frequencies (sums) for sequences where pumps for two or more LHSI pumps (break sizes in Table 13) and sequences where a single LHSI pump is operating (break sizes in Table 15).

LHSI Operating train Condition	Success Frequency per year
f_2	4.16E-06
f_1	1.55E-09

4.3 LERF

Because operation of the STP RCFCs is not dependent on the sump status, and because they are designed to remove decay heat and maintain RCB contamination limits within design limits, the concerns raised in GSI-191 would not result in new early containment failure modes. Contributors to large early containment failure modes may include the following:

1. Containment bypass paths (including interfacing system LOCAs, steam generator tube rupture initiating events, and induced steam generator tube ruptures).
2. Containment isolation failures.
3. High pressure melt ejection phenomena.
4. Core debris impingement on containment (if applicable).
5. Reactor vessel and containment venting (if applicable).
6. In-vessel steam explosions leading to containment failures (alpha mode failures).
7. Hydrogen burns leading to early containment failure.

The following considerations are included in the STP RCB early failure analysis:

1. For STP, GSI-191 phenomena are only applicable for break sizes in the LLOCA range; that is, greater than 6 in equivalent diameters. Since GSI-191 phenomena are only relevant for LLOCAs, containment bypass paths are not applicable.
2. Containment isolation failures are still applicable, but of extremely low frequency. GSI-191 phenomena do not impact the reliability of containment isolation.
3. High pressure melt ejections are not applicable for LLOCAs.

4. Core debris impingement on the containment wall is not applicable to STP.

5. Containment venting features are not applicable to the STP design.

6. In-vessel steam explosions are applicable to GSI-191 scenarios, but are of low probability. GSI-191 phenomena do not impact their probability of causing containment failure.

7. Hydrogen burns leading to early (that is within 4 hours) containment failure are applicable to GSI-191 scenarios, but again are of low probability. Immediately following a LLOCA blowdown, the containment atmosphere is steam inerted. The low RCS pressure conditions following a LLOCA preclude induced interfacing systems LOCAs or induced steam generator tube ruptures. For early flammable conditions, the condensation of steam within containment must occur within 4 hours. Containment spray is very likely to occur during the injection phase but may be lost after switchover to recirculation due to GSI-191 phenomena. Because spray during injection is likely available and the RCFCs are likely to operate throughout the scenarios, the Level 2 model for the STP PRA Revision 7.1 assumes that the steam will be condensed early; that is within 4 hours of the break.

In summary, the early containment failure modes applicable for GSI-191 phenomena are containment isolation failures, in-vessel steam explosions, and early hydrogen burns. The first two are unaffected by GSI-191 phenomena and the last one is conservatively modeled in the PRA in that the containment is assumed deinerted whenever spray injection or recirculation is available. Since STP has three trains of containment spray, containment spray during the injection phase is highly likely.

4.4 ΔLERF scenario development and estimation

GSI-191 phenomena need to be taken into account for ΔLERF calculations given ΔCDF. To ensure that GSI-191 specific scenarios are appropriately considered, calculation for LLOCAs is performed in which sump recirculation is always assumed failed by strainer plugging; that is, as if GSI-191 always caused core damage. The results for a sequence with cutoff of 1E-16 per calendar year are provided below in Table 8 (Johnson, 2015, Page 7).

Table 8: Sensitivity results for large early release given LLOCA with sump strainer plugging assumed as always failed.

Core Damage Frequency	4.183E-06 per calendar year
Large Early Release Frequency	1.044E-08 per calendar year
Conditional probability of Large Early release	2.5E-3

The conditional probability of a large, early release given core damage due to GSI-191 phenomena, P(large early release|core damage), can be estimated as:

$$\text{P(large early release|core damage)} = \frac{\text{LERF}_{\text{LLOCA with SUMP=F}}}{\text{CDF}_{\text{LLOCA with SUMP=F}}} = 2.5\text{E-}03.$$

The change in LERF associated with the change in CDF from scenarios involving GSI-191 phenomena can then be evaluated from:

$$\Delta\text{LERF} = (\Delta\text{CDF})\ \{\text{P(large early release|core damage)}\} = (\Delta\text{CDF})\ (\ 2.5\text{E-}3). \quad (6)$$

The main contributors to large early release from this sensitivity were found to be early hydrogen burns and in-vessel steam explosions (that is, alpha mode).

4.5 Results

STP has two categories of Cases that need to be considered, Case 2, all single train pump configurations or Case 1 all two or three train pump configurations, including the specific condition tested (AREVA, 2008). Within each of these two Cases, one pump configuration is chosen to bound the test for fine fiber accumulation on the strainers. In Section 3.4 (starting on page 26) and Section 6 (starting on page 38), pump configurations that may be limiting for core performance metrics are investigated. For Case 2, when at most one pump of each type is operating, the limiting pump configuration is when all three pumps are aligned to the same strainer. In Case 1, when at most two pumps of the same type are operating, the limiting pump configuration is again when all pumps are aligned to two of the strainers and none are aligned to the third strainer. The tested deterministic case was for this condition; that is with two of the three STP ECCS strainers in operation (single failure criterion) with all pumps (two CSS, two LHSI, and two HHSI) operating. For the pump configurations with three pumps of the same type operating there would be far less fiber accumulation on each strainer than for the tested case. As a consequence, pump configurations with three trains of pumps operating are bounded by the tested case, and are conservatively grouped within Case 1.

However, the single train case corresponds to a case where only one train of the three STP ECCS strainers is in operation. Although this case is beyond design basis, it needs to be considered in the risk analysis since at least twice as much fiber would accumulate on the single strainer than when two or more strainers are in operation. In this case, only 1/2 the tested amount of fine fiber can be assumed to be tolerated.

4.5.1 ΔCDF results

When all cases are considered using (5), a slightly higher ΔCDF is estimated than when two (or more) strainers are assumed in operation (design basis configuration). Table 9

summarizes the ΔCDF estimate for geometric and arithmetic averages from Tregoning et al. (2008) using frequencies for the bounding cases from Table 7 (page 34), f_2 (Case 1) and f_1 (Case 2). As shown, the median ΔCDF is within Region III of the Regulatory Guide 1.174 evaluation ($\ll 1.0E-06$). Interpolation of Table 6 is done using the linear-linear method, (2).

Table 9: Case 1 and Case 2 results for geometric (GM) and arithmetic (AM) aggregations of Tregoning et al. (2008, Tables 7.13 and 7.19) data. The total frequencies, $\hat{\Phi}$(GM) and $\hat{\Phi}$(AM), from (5) are in events/yr. Also shown for comparison are the results for a DEGB-only model for the locations that go to failure.

Continuum Break Model						
Quantile	Case 1 GM	Case 1 AM	Case 2 GM	Case 2 AM	$\hat{\Phi}$ (GM)	$\hat{\Phi}$ (AM)
5^{th}	3.30E-10	7.88E-09	4.41E-09	2.68E-08	3.31E-10	7.89E-09
50^{th}	9.44E-09	2.05E-07	9.92E-08	5.50E-07	9.47E-09	2.05E-07
95^{th}	4.38E-07	5.78E-06	2.15E-06	1.36E-05	4.39E-07	5.79E-06
Mean	1.50E-07	1.90E-06	5.90E-07	4.31E-06	1.50E-07	1.90E-06
DEGB-Only Model						
5^{th}	3.47E-10	7.78E-09	3.35E-09	2.23E-08	3.49E-10	7.78E-09
50^{th}	8.62E-09	1.92E-07	7.60E-08	4.72E-07	8.64E-09	1.92E-07
95^{th}	2.84E-07	6.02E-06	1.72E-06	1.19E-05	2.84E-07	6.03E-06
Mean	9.02E-08	1.82E-06	4.82E-07	3.80E-06	9.03E-08	1.82E-06

As shown in Table 9, only the mean and 95^{th} percentile ($\hat{\Phi}$ (AM)) of the Tregoning et al. arithmetic aggregation estimate exceed the Region III criterion in (NRC, 2011). As described in the letter to the NRC dated May 22, 2014 (ML14149A434), the geometric method of aggregation is the most appropriate estimator of LOCA frequency from (Tregoning et al., 2008).

4.5.2 ΔLERF results

The results for the ΔLERF are summarized in Table 10. These results are obtained by applying P(large early release|core damage) to the mean values of $\hat{\Phi}$ in Table 9 for ΔCDF. As summarized in the table, when (6) is used with Table 8 values considering GSI-191 phenomena and using $\hat{\Phi}$ (GM) mean values for either the continuum model or the DEGB-only model, ΔLERF is $\ll$1.E-07 yr^{-1}.

Table 10: ΔLERF evaluation for geometric and arithmetic means of the Continuum and DEGB-only models

Model	ΔLERF using $\hat{\Phi}$ (GM)	ΔLERF using $\hat{\Phi}$ (AM)
Continuum break model	3.75E-10	4.76E-09
DEGB-only	2.26E-10	4.54E-09

5 RCS Thermal-hydraulics

Section 3 is a description of the debris generation and transport in the RCB. The RoverD thermal-hydraulic calculations for the RCS response to LOCA are solved for mass, momentum and energy as well as for heat transfer from bodies in the flow fields. The calculations are documented in STP Engineering Calculations (TAMU, 2016c,b,a) for small, medium, and large HLBs. The thermal-hydraulic analyses have been adequately described in Powell (2015a, Attachment 1-3, page 28 of 81) and associated RAIs (Connolly, 2016a, Attachment 6; SNPB 3-1, -3, -4, -5, -8, -11, -12, -13, -14, -16, -19), (Powell, 2016, Attachment 1; SNPB 3-2, -6, -7, -15, -17, -18, -20 – -32).[14]

As summarized in the calculations, for the STP reactor design, a complete core blockage starting from the time of ECCS recirculation phase in HLBs will not result in fuel overheating. Therefore, debris blockage is bounded for all HLBs in the STP reactor design.

6 Core performance metrics

In addition to satisfying the strainer performance metrics, certain core performance must be acceptable with the amount of LDFG fines tested as well. There are two metrics, separately evaluated but ultimately having the same consequence, that must be found acceptable to categorize a scenario as deterministic. Decay heat removal considering LDFG blockage of the core cooling channels and freedom from boric acid precipitation must be found acceptable. As discussed in Section 5, HLBs are not subject to LDFG concerns however, CLBs need to be studied for cooling and boric acid concentration.

Ogden et al. (2013) have shown that the amount of fiber penetrating through the ECCS strainer is a function of strainer LDFG loading. In order for the screen performance metrics as tested (again AREVA, 2008, for example) to serve as the 'worst case' condition for deterministic characterization, the amount of fiber passing through the ECCS strainers needs to be less than that tested by the PWROG as acceptable.

[14] A typographical error in ML15246A127, Table 12, "Summary of core blockage scenario simulation conditions" had the RWST temperature (incorrectly) identified as being in units of °C rather than °F.

6.1 Core cooling

The PWROG (2011) has tested performance of the reactor core fuel assemblies under deterministically challenging conditions, and developed a performance metric in terms of the allowable amount of LDFG fiber accumulation on the reactor fuel assemblies. The currently accepted allowable amount of fiber accumulation for STP cores is 15 grams of fiber per FA for core cooling. The PWROG fuel assembly testing was performed to investigate heat removal with particulate, chemical precipitates, and LDFG fiber present in the fuel assemblies but boric acid precipitation was not a consideration in the PWROG testing. As shown in the uncertainty analysis in Section 3 (Table 5), the maximum total fiber captured in the core in a CLB for the design basis case is calculated to be about 2 gm/FA. The maximum possible core accumulation is calculated 4.1 gm/FA for the beyond design basis case (2 LHSI, 0 HHSI, 0 CSS) that is success for core cooling.

However, there are no HLB scenarios with (deterministically) less than 15 gm/FA and therefore HLB scenarios are analyzed as described in Section 5. As summarized in Section 5, all HLB scenarios succeed regardless of the fiber blockage. That is, the analyses cited in Section 5 shows full blockage of all flow into the core during HLBs) will not cause loss of adequate cooling regardless of break size. From a core cooling perspective, the HLB risk-informed scenarios only contribute to failure by potential loss of core cooling through failure of ECCS strainer as described previously.

6.2 Boric acid precipitation

Even though direct core cooling flow is adequate, it is possible that mixing flows, assumed to be available to dilute boric acid concentrations in the core, reactor vessel, and RCS may be inhibited by fiber accumulation on the core during CLBs. However, based on evaluation of fiber loading under expected, design basis, and beyond design basis analyses of core fiber loading, it can be concluded that very small amounts of fiber would accumulate on the STP core following a LOCA. The amounts are small enough that they would not be expected to inhibit dilution flows following a LOCA. In the following, results of FIDOE sensitivity studies for core fiber loadings with different assumed pool loadings and ECCS/CSS flows are summarized.

FIDOE sensitivity analyses, as summarized in Table 11, using the STP fiber penetration data fit (Ogden et al., 2013, Equation 10 and center data, Table 9) were conducted to investigate CLB core fiber accumulation that might be expected for the maximum debris cases (DEGB) in the RoverD risk-informed scenarios. Sensitivity for the design basis pump configuration (two trains with a CSS pump, a LHSI pump, and a HHSI pump) show that, within the measured range of ECCS screen penetration and approximately nominal pump flows, the total accumulation on the core is less than 400 gm (less than 2 gm/FA). For these simulations, 800 lbm (363,200 gm) of transportable (fine fiber) was assumed to arrive in the containment pool prior to start of ECCS recirculation. 800 lbm bounds the maximum

DEGB amount of fine fiber (the fiber assumed to transport to the strainers) from any break (Table 14).

As explained further in what follows, lower ECCS flows (compared to core flow) cause greater core fiber accumulation. Therefore an extreme case, one that is success for core cooling in the STP PRA, is investigated. In this beyond design basis case, two ECCS trains are assumed operating in recirculation but with no CSS pumps and no HHSI pumps operating. The maximum core fiber buildup for the beyond design basis case is 4.4 gm/FA using the 'Center' fit parameters. This small amount of fiber would not be expected to cause significant inhibition of mixing flows. If the 'Upper penetration values' fit parameters of the measured filtration data are used, the fiber accumulated on the core is 5.8 gm/FA. Even in this extreme case, the amount of fiber accumulated would not be expected to significantly impact boric acid dilution flows. This conclusion is similar to the conclusion by the PWROG (2011, Section 10.2, pages 10-3 and 10-4) that much larger fiber loads produced insignificant head loss and by the NRC (2012, Section 3.8, pages 61 and 62) for separation of BAP from concerns raised in GSI-191.

Table 11: Summary of sensitivity studies investigating fiber amounts under different ECCS flow assumptions and maximum fibrous debris loads in the sump pool.

Total strainer flow (gpm)/Comments	CSS flow (gpm)	Total core fiber (gm)	FA fiber (gm/FA)
12,700 / Design case (single failure)	1930	376	1.95
8840 / No CSS pumps	0	539	2.8
5600 / No CSS or HHSI pumps	0	845	4.4
5600 / 'Upper' penetration values Ogden et al. (2013, Table 9)	0	1119	5.8

6.3 Further discussion on relative ECCS and core flows

If it were possible for the ECCS flow to be equal to the core flow (and no CSS flow), the filtration process could be modeled as a simple loop with the strainer and core in series and the core would capture all fiber advected from the ECCS strainers. In addition, if the ECCS strainer filtration efficiency is assumed constant, say f^*, the percentage of mass on the strainer would be f^* and the percentage on the core, $1 - f^*$ (recalling FIDOE models the core as a mass sink).

As the flow through the strainer relative to the flow through the core increases, increasing amounts of the entrained fiber recirculates back to the pool and through the (inefficient) strainer removing the debris according to the percentage f^*. So it follows that increasing the strainer flow rates will always increase the relative amount of debris caught by the strainer. For practical cases of the FIDOE model, increasing ECCS flow increases the filtration rate while reducing the concentration in the pool, both of which reduce the amount of debris that reaches the core.

This behavior can also be deduced from the FIDOE equations as well. In equations (1), $\frac{d}{dt}M_s^k$ is proportional to the strainer flow. Higher flow rates mean higher $\frac{d}{dt}M_s^k$, which in turn means $M_p(t)$ and thus $C_p(t)$ are reduced at a greater rate. In (1b), $\frac{d}{dt}M_c$ is proportional to $C_p(t)$, which (as discussed above) is reduced under higher strainer flow rates. Higher strainer flow rates yield lower rates of core fiber penetration – even with a constant filtration rate.

7 Weld list

In the following, tables summarize the amounts of transported fiber fines for the STP scenarios (Munoz, 2016) in the RoverD assessment. The tested amount of fine fiber is used as the success/fail criteria; other sources of debris have been shown to be bounded by the test (Alion, 2016). Table 13 summarizes the STP RoverD risk-informed scenarios. The total number of welds in each category of pipe size intervals is required (Figure 10, Page 29). The counts of welds are summarized in Table 12. For these scenarios, the minimum amount of fiber (the amount associated with smallest D_i) at each location is listed in the D_i^{small} fines (lbm) column. In determining the smallest break that fails at each location, a systematic sampling methodology with a break size resolution of 0.01 inches and an angular resolution of one degree is used. In other words, for each critical weld location, we sampled 360 jet directions at a break size 0.01 inches smaller than the reported smallest break size and did not find a break that exceeded the threshold. By utilizing this systematic sampling method with high break size and angular resolution, we know that we have found the smallest break that fails at each of the critical weld locations to within a 0.01 inch tolerance.

Table 14 summarizes the amount of transported fiber produced for all STP weld locations in the analysis at the DEGB size. The amounts of debris and the DEGB break sizes are shown.

Table 12: The number of welds (Number) for each nominal pipe size (Size) listed with the inside diameter (ID) of the pipe and the stainless steel pipe schedule or forged non-standard (type). The total number of welds is in each category n is used for the top-down weld counts (TW_n) in (4).

ID	Number	Size	Type
0.612	32	0.75	Sch. 160
0.815	3	1	Sch. 160
1.338	9	1.5	Sch. 160
1.687	85	2	Sch. 160
2.125	6	2.5	Sch. 160
2.624	26	3	Sch. 160
3.438	90	4	Sch. 160
5.187	88	6	Sch. 160
6.813	54	8	Sch. 160

continued next page ...

...Table 12 continued

ID	Number	Size	Type
8.5	30	10	Sch. 160
10.126	131	12	Sch. 160
12.814	10	16	Sch. 160
27.5	16	27.5	Spool/forged
29	20	29	Spool/forged
31	28	31	Spool/forged
Total	628		

Table 13: Data for weld locations in the risk-informed category (exceeding 191.78lbm as tested in AREVA, 2008, pages 29 and 30, Tables 6.1 and 6.2 scaled to 40 modules) listing the i^{th} weld number (No. ordered by increasing D_i^{small}), location name (ID), break size (D_i^{small}), amount of fiber fines at D_i^{small} (D_i^{small} fines), and the difference in mass of fiber fines at D_i^{small} to the mass at DEGB (additional to DEGB), the additional amount of fiber that would be released above that for the smallest break if the pipe instead suffered a DEGB – see Table 14 starting on page 43 for fiber fines mass at the DEGB break size).

No.	Location	D_i^{small} (in)	D_i^{small} fines (lbm)	Additional to DEGB (lbm)
1	16-RC-1412-NSS-8	12.814	226.647	0.000
2	29-RC-1401-NSS-3	13.980	191.895	555.429
3	29-RC-1101-NSS-4	14.170	191.912	600.320
4	29-RC-1201-NSS-4	14.400	191.834	598.519
5	29-RC-1301-NSS-4	14.410	191.780	577.392
6	31-RC-1302-NSS-RSG-1C-ON-SE	14.780	191.853	606.644
7	29-RC-1101-NSS-RSG-1A-IN-SE	15.070	191.924	631.539
8	29-RC-1101-NSS-5.1	15.080	191.864	631.172
9	29-RC-1401-NSS-RSG-1D-IN-SE	15.100	191.793	587.735
10	29-RC-1401-NSS-4.1	15.110	191.813	587.364
11	31-RC-1102-NSS-1.1	15.240	191.813	641.923
12	31-RC-1102-NSS-RSG-1A-ON-SE	15.240	191.840	642.006
13	29-RC-1201-RSG-1B-IN-SE	15.330	191.831	631.676
14	29-RC-1201-NSS-5.1	15.350	191.972	631.193
15	29-RC-1301-RSG-1C-IN-SE	15.350	191.939	609.793
16	31-RC-1202-NSS-1.1	15.350	191.796	638.803
17	31-RC-1202-NSS-RSG-1B-ON-SE	15.350	191.840	638.818
18	29-RC-1301-NSS-5.1	15.360	191.946	609.653
19	31-RC-1202-NSS-4	15.540	191.785	405.956
20	31-RC-1202-NSS-2	15.580	191.836	586.085
21	31-RC-1102-NSS-2	15.630	191.897	587.257
22	31-RC-1302-NSS-2	15.630	191.811	555.337
23	31-RC-1302-NSS-1.1	15.700	191.804	606.693
24	31-RC-1102-NSS-4	15.710	191.792	400.542
25	31-RC-1302-NSS-4	15.920	191.780	372.946
26	29-RC-1101-NSS-1[a]	15.950[a]	58.768[a]	121.503[a]
27	29-RC-1101-NSS-RPV1-N1ASE[a]	15.950[a]	58.995[a]	122.336[a]
28	29-RC-1201-NSS-1[a]	15.950[a]	58.614[a]	123.875[a]
29	29-RC-1201-RPV1-N1BSE[a]	15.950[a]	58.989[a]	126.705[a]

continued next page ...

... Table 13 continued

No.	Location	D_i^{small} (in)	D_i^{small} fines (lbm)	Additional to DEGB (lbm)
30	29-RC-1301-NSS-1[a]	15.950[a]	58.901[a]	122.474[a]
31	29-RC-1301-RPV1-N1CSE[a]	15.950[a]	59.273[a]	125.573[a]
32	29-RC-1401-NSS-1[a]	15.950[a]	59.904[a]	121.310[a]
33	29-RC-1401-NSS-RPV1-N1DSE[a]	15.950[a]	60.189[a]	124.323[a]
34	31-RC-1402-NSS-2	15.990	191.788	519.675
35	31-RC-1402-NSS-RSG-1D-ON-SE	16.490	191.784	575.481
36	31-RC-1402-NSS-1.1	16.500	191.802	575.409
37	27.5-RC-1203-NSS-1	16.620	191.870	325.198
38	27.5-RC-1303-NSS-1	16.620	191.921	282.567
39	27.5-RC-1103-NSS-1	16.650	191.861	333.573
40	31-RC-1202-NSS-8	16.840	191.803	332.013
41	31-RC-1102-NSS-8	17.130	191.789	332.508
42	31-RC-1402-NSS-4	17.480	191.819	331.536
43	31-RC-1302-NSS-8	17.750	191.797	293.212
44	31-RC-1102-NSS-3	17.760	191.830	493.337
45	31-RC-1202-NSS-3	17.820	191.921	495.845
46	31-RC-1102-NSS-9	18.100	191.794	339.628
47	31-RC-1202-NSS-9	18.110	191.883	334.215
48	31-RC-1302-NSS-3	18.140	191.833	469.147
49	27.5-RC-1403-NSS-1	18.150	191.785	251.899
50	31-RC-1302-NSS-9	18.570	191.818	286.977
51	31-RC-1402-NSS-3	19.020	191.877	426.971
52	31-RC-1402-NSS-8	19.690	191.826	253.842
53	31-RC-1402-NSS-9	20.500	191.923	247.299

[a] These locations are RV nozzzle HLB locations with assumed D_i^{small} of 16 inches. The DEGB at these locations produces less than the tested amount.

Table 14: DEGB data (largest break size) for all weld locations showing the number (No.) in order of increasing pipe ID, location ID (Location), break size (DEGB size (in)), and the fiber fines amount (Fiber fines (lbm))

No.	Location	DEGB size (in)	Fiber fines (lbm)
1	0.75-CV-1122-BB1-1	0.614	28.547
2	0.75-CV-1122-BB1-2	0.614	28.548
3	0.75-CV-1124-BB1-1	0.614	28.500
4	0.75-CV-1124-BB1-2	0.614	28.500
5	0.75-CV-1126-BB1-1	0.614	28.500
6	0.75-CV-1126-BB1-2	0.614	28.683
7	0.75-CV-1128-BB1-1	0.614	28.500
8	0.75-CV-1128-BB1-2	0.614	28.500
9	0.75-RC-1001-BB1-1	0.614	28.738
10	0.75-RC-1002-BB2-1	0.614	28.785
11	0.75-RC-1112-BB1-1	0.614	28.787
12	0.75-RC-1114-BB1-1	0.614	28.937
13	0.75-RC-1125-BB1-1	0.614	28.783

continued next page ...

... Table 14 continued

No.	Location	DEGB size (in)	Fiber (lbm)	fines
14	0.75-RC-1125-BB1-2	0.614	28.874	
15	0.75-RC-1126-BB1-1	0.614	28.851	
16	0.75-RC-1212-BB1-1	0.614	28.841	
17	0.75-RC-1214-BB1-1	0.614	28.882	
18	0.75-RC-1221-BB1-1	0.614	28.787	
19	0.75-RC-1221-BB1-2	0.614	28.794	
20	0.75-RC-1312-BB1-1	0.614	28.831	
21	0.75-RC-1324-BB1-1	0.614	28.932	
22	0.75-RC-1423-BB1-1	0.614	29.031	
23	0.75-SI-1130-BB2-1	0.614	28.753	
24	0.75-SI-1132-BB1-1	0.614	28.653	
25	0.75-SI-1218-BB1-1	0.614	28.677	
26	0.75-SI-1223-BB2-1	0.614	28.738	
27	0.75-SI-1315-BB1-1	0.614	28.875	
28	0.75-SI-1323-BB1-1	0.614	28.671	
29	0.75-SI-1327-BB1-1	0.614	28.706	
30	0.75-SI-1327-BB1-2	0.614	28.702	
31	0.75-SI-1327-BB1-3	0.614	28.689	
32	0.75-SI-1328-BB2-1	0.614	28.739	
33	1-RC-1003-BB1-1	0.815	29.280	
34	1-RC-1123-BB1-1	0.815	28.858	
35	1-RC-1422-BB1-1	0.815	29.161	
36	1.5-RC-1412-NSS-1	1.338	30.358	
37	2(1.5)-CV-1122-BB1-1	1.338	28.579	
38	2(1.5)-CV-1122-BB1-2	1.338	28.750	
39	2(1.5)-CV-1124-BB1-1	1.338	28.572	
40	2(1.5)-CV-1124-BB1-2	1.338	28.870	
41	2(1.5)-CV-1126-BB1-1	1.338	29.079	
42	2(1.5)-CV-1126-BB1-2	1.338	29.071	
43	2(1.5)-CV-1128-BB1-1	1.338	28.754	
44	2(1.5)-CV-1128-BB1-2	1.338	29.025	
45	2-CV-1121-BB1-1	1.689	28.760	
46	2-CV-1121-BB1-2	1.689	29.028	
47	2-CV-1121-BB1-3	1.689	29.267	
48	2-CV-1122-BB1-1	1.689	29.420	
49	2-CV-1122-BB1-2	1.689	29.353	
50	2-CV-1122-BB1-3	1.689	29.276	
51	2-CV-1122-BB1-4	1.689	29.252	
52	2-CV-1122-BB1-5	1.689	29.319	
53	2-CV-1122-BB1-6	1.689	28.950	
54	2-CV-1124-BB1-1	1.689	29.263	
55	2-CV-1124-BB1-2	1.689	29.288	
56	2-CV-1124-BB1-3	1.689	29.289	
57	2-CV-1124-BB1-4	1.689	29.406	
58	2-CV-1124-BB1-5	1.689	29.501	
59	2-CV-1124-BB1-6	1.689	29.449	

continued next page ...

... Table 14 continued

No.	Location	DEGB size (in)	Fiber (lbm)	fines
60	2-CV-1124-BB1-7	1.689	29.295	
61	2-CV-1124-BB1-8	1.689	29.279	
62	2-CV-1124-BB1-9	1.689	29.340	
63	2-CV-1124-BB1-10	1.689	29.378	
64	2-CV-1124-BB1-11	1.689	29.339	
65	2-CV-1124-BB1-12	1.689	28.860	
66	2-CV-1124-BB1-13	1.689	28.892	
67	2-CV-1126-BB1-1	1.689	28.735	
68	2-CV-1126-BB1-2	1.689	28.790	
69	2-CV-1126-BB1-3	1.689	28.843	
70	2-CV-1126-BB1-4	1.689	28.879	
71	2-CV-1126-BB1-5	1.689	28.871	
72	2-CV-1126-BB1-6	1.689	28.898	
73	2-CV-1126-BB1-7	1.689	29.002	
74	2-CV-1126-BB1-8	1.689	29.988	
75	2-CV-1126-BB1-9	1.689	30.098	
76	2-CV-1126-BB1-10	1.689	29.431	
77	2-CV-1126-BB1-11	1.689	29.361	
78	2-CV-1128-BB1-1	1.689	28.513	
79	2-CV-1128-BB1-2	1.689	28.671	
80	2-CV-1128-BB1-3	1.689	28.766	
81	2-CV-1128-BB1-3A	1.689	28.825	
82	2-CV-1128-BB1-3B	1.689	28.867	
83	2-CV-1128-BB1-4	1.689	28.864	
84	2-CV-1128-BB1-5	1.689	28.871	
85	2-CV-1128-BB1-6	1.689	28.846	
86	2-CV-1128-BB1-7	1.689	28.963	
87	2-CV-1141-BB1-1	1.689	29.057	
88	2-CV-1141-BB1-2	1.689	28.864	
89	2-RC-1003-BB1-1	1.689	29.267	
90	2-RC-1003-BB1-2	1.689	29.721	
91	2-RC-1120-BB1-1	1.689	29.930	
92	2-RC-1120-BB1-2	1.689	29.621	
93	2-RC-1121-BB1-1	1.689	30.393	
94	2-RC-1121-BB1-2	1.689	29.112	
95	2-RC-1121-BB1-3	1.689	29.142	
96	2-RC-1121-BB1-3A	1.689	29.121	
97	2-RC-1121-BB1-3B	1.689	29.033	
98	2-RC-1121-BB1-4	1.689	28.958	
99	2-RC-1219-BB1-1	1.689	29.885	
100	2-RC-1219-BB1-2	1.689	29.740	
101	2-RC-1220-BB1-1	1.689	30.279	
102	2-RC-1220-BB1-2	1.689	29.049	
103	2-RC-1220-BB1-3	1.689	29.007	
104	2-RC-1220-BB1-4	1.689	28.922	
105	2-RC-1319-BB1-1	1.689	30.081	

continued next page ...

... Table 14 continued

No.	Location	DEGB size (in)	Fiber (lbm)	fines
106	2-RC-1319-BB1-2	1.689	29.639	
107	2-RC-1321-BB1-1	1.689	29.764	
108	2-RC-1321-BB1-4	1.689	29.692	
109	2-RC-1321-BB1-5	1.689	29.818	
110	2-RC-1321-BB1-6	1.689	29.782	
111	2-RC-1417-BB1-1	1.689	29.870	
112	2-RC-1417-BB1-2	1.689	29.796	
113	2-RC-1418-BB1-1	1.689	30.289	
114	2-RC-1418-BB1-2	1.689	29.712	
115	2-RC-1418-BB1-3	1.689	29.627	
116	2-RC-1418-BB1-4	1.689	29.567	
117	2-RC-1418-BB1-5	1.689	29.413	
118	2-RC-1418-BB1-6	1.689	29.228	
119	2-RC-1419-BB1-1	1.689	29.556	
120	2-RC-1419-BB1-2	1.689	29.326	
121	2-RC-1419-BB1-3	1.689	29.355	
122	2-RC-1419-BB1-4	1.689	29.071	
123	2.5-RC-1003-BB1-1	2.125	30.874	
124	2.5-RC-1003-BB1-2	2.125	30.713	
125	2.5-RC-1003-BB1-3	2.125	30.557	
126	2.5-RC-1003-BB1-4	2.125	30.650	
127	2.5-RC-1003-BB1-5	2.125	30.597	
128	2.5-RC-1003-BB1-6	2.125	30.597	
129	3-RC-1003-BB1-1	2.626	31.493	
130	3-RC-1003-BB1-2	2.626	31.429	
131	3-RC-1015-NSS-1	2.626	30.838	
132	3-RC-1015-NSS-2	2.626	30.583	
133	3-RC-1015-NSS-3	2.626	30.327	
134	3-RC-1015-NSS-4	2.626	29.680	
135	3-RC-1015-NSS-5	2.626	29.133	
136	3-RC-1015-NSS-6	2.626	28.573	
137	3-RC-1015-NSS-7	2.626	28.500	
138	3-RC-1015-NSS-8	2.626	28.500	
139	3-RC-1015-NSS-9	2.626	31.390	
140	3-RC-1015-NSS-10	2.626	31.385	
141	3-RC-1015-NSS-11	2.626	31.305	
142	3-RC-1015-NSS-12	2.626	30.662	
143	3-RC-1015-NSS-13	2.626	29.874	
144	3-RC-1015-NSS-14	2.626	28.753	
145	3-RC-1015-NSS-15	2.626	28.649	
146	3-RC-1015-NSS-16	2.626	29.846	
147	3-RC-1106-BB1-25	2.626	32.478	
148	3-RC-1206-BB1-28	2.626	32.414	
149	3-RC-1306-BB1-28	2.626	32.435	
150	3-RC-1406-BB1-25	2.626	32.372	
151	4-CV-1001-BB1-1	3.438	31.276	

continued next page ...

... Table 14 continued

No.	Location	DEGB size (in)	Fiber (lbm)	fines
152	4-CV-1001-BB1-2	3.438	30.367	
153	4-CV-1118-BB1-1	3.438	29.783	
154	4-CV-1118-BB1-2	3.438	30.897	
155	4-CV-1120-BB1-1	3.438	32.714	
156	4-CV-1120-BB1-2	3.438	33.193	
157	4-RC-1000-BB1-1	3.438	35.211	
158	4-RC-1000-BB1-2	3.438	34.358	
159	4-RC-1000-BB1-3	3.438	34.286	
160	4-RC-1000-BB1-4	3.438	32.911	
161	4-RC-1000-BB1-5	3.438	32.728	
162	4-RC-1000-BB1-6	3.438	32.912	
163	4-RC-1000-BB1-7	3.438	33.161	
164	4-RC-1000-BB1-8	3.438	34.234	
165	4-RC-1003-BB1-1	3.438	34.139	
166	4-RC-1003-BB1-2	3.438	33.867	
167	4-RC-1003-BB1-3	3.438	33.771	
168	4-RC-1003-BB1-4	3.438	34.107	
169	4-RC-1123-BB1-1	3.438	38.063	
170	4-RC-1123-BB1-2	3.438	30.377	
171	4-RC-1123-BB1-3	3.438	30.327	
172	4-RC-1123-BB1-4	3.438	30.312	
173	4-RC-1123-BB1-5	3.438	30.201	
174	4-RC-1123-BB1-6	3.438	30.235	
175	4-RC-1123-BB1-7	3.438	30.299	
176	4-RC-1123-BB1-8	3.438	30.297	
177	4-RC-1123-BB1-9	3.438	31.905	
178	4-RC-1123-BB1-10	3.438	31.713	
179	4-RC-1123-BB1-11	3.438	30.814	
180	4-RC-1123-BB1-12	3.438	30.486	
181	4-RC-1123-BB1-13	3.438	30.514	
182	4-RC-1123-BB1-14	3.438	30.006	
183	4-RC-1123-BB1-15	3.438	29.914	
184	4-RC-1123-BB1-16	3.438	32.370	
185	4-RC-1123-BB1-17	3.438	33.463	
186	4-RC-1123-BB1-18	3.438	35.976	
187	4-RC-1123-BB1-19	3.438	35.960	
188	4-RC-1123-BB1-20	3.438	35.490	
189	4-RC-1126-BB1-1	3.438	31.283	
190	4-RC-1126-BB1-2	3.438	32.136	
191	4-RC-1126-BB1-3	3.438	32.358	
192	4-RC-1126-BB1-4	3.438	32.461	
193	4-RC-1126-BB1-5	3.438	33.032	
194	4-RC-1126-BB1-6	3.438	36.398	
195	4-RC-1320-BB1-1	3.438	36.951	
196	4-RC-1320-BB1-2	3.438	36.417	
197	4-RC-1320-BB1-3	3.438	35.741	

continued next page ...

... Table 14 continued

No.	Location	DEGB size (in)	Fiber (lbm)	fines
198	4-RC-1320-BB1-4	3.438	33.707	
199	4-RC-1320-BB1-5	3.438	33.170	
200	4-RC-1320-BB1-6	3.438	33.152	
201	4-RC-1320-BB1-7	3.438	32.820	
202	4-RC-1320-BB1-8	3.438	32.755	
203	4-RC-1320-BB1-9	3.438	32.081	
204	4-RC-1320-BB1-10	3.438	31.748	
205	4-RC-1320-BB1-11	3.438	31.609	
206	4-RC-1320-BB1-12	3.438	31.728	
207	4-RC-1323-BB1-1	3.438	31.940	
208	4-RC-1323-BB1-2	3.438	31.544	
209	4-RC-1323-BB1-3	3.438	30.880	
210	4-RC-1323-BB1-4	3.438	35.778	
211	4-RC-1420-BB1-1	3.438	36.314	
212	4-RC-1422-BB1-1	3.438	36.536	
213	4-RC-1422-BB1-2	3.438	35.712	
214	4-RC-1422-BB1-3	3.438	34.772	
215	4-RC-1422-BB1-4	3.438	35.411	
216	4-RC-1422-BB1-5	3.438	34.782	
217	4-RC-1422-BB1-6	3.438	30.629	
218	4-RC-1422-BB1-7	3.438	30.634	
219	4-RC-1422-BB1-8	3.438	30.640	
220	4-RC-1422-BB1-9	3.438	30.696	
221	4-RC-1422-BB1-10	3.438	30.336	
222	4-RC-1422-BB1-11	3.438	30.342	
223	4-RC-1422-BB1-12	3.438	32.327	
224	4-RC-1422-BB1-13	3.438	32.107	
225	4-RC-1422-BB1-14	3.438	31.766	
226	4-RC-1422-BB1-15	3.438	30.969	
227	4-RC-1422-BB1-16	3.438	30.343	
228	4-RC-1422-BB1-17	3.438	30.174	
229	4-RC-1422-BB1-18	3.438	30.046	
230	4-RC-1422-BB1-19	3.438	29.823	
231	4-RC-1422-BB1-20	3.438	30.231	
232	4-RC-1422-BB1-21	3.438	33.360	
233	4-RC-1422-BB1-22	3.438	34.051	
234	4-RC-1422-BB1-23	3.438	34.222	
235	6-RC-1003-BB1-1	5.189	45.741	
236	6-RC-1003-BB1-2	5.189	45.669	
237	6-RC-1003-BB1-3	5.189	45.660	
238	6-RC-1003-BB1-4	5.189	45.072	
239	6-RC-1003-BB1-5	5.189	44.692	
240	6-RC-1003-BB1-6	5.189	43.951	
241	6-RC-1003-BB1-7	5.189	45.801	
242	6-RC-1003-BB1-8	5.189	49.976	
243	6-RC-1003-BB1-9	5.189	50.316	

continued next page ...

...Table 14 continued

No.	Location	DEGB size (in)	Fiber (lbm)	fines
244	6-RC-1003-BB1-9A	5.189	49.960	
245	6-RC-1003-BB1-9B	5.189	49.872	
246	6-RC-1003-BB1-10	5.189	42.910	
247	6-RC-1003-BB1-11	5.189	43.201	
248	6-RC-1003-BB1-11A	5.189	46.025	
249	6-RC-1003-BB1-11B	5.189	47.853	
250	6-RC-1003-BB1-12	5.189	51.449	
251	6-RC-1003-BB1-13	5.189	55.795	
252	6-RC-1003-BB1-13A	5.189	61.362	
253	6-RC-1003-BB1-14	5.189	65.840	
254	6-RC-1003-BB1-PRZ-1-N2-SE	5.189	65.697	
255	6-RC-1004-NSS-1	5.189	57.542	
256	6-RC-1004-NSS-2	5.189	55.426	
257	6-RC-1004-NSS-3	5.189	51.471	
258	6-RC-1004-NSS-4	5.189	56.858	
259	6-RC-1004-NSS-5	5.189	58.173	
260	6-RC-1004-NSS-6	5.189	50.631	
261	6-RC-1004-NSS-7	5.189	48.061	
262	6-RC-1004-NSS-PRZ-1-N3-SE	5.189	57.542	
263	6-RC-1009-NSS-1	5.189	60.037	
264	6-RC-1009-NSS-2	5.189	58.272	
265	6-RC-1009-NSS-3	5.189	53.355	
266	6-RC-1009-NSS-4	5.189	57.798	
267	6-RC-1009-NSS-5	5.189	61.057	
268	6-RC-1009-NSS-6	5.189	62.192	
269	6-RC-1009-NSS-7	5.189	60.528	
270	6-RC-1009-NSS-8	5.189	57.181	
271	6-RC-1009-NSS-9	5.189	54.230	
272	6-RC-1009-NSS-PRZ-1-N4C-SE	5.189	59.909	
273	6-RC-1012-NSS-1	5.189	63.538	
274	6-RC-1012-NSS-2	5.189	61.962	
275	6-RC-1012-NSS-3	5.189	60.969	
276	6-RC-1012-NSS-4	5.189	60.774	
277	6-RC-1012-NSS-5	5.189	57.736	
278	6-RC-1012-NSS-6	5.189	56.869	
279	6-RC-1012-NSS-7	5.189	55.313	
280	6-RC-1012-NSS-8	5.189	55.794	
281	6-RC-1012-NSS-9	5.189	58.640	
282	6-RC-1012-NSS-10	5.189	55.158	
283	6-RC-1012-NSS-11	5.189	54.561	
284	6-RC-1012-NSS-PRZ-1-N4B-SE	5.189	63.633	
285	6-RC-1015-NSS-1	5.189	62.593	
286	6-RC-1015-NSS-2	5.189	60.658	
287	6-RC-1015-NSS-3	5.189	59.156	
288	6-RC-1015-NSS-4	5.189	60.633	
289	6-RC-1015-NSS-5	5.189	63.025	

continued next page ...

... Table 14 continued

No.	Location	DEGB size (in)	Fiber (lbm)	fines
290	6-RC-1015-NSS-6	5.189	63.800	
291	6-RC-1015-NSS-7	5.189	63.965	
292	6-RC-1015-NSS-8	5.189	60.651	
293	6-RC-1015-NSS-9	5.189	58.022	
294	6-RC-1015-NSS-10	5.189	54.467	
295	6-RC-1015-NSS-11	5.189	42.368	
296	6-RC-1015-NSS-12	5.189	40.157	
297	6-RC-1015-NSS-13	5.189	39.826	
298	6-RC-1015-NSS-14	5.189	41.025	
299	6-RC-1015-NSS-15	5.189	41.074	
300	6-SI-1108-BB1-1	5.189	29.044	
301	6-SI-1108-BB1-2	5.189	29.060	
302	6-SI-1108-BB1-3	5.189	29.280	
303	6-SI-1108-BB1-4	5.189	38.063	
304	6-SI-1111-BB1-1	5.189	32.208	
305	6-SI-1111-BB1-2	5.189	32.053	
306	6-SI-1208-BB1-1	5.189	29.034	
307	6-SI-1208-BB1-2	5.189	29.046	
308	6-SI-1208-BB1-3	5.189	29.279	
309	6-SI-1208-BB1-4	5.189	36.640	
310	6-SI-1211-BB1-1	5.189	31.222	
311	6-SI-1211-BB1-2	5.189	31.240	
312	6-SI-1308-BB1-1	5.189	32.163	
313	6-SI-1308-BB1-2	5.189	30.555	
314	6-SI-1308-BB1-3	5.189	30.600	
315	6-SI-1308-BB1-4	5.189	31.073	
316	6-SI-1327-BB1-1	5.189	43.600	
317	6-SI-1327-BB1-2	5.189	42.996	
318	6-SI-1327-BB1-3	5.189	42.830	
319	6-SI-1327-BB1-4	5.189	43.462	
320	6-SI-1327-BB1-5	5.189	42.548	
321	6-SI-1327-BB1-6	5.189	41.844	
322	6-SI-1327-BB1-7	5.189	40.814	
323	8-RC-1114-BB1-1	6.813	51.000	
324	8-RC-1114-BB1-2	6.813	49.482	
325	8-RC-1114-BB1-3	6.813	51.252	
326	8-RC-1114-BB1-4	6.813	54.400	
327	8-RC-1114-BB1-5	6.813	58.515	
328	8-RC-1114-BB1-6	6.813	62.131	
329	8-RC-1214-BB1-1	6.813	51.380	
330	8-RC-1214-BB1-2	6.813	49.952	
331	8-RC-1214-BB1-3	6.813	51.507	
332	8-RC-1214-BB1-4	6.813	54.477	
333	8-RC-1214-BB1-5	6.813	58.116	
334	8-RC-1214-BB1-6	6.813	61.627	
335	8-RC-1324-BB1-1	6.813	53.769	

continued next page ...

...Table 14 continued

No.	Location	DEGB size (in)	Fiber (lbm)	fines
336	8-RC-1324-BB1-2	6.813	52.347	
337	8-RC-1324-BB1-3	6.813	53.423	
338	8-RC-1324-BB1-4	6.813	54.522	
339	8-RC-1324-BB1-5	6.813	58.647	
340	8-RC-1324-BB1-6	6.813	62.424	
341	8-RH-1108-BB1-1	6.813	32.774	
342	8-RH-1108-BB1-2	6.813	33.079	
343	8-RH-1112-BB1-1	6.813	52.660	
344	8-RH-1112-BB1-1A	6.813	51.419	
345	8-RH-1112-BB1-2	6.813	51.227	
346	8-RH-1208-BB1-1	6.813	31.631	
347	8-RH-1208-BB1-2	6.813	31.865	
348	8-RH-1212-BB1-1	6.813	54.017	
349	8-RH-1212-BB1-2	6.813	50.407	
350	8-RH-1308-BB1-1	6.813	39.587	
351	8-RH-1308-BB1-2	6.813	37.465	
352	8-RH-1315-BB1-1	6.813	51.206	
353	8-SI-1108-BB1-1	6.813	45.559	
354	8-SI-1108-BB1-2	6.813	49.112	
355	8-SI-1108-BB1-3	6.813	53.060	
356	8-SI-1108-BB1-4	6.813	55.782	
357	8-SI-1108-BB1-5	6.813	53.245	
358	8-SI-1208-BB1-1	6.813	45.092	
359	8-SI-1208-BB1-2	6.813	47.250	
360	8-SI-1208-BB1-3	6.813	52.724	
361	8-SI-1208-BB1-3A	6.813	55.783	
362	8-SI-1208-BB1-4	6.813	52.880	
363	8-SI-1327-BB1-1	6.813	49.871	
364	8-SI-1327-BB1-2	6.813	49.242	
365	8-SI-1327-BB1-3	6.813	48.957	
366	8-SI-1327-BB1-4	6.813	48.065	
367	8-SI-1327-BB1-5	6.813	46.052	
368	8-SI-1327-BB1-6	6.813	48.058	
369	8-SI-1327-BB1-7	6.813	52.787	
370	8-SI-1327-BB1-8	6.813	58.227	
371	8-SI-1327-BB1-9	6.813	59.661	
372	8-SI-1327-BB1-10	6.813	63.207	
373	8-SI-1327-BB1-11	6.813	57.440	
374	10-RH-1108-BB1-1	8.5	34.959	
375	10-RH-1108-BB1-1A	8.5	35.238	
376	10-RH-1108-BB1-2	8.5	35.316	
377	10-RH-1108-BB1-3	8.5	35.497	
378	10-RH-1108-BB1-4	8.5	35.670	
379	10-RH-1108-BB1-5	8.5	36.078	
380	10-RH-1108-BB1-6	8.5	36.210	
381	10-RH-1108-BB1-7	8.5	37.710	

continued next page ...

...Table 14 continued

No.	Location	DEGB size (in)	Fiber (lbm)	fines
382	10-RH-1108-BB1-8	8.5	52.935	
383	10-RH-1108-BB1-9	8.5	52.678	
384	10-RH-1108-BB1-10	8.5	52.143	
385	10-RH-1208-BB1-1	8.5	33.480	
386	10-RH-1208-BB1-2	8.5	33.759	
387	10-RH-1208-BB1-3	8.5	33.905	
388	10-RH-1208-BB1-4	8.5	34.530	
389	10-RH-1208-BB1-5	8.5	35.017	
390	10-RH-1208-BB1-6	8.5	35.027	
391	10-RH-1208-BB1-7	8.5	36.654	
392	10-RH-1208-BB1-8	8.5	47.727	
393	10-RH-1208-BB1-9	8.5	49.228	
394	10-RH-1208-BB1-10	8.5	49.124	
395	10-RH-1208-BB1-11	8.5	48.140	
396	10-RH-1308-BB1-1	8.5	39.719	
397	10-RH-1308-BB1-2	8.5	32.907	
398	10-RH-1308-BB1-3	8.5	32.857	
399	10-RH-1308-BB1-4	8.5	32.990	
400	10-RH-1308-BB1-5	8.5	33.329	
401	10-RH-1308-BB1-6	8.5	34.702	
402	10-RH-1308-BB1-7	8.5	34.741	
403	10-RH-1308-BB1-8	8.5	35.441	
404	12-RC-1112-BB1-1	10.126	102.659	
405	12-RC-1112-BB1-2	10.126	90.821	
406	12-RC-1112-BB1-3	10.126	83.800	
407	12-RC-1112-BB1-4	10.126	79.435	
408	12-RC-1112-BB1-5	10.126	77.060	
409	12-RC-1112-BB1-6	10.126	80.598	
410	12-RC-1112-BB1-7	10.126	83.210	
411	12-RC-1112-BB1-8	10.126	86.264	
412	12-RC-1112-BB1-9	10.126	76.040	
413	12-RC-1112-BB1-10	10.126	73.238	
414	12-RC-1112-BB1-11	10.126	71.885	
415	12-RC-1125-BB1-1	10.126	55.548	
416	12-RC-1125-BB1-2	10.126	53.877	
417	12-RC-1125-BB1-3	10.126	53.586	
418	12-RC-1125-BB1-4	10.126	53.136	
419	12-RC-1125-BB1-5	10.126	52.489	
420	12-RC-1125-BB1-6	10.126	55.249	
421	12-RC-1125-BB1-7	10.126	56.426	
422	12-RC-1125-BB1-8	10.126	102.699	
423	12-RC-1125-BB1-9	10.126	132.978	
424	12-RC-1125-BB1-10	10.126	137.464	
425	12-RC-1125-BB1-11	10.126	138.713	
426	12-RC-1125-BB1-12	10.126	132.401	
427	12-RC-1125-BB1-13	10.126	105.968	

continued next page ...

... Table 14 continued

No.	Location	DEGB size (in)	Fiber (lbm)	fines
428	12-RC-1212-BB1-1	10.126	97.000	
429	12-RC-1212-BB1-2	10.126	88.122	
430	12-RC-1212-BB1-3	10.126	83.504	
431	12-RC-1212-BB1-4	10.126	77.555	
432	12-RC-1212-BB1-5	10.126	76.024	
433	12-RC-1212-BB1-6	10.126	81.140	
434	12-RC-1212-BB1-7	10.126	83.379	
435	12-RC-1212-BB1-8	10.126	92.525	
436	12-RC-1221-BB1-1	10.126	51.113	
437	12-RC-1221-BB1-2	10.126	49.820	
438	12-RC-1221-BB1-3	10.126	50.452	
439	12-RC-1221-BB1-4	10.126	51.780	
440	12-RC-1221-BB1-5	10.126	52.889	
441	12-RC-1221-BB1-6	10.126	54.268	
442	12-RC-1221-BB1-7	10.126	54.836	
443	12-RC-1221-BB1-8	10.126	97.830	
444	12-RC-1221-BB1-9	10.126	134.012	
445	12-RC-1221-BB1-10	10.126	137.988	
446	12-RC-1221-BB1-11	10.126	147.820	
447	12-RC-1221-BB1-12	10.126	137.750	
448	12-RC-1221-BB1-13	10.126	130.840	
449	12-RC-1221-BB1-14	10.126	102.462	
450	12-RC-1312-BB1-1	10.126	97.760	
451	12-RC-1312-BB1-2	10.126	88.850	
452	12-RC-1312-BB1-3	10.126	84.110	
453	12-RC-1312-BB1-4	10.126	78.031	
454	12-RC-1312-BB1-5	10.126	76.767	
455	12-RC-1312-BB1-6	10.126	81.675	
456	12-RC-1312-BB1-7	10.126	83.691	
457	12-RC-1312-BB1-8	10.126	96.047	
458	12-RC-1312-BB1-9	10.126	83.607	
459	12-RC-1312-BB1-10	10.126	81.759	
460	12-RC-1312-BB1-11	10.126	77.903	
461	12-RC-1322-BB1-1	10.126	140.068	
462	12-RC-1322-BB1-1A	10.126	139.631	
463	12-RC-1322-BB1-2	10.126	134.958	
464	12-RC-1322-BB1-3	10.126	129.669	
465	12-RC-1322-BB1-4	10.126	103.194	
466	12-RH-1101-BB1-1	10.126	72.298	
467	12-RH-1101-BB1-2	10.126	67.516	
468	12-RH-1101-BB1-3	10.126	68.824	
469	12-RH-1101-BB1-3A	10.126	88.258	
470	12-RH-1101-BB1-4	10.126	85.288	
471	12-RH-1101-BB1-5	10.126	75.738	
472	12-RH-1101-BB1-6	10.126	74.751	
473	12-RH-1101-BB1-7	10.126	74.506	

continued next page ...

... Table 14 continued

No.	Location	DEGB size (in)	Fiber (lbm)	fines
474	12-RH-1101-BB1-8	10.126	66.676	
475	12-RH-1101-BB1-9	10.126	45.303	
476	12-RH-1101-BB1-10	10.126	46.307	
477	12-RH-1101-BB1-11	10.126	45.430	
478	12-RH-1101-BB1-12	10.126	41.020	
479	12-RH-1101-BB1-13	10.126	45.229	
480	12-RH-1101-BB1-14	10.126	42.090	
481	12-RH-1101-BB1-15	10.126	41.712	
482	12-RH-1101-BB1-16	10.126	42.817	
483	12-RH-1201-BB1-1	10.126	87.678	
484	12-RH-1201-BB1-2	10.126	82.301	
485	12-RH-1201-BB1-3	10.126	77.973	
486	12-RH-1201-BB1-4	10.126	74.150	
487	12-RH-1201-BB1-5	10.126	74.696	
488	12-RH-1201-BB1-6	10.126	89.970	
489	12-RH-1201-BB1-7	10.126	79.735	
490	12-RH-1201-BB1-8	10.126	78.740	
491	12-RH-1201-BB1-9	10.126	79.421	
492	12-RH-1201-BB1-10	10.126	70.956	
493	12-RH-1201-BB1-11	10.126	48.468	
494	12-RH-1201-BB1-12	10.126	46.867	
495	12-RH-1201-BB1-13	10.126	46.512	
496	12-RH-1201-BB1-14	10.126	42.832	
497	12-RH-1201-BB1-15	10.126	40.054	
498	12-RH-1201-BB1-16	10.126	40.334	
499	12-RH-1201-BB1-17	10.126	40.979	
500	12-RH-1301-BB1-1	10.126	74.021	
501	12-RH-1301-BB1-2	10.126	71.562	
502	12-RH-1301-BB1-3	10.126	71.051	
503	12-RH-1301-BB1-4	10.126	71.681	
504	12-RH-1301-BB1-5	10.126	67.079	
505	12-RH-1301-BB1-5A	10.126	43.772	
506	12-RH-1301-BB1-6	10.126	44.182	
507	12-RH-1301-BB1-7	10.126	45.256	
508	12-RH-1301-BB1-8	10.126	43.455	
509	12-RH-1301-BB1-9	10.126	42.971	
510	12-RH-1301-BB1-10	10.126	43.021	
511	12-SI-1125-BB1-1	10.126	51.120	
512	12-SI-1125-BB1-2	10.126	53.904	
513	12-SI-1125-BB1-3	10.126	54.668	
514	12-SI-1125-BB1-4	10.126	54.762	
515	12-SI-1218-BB1-1	10.126	47.245	
516	12-SI-1218-BB1-2	10.126	49.659	
517	12-SI-1218-BB1-3	10.126	50.548	
518	12-SI-1218-BB1-4	10.126	50.770	
519	12-SI-1315-BB1-1	10.126	35.600	

continued next page ...

...Table 14 continued

No.	Location	DEGB size (in)	Fiber (lbm)	fines
520	12-SI-1315-BB1-2	10.126	36.280	
521	12-SI-1315-BB1-3	10.126	37.962	
522	12-SI-1315-BB1-4	10.126	38.207	
523	12-SI-1315-BB1-5	10.126	38.178	
524	12-SI-1315-BB1-6	10.126	78.837	
525	12-SI-1315-BB1-7	10.126	108.774	
526	12-SI-1315-BB1-8	10.126	120.470	
527	12-SI-1315-BB1-9	10.126	125.120	
528	12-SI-1315-BB1-10	10.126	129.673	
529	16-RC-1412-NSS-1	12.814	100.521	
530	16-RC-1412-NSS-3	12.814	44.074	
531	16-RC-1412-NSS-4	12.814	40.969	
532	16-RC-1412-NSS-5	12.814	122.890	
533	16-RC-1412-NSS-6	12.814	145.632	
534	16-RC-1412-NSS-7	12.814	159.539	
535	16-RC-1412-NSS-8	12.814	226.647	
536	16-RC-1412-NSS-9	12.814	181.076	
537	16-RC-1412-NSS-PRZ-1-N1-SE	12.814	101.594	
538	27.5-RC-1103-NSS-1	27.5	525.433	
539	27.5-RC-1103-NSS-3	3.438	38.798	
540	27.5-RC-1103-NSS-4	10.126	79.463	
541	27.5-RC-1103-NSS-5	3.438	37.000	
542	27.5-RC-1103-NSS-6	27.5	153.815	
543	27.5-RC-1103-NSS-7	27.5	152.923	
544	27.5-RC-1103-NSS-RPV1-N2ASE	27.5	155.883	
545	27.5-RC-1203-NSS-1	27.5	517.067	
546	27.5-RC-1203-NSS-3	10.126	90.523	
547	27.5-RC-1203-NSS-4	27.5	154.662	
548	27.5-RC-1203-NSS-5	27.5	156.057	
549	27.5-RC-1203-NSS-RPV1-N2BSE	27.5	156.890	
550	27.5-RC-1303-NSS-1	27.5	474.488	
551	27.5-RC-1303-NSS-3	10.126	92.823	
552	27.5-RC-1303-NSS-4	3.438	36.276	
553	27.5-RC-1303-NSS-5	27.5	133.504	
554	27.5-RC-1303-NSS-6	27.5	137.616	
555	27.5-RC-1303-NSS-RPV1-N2CSE	27.5	138.302	
556	27.5-RC-1403-NSS-1	27.5	443.685	
557	27.5-RC-1403-NSS-3	3.438	37.325	
558	27.5-RC-1403-NSS-4	3.438	37.113	
559	27.5-RC-1403-NSS-5	27.5	127.450	
560	27.5-RC-1403-NSS-6	27.5	133.732	
561	27.5-RC-1403-NSS-RPV1-N2DSE	27.5	135.049	
562	29-RC-1101-NSS-1	29	180.271	
563	29-RC-1101-NSS-2	6.813	62.906	
564	29-RC-1101-NSS-3	10.126	104.133	
565	29-RC-1101-NSS-4	29	792.232	

continued next page ...

... Table 14 continued

No.	Location	DEGB size (in)	Fiber (lbm)	fines
566	29-RC-1101-NSS-5.1	29	823.036	
567	29-RC-1101-NSS-RPV1-N1ASE	29	181.331	
568	29-RC-1101-NSS-RSG-1A-IN-SE	29	823.463	
569	29-RC-1201-NSS-1	29	182.489	
570	29-RC-1201-NSS-2	6.813	63.233	
571	29-RC-1201-NSS-3	10.126	101.944	
572	29-RC-1201-NSS-4	29	790.353	
573	29-RC-1201-NSS-5.1	29	823.166	
574	29-RC-1201-RPV1-N1BSE	29	185.694	
575	29-RC-1201-RSG-1B-IN-SE	29	823.507	
576	29-RC-1301-NSS-1	29	181.375	
577	29-RC-1301-NSS-2	6.813	64.219	
578	29-RC-1301-NSS-3	10.126	102.019	
579	29-RC-1301-NSS-4	29	769.172	
580	29-RC-1301-NSS-5.1	29	801.599	
581	29-RC-1301-RPV1-N1CSE	29	184.846	
582	29-RC-1301-RSG-1C-IN-SE	29	801.732	
583	29-RC-1401-NSS-1	29	181.214	
584	29-RC-1401-NSS-2	12.814	179.718	
585	29-RC-1401-NSS-3	29	747.324	
586	29-RC-1401-NSS-4.1	29	779.177	
587	29-RC-1401-NSS-RPV1-N1DSE	29	184.512	
588	29-RC-1401-NSS-RSG-1D-IN-SE	29	779.528	
589	31-RC-1102-NSS-1.1	31	833.735	
590	31-RC-1102-NSS-2	31	779.154	
591	31-RC-1102-NSS-3	31	685.167	
592	31-RC-1102-NSS-4	31	592.334	
593	31-RC-1102-NSS-5	1.689	30.136	
594	31-RC-1102-NSS-6	1.689	30.522	
595	31-RC-1102-NSS-7	2.626	33.235	
596	31-RC-1102-NSS-8	31	524.297	
597	31-RC-1102-NSS-9	31	531.422	
598	31-RC-1102-NSS-RSG-1A-ON-SE	31	833.845	
599	31-RC-1202-NSS-1.1	31	830.600	
600	31-RC-1202-NSS-2	31	777.921	
601	31-RC-1202-NSS-3	31	687.766	
602	31-RC-1202-NSS-4	31	597.741	
603	31-RC-1202-NSS-5	1.689	30.153	
604	31-RC-1202-NSS-6	2.626	33.262	
605	31-RC-1202-NSS-7	1.689	30.469	
606	31-RC-1202-NSS-8	31	523.816	
607	31-RC-1202-NSS-9	31	526.097	
608	31-RC-1202-NSS-RSG-1B-ON-SE	31	830.657	
609	31-RC-1302-NSS-1.1	31	798.498	
610	31-RC-1302-NSS-2	31	747.148	
611	31-RC-1302-NSS-3	31	660.980	

continued next page ...

...Table 14 continued

No.	Location	DEGB size (in)	Fiber fines (lbm)
612	31-RC-1302-NSS-4	31	564.726
613	31-RC-1302-NSS-5	1.689	30.177
614	31-RC-1302-NSS-6	2.626	33.197
615	31-RC-1302-NSS-7	3.438	37.318
616	31-RC-1302-NSS-8	31	485.009
617	31-RC-1302-NSS-9	31	478.796
618	31-RC-1302-NSS-RSG-1C-ON-SE	31	798.498
619	31-RC-1402-NSS-1.1	31	767.211
620	31-RC-1402-NSS-2	31	711.463
621	31-RC-1402-NSS-3	31	618.848
622	31-RC-1402-NSS-4	31	523.355
623	31-RC-1402-NSS-5	1.689	30.136
624	31-RC-1402-NSS-6	2.626	33.231
625	31-RC-1402-NSS-7	1.689	30.444
626	31-RC-1402-NSS-8	31	445.668
627	31-RC-1402-NSS-9	31	439.222
628	31-RC-1402-NSS-RSG-1D-ON-SE	31	767.265

Table 15: Single train data for weld locations in the risk-informed category listing the i^{th} weld number (No. ordered by increasing D_i^{small}), location (Break location), break size (D_i^{small} (in)), and mass of fiber in the sump for the scenario (D_i^{small} fines (lbm))

No.	Break location	D_i^{small} (in)	D_i^{small} fines (lbm)
1	16-RC-1412-NSS-8	9.34	95.95
2	31-RC-1102-NSS-1.1	9.56	95.951
3	31-RC-1102-NSS-RSG-1A-ON-SE	9.56	95.904
4	31-RC-1202-NSS-1.1	9.65	95.9
5	31-RC-1202-NSS-RSG-1B-ON-SE	9.65	95.901
6	31-RC-1302-NSS-RSG-1C-ON-SE	9.7	95.968
7	12-RC-1221-BB1-9	9.72	96.009
8	12-RC-1221-BB1-11	9.72	95.906
9	12-RC-1125-BB1-9	9.75	95.892
10	29-RC-1101-NSS-RSG-1A-IN-SE	9.76	95.895
11	29-RC-1101-NSS-5.1	9.78	95.997
12	29-RC-1401-NSS-3	9.81	95.902
13	12-SI-1315-BB1-8	9.84	95.968
14	29-RC-1301-NSS-4	9.84	95.929
15	12-RC-1322-BB1-1	9.9	95.893
16	29-RC-1101-NSS-4	9.9	96.009
17	31-RC-1302-NSS-1.1	9.9	95.982
18	29-RC-1301-NSS-5.1	9.92	95.925
19	29-RC-1301-RSG-1C-IN-SE	9.92	95.945
20	12-RC-1322-BB1-1A	9.93	95.921
21	12-RC-1125-BB1-11	9.94	95.911
22	29-RC-1201-NSS-4	9.94	95.931

continued next page ...

...Table 15 continued

No.	Break location	D_i^{small} (in)	D_i^{small} fines (lbm)
23	29-RC-1201-NSS-5.1	9.99	95.914
24	29-RC-1201-RSG-1B-IN-SE	9.99	95.964
25	31-RC-1202-NSS-2	9.99	95.89
26	12-RC-1125-BB1-10	10.006	95.967
27	12-RC-1221-BB1-12	10.016	95.915
28	29-RC-1401-NSS-RSG-1D-IN-SE	10.03	95.969
29	29-RC-1401-NSS-4.1	10.04	95.921
30	12-RC-1322-BB1-2	10.066	95.893
31	31-RC-1102-NSS-2	10.07	95.964
32	12-RC-1221-BB1-10	10.106	95.933
33	12-RC-1112-BB1-1	10.126	102.659
34	12-RC-1125-BB1-8	10.126	102.699
35	12-RC-1125-BB1-12	10.126	132.401
36	12-RC-1125-BB1-13	10.126	105.968
37	12-RC-1212-BB1-1	10.126	97
38	12-RC-1221-BB1-8	10.126	97.83
39	12-RC-1221-BB1-13	10.126	130.84
40	12-RC-1221-BB1-14	10.126	102.462
41	12-RC-1312-BB1-1	10.126	97.76
42	12-RC-1312-BB1-8	10.126	96.047
43	12-RC-1322-BB1-3	10.126	129.669
44	12-RC-1322-BB1-4	10.126	103.194
45	12-SI-1315-BB1-7	10.126	108.774
46	12-SI-1315-BB1-9	10.126	125.12
47	12-SI-1315-BB1-10	10.126	129.673
48	29-RC-1101-NSS-3	10.126	104.133
49	29-RC-1201-NSS-3	10.126	101.944
50	29-RC-1301-NSS-3	10.126	102.019
51	31-RC-1302-NSS-2	10.14	95.946
52	31-RC-1402-NSS-1.1	10.22	95.963
53	31-RC-1402-NSS-RSG-1D-ON-SE	10.22	95.98
54	16-RC-1412-NSS-7	10.41	95.912
55	31-RC-1402-NSS-2	10.54	95.894
56	16-RC-1412-NSS-9	10.69	95.894
57	29-RC-1401-NSS-2	10.7	95.892
58	16-RC-1412-NSS-6	10.74	95.978
59	31-RC-1202-NSS-8	10.88	95.891
60	27.5-RC-1303-NSS-1	10.91	95.916
61	27.5-RC-1203-NSS-1	10.93	95.947
62	27.5-RC-1103-NSS-1	10.99	96.007
63	31-RC-1202-NSS-4	11	95.915
64	31-RC-1102-NSS-8	11.09	95.906
65	31-RC-1102-NSS-4	11.1	95.999
66	31-RC-1302-NSS-4	11.17	95.915
67	31-RC-1302-NSS-8	11.28	95.971
68	31-RC-1202-NSS-3	11.31	95.921
69	31-RC-1102-NSS-3	11.37	95.895

continued next page ...

...Table 15 continued

No.	Break location	D_i^{small} (in)	D_i^{small} fines (lbm)
70	31-RC-1302-NSS-3	11.38	96.013
71	31-RC-1202-NSS-9	11.48	95.909
72	31-RC-1102-NSS-9	11.49	95.929
73	31-RC-1302-NSS-9	11.67	95.912
74	16-RC-1412-NSS-5	11.96	95.919
75	27.5-RC-1403-NSS-1	12.07	95.904
76	31-RC-1402-NSS-3	12.21	95.945
77	31-RC-1402-NSS-4	12.35	95.984
78	16-RC-1412-NSS-1	12.814	100.521
79	16-RC-1412-NSS-PRZ-1-N1-SE	12.814	101.594
80	31-RC-1402-NSS-8	13.01	95.99
81	31-RC-1402-NSS-9	13.7	95.891
82	29-RC-1401-NSS-1	15.95	59.904
83	29-RC-1301-NSS-1	15.95	58.901
84	29-RC-1401-NSS-RPV1-N1DSE	15.95	60.189
85	29-RC-1301-RPV1-N1CSE	15.95	59.273
86	29-RC-1101-NSS-1	15.95	58.768
87	29-RC-1101-NSS-RPV1-N1ASE	15.95	58.995
88	29-RC-1201-NSS-1	15.95	58.614
89	29-RC-1201-RPV1-N1BSE	15.95	58.989
90	27.5-RC-1103-NSS-RPV1-N2ASE	22.57	95.899
91	27.5-RC-1203-NSS-5	22.61	95.904
92	27.5-RC-1203-NSS-RPV1-N2BSE	22.68	95.894
93	27.5-RC-1203-NSS-4	24.65	95.937
94	27.5-RC-1103-NSS-6	24.94	95.897
95	27.5-RC-1103-NSS-7	25.41	95.891
96	27.5-RC-1303-NSS-RPV1-N2CSE	26.78	95.911
97	27.5-RC-1303-NSS-6	26.82	95.891
98	27.5-RC-1303-NSS-5	27.5	133.504
99	27.5-RC-1403-NSS-5	27.5	127.45
100	27.5-RC-1403-NSS-6	27.5	133.732
101	27.5-RC-1403-NSS-RPV1-N2DSE	27.5	135.049

Acknowledgements and primary contributions

Work presented in this article was developed by YK.risk, LLC, funded by STPNOC contract BO5657, Revision 0 and Revision 1, and by Alion Science and Technology through contract BO4461, Revision 5. Reduction of CASA results was performed by Jeremy Tejada under the direction of John Hasenbein and funded by STPNOC grant BO4425. Development of the strainer mass conservation equations was supported by Alex Zolan under the direction of John Hasenbein and funded by STPNOC grant BO4425, Revision 4. Seyed Reihani contributed to developing the mass conservation equations at UIUC under STPNOC grant BO5270, Revision 3. The top down frequency methodology was originally developed by Elmira Popova at UT Austin, funded by STPNOC grant BO4425, Revision 0. Further development for implementation RoverD was supported by David Johnson and Don Wakefield at ABS Consulting under STPNOC contract BO5760, Revision 1 and Bruce Letellier at Alionscience and Technology under STPNOC contract BO4461, Revision 6. Work contributed by Ernie Kee is funded by STPNOC under YK.risk, LLC contract BO5657, Revision 1.

References

Alion (2016). STP Consolidated Debris Analysis and GSI-191 Risk Assessment. ALION-CAL STP-9277-01 Rev. 0, Alion Science & Technology, Albuquerque, NM.

Alion Science & Technology (2008). GSI-191 Containment Recirculation Sump Evaluation: Debris Generation. ALION-CAL-STPEGS 2916-002, Revision 3, (Reference 5 to STP STI 33647079), Alion Science & Technology, Albuquerque, NM.

Alion Science & Technology (2009). Insulation Debris Size Distribution for Use in GSI-191 Resolution. ALION-REP-ALION 2806-01, Revision 4, ML15091A440, Alion Science & Technology, Albuquerque, NM.

Alion Science & Technology (2011). Erosion Testing of Small Pieces of Low Density Fiberglass Debris – Test Report. ALION-REP-ALION 1006-04, Revision 1, ML14202A045, Alion Science & Technology, Albuquerque, NM.

Alion Science & Technology (2014). Risk-Informed GSI-191 Debris Transport Calculation. ALION-CAL-STP 8511-08, Revision 3, (Reference in ML15091A440), Alion Science & Technology, Albuquerque, NM.

Alion Science & Technology (2015, April). CASA Grande Theory Manual. ALION-SPP ALION-I009-10, STP STI 34179370, Alion Science & Technology, Albuquerque, NM.

AREVA (2008, August). South Texas Project Test Report for ECCS Strainer Testing. AREVA NP Document 66-9088089-000, 0415-010007WN, Rev. A, AREVA NP, 7207 IBM Drive, Charlotte, NC 28262.

Connolly, J. (2016a, May). First Set of Responses to April 11, 2016 Requests for Additional Information Regarding STP Risk-Informed GSI-191 Licensing Application. ML16154A117, Letter from James Connolly to the USNRC Document Control Desk.

Connolly, J. (2016b, July). Third Set of Responses to April 11, 2016 Requests for Additional Information Regarding STP Risk-Informed GSI-191 Licensing Application. ML16209A226, Letter from James Connolly to the USNRC Document Control Desk.

Harrison, A. W. (2015, December 01). Ernie's slides. ML14349A788, Letter from Harrison, Albon to Singal, Balwant.

Hasenbein, J. (2015, May). Order Relations for Concave Interpolation Methods. Technical Report 2015-001, The University of Texas at Austin, Austin, TX.

Hasenbein, J., A. Zolan, and J. Tejada (2015, November). Fiber Diffusion Operations Engine (FiDOE) Software Quality Assurance Documentation. Technical Report, Software Quality Assurance FIDOE15May27, STP STI 34376028, The University of Texas at Austin, Austin, TX.

Howard, C. K. (2015, August). Preparation of Calculations. STP Engineering Procedure.

Johnson, D. (2015, June). PRA Calculations in Support of RoverD White Paper Development. Letter Report STP-338116-O-02, STP STI 34176256, ABSG Consulting Inc., Irvine, CA 92602.

Munoz, D. (2016, September). Transmittal of April 2016 Current Baseline, RoverD Fiber Assessment Results. LTR-DAM 2K16-STP-2 Rev. 1; STP-9277-01; BO4461 Rev. 007, Alion Science & Technology, 6200 Uptown Blvd., Suite 200, Albuquerque, NM 87110, Tel: 505.872.1089 Ext. 15.

NEI (2004, May). Pressurized Water Reactor Sump Performance Evaluation Methodology. Technical Report 04-07, Nuclear Energy Institute, 1776 I Street, Washington, DC.

NRC (2011). Regulatory Guide 1.174: An Approach for Using Probabilistic Risk Assessment In Risk-Informed Decisions On Plant-Specific Changes to the Licensing Basis, Revision 2, Nuclear Regulatory Commission, Washington, DC.

NRC (2012, undated). FINAL SAFETY EVALUATION BY THE OFFICE OF NUCLEAR REACTOR REGULATION TOPICAL REPORT WCAP-16793-NP, REVISION 2 EVALUATION OF LONG-TERM COOLING CONSIDERING PARTICULATE, FIBROUS AND CHEMICAL DEBRIS IN THE RECIRCULATING FLUID, PRESSURIZED WATER REACTOR OWNERS GROUP PROJECT NO. 694. NRC Safety Evaluation.

Ogden, N., D. Morton, and J. Tejada (2013, June). South Texas Project Risk-Informed GSI-191 Evaluation: Filtration as a Function of Debris Mass on the Strainer: Fitting a Parametric Physics-Based Model. Technical report, STP–RIGSI191–V03.06, The University of Texas at Austin, Austin, TX.

Powell, G. (2015a, August 20). Supplement 2 to STP Pilot Submittal and Requests for Exemptions and License Amendment for a Risk-Informed Approach to Address Generic Safety Issue (GSI)-1 91 and Respond to Generic Letter (GL) 2004-02. ML15246A126 , Letter from Gerald T. Powell to the USNRC Document Control Desk.

Powell, G. T. (2013, November 13). Supplement 1 to Revised STP Pilot Submittal for a Risk-Informed Approach to Resolving Generic Safety Issue (GSI)-191 to Supersede and Replace the Revised Pilot Submittal. ML13323A183, Letter from Gerald T. Powell to the USNRC Document Control Desk; STP Letter NOC-AE-13003043.

Powell, G. T. (2015b, March 25). Description of Revised Risk-Informed Methodology and Responses to Round 2 Requests for Additional Information Regarding STP Risk-Informed GSI-191 Licensing Application. ML15091A440, Letter from Gerald T. Powell to the USNRC Document Control Desk, NOC-AE-15003220.

Powell, G. T. (2015c, January). Response to Request for Additional Information re Use of RELAP5 in Analyses for Risk-Informed GSI-191 Licensing Application. ML14009A307, Letter from Gerald T. Powell to the USNRC Document Control Desk.

Powell, G. T. (2016, July). Third Set of Responses to April 11, 2016 Requests for Additional Information Regarding STP Risk-Informed GSl-191 Licensing Application. ML16229A189, Letter from Gerald T. Powell to the USNRC Document Control Desk.

PWROG (2011, October). Evaluation of Long - Term Cooling Considering Particulate, Fibrous and Chemical Debris in the Recirculating Fluid. WCAP 16793, Revision 2, Pressurized Water Reactor Owners Group, Pittsburgh, PA.

Rao, D., C. Shaffer, and E. Haskin (1998, February). Drywell Debris Transport Study. NUREG/CR 6369, USNRC, Washington, DC.

STPNOC (2015, February 4). STP Risk-Informed Approach to GSI-191. ML15034A114, NRC public meeting slides.

TAMU (2016a). Large Hot Leg Break Transient. STP Engineering Calculation 0PGP04-ZG-0307, RC09969, STP STI 34327914, Texas A&M University, Wadsworth, TX.

TAMU (2016b). RELAP5 GSI-191 Medium Hot Leg Break Transient. STP Engineering Calculation 0PGP04-ZG-0307, RC09968, STP STI 34327913, Texas A&M University, Wadsworth, TX.

TAMU (2016c). RELAP5 GSI-191 Small Hot Leg Break Transient. STP Engineering Calculation 0PGP04-ZG-0307, RC09967, STP STI 34327912, Texas A&M University, Wadsworth, TX.

Tregoning, R., L. Abramson, and P. Scott (2008, April). Estimating Loss-of-Coolant Accident (LOCA) Frequencies Through the Elicitation Process. NUREG/CR 1829, Nuclear Regulatory Commission, Washngton, DC.

Zolan, A., J. Hasenbein, and J. Tejada (2016, April). Risk Unifying Frequency Functional (RUFF) Software Quality Assurance Documentation. Technical Report, Software Quality Assurance 2015-003 Rev. 2, STP STI 34375720, The University of Texas at Austin, Austin, TX.

8 Acronyms

BAP	Boric Acid Precipitation
BB	Core Barrel Bypass
CAD	Computer Aided Design
CASA	Containment Accident Stochastic Analysis (CASA) Grande
CDF	Core Damage Frequency
CFD	Computational fluid dynamics
ΔCDF	Change in core damage frequency above a baseline level
ΔLERF	Change in large early release frequency above a baseline level
CLB	Cold Leg Break
CSS	Containment Spray System
DEGB	Double-Ended Guillotine Break
ECCS	Emergency Core Cooling System
FA	Fuel Assembly. Several fuel assemblies are loaded in the reactor vessel to form the reactor core
FIDOE	FIber Diffusion Operations Engine; application that solves fiber mass conservation
GSI-191	Generic Safety Issue 191 - the NRC Generic Safety Issue number 191
HHSI	High Head Safety Injection
HLB	Hot Leg Break
IOZ	Inorganic zinc
LDFG	Low Density Fiberglass (such as NUKON^{TM})
LERF	Large Early Release Frequency
LHSI	Low Head Safety Injection
LLOCA	Large Break Loss of Coolant Accident
LOCA	Loss of Coolant Accident
PRA	Probabilistic Risk Assessment
PWROG	Pressurized Water Reactor Owners Group
RCB	Reactor Containment Building
RCFC	Reactor Containment Fan Coolers
RCP	Reactor Coolant Pump
RCS	Reactor Coolant System
RoverD	Risk-informed Over Deterministic
RUFF	Risk Uncertainty Frequency Function. The application for interpolating NUREG 1829 frequencies
RV	Reactor vessel and reactor core
RWST	Refueling Water Storage Tank
SSO	Sump Switch Over
STP	South Texas Project
STL	stereolithography file format
STPNOC	The STP Nuclear Operating Company
ZOI	Zone of Influence

9 Nomenclature

$C_p(\cdot)$	Concentration of fine fiber in the containment pool
D_i	Break diameter at any weld location
$\mathbb{D}_1$	Inside diameter of the smallest pipe of NP pipes having one or more welds in the risk-informed category
D_i^{small}	Smallest break diameter at any weld location that results in an amount of fine fiber transported to the containment pool exceeding the amount tested (there is no break size smaller that can produce more fines than the D_i^{small} at the corresponding weld)
f_i, f_1, f_2	Generally, f_i is the break frequency corresponding to D_i evaluated from NUREG 1829. f_1, f_2 are separately used to refer to the success frequencies in plant states 1 and 2
f^*	An arbitrary fixed value of strainer filtration efficiency between 0 and 1
$f(\cdot)$	Filtration efficiency. When using the measured data fit in FIDOE, it is dependent on the amount of fiber mass on the strainer
$F(\cdot)$	The frequency of breaks that exceed a criterion at each weld i in the risk-informed category
ϕ_x	Interpolated frequency at x in the data interval, $\{a, b\}$
ϕ_a	Frequency at start of the data interval, $\{a, b\}$
ϕ_b	Frequency at end of the data interval, $\{a, b\}$
$\hat{\Phi}$	The total weighted frequency that includes different plant states
Φ	The overall frequency, evaluated from NUREG 1829 at any particular quantile or mean, with which a criterion is exceeded
γ	Fraction of the CSS flow to the total strainer flow
i	Index of weld locations in the risk-informed category, $i = 1, \ldots, I$
j	Index of categories of pipe ID extents of pipes with welds in the risk-informed category from the smallest to largest pipe ID, $j = 1, \ldots, NP$
k	Index over all the ECCS strainer values in each of the three strainers, $\{A, B, C\}$
λ	Fraction of the total flow entering the RCS that flows through the reactor core
$M_c(\cdot)$	Mass of fine fiber captured on the reactor core
$M_p(\cdot)$	Mass of fine fiber in the containment pool
$M_s(\cdot)$	Mass of fine fiber captured on the strainer

NP	Number of pipe inside diameters corresponding to pipes with one or more welds in the risk-informed category
$Q_s(\cdot)$	Total flow through the strainer
$Q_c(\cdot)$	Total flow through the reactor core
R_n	The set of all welds in the risk-informed category associated with pipes of category n
TW_n	Total number of welds in pipe category, n, $n = 1, \ldots, NP$
V_p	Volume of water in the containment pool
x	Any break size in an evaluation of NUREG 1829 where the exceedance frequency for that size is the NUREG 1829 exceedance frequency

1-4 Resolution of NRC Comments on Responses to Round 3 and 4 RAIs

SNPB Round 3 RAIs:

Follow-up SNPB-3-1 Cladding Oxide

Initial RAI: *Demonstrate that the thickness of the cladding oxide and the deposits of material on the fuel do not exceed 0.050 inches in any fuel region.*

Follow-up question:

In its response, STPNOC referenced an analysis performed by Westinghouse. It is not clear to the NRC staff that the analysis referred to in the RAI response is applicable to STP due to the fiber loading assumed in the analysis. The same referenced analysis also provided a prediction of the peak centerline temperature (PCT) experienced during the long term core cooling phase, but STPNOC determined that the PCT analysis was not applicable due to the amount of debris used in the analysis. If the analysis' prediction of PCT was not applicable to STP, it would follow that the same analysis' prediction of clad oxide thickness would also not be applicable. Explain how the analysis referenced is, in fact, applicable and an appropriate basis to satisfy the initial RAI criteria.

STPNOC Response

Please note that the PCT figure of merit in the STPNOC response referenced in the RAI is "peak clad temperature". The thickness of the cladding oxide and the deposits of material on STP fuel do not exceed 0.050 inches in any fuel region as demonstrated in the STP-specific LOCA DM calculation and in the generic analysis documented in WCAP 16793 (see also starting on page 74 of 77 of ML083520326, STP RAI #31 and 36). The deposit layer thickness for STP fuel is 13.64 mils. The STP-specific analysis conservatively assumed 38.832 lbm of fiber (approximately 91 gm/FA) bypassed the strainers into the RCS however, less than half that amount bypasses the STP strainers in a HLB that is success at the strainer. In both of these analyses it was shown that STP cladding material would have less than 50 mil of deposits.

Additional information

STP further applies the results and assumptions used in the Westinghouse LOCA-DM calculation for assessing PCT under full core and core bypass blockage by assuming the same amount of impedance to heat transfer as assumed in the LOCA-DM analyses. That is, Westinghouse assumes sufficient upward flow through the core and core bypass with heat transfer impeded by the deposits whereas STP assumes the core and core bypass are fully blocked and the core has the same impediment to heat transfer due to deposits. As mentioned above, the level of deposition (and therefore impediment to heat transfer) is conservatively assessed compared to STP RCS fiber quantities. Note that HLB is limiting for core fiber accumulation.

Summary
Both the STP and Westinghouse TH analyses assume a clad thermal resistance due to deposits accumulated on the cladding that is independent on the flow condition. Flow assumptions through the core must be adopted in order to obtain a PCT consistent with the clad thermal conductivity and deposits on the clad (impedance to heat transfer). Westinghouse assumes continued flow up through the core and core bypass. STP assumes the core and core bypass (a more restrictive flow condition) are fully blocked.

Follow-up SNPB-3-2 Accident Scenario Progression

Initial RAI: *Provide a description of the accident progression of the accident scenarios being simulated using the LTCC EM. This description should start at the initiation of the break, define each phase, and the important phenomena occurring in that phase in the various locations of the RCS (e.g., core, reactor vessel, steam generators - both primary and secondary side, loops, pressurizer, pumps, containment)*

Follow-up question:

In their response, STPNOC provided a detailed write-up of the accident scenario, along with a number of plots describing key phenomena. However, the following items need to be addressed in the explanation of the accident progression scenario:

- A basis was not provided for the time delay between sump switchover and full core blockage. STPNOC chose 360 seconds, but did not justify this time period.

STPNOC Response
STP assumes the time to complete blockage of the core and core bypass is when the amount of debris that enters the RCS is equivalent to 15 gm/FA. This is a conservative assumption because, in order to have blocked both the core and the

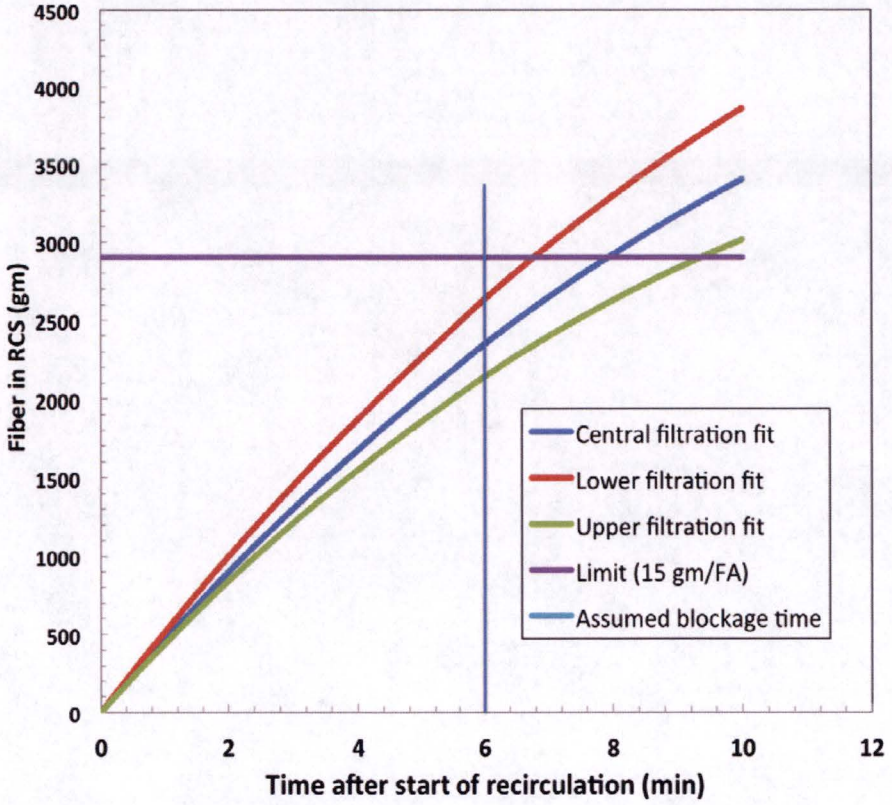

core bypass, much more than 15 gm/FA is required. That is, additional fiber beyond 15 gm/FA would be needed to block the BB bypass, for example. In addition, any fiber not caught in the core or BB bypass would go out the HLB which would result in further reduction in the amount entering the RCS; FiDOE assumes all debris entering the RCS from a HLB is trapped on the core.

The amount of debris entering the RCS required to just reach 15 gm/FA is approximately 2900 gm (15gm/FA X 193FA). FiDOE time histories for design debris amount (approximately 192 lbm) and design train configuration (two trains) for different measured filtration fits (lower, central, and upper) is shown in the figure. As can be seen, 360 seconds (6 min) is a conservatively short time to assume that core and core bypass blockage has occurred due to 15 gm/FA, especially since there would be negligible chemical head loss this early.

- The LTCC EM has a conservation equation for boron density, but STPNOC did not specify whether boron density effects were modeled in the simulation.

STPNOC Response

The STP LTCC EM includes a (mass) conservation equation for boron density however, by use of input, the mass of boron in the system is 0.0. That is, there is no boron assumed in the RCS sources (ECCS flows, CS flows, RWST water, or ECCS Accumulators). Also, no boron mass is entered as an initial condition in the RCS. Therefore, although a mass conservation equation is present, no boron is present, accumulated, or depleted in the STP LTCC EM. Effects of the boron density are not modeled in the simulation.

- The heat stored in the steam generators needs to be appropriately treated to ensure correct flow, as the steam generators become the dominant flow path following full core blockage. Are the levels of auxiliary feedwater used in this analysis consistent with plant procedures following a LOCA? Has all of the secondary metal mass been accounted for the in the simulation? Have the correct material properties been used (e.g., heat capacity of the steam generator tubes)?

STPNOC Response

The approach used in modeling the steam generators (SGs) in the LTCC EM is adequate to the scope of the simulation proposed. The model of the SGs include sufficient details of the primary and secondary fluid regions to simulate the behavior of the reactor system during the LTCC, including the effects of the SG secondary side on the primary coolant flow reaching the top of the core during the Post-Core Blockage LTCC phase.

<u>Geometry.</u>
The detail included in the RELAP5-3D LTCC EM is adequate to conduct the simulation of the proposed accident scenarios (16", 6", and 2" HLB). All the regions of the SG are modeled in the EM including the primary side (U-tubes and metal walls) and secondary side (downcomer, boiler, steam separator, upper dome, MFW, and AFW injection). Description of the SG internal volumes (primary and secondary side) dimensions, assumptions, and nodalization technique is described in the steady-state calculation document RC09989 [1]. In the same document adequate comparison with plant operating conditions is presented to verify the adequateness of the model.

<u>Plant LOCA Operations</u>
The SGs' secondary side boundary conditions used in the LTCC EM are consistent with the plant procedures following a LOCA scenario. In particular:

- MFW flow is isolated based on the primary low-pressure signal
- The MSIV closure is controlled by the reactor trip signal
- The AFW injection start is controlled by the reactor trip signals

- Set points and delays are accounted and aligned with the plant characteristics.
- The AFW thermodynamic conditions are consistent with the plant characteristics
- The AFW flow rate is controlled in order to reach and maintain the liquid level in the SG's secondary side above the U-tubes bundle.

Metal Masses (Passive Structures)
The LTCC EM include heat structures representing the u-tube walls. These heat structures simulate:

- The heat transfer mechanisms (convection, conduction) from the primary coolant to the secondary coolant during normal operation (steady-state)
- The heat transfer mechanisms (convection, conduction) between the primary and secondary coolants during the accident

Masses of the u-tube are modeled in the EM. The material selected for the u-tube represents the STP SG's characteristics. Thermal properties of the material selected (thermal conductivity and heat capacity) are tabulated as function of the temperature in the RELAP5-3D steady-state input file. These thermal properties represent the thermal characteristics of the of the u-tube's walls in the STP plant.

Additional Secondary Side SGs' Metal Masses
Although the LTCC EM does not model metal masses in the SGs' secondary side, a sensitivity study is conducted to demonstrate that the effect of the heat stored in the secondary metal masses on the primary system behavior during the Post-Core Blockage LTCC phase is negligible. The PCT is used as figure of merit in the sensitivity. Assumptions, boundary conditions, modeling and simulation techniques, and results of the sensitivity are described below.

SG Secondary Side Metal Masses Sensitivity
The sensitivity study is conducted to evaluate the effects of the SG secondary metal masses (sensitivity input parameter) on the PCT (figure of merit) during the post-core blockage LTCC phase of a 16" HLB LOCA scenario. The initial conditions for the simulations are the same of the ones produced by the LTCC EM described in the RAI-3-02. The initial conditions are imposed by using the restart feature of RELAP5-3D.
The sensitivity simulation is started at t=2000 s, which corresponds to the first available restart time from the LTCC EM – Base case immediately before the core blockage time (2099 s). The input file of the sensitivity case is expanded to conservatively include heat structures simulating the total dry mass of the SG. The total dry mass of the SG includes the mass of:

- SG pressure shell (including inlet/outlet plena, cylindrical walls, and upper head),
- separators and dryers,
- tube bundle wrapper (shroud)
- tube support plates and tube plate
- U-tubes
- Any other internal structure

The total dry mass of the SG specified in the sensitivity model is equal to 1,045,000 lbm. This mass is equally split between two passive heat structures (SH- X701 and SH-X702) identified in Figure 1.

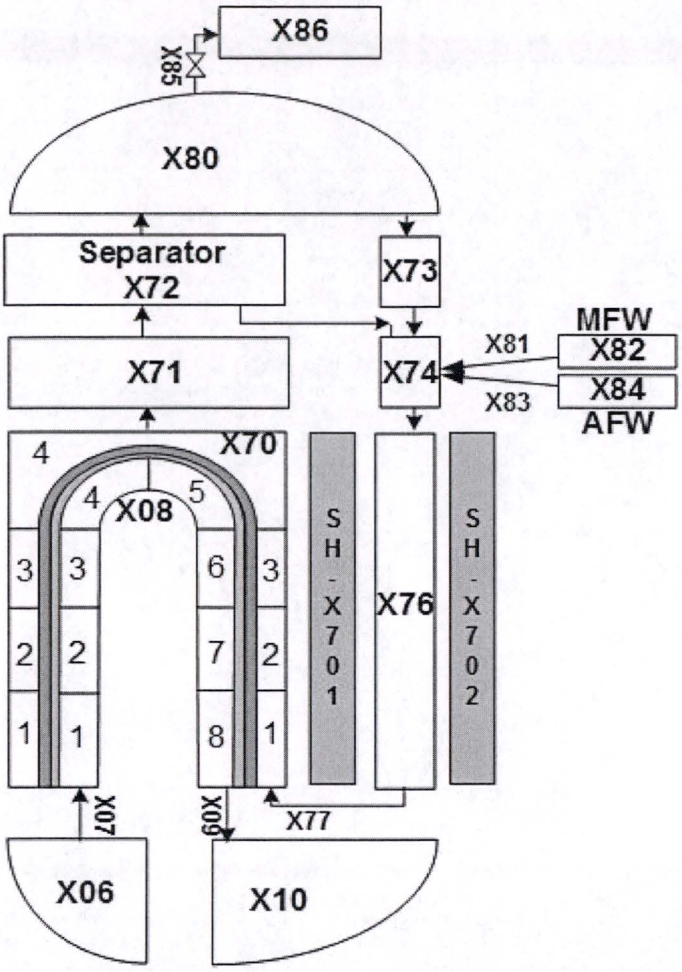

Figure 1. Steam Generator Nodalization and Passive Heat Structures (Sensitivity)

These passive heat structures are assumed in contact only with the lower volumes of the secondary side. This maximizes the heat transfer to the secondary fluid during the LTCC phase, when the liquid level is maintained within this region. SH-X702 is in contact with the hydrodynamic component X76 (simulating the SG downcomer), and isolated on the other side. SH-X701 is in contact with the downcomer (X76) and the boiler (X70) on the left and right sides respectively.

Thermal properties (thermal conductivity and heat capacity) are tabulated as a function of the temperature.

Since the SG U-tubes are simulated with a separate heat structure (see Figure 1, dark profile between X70 and X08), the mass of the U-tubes are accounted twice in the sensitivity model to increase conservatism.

The initial temperatures of the additional heat structures SH-X701 and SH-X702 are conservatively imposed to be equal to the temperature of the secondary side during normal operation.

Simulation Results - PCT

The comparison of the PCT of the LTCC EM and the sensitivity case is shown in Figure 2. PCT is plotted with solid lines. The core coolant saturation temperature is also plotted in the same figure (dotted lines). No major differences are noticeable. The PCT for the two cases is comparable.

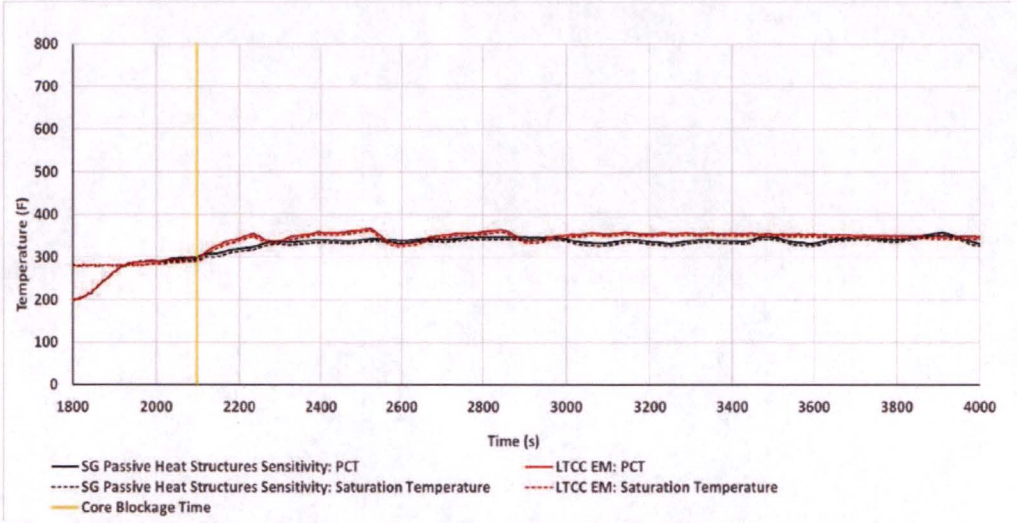

Figure 2. PCT during the Post-Core Blockage LTCC Phase

The secondary fluid average temperature (average of the temperature of the fluid in the nodes of the boiler (X7001-04) is compared in Figure 3. The comparison shows that the average temperature of the secondary side is higher for the sensitivity case due to heat transferred from the metal masses included in the model.

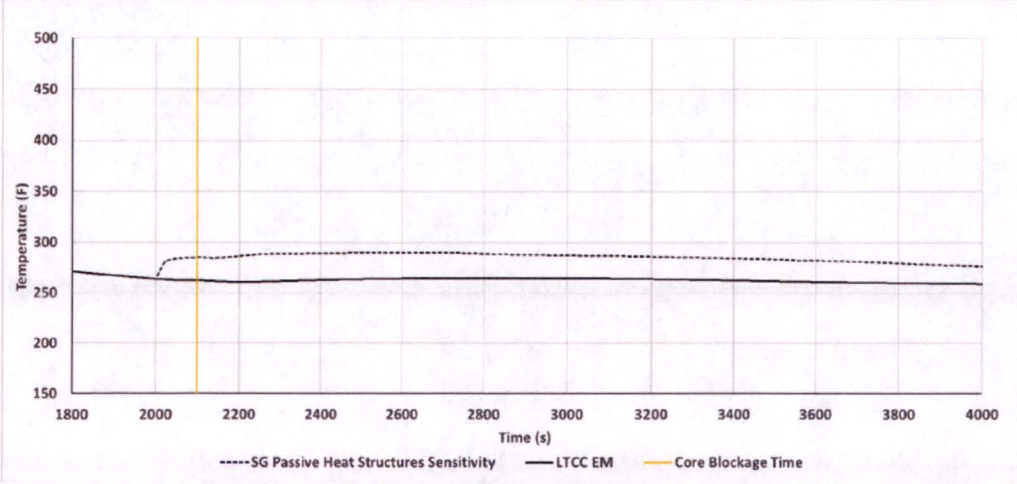

Figure 3. Secondary Coolant Average Temperature

The total heat transferred between primary and secondary fluids within the first hour after the core blockage time is shown in Table 1.

Table 1

Case	Total SG-Primary Energy Transferred (BTU)
LTCC EM	1.12 E+10
Sensitivity	6.96 E+10

Simulation results confirm that the energy released to the primary coolant flowing through the SGs' U-tubes is higher in the sensitivity case due to the presence of the additional metal masses.

The total energy produced in the core (decay heat) within the first hour after the core blockage time for both cases is 1.92 E+08 BTU (this is calculated as the time-integral of the total core decay power).

The SG secondary collapsed liquid level is plotted in Figure 4. The behavior of all four SGs is found to be similar. The figure shows the simulation results of the SG of the broken loop (Loop 3). Main features of the liquid level are explained in the figure.

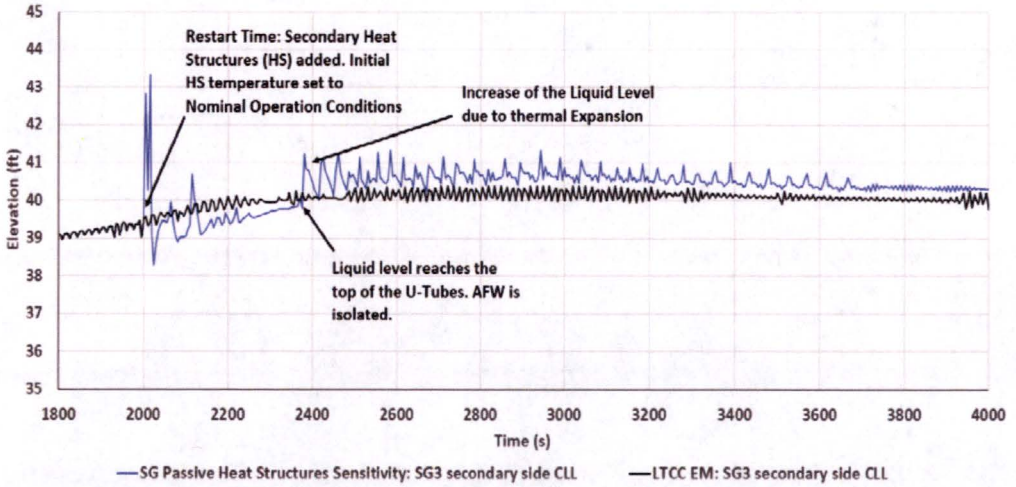

Figure 4. Secondary Collapsed Liquid Level (Loop 3 – Broken Loop)

Conclusions
A sensitivity case is conducted to study the effects of metal structures in the secondary side of the steam generators.

The mass of the metal structures, the initial temperature, and the location of the heat structures are defined to maximize the energy stored in the secondary side at the core blockage time.

The simulation results confirmed that the effects of the secondary metal structures on the on the PCT is negligible.

[1]. RC09989, RELAP5-3D Steady-State Model, Revision 0.

- Though only the 16-inch hot leg break analysis was provided, STPNOC did not justify or demonstrate that the 16-inch hot leg break bounds smaller hot leg breaks. Justify that the 16-inch hot leg break analysis bounds the smaller hot leg break scenarios.

STPNOC Response

The 16-inch HLB LOCA scenario progression is described as part of the response to the SNPB-3-02. The accident progression simulated with the LTCC EM can be summarized as follow:

- Immediately after the break event, the primary system experiences a fast depressurization where water and steam are discharged from the break.
- Reactor scram and ECCS actuation occur, controlled by low pressure signal.
- Due to the location of the break, injection of liquid water from the cold side is sustained by the ECCS injection system (HHSI, Accumulators, and LHSI).
- Core liquid inventory increases rapidly after the actuation of the accumulators and SI pump. Pre-Core Blockage LTCC starts when the core is fully flooded (Core Collapsed Liquid Level = 14 feet).
- When RWST water is depleted, injection starts from the sump (SSO time).
- The total liquid inventory in the core and in the primary system is sufficient to supply the liquid water to the core immediately after the core blockage event.
- Liquid inventory in the core decreases until flow through alternative flow paths (steam generators u-tubes) is established.
- Liquid water flow is maintained at the top of the core through the steam generators during the Post-Core Blockage LTCC.

Different important thermal-hydraulic parameters can be identified from the description provided. These parameters (listed and described below) can be used as figure of merit to confirm that the large break scenarios bound smaller hot leg breaks.

Sump Switchover time

The sump switchover (SSO) time and, subsequently, the core blockage time, is one of the most important parameters defining the thermal-hydraulic initial conditions of the reactor system for the post-core blockage LTCC phase. The SSO time is defined based on the RWST volume available for injection, and the injection rate of the SI system and CS system. The rate of injection has three[1] contributors:

- The High Head Safety Injection (HHSI) pumps
- The Low Head Safety Injection (LHSI) pumps
- The Containment Spray (CS) pumps

The rate of injection of the HHSI and LHSI depends on the pressure of the primary system and, based on the pump characteristics, is expected to increase at lower primary system pressures. The contribution of the CS pumps may be assumed to be constant throughout the accident progression[2]. The primary pressure during the accident progression is strongly dependent on the break size. In particular, larger breaks are expected to experience a faster depressurization, stabilizing the primary system at a lower pressure. Subsequently, the total ECCS injection is expected to be higher during large break scenario than smaller breaks. The SSO time for the three HLB scenarios simulated is reported in the table below.

	Break Size		
	16"	6"	2"
SSO Time (s)	1740	2302	3729

Decay Power at Core Blockage and Core Boil-off Rate

The LTCC EM calculates the decay power using the ANS-1979 model. Based on the considerations on the SSO time provided in the previous paragraph, the decay power at time of core blockage is higher for larger breaks since the core blockage event occurs earlier in the transient. The amount of water required to compensate the boil-off rate and cool down the reactor core during at the post-core blockage LTCC is relatively larger in the 16-inch HLB scenario than smaller break scenarios. The core decay power at the time of core blockage for the three HLB scenarios simulated is reported in the table below.

	Break Size		
	16"	6"	2"
Decay Power @ Core Blockage (MW)	68.25	63.01	54.92

[1] Accumulators do not contribute to the RWST depletion
[2] The CS pumps injection volumetric flow rate ramps up at pump startup and stabilizes to a nominal value defined by the pump and injection pipeline characteristics.

Core Collapsed Liquid Level

In the seconds after the core blockage, the liquid water in the core reaches saturation and starts boiling. The boil-off rate depends on the core decay power (as mentioned in the previous sections). The steam leaving the core is replaced by liquid water entering the top of the core in opposite direction. Higher boil-off rates are expected right after the core blockage during larger break scenarios. Subsequently, the core mass inventory during the post-core blockage LTCC is expected to be smaller for larger break scenarios. In the following figure, the core collapsed liquid level is plotted for the cases simulated. In the figure, the core blockage time is set to zero for all the break scenarios to facilitate the comparison. Due to the higher decay power at the SSO (occurring 360 seconds before the core blockage time) in large breaks, voids are created in the core even before the core blockage time. The core collapsed liquid level decreases rapidly after the core blockage time in large breaks due to the smaller water inventory at the top of the core. Smaller breaks (6" and 2" in the figure) would have a core fully covered at the core blockage time (core collapsed liquid level = 14 ft) and a larger inventory of water available at the top of the core. This effect, combined with a lower decay power level in the core, allows a slower decrease in the core liquid inventory, which will stabilize to a higher level.

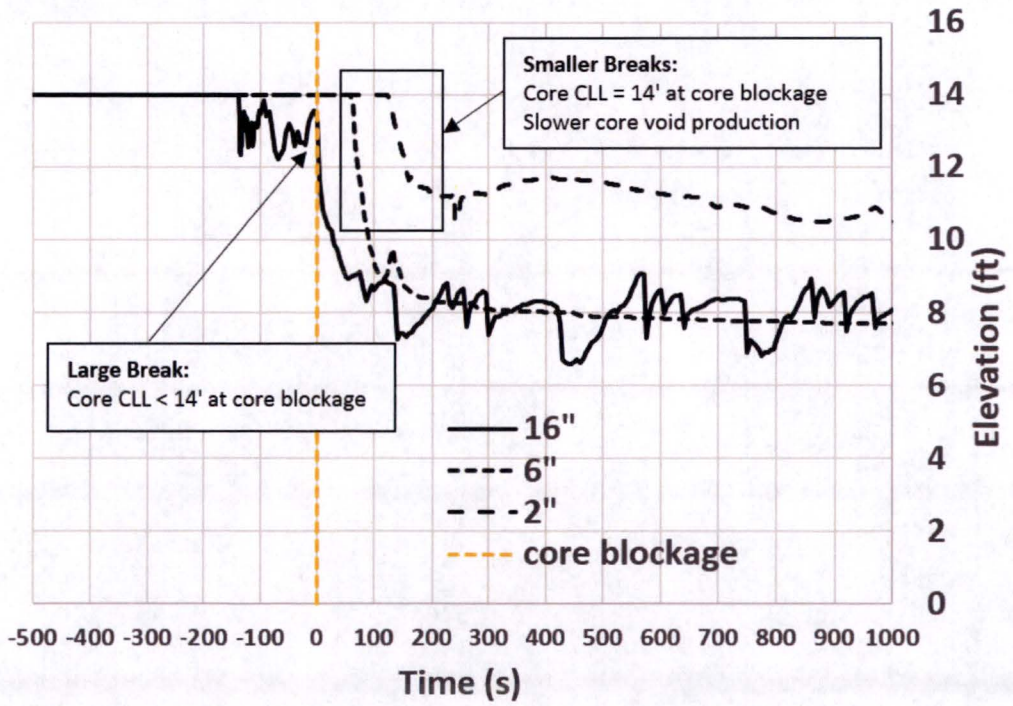

Other Considerations: Boundary Conditions

The simulations of the 6" and 2" HLB scenarios and core blockages are executed under the same boundary conditions of the large break (16") scenario. RWST volume available for injection, RWST water temperature, ECCS injection characteristics, and all other boundary conditions are imported from the 16" break simulation. Of particular importance is the sump pool temperature profile which is also assumed to be the same of the one imposed as boundary condition for the large hot leg break. Considerations on the heat transfer mechanisms in the reactor containment, and simulation results of different break sizes available in literature [1] show that the sump pool temperature at the SSO time is relatively lower for smaller breaks compared to large breaks.

The cladding temperature for the three accident scenarios simulated (16", 6", and 2" HLB) is shown in the figure below. In the figure, the following features can be seen:

- During the pre-core blockage LTCC and before the SSO time, cladding temperature is determined by the amount of flow forced through the core. The flow is lower for smaller breaks (no LHSI pumps running due to the high pressure of the primary system[3]). Subsequently, cladding temperature of small breaks (2" in the figure) is found to be higher than larger breaks.
- At SSO, the increase in the injection temperature produces an increase of the cladding temperature. ECCS flow is still forced through the core from the bottom.
- When core and core bypass are fully blocked, cladding temperature rises. Subcooled and saturated heat transfer regimes are seen in the core for the scenarios simulated. During the post-core blockage LTCC phase, the cladding temperature stabilizes to a level slightly above the saturation temperature at the pressure of the core as shown in the figure (dashed lines identify the saturation temperature and solid lines identify PCT). Differences in the cladding temperature shown in the figure below are due to the difference in the saturation temperature (primary pressure) for the break sizes analyzed.

[3] No manual operations to cool down and depressurize the primary system are modeled in the LTCC EM. This condition generates a relatively high pressure of the primary system and a subsequent low ECCS flow rate through the core.

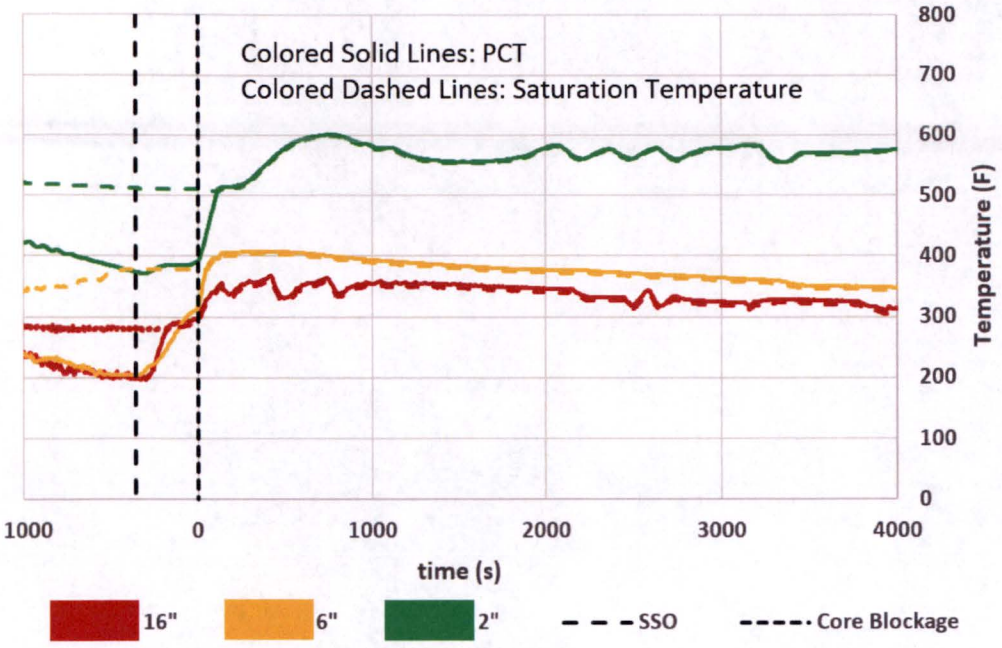

Final Remarks and Conclusions

The simulations of the three HLB scenarios are executed under the same boundary conditions. The important phenomena observed in the simulations are similar. Nevertheless, the large break scenario shows bounding initial conditions for the post-core blockage LTCC simulation, specifically in regards to the status of important thermal-hydraulic parameters of the reactor system at the SSO time:

- Decay power level,
- Water inventory in the core (Core CLL)
- Water inventory in the primary system

The arguments and discussion provided above confirm that the overall simulation results for the large HLB LTCC scenario are bounding the ones for smaller breaks.

[1]. NUREG/CR-6770, "GSI-191: Thermal-Hydraulic Response of PWR Reactor Coolant System & Containments to Selected Accident Sequences". August 2002. (http://www.nrc.gov/reading-rm/doc-collections/nuregs/contract/cr6770/)

- Provide a clear and in-depth description of counter-current flow limit (CCFL) at the core exit (e.g., plots of vapor and liquid flow at the exit, a description of relevance of the provided figure).

STPNOC Response

The simulation results for the 16" HLB LOCA scenario (described in the response to RAI-SNPB-3-02) show that the core is fully covered at the time of core blockage. When the core is fully blocked, vapor is produced and discharged from the top of the core, proceeding upward toward the break. Liquid water reaching the top of the core through alternative flow paths, tends to enter the core by gravity.
The vapor and liquid velocities simulated at the core exit (Junction 84502) are plotted in Figure 1.

The following features are marked in the figure.

1. During the pre-core blockage LTCC, the ECCS water is forced to flow through the core from the core inlet. The core is fully covered. The velocity of the liquid is positive (upward). Vapor velocity is set by the code equal to the liquid velocity since the void fraction is zero (no vapor).
2. At the sump switchover time, ECCS temperature increases. When higher temperature water reaches the core, voids are produced due to reduced sub-cooling of the inlet liquid. Velocities of both liquid and steam are positive (upward).
3. At core blockage, liquid velocity gradually decreases to zero. Voids increase in the core.
4. Liquid velocity is negative (downward). Liquid is now entering the core from the top. Steam leaves the core from the top toward the break in hot leg. The steam velocity is positive (upward).

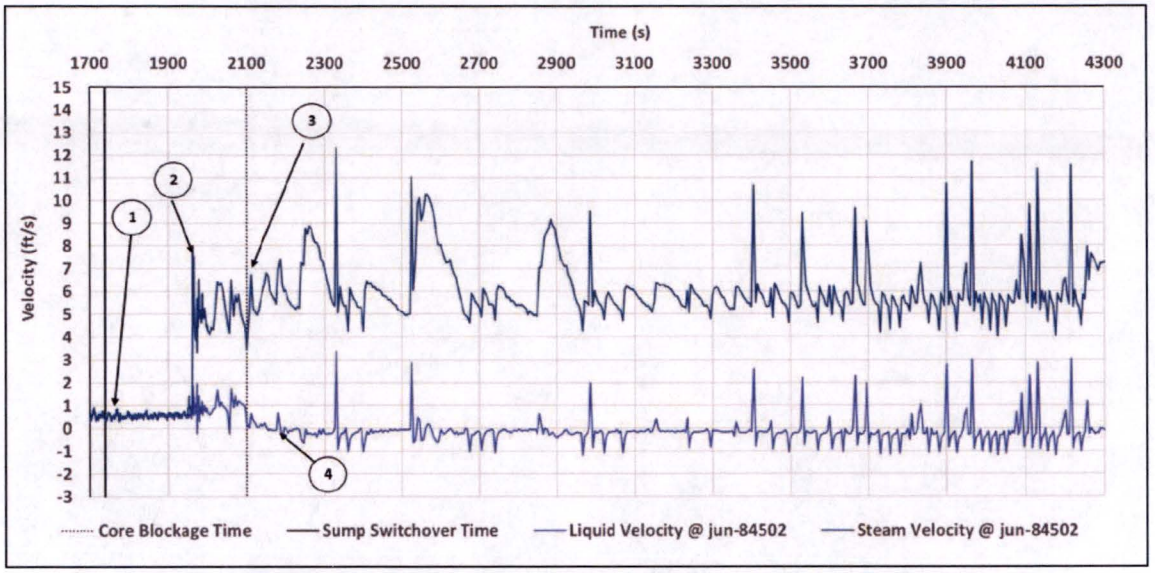

Figure 1. Liquid and Steam Velocities at Core Exit

Conditions for CCFL may occur, based on vapor and liquid velocities, void fraction, and coolant thermodynamic conditions. The CCFL model available in RELAP5-3D and the coefficients used in the STP LTCC EM are described in detail in the response to RAI-SNPB-3-13 follow up; the response also describes the conditions under which the model is enabled. The model is enabled when upward vapor velocity and other thermodynamic conditions (void fraction, liquid and gas densities) contribute to the increase in the gas dimensionless superficial velocity H_g outside the accessibility area.

The RELAP5-3D simulation output includes variables to track when the CCFL model is enabled. The variable *ccflf* is the junction CCFL flag. Its value is "0" if the flow is not CCFL-limited, and "1" if the flow is CCFL-limited. A control variable is defined in the input file to calculate the time integral of the variable *ccflf*. The value of this integral at a given time, t, provides an indication of the cumulative time at which the flow at the core exit was CCFL-limited. This integral is plotted in Figure 2 together with the core exit liquid and steam velocities (also shown in Figure 1). The figure clearly shows that immediately after the core blockage, conditions for CCFL are established at the top of the core.

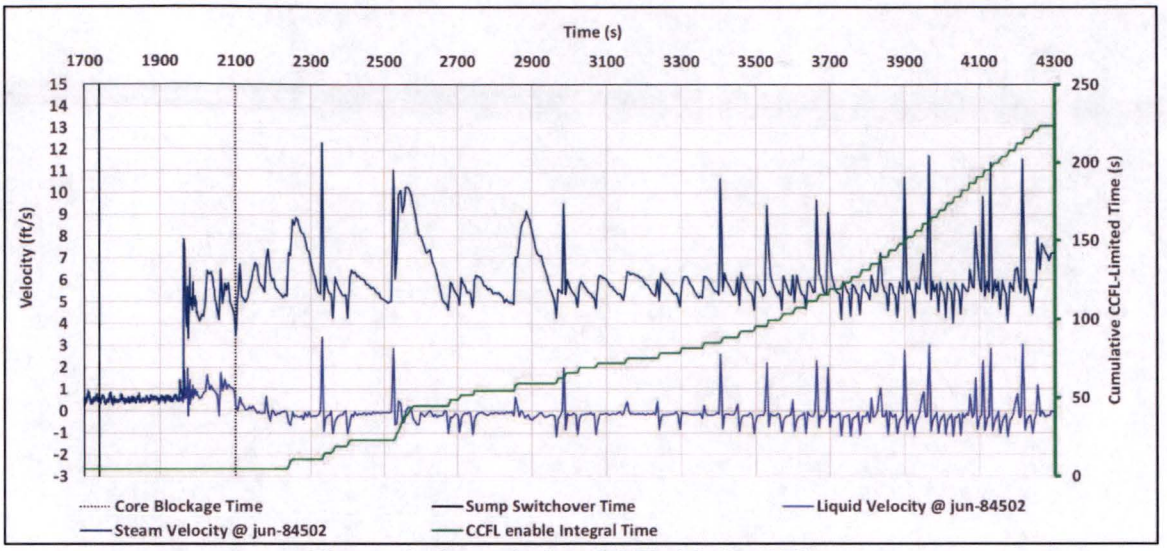

Figure 2. Cumulative CCFL-Limited Time

Follow-up SNPB-3-5 Debris at grid spacers

Initial RAI: Describe how the LTCC EM accounts for potential blockages at spacer grid in the core above the bottom grid.

Follow-up question:

In its response, STPNOC referenced a previous submittal. In this previous analysis, STP demonstrated that the amount of CRUD which could be expected to be released would be less than 2 pounds. The NRC staff agrees with STPNOC that this small amount of fine particles would have minimal impact on the flow through the spacer grids. STP also referenced WCAP-16793-NP (Reference 26) to address the ability of fibrous debris to collect at grid spacers. In section 3.4.4 of their Safety Evaluation (Reference 27), the NRC staff concluded that when the quantity of debris is within the acceptance limits specified in the WCAP (e.g., 15 grams per fuel assembly), the effect of fibrous debris accumulation on spacer grids in the core will be minimal. This conclusion was based on the observation made during testing that while fiber was deposited on spacer grids in the core, it did not impede cooling. It was not clear to the NRC staff that the same conclusion made in WCAP-16793-NP-A would be applicable to STP, as the fiber loading analyzed by STP in the long term core cooling analysis is much higher than what was tested in WCAP-16793-NP-A).

STPNOC Response

The response below is with respect to hot-leg breaks. Cold-leg breaks have been shown to have substantially less than 15 gm/FA, such that LTCC is not affected.

The STP LTCC EM conservatively assumes full blockage occurs at 15 gm/FA and that the blockage (as stated in WCAP-16793-NP-A) preferentially accumulates on the first grid spacer (the core entrance). It is reasonable to assume that addition of more debris would,

because filtration is more efficient where debris is concentrated, collect at the bottom grid rather than passing through the more effective core entrance debris bed, consistent with the assumption in the STP LTCC EM. In addition, the STP LTCC EM assumes all fiber that enters the RCS is collected in the core.

On the amount of debris entering the RCS

Per STPNOC's FiDOE evaluation, the maximum amount of fiber that enters the RCS is less than 50 gm/FA. As described in SNPB 3-02, under the 100% collection assumption, more than 6 minutes elapses before the total amount of debris entering the RCS reaches 15 gm/FA. During this time, the RCS is filling in volumes such as the steam generator tubes and the RV upper head with water at the same debris concentration as the water entering the core.

On the core accumulation

The flow through the baffle barrel (BB) bypass would have no debris blockage until the core is fully blocked (otherwise, the core would have less than 15 gm/FA collected); alternatively, the fiber collects in the BB and not on the core. Either way, the STP LTCC EM adds conservatism by assuming that what when 15 gm/FA enters the RCS, the core and core bypass is fully blocked.

Similar to the CLB scenario, the debris in the RCS volumes and the debris that passes through the BB bypass (debris other than that captured in the core) during the first 6 minutes is discharged from the break and re-filtered through the ECCS sump screens, greatly reducing the amount of debris available to return to the core. The STP LTCC EM conservatively ignores this filtration mechanism and assumes 100% of debris entering the RCS is captured in the core.

On the WCAP test case

The tested limit of 15 gm/FA was arrived at by finding the maximum amount of debris that can be tolerated with a full chemical precipitate loading. It is very unlikely that chemical precipitates would be formed, based on testing performed by the NRC (NUREG/CR-6914) and STPNOC (ML13323B202, ML13323B209). However, in the unlikely event significant amounts of chemical precipitates were to form, it would be several hours after recirculation starts at which time much lower cooling demand would be required (that is, higher loadings could be tolerated).

The WCAP test case ignores the effect of collection on the ECCS strainer of the debris that circulated through the test loop. That is, the testing was conducted in such a way that all the debris that was introduced went to the fuel assembly without ECCS screen filtration. Very little debris can accumulate on the core when the debris in the ECCS flow above that required to remove decay heat, and which bypasses the core is allowed to be captured on the ECCS screen.

On the break flow and ECCS flow

After the time core blockage is conservatively assumed in the STP LTCC EM, the fiber that accumulates in SGs, RV Upper Plenum, RV Upper Head, and RCS piping contains the remaining 35 gm/FA. The only fraction of the remaining 35 gm/FA that enters the core is that needed to overcome decay heat; the rest leaves through the break and is (mostly) captured on the debris-loaded ECCS sump screens. This situation is similar to the CLB scenario in that only the fraction of ECCS flow required to satisfy the core decay heat flow demand enters the core and the rest is bypassed. As in the CLB scenario, only a very few grams (less than 5 gm/FA) per FA would enter the core.

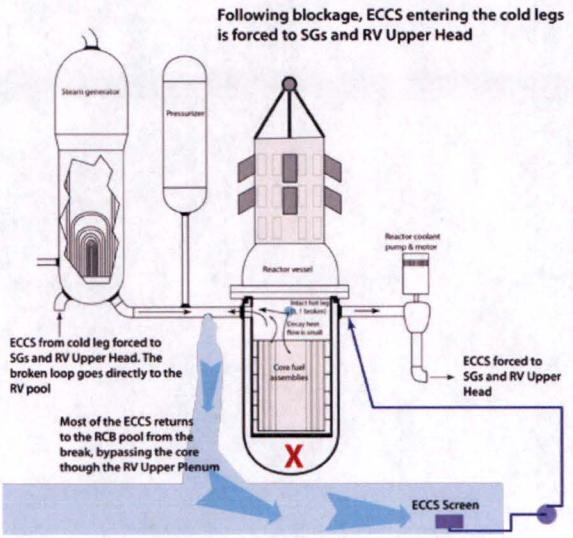

Summary

- When all the conservatisms included in the STP LTCC EM are taken into consideration for the hot-leg break, it is reasonable to assume most of the 35 gm/FA, in excess of the 15 gm/FA assumed to block the core, never reaches the core and would not impede cooling.
- Based on observations made on chemical precipitate behavior in STP post-LOCA sump fluids, it is reasonable to assume that core cooling would be satisfied with higher debris loads than 15 gm/FA; at least for several hours following initiation of the LTCC phase.
- The actual amount of debris entering the core would be much less than the amount that enters the RCS (50 gm/FA) and much closer to what was tested in WCAP-16793-NP-A.

Follow-up SNPB-3-7 Initial and Boundary Conditions for the Long-Term Phase

Initial RAI: Demonstrate that the initial and boundary conditions for each accident scenario at the beginning of the long-term phase are consistent with those conditions which are expected. This demonstration should analyze the RELAP5-3D calculations for the conditions at the beginning of reflood and show that those calculations are reasonable compared with known behavior. This analysis should include comparison between the conditions calculated by RELAP5-3D and the current large and small break LOCA safety analyses.

Follow-up question:

Discuss the initial and boundary conditions at the beginning of the long-term phase (i.e., phase 4), and provide a justification that these initial and boundary conditions are appropriate.

STPNOC Response

The LTCC phase (referred to as Phases 3 and 4 in SNPB 3-06) initial conditions and boundary conditions as simulated by the STP LTCC EM appropriately adopt conservative values such that, as these phases are simulated, the PCT figure of merit conservatively bounds the expected response that would be realized in the unlikely event the hypothesized HLB LOCA scenarios could occur.

The simulation results (the initial conditions for next phases) at the end of Phase 2 are consistent with expected behavior of the primary system during HLB LOCA events. In particular:

- Due to the break location (HLB), the ECCS flow injected into the cold legs is expected to move preferentially toward the reactor vessel and, subsequently, through the reactor core.
- The reactor core is flooded and fully covered at the end of the refill/reflood phase and the level of sub-cooling at the core exit depends on the total core flow rate; the core cladding temperature depends on forced convection of ECCS coolant through the core and decay heat.
- The SSO time results from the depletion of the water in the RWST at the rate of the total ECCS and CS injection (HHSI, LHSI, and CS pumps).

The initial conditions for the LTCC are consistent with the expected behavior of the plant during HLB scenarios. Based on the conservatism in the boundary conditions imposed in the STP LTCC EM, the simulation results of the phases proceeding the LTCC phase are considered to be satisfactory and appropriate as initial conditions for the pre- and post-core blockage LTCC simulations.

In the following, the primary initial conditions and boundary conditions are further summarized

- Minimum RWST available volume:
  Maximizes decay heat input by minimizing the actual time to empty (entering Phases 3 and 4) Minimizes the cooling water available for core refill/reflood in Phases 1 and 2.
- Maximum RWST temperature:
  Increases ECCS enthalpy, thereby increasing the RCS pressure in Phases 1 and 2, creating higher temperature and pressure at the start of Phases 3 and 4. Minimizes the level of sub-cooling of the water in the primary system at the beginning of phases 3 and 4.
- Average ECCS flow:
  The STP LTCC EM uses a value between minimum and maximum ECCS pumping capability which helps minimize (by not using minimum flow) the time to Phases 3 and 4 resulting in higher decay heat load in subsequent Phases; and (by not using maximum flow) decreases the water flow rate available for refill/reflood.
- Core flooding:
  The core outlet CCFL parameters are selected such that the liquid accessibility is minimized.

- Void coefficient/reactor trip:
  The full assumed reactor trip delay time is conservatively assumed by ignoring the void feedback effect which would result in effectively immediate reactor shutdown at the start of the hypothesized event.
- SBLOCA operator action:
  The STP LTCC EM ignores (in SBLOCA) the operator action to cool down and depressurize the RCS using the Steam Generators. This results in much higher pressure and temperature at the start of Phases 3 and 4 due to the STP HHSI head-flow characteristics. This assumption also minimizes the ECCS flow during smaller breaks.
- ECCS Cooling:
  In Phases 3 and 4, cooling of the LHSI ECCS flow from the RHR Heat exchangers is ignored, increasing the enthalpy of the ECCS water supplied to the RCS. Sump water cooling is ignored throughout Phases 3 and 4 thereby artificially increasing the ECCS enthalpy during these phases.
- Vessel Flow Splits:
- The STP LTCC EM minimizes the flow through the core by lumping some of the alternative flow paths (core periphery and rod cluster control guide thimbles) into the core bypass channel. This channel is assumed to be fully blocked during the post-core blockage LTCC phase.

Follow-up SNPB-3-13 Validation of closure relationships

Initial RAI: For the closure relationships identified, provide appropriate validation for the use of this relationship over its expected application domain. This validation should include comparisons to separate effects tests and/or integral test data and appropriately address the model's uncertainty. Where appropriate, discuss any similarity criteria, scaling rationale, assumptions, simplifications, and/or compensating errors.

Follow-up question:

Provide an analysis of the validation for the closure relationships important for the long-term core cooling (LTCC) evaluation methodology (EV). Analysis of the validation of the closure relationships is recommended with consideration towards similarity criteria, scaling, experimental uncertainty, the potential for compensating errors, and the comparison between predicted and measured results to determine if the closure relationships for the LTCC EM have sufficient validation for their use in the EM.

STPNOC Response

The RELAP5-3D thermal-hydraulic model solves eight field equations for eight primary dependent variables (pressure, phasic specific internal energies, vapor/gas volume fraction, phasic velocities, noncondensable quality, and boron density). Closure of the field equations is provided through the use of constitutive relations and correlations.

The closure relationships included in the RELAP5-3D computer code are adequate to simulate the HLB LOCA scenarios included in the LTCC EM, and to predict the behavior of the primary system during the blowdown, refill/reflood, and pre- and post-core blockage LTCC phases of the accident. While detailed description of each closure relationship, scalability and applicability, implementation and validation, and other details are available in the RELAP5-3D user's manual (Volume 4), considerations on the validity and applicability of these closure relationships are provided below. A more detailed description of the closure relationships for the most important phenomena of the post-core blockage LTCC phase is also provided.

The RELAP5-3D closure relationships can be classified into five main categories.

- Flow Regime Maps
- Closure Relations for the Fluid Energy Equations
- Momentum Equation Closure Relations
- Flow Process Models
- Other Models

1.0 Flow Regime Maps

RELAP5-3D includes models for defining flow regimes and flow-regime-related models for interphase friction, the coefficient of virtual mass, wall friction, wall heat transfer, and interphase heat and mass transfer. Four flow-regime maps are used in the RELAP5-3D code to predict: (a) a horizontal map for flow in pipes; (b) a vertical map for flow in pipes, annuli, and bundles; (c) a high mixing map for flow through pumps; and (d) an ECC mixer map for flow in the horizontal pipes near the ECC injection port.
The models included in the RELAP5-3D code are adequate to predict the flow regimes in the regions of the primary system during the phases of the LOCA, including the pre- and post-core blockage LTCC phases.

2.0 Closure Relations for the Fluid Energy Equations

Heat transfer correlations are used to provide closure for the energy equations. This includes bulk interfacial, wall-to-fluid, and Critical Heat Flux (CHF) heat transfer correlations, and reflood model. Each correlation is designed to represent energy transfer under a specific set of thermal-hydraulic and thermodynamic conditions. The correlations included in the RELAP5-3D code and the conditions under which these correlations are used in the LTCC EM, are adequate to predict the heat transfer phenomena in the core, and steam generators (primary and secondary side) during the phases of the LOCA, including the pre- and post-core blockage LTCC phases.

2.1 Core Heat Transfer Regimes during Post-Core Blockage LTCC Phase

The simulation results of the post-core blockage phase show that the liquid inventory in the core is maintained sufficiently high to establish the conditions for subcooled and/or saturated heat transfer regimes in the core. A more detailed description of the sub-cooled and saturated heat transfer correlation and its validity is described below.

The RELAP5 code uses classical and widely-adopted Chen correlation [1] for both subcooled and saturated nucleate boiling HT.

2.1.1 Saturated nucleate boiling model

The nucleate boiling correlation proposed by Chen has a macroscopic convection term plus a microscopic boiling term:

$$q'' = h_{mac}(T_w - T_{spt})F + h_{mic}(T_w - T_{spt})S \quad (1)$$

Chen chose Dittus-Boelter times a Reynolds number factor, F, for the convection part and Forster-Zuber [2] pool boiling times a suppression factor, S, for the boiling part, where h_{mac} is the Dittus-Boelter equation,

$$h_{mac} = \frac{k}{D}\mathrm{Nu}_{DB};\quad \mathrm{Nu}_{DB} = 0.023\left(\frac{k}{D}\right)\mathrm{Re}^{0.8}\,\mathrm{Pr}^{0.4} \quad (2)$$

and the Forster-Zuber equation is

$$h_{mic} = 0.00122\left(\frac{k_f^{0.79}C_{pf}^{0.45}\rho_f^{0.49}g_c^{0.25}}{\sigma^{0.5}\mu_f^{0.29}h_{fg}^{0.24}\rho_g^{0.24}}\right)\Delta T_w^{0.24}\Delta P^{0.75} \quad (3)$$

where the subscript *f* means liquid, the subscript *g* means vapor/gas, g_c is the gravitational conversion factor, which equals unity in SI units, $\Delta T_W = T_W - T_{spt}$ (based on total pressure), and ΔP is the pressure based on wall temperature minus total pressure.

A plot of the *F* factor is shown in Figure 1(a). The suppression factor *S* shown in Figure 1(b), is the ratio of effective superheat to wall superheat. The S factor accounts for decreased boiling heat transfer because the effective superheat across the boundary layer is less than the superheat based on a wall temperature. The *F* and *S* factors are determined by an iterative process. First, *F* is calculated assuming a functional relationship with the Martinelli flow parameter, χ_{tt}, and the ratio of the two-phase to liquid Reynolds numbers. With *F* determined, the convective component is extracted from the total heat transfer, leaving the boiling component. Then, S is determined assuming it to be a function of the local two-phase Reynolds number. The process is continued for 10 iterations. The solid lines drawn through the data ranges of Figure 1(a) and Figure 1(b) are taken as the values for *F* and *S*.

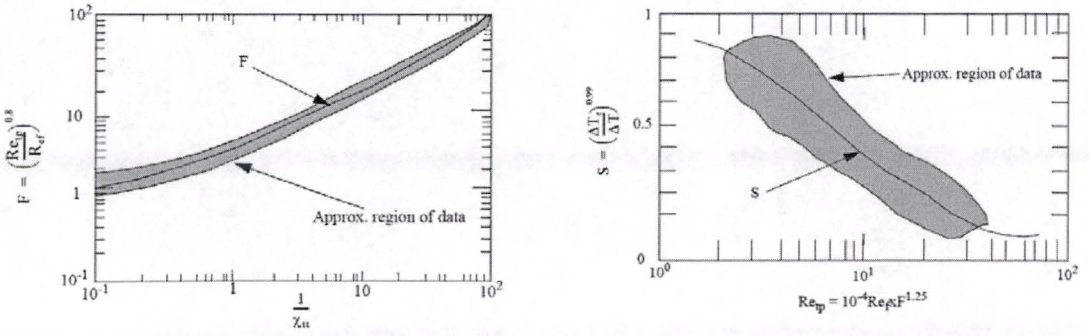

(a) (b)

Figure 1: (a) Reynolds number factor F and (b) suppression factor S

Table 1 indicates data for water, for which the correlation was developed and tested [3-7]. The mean percent deviations between the correlation and the data sets are presented in the last column.

Recent development [8] has extended the database over which the correlation has been exposed. The maximum pressure of the database was increased to 7.0 MPa for saturated water. These conditions are similar to the ones expected during the post-core blockage LTCC phase.

Table 1: Range of conditions tested by Chen for water data

Reference	Geometry	Flow direction	Pressure (MPa)	Liquid velocity (m/s)	Quality (%)	Heat flux (kW/m^2)	Average error (%)
Dengler-Addoms	Tube	Up	0.05 - 0.27	0.06 - 1.5	15 - 71	88 - 63	14.7
Schrock-Grossman	Tube	Up	0.29 - 3.48	0.24 - 4.5	3 - 50	205 - 240	15.1
Sani	Tube	Down	0.11 - 0.21	0.24 - 0.82	2 - 14	44 - 158	8.5
Bennett et al.	Annulus	Up	0.10 - 0.24	0.06 - 0.27	1 - 59	55 - 101	10.8
Wright	Tube	Down	0.11 - 0.47	0.54 - 3.41	1 - 19	41 - 278	15.4

2.1.2 Subcooled nucleate boiling models

The model basis is the same as for saturated nucleate boiling expressed by Equation (1), with changes proposed by Bjornard and Griffith [9] where a modified F factor (F') is defined as function of the level of sub-cooling.

2.2 General Considerations

The approach and correlation proposed by Chen is one of the most used methods to predict the wall-to-fluid heat transfer coefficient under nuclear boiling conditions. The correlation implemented in RELAP5-3D and the use of this correlation to predict the cladding temperature during the post-core blockage LTCC phase is adequate for the simulation conditions in use in the LTCC EM.

2.3 References

[1] J. C. Chen, "A Correlation for Boiling Heat Transfer to Saturated Fluids in Convective Flow," *Process Design and Development, 5,* 1966, pp. 322-327.
[2] H. K. Forster and N. Zuber, "Dynamics of Vapor Bubbles and Boiling Heat Transfer," *AIChE Journal, 1,* No. 4, December 1955, pp. 531-535.
[3] G. E. Dengler and J. N. Addoms, *Chemical Engineering Progress Symposium Series, 52,* 18, 1956, pp. 95-103.
[4] V. E. Schrock and L. M. Grossman, "Forced Convection Boiling in Tubes," *Nuclear Science and Engineering, 12,* 1962, pp. 474-481.

[5] R. L. Sani, *Downflow Boiling and Nonboiling Heat Transfer in a Uniformly Heated Tube,* UCRL-9023, 1960.
[6] J. A. R. Bennett et al., *Heat Transfer to Two-Phase Gas Liquid Systems,* AERE-R3159, 1959.
[7] R. M. Wright, *Downflow Forced-Convection Boiling of Water in Uniformly Heated Tubes,* UCRL-9744, August 1961.
[8] K. E. Gungor and R. H. S. Winterton, "A General Correlation for Flow Boiling in Tubes and Annuli," *International Journal of Heat and Mass Transfer, 29,* 1986, pp. 351-356.
[9] T. A. Bjornard and P. Griffith, "PWR Blowdown Heat Transfer," *American Society of Mechanical Engineers Winter Annual Meeting, Atlanta, GA, November 27 - December 2, 1977,in: O. C. Jones and S.*

3.0 Momentum Equation Closure Relations

Closure relationships required for the momentum equation include the interphase friction, the wall friction, and the entrainment model. The correlations adopted by the RELAP5-3D code are adequate to predict the relevant phenomena in primary system during the phases of the LOCA, including the pre- and post-core blockage LTCC phases.

4.0 Flow Process Models

These models are included in the RELAP5-3D code to predict special flow phenomena of interest, including phenomena of particular interest during a LOCA scenario. These models include abrupt contraction and expansion, choked flow, stratification entrainment/pull-through, and CCFL. The CCFL is found to be the most important phenomena to occur during the post-core blockage LTCC phase of the scenarios under consideration. A detailed description of the closure relationship used in RELAP5-3D is reported below.

4.1 Counter-Current Flow Limitation (CCFL) Correlation

CCFL is a high-ranked phenomenon that requires empirical support; the STP LTCC EM model CCFL correlation uses bounding values found by examining a large parameter space that covers the conditions encountered in the LTCC simulations.

The simulations performed with the LTCC EM show that, during the post-core blockage phase, conditions for CCFL at the top of the core may occur (see Appendix A). During this phase, vapor produced leaves the core by flowing upward through the core outlet, while liquid water (reaching the top of the core through alternative flow paths) moves downward toward the core. Conditions that affect the CCFL at the top of the core include the liquid and vapor velocities, the liquid and vapor properties, and the geometry.

This condition is considered one of the most important phenomena during the Post-Core Blockage LTCC phase as it affects the behavior of the liquid entering the top of the core during this phase and, subsequently, the core coolability.

The response is divided into four sections:
Model Description: First, a general description of the correlations available in RELAP5-3D and their formulation is provided.

Assumptions and Boundary Conditions: Description of how the models are used in the LTCC EM, and the assumptions made on the CCFL coefficients is then described, to

confirm the appropriateness of the boundary conditions adopted in the LTCC EM for the simulations performed.

Code Validation: At the end, a list of validation cases performed by the code developers is included.

Conclusions: Final conclusions are stated at the end based on the evidence provided in the response.

4.1.1 Model Description

RELAP5-3D code includes three forms of the CCFL correlation – Wallis form [1], Kutateladze form, and Benkoff [2] form – a form in between the Wallis and Kutateladze forms and used in TRAC-PF1 code. A description of these models and their formulation in RELAP5-3D is provided below.

The CCFL correlations can be expressed in the following general equation [2]:

$$H_g^{1/2} + mH_f^{1/2} = c \quad (1)$$

where H_g is the dimensionless vapor/gas flux, H_f is the dimensionless liquid flux, c is the vapor/gas intercept (value of $H_g^{1/2}$ when $H_f = 0$, i.e., complete flooding), and m is the "(negative) slope", that is the vapor/gas intercept divided by the liquid intercept (the value of $H_f^{1/2}$ when $H_g = 0$). A typical plot of $H_g^{1/2}$ versus $H_f^{1/2}$ is shown in Figure 1. The dimensionless fluxes have the form

$$H_g = j_g \left[\frac{\rho_g}{gw(\rho_f - \rho_g)} \right]^{1/2}, \quad (2)$$

$$H_f = j_f \left[\frac{\rho_f}{gw(\rho_f - \rho_g)} \right]^{1/2}, \quad (3)$$

where j_g is the vapor/gas superficial velocity ($\alpha_g v_g$), j_f is the liquid superficial velocity ($\alpha_f v_f$), ρ_g is the vapor/gas density, ρ_g is the liquid density, α_g is the vapor/gas volume fraction, α_f is the liquid volume fraction, g is the gravitational acceleration, and w is the length scale and is given by the expression

$$w = D_j^{1-\beta} L^{\beta} \quad (4)$$

where β is a user-input constant. Also, D_j is the junction hydraulic diameter and L is the Laplace capillary length constant, given by

$$L = \left[\frac{\sigma}{g(\rho_f - \rho_g)} \right]^{1/2}, \quad (5)$$

where σ is the surface tension.

In Equation (4), β can be a number from 0 to 1. For $\beta = 0$, the Wallis form of the CCFL equation is obtained; and for $\beta = 1$, the Kutateladze form of the CCFL equation is obtained. For $0 < \beta < 1$, Bankoff form in between the Wallis and Kutateladze forms is obtained.

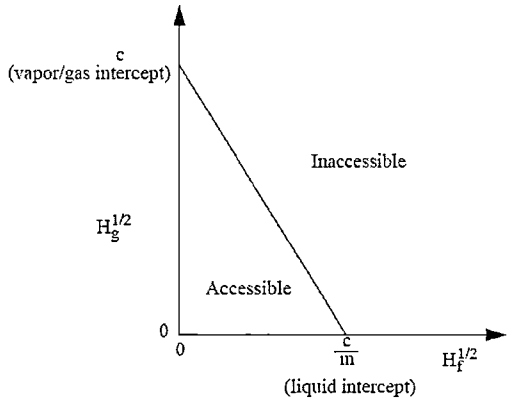

Figure 1. Plot of $H_g^{1/2}$ versus $H_f^{1/2}$ for a typical CCFL correlation.

First, according to Bankoff et al.'s guidelines, coefficients β, c, and m in the generalized CCFL model above (Equations (1) through (5)) can be estimated based on experimental data:

$$\beta = \tanh(\gamma k_c D_j), \tag{6}$$

$$m = 1, \tag{7}$$

$$c = \begin{cases} 1.07 + 4.33 \times 10^{-3} D^* & D^* < 200 \\ 2 & D^* \geq 200 \end{cases} \tag{8}$$

where the critical wave number $k_c = 2\pi / t$ corresponds to the maximum wavelength that can be sustained on an interface of length t (the plate thickness), and γ is the perforation ratio (fraction of plate area occupied by holes); and D^* is a Bond number defined as

$$D^* = n\pi D \left[\frac{g(\rho_f - \rho_g)}{\sigma} \right]^{1/2}, \tag{9}$$

with *n* the number of holes and *D* the plate diameter.

The formulation of the coefficients listed in Equations (6) – (9), and the models adopted in RELAP5-3D, is similar to the approach adopted in TRACE computer code and in the TRACE code manuals in regard to the CCFL [11].

4.1.2 Assumptions and Boundary Conditions

Figure 2 presents various CCFL experimental data for a perforated plate with different hole diameters (d), plate thicknesses (t), number of holes (n), and pitches (p) in the graph of $j_g^{1/2}$ vs. $j_f^{1/2}$.

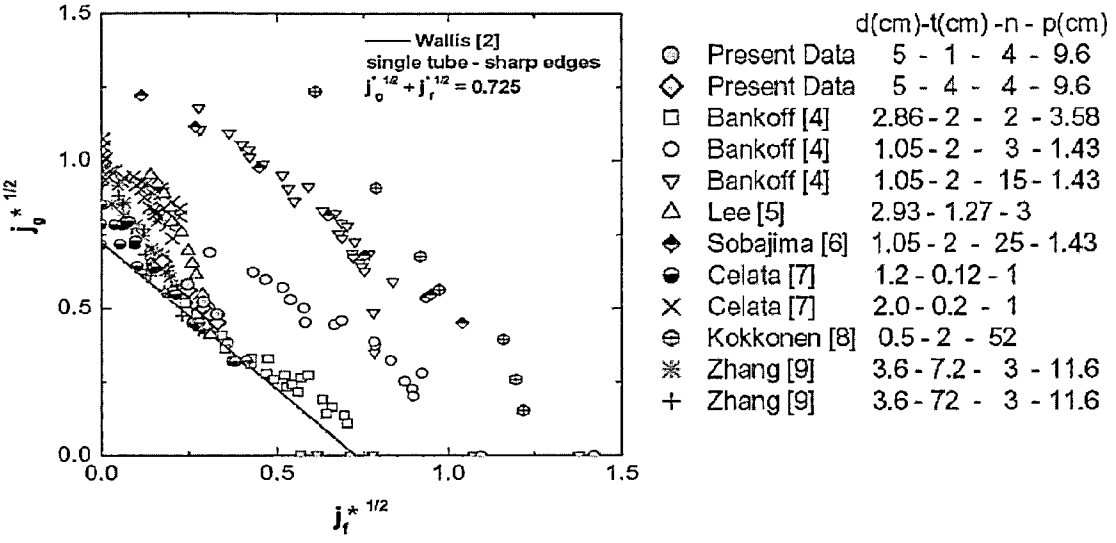

Figure 2. CCFL data for various conditions (reproduced from [4])

The data indicates that the number of holes is the most critical factor determining the "accessibility area", while other factors are relatively less important.

As the number of holes in the plate increases, the experimental data tend to shift upward (i.e., toward larger c) maintaining the same slope (m ~ 1). This is the case for the data produced by Bankoff [3] (n=2, 3, and 15), Sobajima [6] (n=25), and Kokkonen [8] (n=52).

In the same figure, the condition investigated by Wallis (vertical pipe, sharp-edged, c=0.725, m=1) is also shown (experimental points not included).

It can be noted that for perforated plates with large number of holes, experimental data may be bounded by the conditions (c=1, m=1). This condition is the one adopted in the LTCC EM.

Additional sensitivity analysis is conducted to include limiting cases for the CCFL. In particular, the coefficients proposed by Wallis (c=0.725, m=1) to account for edge effects for vertical sharp-edged pipes appear to be the most limiting conditions, as shown in Figure 2.

A list of conditions applied to the simulations performed is included in Table 1[4].

[4] Sensitivities are conducted starting from the 16" HLB scenario included in the LTCC EM, by simply changing the CCFL coefficients at the core outlet junction.

Table 1. CCFL Conditions used (LTCC EM and Sensitivities)

Case	β	c	m	Notes
LTCC EM - Base	0	1	1	Wallis – Smooth-edges. Bounding condition
Sensitivity 1	0.038422	2	1	Bankoff – STP Geometry
Sensitivity 2	0	0.725	1	Wallis – Sharp-edges. Worst Condition

The conditions calculated with Equations (6) – (9) for the STP geometry (Sensitivity 2) put in evidence the following:

- Coefficient β is close to zero. This can be interpreted as a negligible effect of the surface tension for this geometry. Subsequently the Bankoff model becomes similar to the Wallis model.
- The value of intercept c is larger than the condition proposed by Wallis for smooth-edged pipes, confirming that the conditions assumed for the LTCC EM – Base are bounding the expected phenomenon in the STP top core geometry.

The Sensitivity 2 was included in the list of sensitivities since it includes the worst conditions for the CCFL, by minimizing the accessibility area. Although these conditions do not realistically represent the geometry under consideration, the simulation results show sufficient liquid flow through the top of the core, maintaining adequate core cooling.

Figure 3 graphically represents these condition together with the available experimental data.

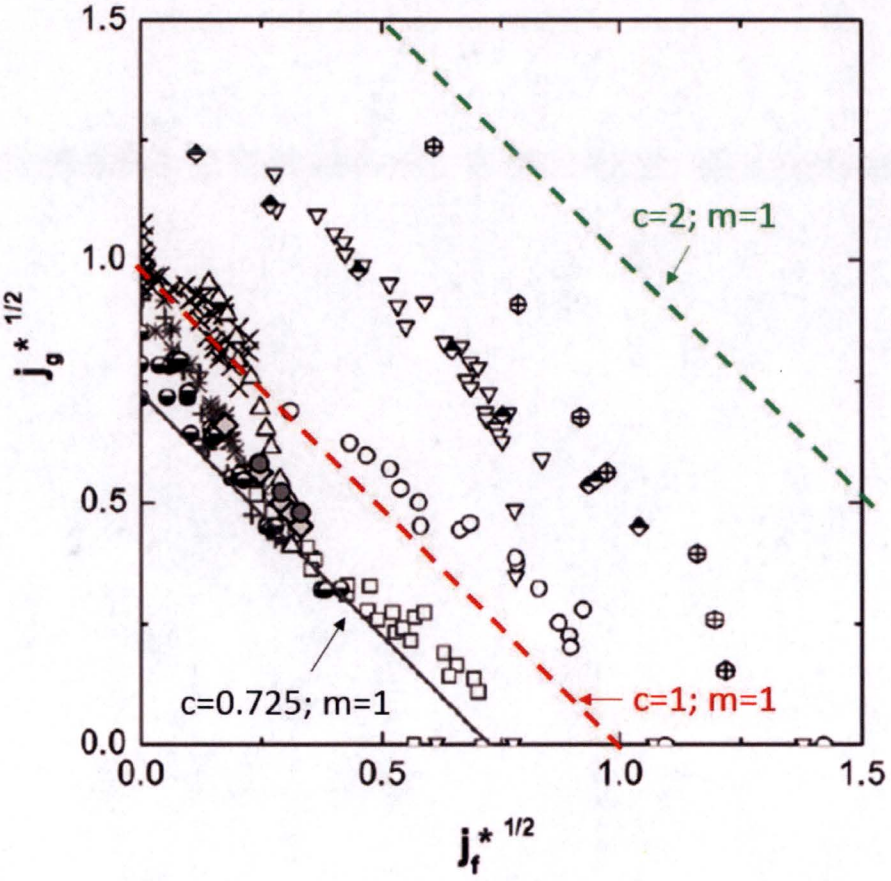

Figure 3. CCFL Coefficients – LTCC EM and Sensitivities

The line representing the conditions used in the LTCC EM (c = 1 and m=1) can be regarded as a conservative choice for medium and high number of holes, minimizing the accessibility area.

The conditions used in the Sensitivity 2 (c= 0.725, and m = 1) recommended by Wallis [1] for the sharp-edged pipes – is observed to cover all the CCFL data, and thus, this line can be regarded as the most conservative condition (with the smallest range of the accessibility of CCFL).

The PCT (Figure of Merit) as a function of the time during the Post-Core Blockage LTCC for the cases listed in Table 1 is plotted in Figure 4. The figure shows that under the conditions imposed in the LTCC EM (c=1, m=1), and also under worst conditions of the Sensitivity 2 (c=0.725, m=1), the PCT is maintained well below the limit of 800 °F.

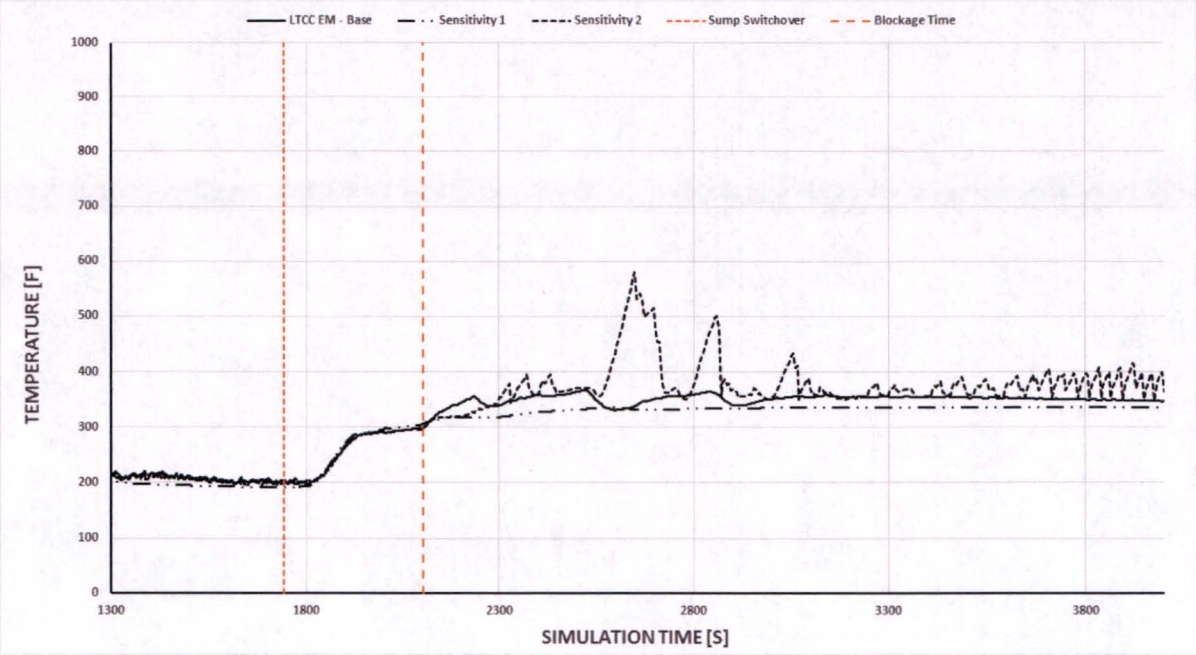

Figure 4. Simulation Results – PCT

4.1.3 Code Validation

Two separate effects tests are used in the RELAP5-3D code assessment, for the CCFL model. These tests and the outcome of the code comparison is briefly discussed below. Additional detail on the facility description, RELAP5-3D model and results is provided in Appendix A and B respectively (see also volume 4 of the RELAP5-3D users' manual).

Dukler-Smith air-water flooding— CCFL in vertical tube (See Appendix 4A or Section 4.15 in manual Vol. 3 for the details.)

Upper plenum test facility (UPTF) Test 6, Run 131— downcomer CCFL (See Appendix 4B or Section 4.16 in manual Vol. 3 for the details.)

The Dukler-Smith air-water flooding experiments assessed the Wallis CCFL model. Semi- and nearly-implicit predictions were in reasonable agreement with the Dukler-Smith experiment data for countercurrent air-water flow in a single tube over the range of air flows from 0.0126 to 0.126 kg/s. The assessment also shows that the Wallis correlation is implemented correctly.

UPTF downcomer CCFL Test 6, Run 131 was used to compare the relative performance of the annulus and pipe components for simulating the refill of the lower plenum during a loss-of-coolant accident. The two components are similar except that all the liquid is

placed in the film, with no liquid allowed in drops, in the annulus component when in the annular-mist flow regime. Liquid is allowed in both the film and drops in the annular-mist flow regime in the pipe component. Both the semi- and nearly implicit calculations were judged to be in reasonable agreement with the measured liquid level data for UPTF Test 6, Run 131. The calculated refill was similar to that observed in the test. The RELAP5-3D calculation in which the downcomer was modeled with annulus components was in better agreement with the measured results than when pipe components were used. The flow regime model in the annulus component, which puts all the liquid in the film, resulted in a better prediction of the lower plenum refill for the UPTF test. The pipe component provided a conservative prediction of the amount of liquid in the lower plenum.

4.1.4 Conclusions

The CCFL condition is identified as one of the most important phenomena during the Post-Core Blockage Phase. Due to the relatively high upward vapor velocity at the top of the core right after core blockage, conditions for CCFL may be expected in this region. CCFL closure relationships are available in RELAP5-3D. Assessment of the code capabilities and in predicting this phenomenon and the correctness of the use of such correlations was conducted and described. The assessment has confirmed that:

1) RELAP5-3D includes models for predicting the CCFL phenomenon. These models and the implementation/formulation approach adopted by the code developers are similar of the ones included in the TRACE computer code.
2) The code validation performed by INL confirmed that the correct implementation of these correlations.
3) The use of these correlations and the related coefficients in the LTCC EM is confirmed to be adequate for the geometry and the conditions under consideration. In particular, the coefficient included in the LTCC EM are bounding experimental data for perforated plates.
4) Sensitivity study is conducted to confirm that margin to the boundary conditions included in the EM is accounted.

The proposed LTCC EM is adequate to predict the expected phenomena of CCFL at the top of the core for the conditions expected during the Post-Blockage LTCC.

4.1.5 References

[1] G. B. Wallis, One-dimensional Two-phase Flow, McGraw-Hill, New York, 336-345, 1969.

[2] S. G. Bankoff and S. C. Lee, Multiphase Science and Technology, Vol. 2 (Edited by G.F. Hewitt, J.M. Delhaye, N. Zuber), Chapter 2, A Critical Review of the Flooding Literature, Hemisphere, New York (1985).

[3] S. G. Bankoff, R. S. Tankin, M. C. Yuen and C. L. Hsieh, "Countercurrent Flow of Air/Water and Steam/Water Through a Horizontal Perforated Plate," Int. J. Heat Mass Transfer, 24, 8, 1381-1395 (1981).

[4] H. C. No, K.-W Lee, C.-H. Song, "An Experimental Study of Air-water Countercurrent Flow Limitation in the Upper Plenum with a Multi-hole Plate," Nucl. Eng. Tech. 37, 557-564 (2005).

[5] H. M. Lee, G. E. McCarthy and C. L. Tien, "Liquid Carryover and Entrainment in Air-water Countercurrent Flooding," EPRI report, NP-2344 (1982).

[6] M. Sobajima, "Experimental Modeling of Steam-Water Countercurrent Flow Limit for Perforated Plates," J. Nuclear Science and Technology, 22, 9, 723-732 (1985).

[7] G. P. Celata, N. Cumo, G. E. Farello, and T. Setaro, "The Influence of Flow Obstructions on the Flooding Phenomenon in Vertical Channels," Int. J. Multiphase Flow, 15, 2, 227-239 (1989).

[8] I. Kokkonen and H. Tuomisto, "Air/Water Countercurrent Flow Limitation Experiments with Full-Scale Fuel Bundle Structures," Experimental Thermal and Fluid Science, 3, 581-587 (1990).

[9] J. Zhang, J. M. Seynhaeve and M. Giot, "Experiments on the Hydrodynamics of Air-Water Countercurrent Flow Through Vertical Short Multitube Geometries," Experimental Thermal and Fluid Science, 5, 755-769 (1992).

[10] C. L. Tien, K. S. Chung, and C. P. Lin, Flooding in Two-Phase Countercurrent Flows, EPRI NP-1283, December 1979.

[11]. ML071000097, "TRACE V5.0, Theory Manual – Fields Equations, Solution Methods, and Physical Models"

Appendix 4-A. Dukler-Smith Air-Water Flooding (Section 4.15 in Manual Vol.4)

Dukler and Smith [A1] conducted a simple flooding experiment at the University of Houston to study the interaction between a falling liquid film with an upflowing gas core. A RELAP5 model for the Dukler-Smith CCFL test facility was developed for earlier assessments using these experiment data. The work of Riemke [A2] and Davis [A3] is representative of these earlier assessments. This work draws heavily on the earlier assessments, basically repeating the assessment for the latest code version.

Experimental facility description

A schematic of the Dukler-Smith experiment facility is shown in Figure A-1(a). The flow system consisted of a 1.52-m (5-ft) length of 0.051-m (2-in.) inner diameter Plexiglas pipe used as a calming section for the incoming air, a 0.305-m (1-ft) diameter section of Plexiglas pipe for both introducing the air to the test section and removing the falling liquid film, a 3.96-m (13-ft) test section consisting of 0.051-m (2-in.) diameter Plexiglas pipe, and an exit section for removing the air, entrainment, and the liquid film flowing up. Measurements were taken of the pertinent flow rates, pressure gradients, and the liquid film thickness over a wide range of gas and liquid flow rates in the flooding region. The liquid film upflow, downflow, and entrainment rates were determined by weighing the liquid flow for a fixed period of time (see discharge lines to weigh tanks labeled B in Figure A-1(a)). Most of the instantaneous measured parameters oscillated once quasi-steady state conditions were reached, and it was necessary to time-average these parameters. Dukler and Smith indicate that the CCFL process is basically an unstable process that is driving the oscillations. In the RELAP5-3D simulations the air and water flow predictions at the measuring point also showed oscillations. The predictions were averaged over 30 s for purposes of showing comparisons to the data.

Input model description

The experiment was modeled using the nodalization shown in Figure A-1(b). The air injection is specified by a time-dependent junction (Component 102) to match the experiment value. The homogeneous (single-velocity momentum equation) option was specified at the air injection point (Junction 10103) to prevent liquid from flowing down the air injection pipe. The falling liquid film drained through Junction 10102. Inlet liquid flow rate was also specified by a time-dependent junction (Component 106) to match the measured value. The falling liquid film drained through a time-dependent junction (Component 195) where the outlet flow was set by a control system to maintain a fixed level in Pipe 190. A pressure of 0.104 MPa was specified for the drain tank (Component 200). Pressure in the test rig was controlled to 0.1 MPa by a time-dependent volume (Component 110).

Dukler discussed more than one CCFL correlation, but the one that appeared to be best for his test is a Wallis [A4] form of the correlation: $j_g^{1/2} + mj_f^{1/2} = c$, where j is defined as the non-dimensional superficial velocity, subscripts g and f refer to gas and liquid respectively, m is the slope, and c is the gas intercept constant. This correlation was found to be reasonable for air/water systems where standing waves appeared on the surface of the liquid film. Dukler found this to occur in his experiment. Wallis [A4] indicated that m = 1 and C varied between 0.88 and 1.0 for small diameter round tubes. The RELAP5-3D input model activated the CCFL model at the junction between Components 104 and 105. The CCFL input data for this junction used the following values: junction hydraulic diameter = 0.0508 m, flooding correlation form =0.0 (Wallis CCFL form), gas intercept c = 0.88, and slope m = 1.0.

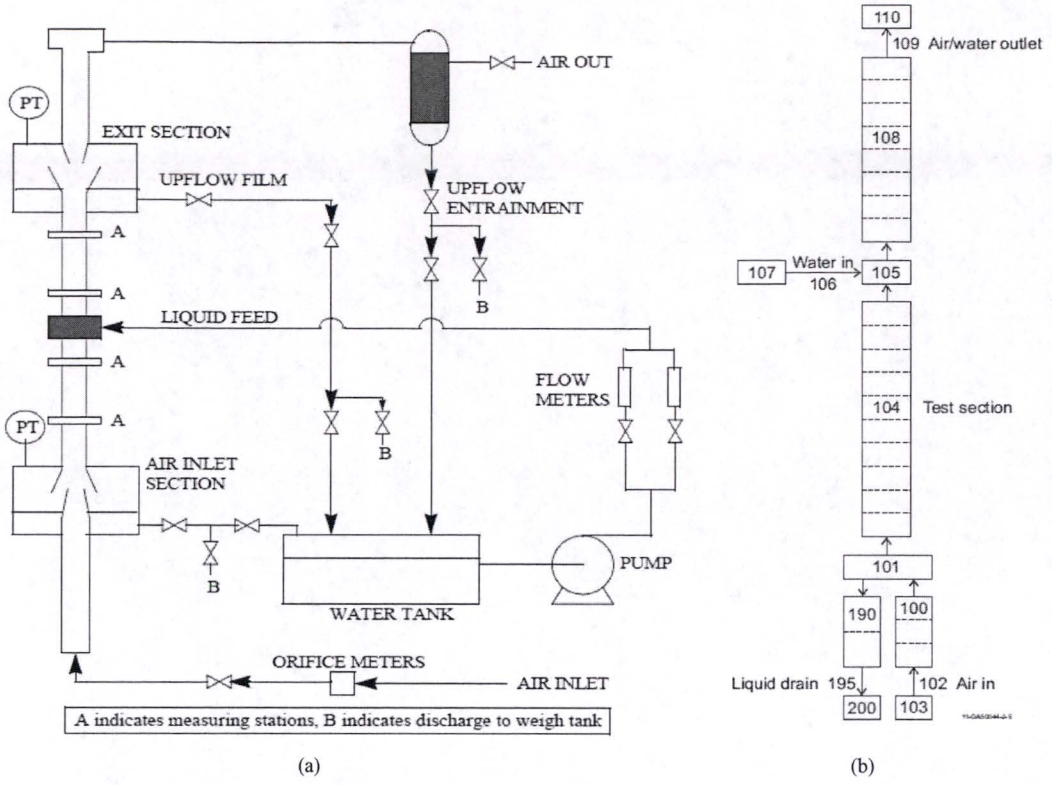

Figure A-1: (a) Schematic of the Dukler-Smith Air-Water Test Facility (from [11]) and (b) nodalization diagram for the Dukler-Smith test facility (from RELAP manual)

Data Comparisons and Results

The requested time step size for both the semi-implicit and nearly-implicit advancement scheme calculations was 0.005 s. Calculations were run with values of liquid and air injection flows consistent with the data. Figure A-2(a) compares the calculated liquid downflow rates with data at the given liquid injection flow rate. Good agreement with the data is observed in the predictions with both the semi-implicit and nearly-implicit advancement schemes. At the higher liquid injection rates, the calculated liquid downflow was less than the data, indicating more of the injected liquid was entrained and exited through the top. A possible reason for the under-calculated liquid downflow is that the values for the gas intercept and slope do not fit the data. As shown in Figure A-2(b), the semi-implicit calculated results are in excellent agreement with the flooding correlation of Wallis as the x-intercept (square root of superficial vapor velocity) for the predictions is 0.88 and the slope is 1.0. Thus the code is working properly based on the intercept and slope values input to the model.

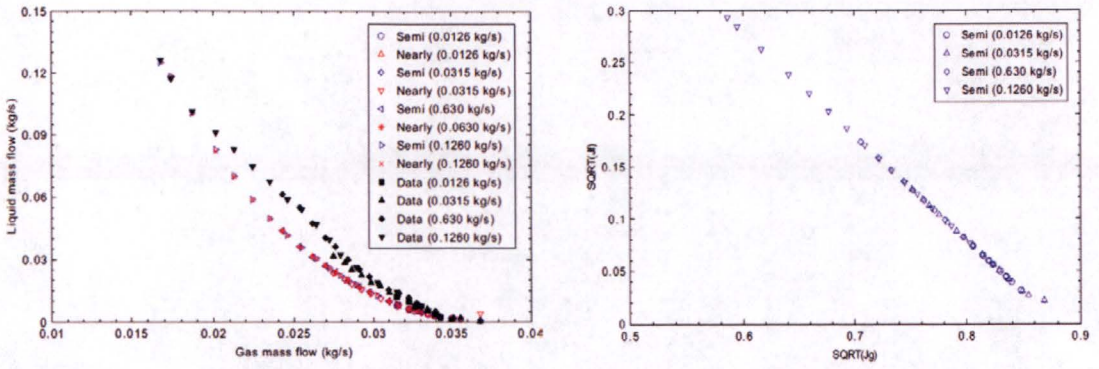

(a) (b)

Figure A-2. Comparison of RELAP5-3D predictions to Dukler-Smith data: (a) liquid mass flow vs. gas mass flow and (b) superficial liquid velocity vs. superficial gas velocity

Conclusions and Assessment Findings

RELAP5-3D predictions are in reasonable agreement with the Dukler-Smith experiment data for countercurrent air-water flow in a single tube over the range of air flows from 0.0126 to 0.126 kg/s. The assessment also shows that the Wallis correlation is implemented correctly.

References

[A1] A. E. Dukler and L. Smith, *Two Phase Interactions in Counter-Current Flow: Studies of the Flooding Mechanism*, NUREG/CR-0617, January 1979.

[A2] R. A. Riemke, "Countercurrent Flow Limitation Model for RELAP5/MOD3," *Nuclear Technology*, Vol. 93, pp 166-173, February 1991.

[A3] C. B. Davis, *Validation Report: RELAP5-3D Flooding Model, Code Version 1.3.5*, R5/3D-01-05, October 2, 2001.

[A4] G. F. Hewitt and G. B. Wallis, *Flooding and Associated Phenomena in Falling Film Flow in a Tube*, UKAEA Report AERE-R 4022, 1963.

Appendix 4-B. UPTF Downcomer CCFL Test 6, Run 131 (Section 4.16 in Manual vol.3)

Experiments were performed in the Upper Plenum Test Facility (UPTF) to obtain full-scale data on downcomer/lower plenum refill behavior during a loss-of-coolant accident initiated by a large break. The experiments provided a counterpart to testing that was done previously in scaled facilities.

Code Models Assessed

The relative performance of the annulus and pipe components for simulating the refill of the lower plenum during a loss-of-coolant accident was compared. The two components are similar except that all the liquid is placed in the film, with no liquid allowed in drops, in the annulus component when in the annular-mist flow regime. Liquid is allowed in both the film and drops in the annular-mist flow regime in the pipe component.

Experiment Facility Description

UPTF is a full-scale model of a four-loop 1300-MWe pressurized water reactor (PWR), including the reactor vessel, downcomer, lower plenum, upper plenum, and coolant loops. Simulators are used to represent the core, primary coolant pumps, steam generators, and containment. A schematic view of the test facility is shown in Figure B-1. Key dimensions are presented in Figure B-2. The test vessel, core barrel, and internals are full-size representations of a PWR, with four full-scale hot and cold legs that simulate three intact loops and one broken loop. Figure B-3 shows the positions of the four loops relative to the downcomer.

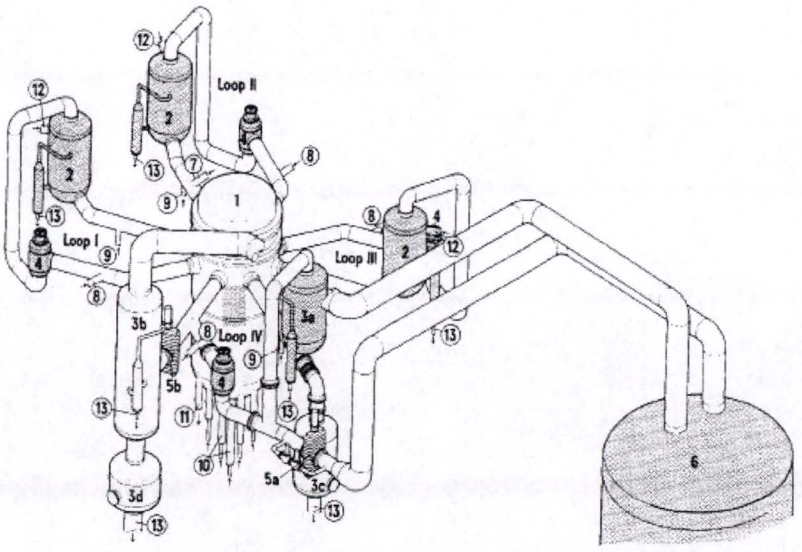

1 Test Vessel
2 Steam Generator Simulator (Intact Loop)
3a Steam Generator Simulator/ Water Separator (Broken Loop Hot Leg)
3b Water Separator (Broken Loop Cold Leg)
3c Drainage Vessel for Hot Leg
3d Drainage Vessel for Cold Leg
4 Pump Simulator
5a Break Valve (Hot Leg)
5b Break Valve (Cold Leg)
6 Containment Simulator
(7) Surgeline-Nozzle
(8) ECC-Injection Nozzles (Cold Leg)
(9) ECC-Injection Nozzles (Hot Leg)
(10) Core Simulator Injection Nozzle
(11) TV-Drainage Nozzle
(12) Steam Injection Nozzle
(13) Drainage Nozzle

Simulator

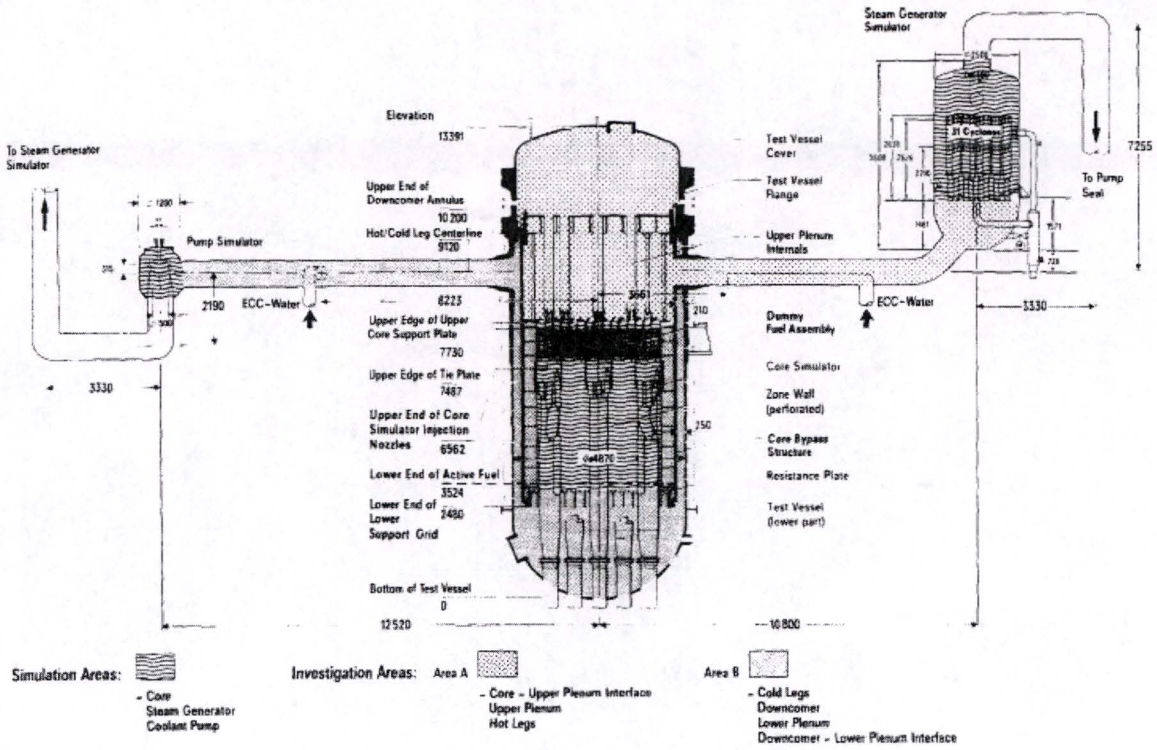

Figure B-2. Key dimensions of the UPTF

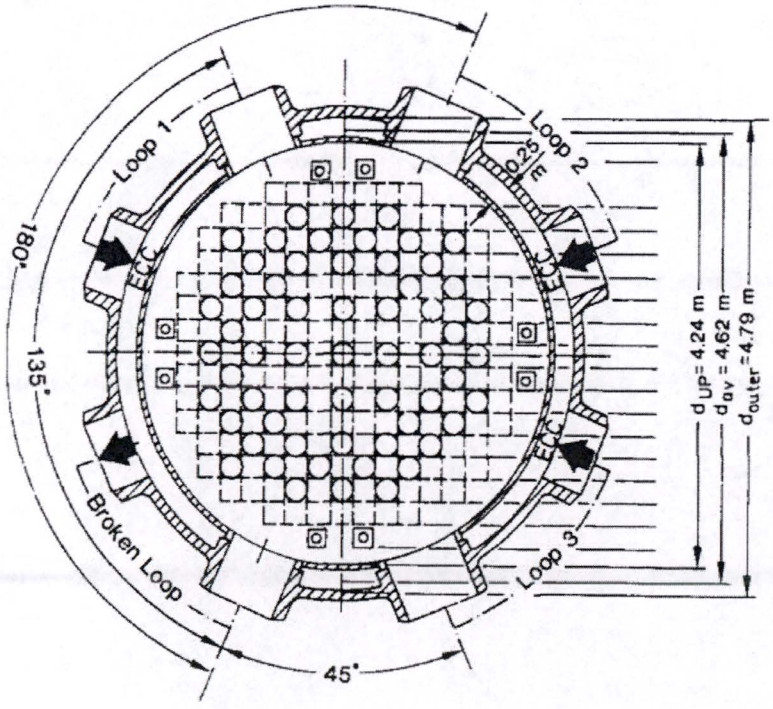

Figure B-3. Cross-section of the UPTF reactor vessel

Test 6 [B1, B2] was a quasi-steady-state experiment that was carried out to obtain full-scale data on downcomer/lower plenum refill behavior. Predetermined steam and emergency core cooling (ECC) water flow rates were injected into the system to determine the penetration of ECC water into the downcomer and lower plenum as a function of steam flow up the downcomer. Run 131 was selected for analysis. The system was initially filled with slightly superheated steam at about 2.5E5 Pa. The test was initiated by starting the steam flow from the core and steam generator simulators. ECC injection into the cold legs of the three intact loops began about 12 s later. The temperature of the ECC water was initially near saturated conditions. However, the steam flow caused the pressure to increase during the test, which caused the subcooling to increase. About 1 kg/s of nitrogen was injected along with the ECC to simulate noncondensable coming out of solution. The injection flow rates were terminated near 80 s. The pump simulators were closed during the test so that all the injected steam had to flow through the downcomer. Boundary conditions for Run 131 are summarized in Table B-1.

Table B-1. Summary of Test 6, Run 131 boundary conditions.

Parameter	Value
Total steam injection rate, kg/s	396
Total ECC injection rate, kg/s	1,447
ECC subcooling, K	58

Input Model Description

The RELAP5-3D nodalization used to simulate Run 131 is shown in Figure B-4. The model explicitly represented all four coolant loops. The break (Component 505) connected Loop 4 to the containment simulator (Component 599). The downcomer was divided into two halves, with Components 111 and 112 connected to the "broken" side (Loops 1 and 4) while Components 121 and 122 were connected to the "intact" side (Loops 2 and 3). These downcomer flow paths were connected in crossflow using single and multiple junctions (Components 118 and 119). The lower plenum was divided axially into two control volumes (Components 150 and 160), each containing approximately the same fluid volume. The core and hot legs were combined into a single volume (Component 180). A time-dependent junction (Component 198) supplied steam flow to the core. The ECC and nitrogen flows were supplied by time-dependent junctions (Components 398, 498, and 698).

Standard code options were applied except that the choking model was turned off at all junctions except for the break because of the low pressure at which the test was conducted (in order to prevent unphysical choking at the other junctions).

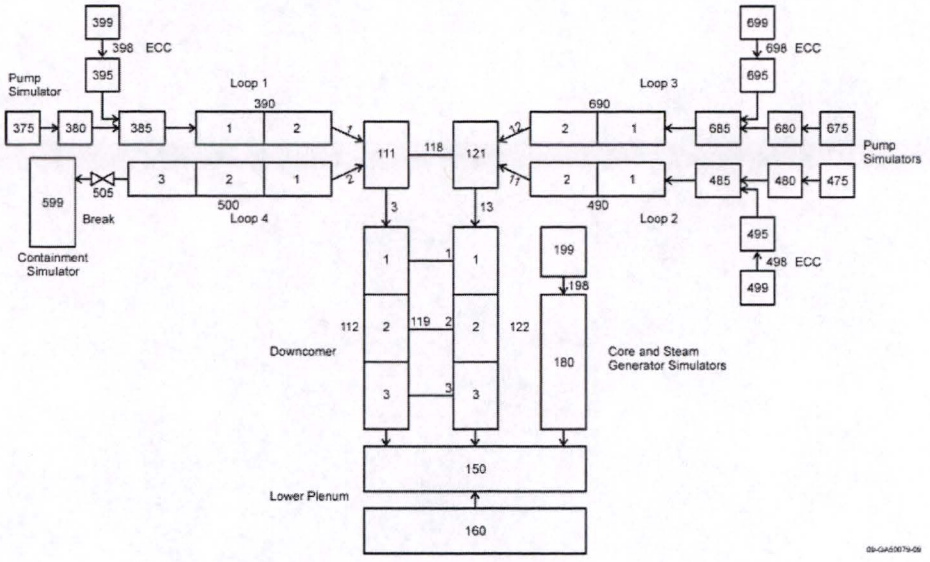

Figure B-4. RELAP5-3D nodalization for UPTF Test 6.

Data Comparisons and Results

Three RELAP5-3D calculations were initially performed, each with a requested time step of 0.01 s. The first two calculations used the semi-implicit numerical scheme. The downcomer was modeled with four annulus components (111, 112, 121, and 122) in the first calculation and four pipe components in the second calculation. The third calculation was identical to the first one except that it used the nearly-implicit numerical scheme. Figure B-5 shows the calculated pressure in the downcomer during the test. The initiation of steam flow, which corresponds to 0 s on the figure, caused the pressure to increase. The pressure increased again near 14 s when ECC reached the break, which reduced the volumetric flow out the break. The termination of steam and ECC flows near 80 s caused the pressure to decrease. Measured results are not presented because only limited data for UPTF Test 6 are publicly available.

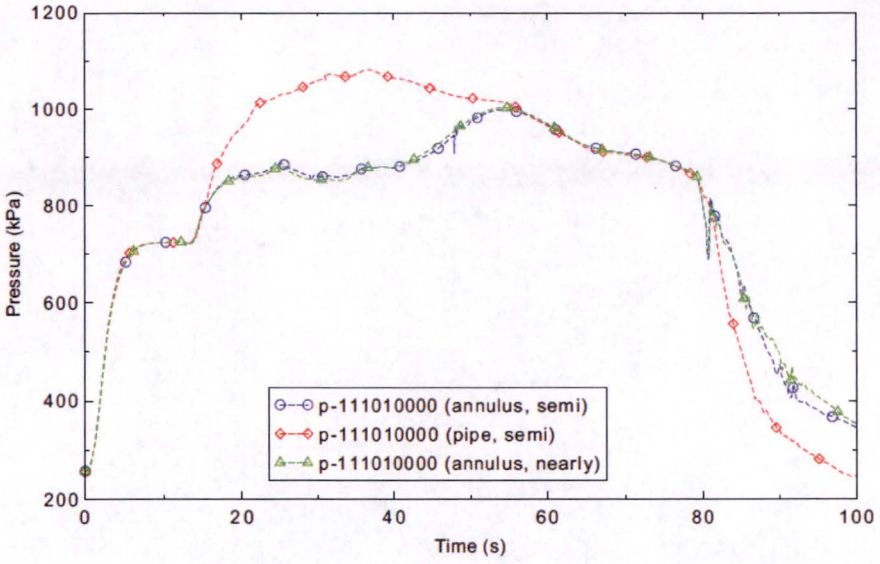

Figure B-5. Calculated downcomer pressure in UPTF Test 6, Run 131

The capability of the code to calculate the refill of the lower plenum is illustrated in Figure B-6, which shows measured and calculated collapsed liquid levels. The calculated values were obtained from the total liquid volume in the lower plenum and converted to liquid levels after accounting for the curvature of the lower head as well as the internals in the lower plenum. This method accounts for the varying flow area as a function of height and thus allows a more realistic indication of the liquid level than the traditional collapsed liquid level, which is obtained as the liquid volume fraction times the height summed over the number of volumes. The discussion will initially concentrate on the first calculation, which used annulus components and the semi-implicit numerical scheme. The gradual increase in the calculated liquid level prior to 15 s was due to the accumulation of droplets that were formed by condensation of the injected steam from the core. ECC first reached the lower plenum at 15.8 s. The liquid level increased relatively rapidly until 40 s, when the rate of increase decreased significantly until the steam and ECC injection ended near 80 s. The ending of the injection caused the pressure to fall as shown previously in Figure 4.16-5. The subsequent flashing in the lower plenum caused a reduction in the liquid level as the steam produced carried liquid from the lower plenum to the break. The calculated behavior was generally similar to the experiment except that the water began to reach the lower plenum about 6 s earlier than in the test and the level decrease after 80 s was much more pronounced than in the test. The calculated and measured rates of level increase were similar during the refill period. The increase in the indicated level at the start of the test is attributed to the effect of the steam flow on the differential pressure taps, rather than the presence of actual liquid because ECC flow did not begin until about 12 s. The different flow regime model used in the pipe component resulted in a delay in the liquid reaching the lower plenum and a substantially slower rate of refill. The calculated results with the nearly- and semi-implicit numerical schemes were similar.

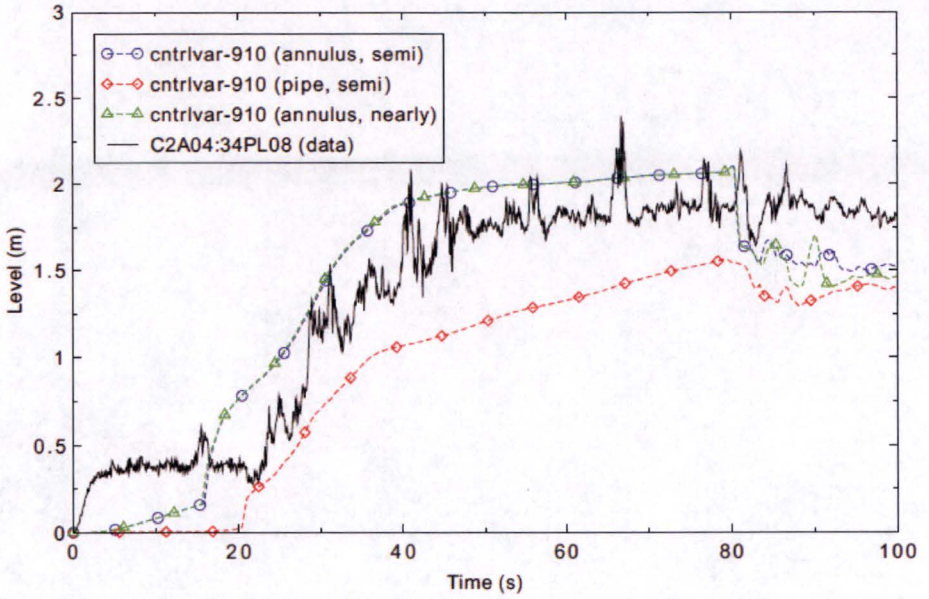

Figure B-6. Measured and calculated collapsed liquid level in the lower plenum in UPTF Test 6, Run 131.

Figures B-7 and B-8 show the calculated mass flow rate and fluid density in the broken cold leg, respectively. The figures indicate that ECC first reached the break near 14 s. Thereafter the mass flow and density increased substantially due to the bypass of ECC. More bypass was initially obtained in the calculation with the pipe component. The flow rate and density also increased substantially in the two annulus calculations when the injection flow rates were terminated near 80 s. The flashing in the lower plenum that was caused by the pressure decrease caused liquid to be entrained from the lower plenum to the break, resulting in an increase in the flow rate and density in the broken loop.

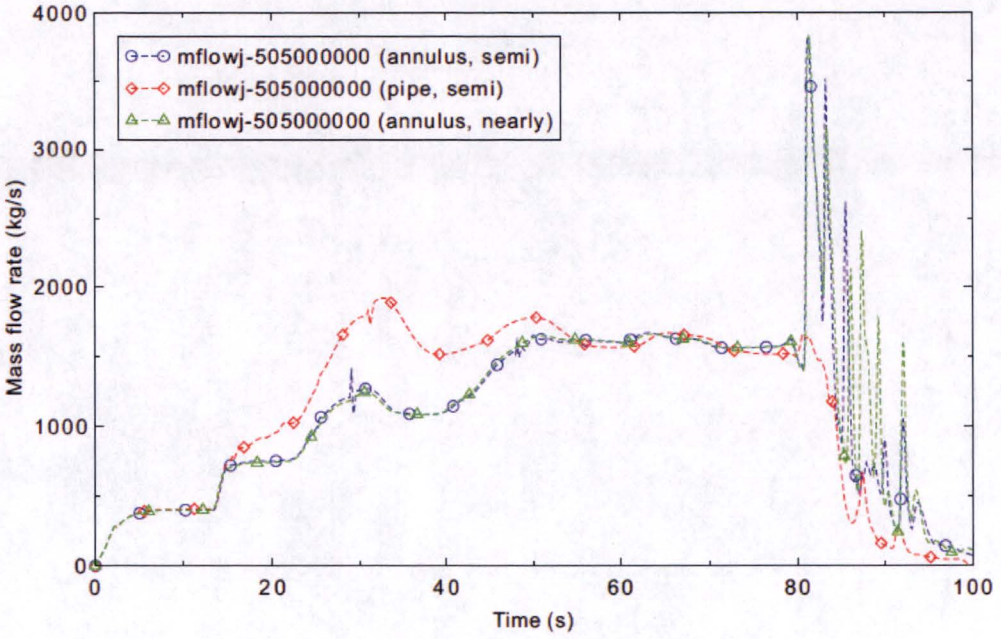

Figure B-7. Calculated break mass flow in UPTF Test 6, Run 131.

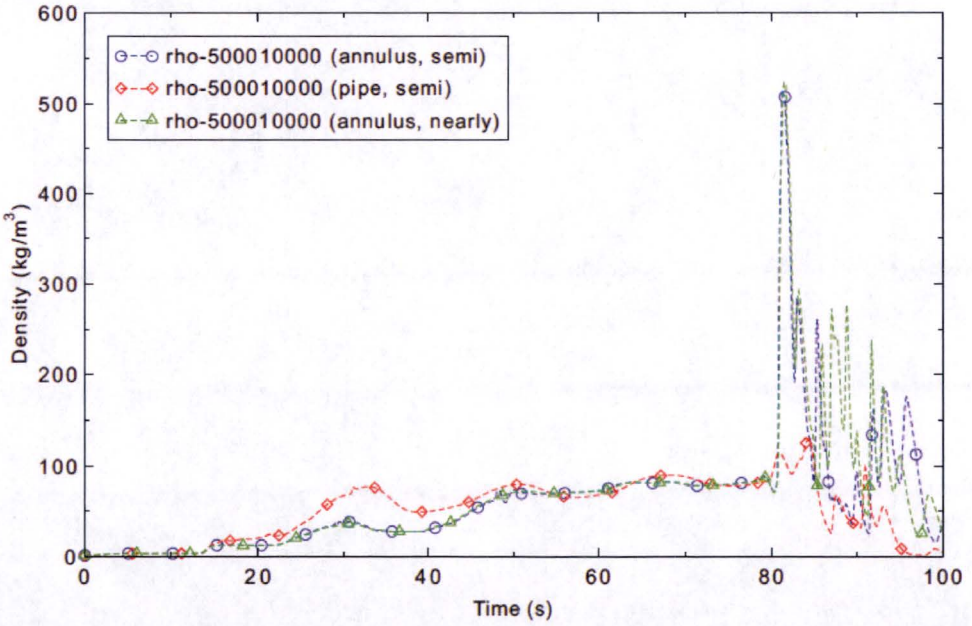

Figure B-8. Calculated fluid density in the broken cold leg in UPTF Test 6, Run 131.

An additional sensitivity calculation was performed to investigate the effects of the lower plenum nodalization. In this sensitivity calculation, the lower plenum was modeled with one control volume (Component 150) rather than the two volumes used previously. Figure B-9 shows that the initial refill of the lower plenum was similar with both models. However, the refill of the lower plenum slowed earlier when the single volume was used. The two

calculations bracketed the data between 40 and 80 s, with the single volume lower plenum under predicting the level and the two-volume model over predicting it. The sensitivity calculation demonstrates that the total amount of liquid stored in the lower plenum at the end of the refill period depends on the nodalization.

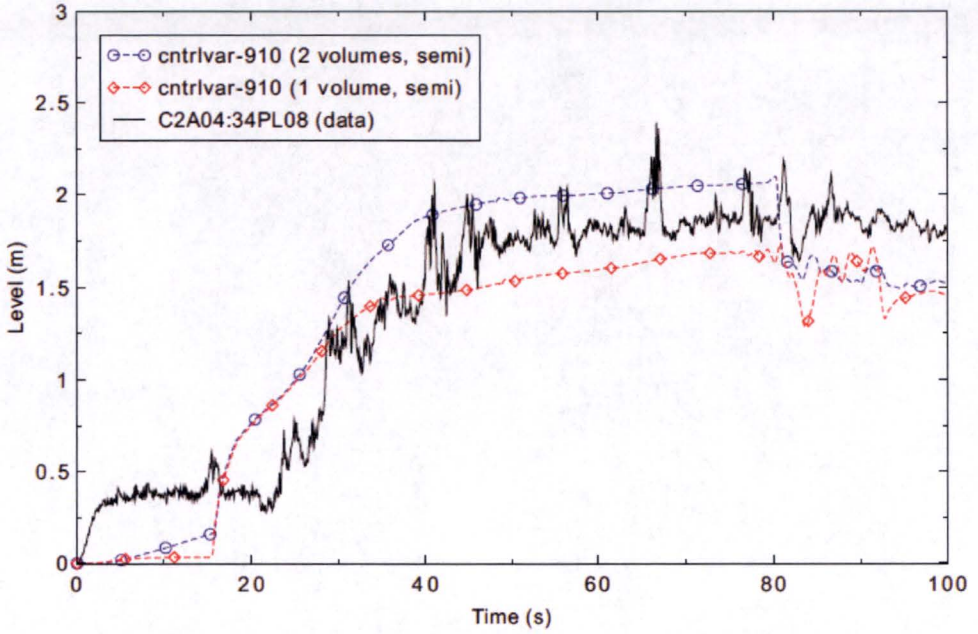

Figure B-9. The effect of nodalization on collapsed liquid level in UPTF Test 6, Run 131.

Conclusions and Assessment Findings

The RELAP5-3D calculations are judged to be in reasonable agreement with the measured liquid level data for UPTF Test 6, Run 131. The calculated refill was similar to that observed in the test, but started about 6 s earlier.

The RELAP5-3D calculation in which the downcomer was modeled with annulus components was in better agreement with the measured results than when pipe components were used. The annular mist flow regime model in the annulus component, which puts all the liquid in the film, resulted in a better prediction of the lower plenum refill for the UPTF test. The pipe component provided a conservative prediction of the amount of liquid in the lower plenum. The semi- and nearly-implicit calculations produced similar results. The liquid inventory in the lower plenum at the end of the refill period depends on the nodalization.

References

[B1] J. Liebert and P. Weiss, "UPTF Experiment Effect of Full-Scale Geometry on Countercurrent Flow Behaviour in PWR Downcomer," *Proceedings of Fourth International Topical Meeting on Nuclear Reactor Thermal-Hydraulics, NURETH-4, Karlsruhe, F.R.G., October 10-13, 1989*, Volume 1, pp. 67 - 74.

[B2] H. Glaeser, "Downcomer and tie plate countercurrent flow in the Upper Plenum Test Facility (UPTF)," *Nuclear Engineering and Design*, 133 (1992), pp. 259-283.

5. Other Models

This includes models for special components (pumps, separator/dryer), heat conduction, and reflood model, and reactor kinetics. These models are not used or have a minor importance in the LTCC EM.

6. Conclusions

Closure relationships and correlations are available in RELAP5-3D to provide closure of the field equations.

The most Important and relevant phenomenon during the post-core blockage LTCC phase of a HB LOCA is identified to be the CCFL. The models used in RELAP5-3D to predict this phenomenon are explained in detail, and evidence is provided to support the validity and adequacy of the models as implemented in the code, and the settings used in the LTCC EM.

Based on the simulation results, the heat transfer regime observed in the core is the nucleate boiling. Additional details of the use of specialized correlations for predicting the heat transfer coefficient under these conditions is provided.

The closure relationships included in the RELAP5-3D computer code are adequate to simulate the HLB LOCA scenarios included in the LTCC EM, and to predict the behavior of the primary system during the blowdown, refill/reflood, and pre- and post-core blockage LTCC phases of the accident.

Follow-up SNPB-3-17 Validation of the evaluation model

Initial RAI: *Provide appropriate validation demonstrating that the LTCC EM will result in a reasonable prediction of the important figures of merit for the accident scenarios considered. Demonstrate that the validation covers the range of the accident scenarios used in the LTCC EM. This validation should include comparisons to integral test data and appropriately address the model's uncertainty. Where appropriate, discuss any similarity criteria, scaling rationale, assumptions, simplifications, and/or compensating errors.*

Follow-up question:

In their response, STPNOC provided a summary of the verification of the adequacy of the parameters used in the LTCC EM, a summary verification of the input models, and a summary of the judgment of the simulation results. While the information provided to justify the simulation results discusses various tasks that were performed to ensure the simulation is correct, that information falls more into quality assurance as it demonstrates that the inputs are correct and that the EM is predictable. Provide validation to demonstrate that the results from the EM are a reasonable prediction of the laws of nature.

Provide information to support the trustworthiness of the overall results of the LTCC EM. While such information is usually provided by comparison to an integrated experiment, the NRC staff is aware that such experiments are not available. However, a case can still be made, based on the relative simplicity of the simulation, the well-known phenomena modeled, and details of the numerous conservative assumptions, that the result of the LTCC EM can be trusted as a reasonable prediction.

STPNOC Response

The STP LTCC EM uses PCT as the figure of merit indicating adequate core flow during the hypothesized core blockage HLB scenarios. The LTCC EM results in a reasonable prediction PCT for the accident scenarios considered (ranging from SBLOCA to LBLOCA in the range 2—16 inches) based on the validation results summarized below.

General comments

The STP LTCC EM is restricted to HLB scenarios which are well-known to be less challenging to Westinghouse PWR ECCS performance from the many analyses and experiments performed since the early 1970's. Cold leg breaks are addressed with the debris mass balance methodology described in Attachment 1-3, and do not require a thermal-hydraulic analyses as part of the LTCC EM.

HLB scenarios are less limiting because the break flow imbalance (loop resistances) favors continued flow up through the core (discussed in SNPB 3-2). In traditional HLB scenario analyses, the core is supplied with flow for the entire transient duration. The STP LTCC EM is completely consistent with the long-standing understanding of the HLB scenarios prior to the specific LTCC scenario variation for GSI-191 consideration whereby the core and core bypass are assumed blocked. Following core blockage in the LTCC assumption, the expected trends are observed in the STP LTCC EM analyses; flow is stopped in the core resulting in reduced heat transfer capability, increased voiding as the inventory boils off, and a rise in the clad temperatures. Because the ECCS flow is supplied at high pressure

and at rates much greater than the core cooling requirement, the core, which is at an elevation lower than the supplied water, is eventually refilled by the ECCS.

Resistance to refill (CCFL) from above the core (following the core blockage assumption) is known to be related to gas velocities that are higher in two phase flow regimes where the liquid phase reduces the flow area. The STP LTCC EM is consistent with intuition here as well; in the later phase of the scenario, core decay heat is much lower, resulting in lower vapor velocities. CCFL is addressed in more detail in the supplemental response to SNPB RAI 3-13.

To ensure uncertainties are bounded in the STP LTCC EM, several uncertainties have been identified and ranked as described in the response to SNPB RAI 3-22; the uncertainties have been considered and bounded by assumptions as described. By including bounding assumptions for uncertainties in all models and specific assumptions in specific simulations, validation of the STP LTCC EM can be limited to assessing the simulated response against expected behaviors and trends.

SBLOCA

The SBLOCA scenarios are dominated by single-phase flow and the ability to remove decay heat through the steam generator in natural circulation. However, the operator action to cool down using the steam generators as directed by the EOPs is not modeled in the STP LTCC EM; therefore, the plant response only reflects decay heat removal through the break flow. The relatively low break flow rates in SBLOCA also reduce core up-flow (HLB scenarios).

Based on the assumptions and conservatisms included in the SBLOCA simulation, less decay heat can be removed through the break, and along with ECCS head increase due to lower flow rates than for the designed LBLOCA, the system temperature and pressure response is slightly higher than for LBLOCA and, for the reasons mentioned, the PCT in SBLOCA (as modeled) is slightly higher than for LBLOCA. Because the RCS water inventory is maintained by ECCS in SBLOCA, heat removal is not challenged.

Based on the overall model conservatisms and the additional assumption of no operator action, the simulated response is completely consistent with expected response in the actual plant setting if all the simulated conservatisms assumptions were realized.

LBLOCA

LBLOCA scenarios are dominated by two-phase flow and large pressure gradients, especially in the initial blowdown phases of the simulation. These large pressure gradients force large up-flow rates through the core until core blockage. The STP LTCC EM reflects this expected response and, unlike in CLB scenarios, full ECCS flow rates are expected to just refill the system up to the break elevations. In the LBLOCA cases, lower system pressures and temperatures result due to the lower saturation pressures.

Following the initial blowdown, during the LTCC phase with core blockage, the RCS flows are dominated by body forces, completely consistent with an "open system" behavior. That is, the ECCS flows, which exceed the core decay heat load demand, must simply fill to the

highest elevation before flowing further. Because the core elevation is low, and other paths that are filled are at higher elevations, flow to the core begins when these paths overflow. This behavior is consistent with behavior of gravity-driven flows.

In addition to the results from the base model simulations, several sensitivity analyses were performed as documented in SNPB RAI 3-20. In those sensitivity analyses, as shown in the response, the trends are consistent with the understanding of the expected behavior.

The STP LTCC EM LBLOCA model simulated response is completely consistent with expected response in the actual plant setting if all the simulated conservative assumptions were realized.

Follow-up SNPB-3-18 Mesh size sensitivity

Initial RAI: *Demonstrate that the LTCC results are independent of mesh size for the accident scenarios under consideration.*

Follow-up question:

In its response, STPNOC provided a mesh sensitivity study on the radial mesh in the core. The base case uses a single set of axial nodes for the core region. In the mesh sensitivity, the licensee created another axial set of nodes to specifically model the hot channel in the core. This sensitivity study was performed to maximize the likelihood for CCFL to occur, as this would reduce the quantity of liquid which could act to cool the core. The results of the sensitivity study confirmed that there was no appreciable difference in the PCT of the two-channel core versus the one-channel core. However, STPNOC did not provide enough information to determine why these results occurred or if the second channel had any impact at all on the analysis. In order for the NRC staff to understand the radial mesh sensitivity study, STPNOC is requested to address:

- Was there a difference in CCFL between the average and hot channel?

STPNOC Response

While the CCFL phenomenology remains the same in both channels, the simulation shows that conditions for CCFL occur more frequently at the top of the hot channel than the average channel. The cumulative CCFL-limited time (defined as time integral of the RELAP5-3D variable *ccflf,* described in detail in the response to RAI-SNPB-3-02 follow up, bullet 5), is plotted for the average and hot channels' exit in Figure 1.

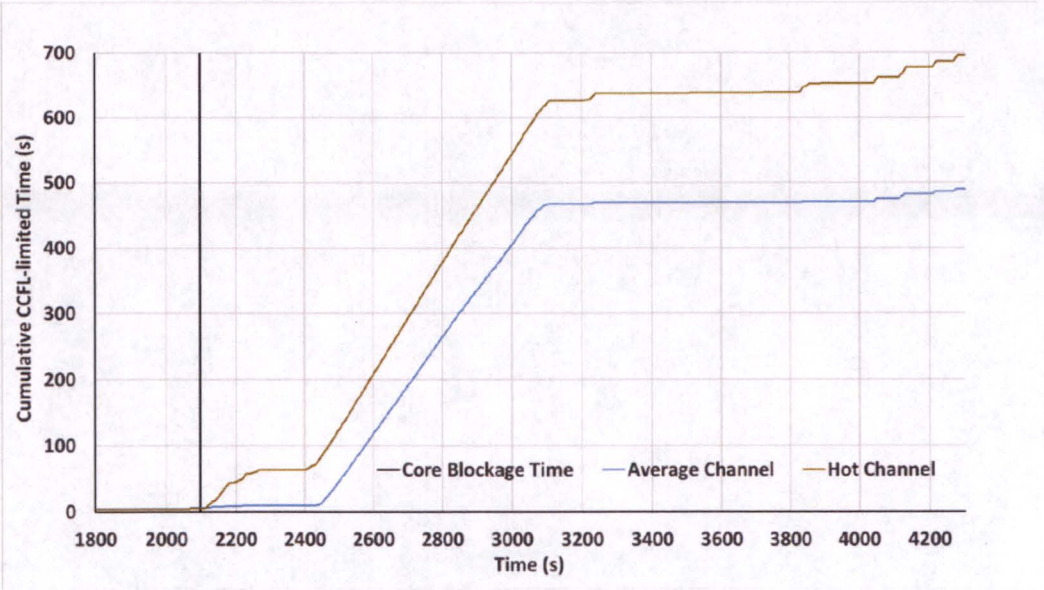

Figure 1. Cumulative CCFL-limited Time

- Was the PCT taken from the hot channel, from the average channel, or from both?

STPNOC Response

The PCT is calculated as the maximum of the temperature of all nodes of the three heat structures defined in the LTCC EM (HS 6050, 6060, and 6061, representing the cladding of the average assembly, hot assembly, and hottest rod, respectively) at each time step of the simulation. As also discussed below (see temperature profiles in Figure 2), the highest temperature of the cladding is recorded at the heat structures of the hot channel.

- What were the temperature profiles of the different channels?

STPNOC Response

Axial temperature profiles of the cladding in the average assembly, hot assembly, and hottest rod are plotted in the figures below. The profiles are taken from two different times during the post-core blockage LTCC phase. In particular:

- Figure 2 shows the cladding temperature profile at the time CCFL is not active
- Figure 3 shows the cladding temperature profile at the time CCFL is active on both average and hot channels

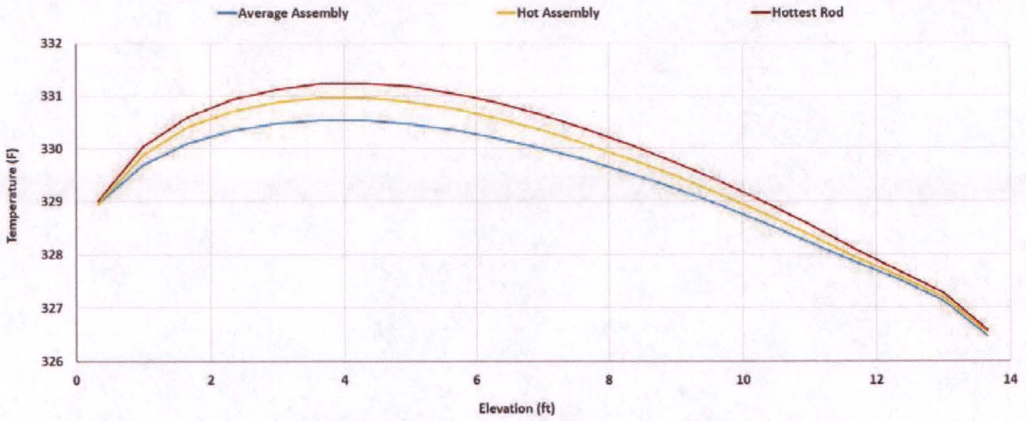

Figure 2. Cladding Temperature Profile – CCFL Not Active

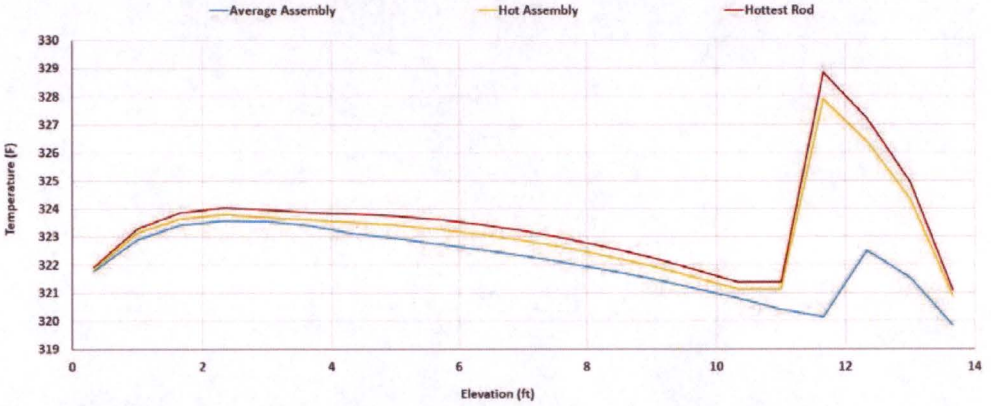

Figure 3. Cladding Temperature Profile – CCFL Active

NOTE: Y-axis scale is zoomed to show the difference in the temperature profiles. When CCFL is not active, liquid can enter the core, enhancing the cooling of the top of the core (Figure 2). Under these conditions, higher temperatures are simulated near the bottom half of the core.

When CCFL is active, liquid is prevented from entering the core and cooling at the top is degraded. Under these conditions, higher temperatures are simulated near the top of the core.

- Did STPNOC notice any difference in the flow through the hot channel?

STPNOC Response

The liquid and vapor velocities at the exit of the average channel (junction 84502) and hot channel (junction 84503) are plotted in Figure 4. Similar considerations provided in the response to RAI-SNPB-3-02 (bullet 5) can be made for this case:

(1) During the pre-core blockage LTCC, the ECCS water is forced to flow through the core (both average and hot channels) from the inlet. Both channels are fully

covered. The velocity of the liquid is positive (upward) in both channels. Vapor velocity is set by the code equal to the liquid velocity since the void fraction is zero (no vapor).

(2) At the sump switchover time, ECCS temperature increases. When higher temperature water reaches the core, voids are produced due to reduced sub-cooling of the inlet liquid. Velocities of both liquid and steam are positive (upward). As expected, hot channel exit velocities are higher than the average channel exit velocities.

(3) At core blockage, liquid velocity gradually decreases on both channels. Voids increase in the core. Liquid velocity is negative (downward) for both average and hot channels. Liquid is now entering the core from the top. Steam leaves the core from the top toward the break in hot leg. The steam velocity is positive (upward). Steam velocity of the hot channels is higher than the average channel.

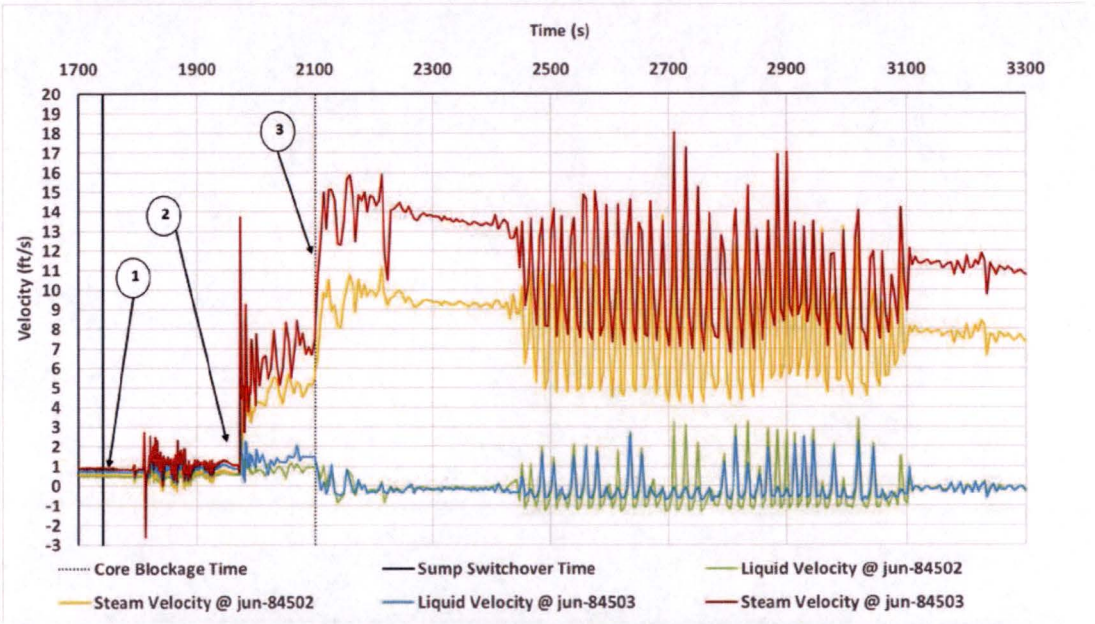

Figure 4. Liquid and Vapor Velocity at Core Exit

- Additionally, the only mesh size sensitivity study discussed by STPNOC was a radial mesh size sensitivity study. Depending on the scenario, NRC staff have found varying levels of sensitivity to axial nodalization. Did STPNOC perform an axial nodalization study? If so, provide a discussion of the results.

STPNOC Response

STPNOC has conducted a sensitivity study to confirm that effects of the core axial nodalization to the PCT simulated during the LTCC with core blockage are negligible. The RELAP5-3D input file used to execute the simulation is generated from the LTCC EM 16" HLB LOCA input file (base case), with the change on the core axial nodalization.

Base Case: 21 axial nodes
Sensitivity: 10 axial nodes
All boundary conditions for the simulation are the same as the ones applied to the base case.

Simulation Results and Comments

Table 1 lists the simulation timing for the base case and the sensitivity case, showing no appreciable differences in the accident progression.
The PCT (figure of merit) is plotted in Figure 5. No appreciable difference in the cladding temperature is observed.

Table 1. Simulation Timing

Phase	Event	Simulation Time (s)	
		Base Case	Sensitivity
Blowdown	Break Opening	300	300
	Low PZR pressure Signal	306	306
	MFW isolation	308	308
	Reactor Trip	308	308
	Reactor Fully Scrammed	311	311
	HPSI Pumps Activation	312	312
	RCP Trip	314	314
	LPSI Pumps Activation	316	316
Refill/Reflood	AFW Actuation	338	338
	Accumulator Actuation	383	383
	Minimum Core Collapsed Liquid Level	417	396
	Core Full	434	442
LTCC	SSO	1740	1739
	Core Blockage	2100	2099

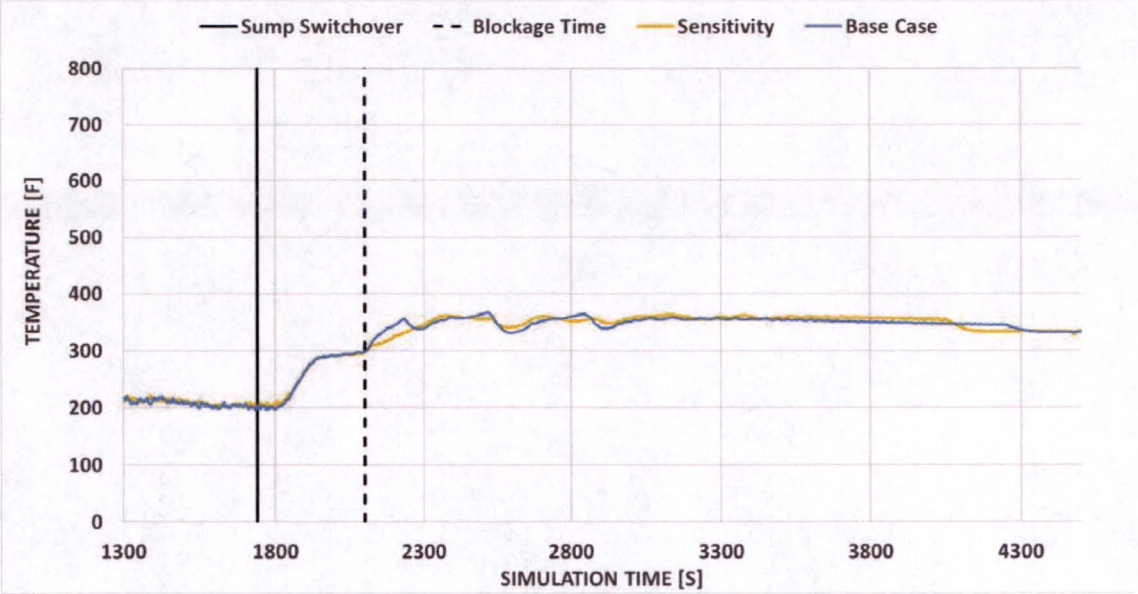

Figure 5. PCT

Follow-up SNPB-3-19 Initial Test Cases

Initial RAI: *Provide a summary of the assessment cases performed in order to demonstrate that RELAP5-3D has been installed and is being used appropriately.*

Follow-up question:

In its response, STPNOC provided an explanation of the initial test cases, but it was not clear if these test cases were the complete set recommended by the developers of RELAP5-3D to verify a correct installation, or merely a subset. Additionally, STPNOC did not discuss the success criteria for each of the test cases and did not confirm that the criteria was satisfied. Confirm that the test cases run were the complete set recommended by the RELAP5-3D developers and provide the results of each case.

STPNOC RESPONSE

The RELAP5-3D software has been installed and currently in use in compliance with the South Texas Project Electric Generating Station Software Quality Assurance Program 0PGP07-ZA-0014 revision 10 [1].

Fifty-nine (59) run-time environment (RTE) test cases are included in the RELAP5-3D installation CD. Each of the cases are is reviewed for applicability and scope of the GSI-191 thermal-hydraulic analyses. Of the 59 cases, eleven (11) cases are relevant to the GSI-191 simulations and are include in the RTE test matrix.

The selected cases are executed and the simulation results (output) are compared with the outputs included in the RELAP5-3D installation CD.

The acceptance criterion applied is that there should be reasonable agreement in the results between the local version of the code and the outputs included in the RELAP5-3D installation CD. The comparison is performed considering that output variations due to running the code with different computer name and precision, CPU time, file paths, dates, times, operating system, and hardware are expected. Nevertheless, no significant variations in the calculated results are expected.

The table below summarizes the results of the output comparison performed [1]. The RTE testing show that the test cases have verified the software functionality by successfully comparing the test case outputs (results) with the reference outputs provided by INL in the installation CD.

Software Name:	**RELAP5-3D**	Software Rev.:	**4.1.3**	
Tester:	Timothy Crook	Test Date:	11/20/2015	
Test Plan No.:	See Section 4.0	Test Case No.:	See Table 3-1	
Case #	**Test Requirement**	**Test Results**		**Pass/Fail**
2	Acceptance criterion: Reasonable agreement of the test results between the installed version and the INL supplied outputs (Comparison of output files)	There were no technical differences in the results between the outputs generated with the installed version and the INL supplied outputs.		Pass
4	Same as above	Same as above		Pass
5	Same as above	Same as above		Pass
17	Same as above	Same as above		Pass
19	Same as above	Same as above		Pass
20	Same as above	Same as above		Pass
21	Same as above	Same as above		Pass
25	Same as above	Same as above		Pass
42	Same as above	Same as above		Pass
50	Same as above	Same as above		Pass
52	Same as above	Same as above		Pass

[1]. 0PGP07-ZA-0014 "Software Quality Assurance Program" STI 33856275 rev.10, 04/17/2014.

Follow-up SNPB-3-20 Specific sensitivity studies

Initial RAI: *During the audit, the NRC staff identified a number of sensitivity studies that would be important for the review of the proposed long term core cooling evaluation methodology. STP should perform the following sensitivity studies and submit plots of the relevant figures of merit and important timings for long term core cooling analysis:*

a) Appendix K decay heat load with single worst failure and steam generator tube plugging
b) Axial power shape
c) Break sensitivity study with appropriate break size resolution
d) No bypass blockage

Follow-up question:

In its response, STPNOC provided an overall summary of the sensitivity studies. However, this summary did not provide important details such as the plots of the figures of merit and justifications for the selections of certain input parameters. Provide the following:

- Plots of the figures of merit
- Discussion of the values of the important inputs chosen for the sensitivities. Where did those values originate and are they typical values (were the top and bottom peaked power shapes typical of top and bottom power peaking, why are the inputs for sensitivity 'a' so much different from the rest and are those values typical of plant or accident conditions, etc.)
- A summary of how the overall accident progression differed from the nominal case in each sensitivity study
- A more detailed discussion of the barrel-bypass sensitivity, including a reference to the PWROG testing performed to show the effect of fiber on flow orifices

STPNOC RESPONSE

Sensitivities are performed to study the effects of selected thermal-hydraulic parameters on the core coolability during the post-core blockage LTCC. The PCT is used as figure of merit for all cases. The PCT is calculated as the maximum of the temperature of all nodes of the three heat structures representing the cladding surface in the core. The 16" HLB LOCA scenario is used as reference case (identified as "base case" below).

SENSITIVITY a) Appendix K decay heat load with single worst failure and steam generator tube plugging.

Boundary Conditions and other Assumptions
The following conditions are assumed for this sensitivity:

- Augmented decay power (+20%) from the ANS-79 model used in the base case.

- Single train failure (1 HHSI + 1LHSI + 1CS). The failure is assumed to occur at the beginning of the transient. In order to minimize the total ECCS flow available for cooling, the unavailable SI train is assumed to be in one of the intact loops (loop 2).
- SG tube plugging equal to 10%.

As described in the answer to SNBP-3-22, several conservatisms are included in the LTCC EM by imposing margin to the nominal (best-estimate) values of important thermal-hydraulic parameters. This includes conservatisms on:

- the RWST usable volume to minimize the SSO time
- the RWST water temperature, to minimize the level of sub-cooling of the injected water during the safety injection phase (before core blockage)
- the sump pool temperature, to minimize the level of sub-cooling of the injected water during the recirculation phase (after core blockage)
- the effect of the RHR heat exchanger on the temperature of the ECCS injection. The LTCC EM does not account for the cooling effect of the RHR HXs. The RHR HXs are assumed to be unavailable following core blockage, to minimize the sub-cooling of the injected water during the recirculation phase (after core blockage)
- Core blockage and core barrel/baffle bypass fractions, assumed 100% and instantaneous at 15 gm/FA (there would be no blockage in the BB bypass)

These conservatisms added to the conditions assumed in the sensitivities (+20% decay heat; ECCS worst train failure, and maximum SG plugging) require relaxation to prevent core uncovery.

Some of the thermal-hydraulic parameters listed above are set to their nominal values in this sensitivity. Description of these parameters is provided below.

RWST Usable Volume

In the LTCC EM, the RWST usable water volume is set to to 360,000 gallons, as per STP design basis calculation MC-5037 Rev. 9. The nominal (best-estimate) usable RWST volume is approximately 458,000 gallons. The RWST volume used for this sensitivity is set to the nominal value of 458,000 gallons.

RWST Water Temperature

In the LTCC EM, the RWST water temperature is set to 130 °F as per the UFSAR. The nominal RWST water temperature is equal to 85 °F (based on STP Accident Analysis Design Basis). The RWST water temperature used in this sensitivity is to the nominal value of 85 °F.

Sump Pool Temperature

The sump pool temperature profile used in the base case LTCC EM is the STP design basis calculation NC7032.
The temperature imposed in this sensitivity represents a nominal best estimate sump pool temperature at the SSO time for a large break of a typical PWR. This value is taken from

the NUREG-6770 [1], and assumed to be constant during the post-core blockage LTCC phase.

Other Boundary Conditions

All other boundary conditions are the ones used in the LTCC EM – Base Case.

Simulation Results

The accident scenario progression is summarized in Table 1. The accident progression simulated in the sensitivity (Case a) are aligned with the event timing of the LTCC EM-Base Case from the break opening until the core is fully flooded.
Due to the lower total ECCS flow rate in the sensitivity a, resulting from the assumed failure of the of one train of ECCS, and the larger RWST usable volume, the SSO time and, subsequently, the core blockage time are found to occur at a later time.

Table 1. Accident Progression Time Table (Sensitivity a)

Phase	Event	Simulation Time (s)	
		Base Case	a
Blowdown	Break Opening	300	300
	Low PZR pressure Signal	306	306
	MFW isolation	308	308
	Reactor Trip	308	308
	Reactor Fully Scrammed	311	311
	HPSI Pumps Activation	312	312
	RCP Trip	314	314
	LPSI Pumps Activation	316	316
Refill/Reflood	AFW Actuation	338	338
	Accumulator Actuation	383	381
	Minimum Core Collapsed Liquid Level	417	422
	Core Full	434	439
LTCC	SSO	1740	2654
	Core Blockage	2100	3014

Figure 1 shows the comparison of the PCT during the pre- and post-core blockage LTCC phases. The saturation temperature of the coolant in the core for both cases is also included in the figure.

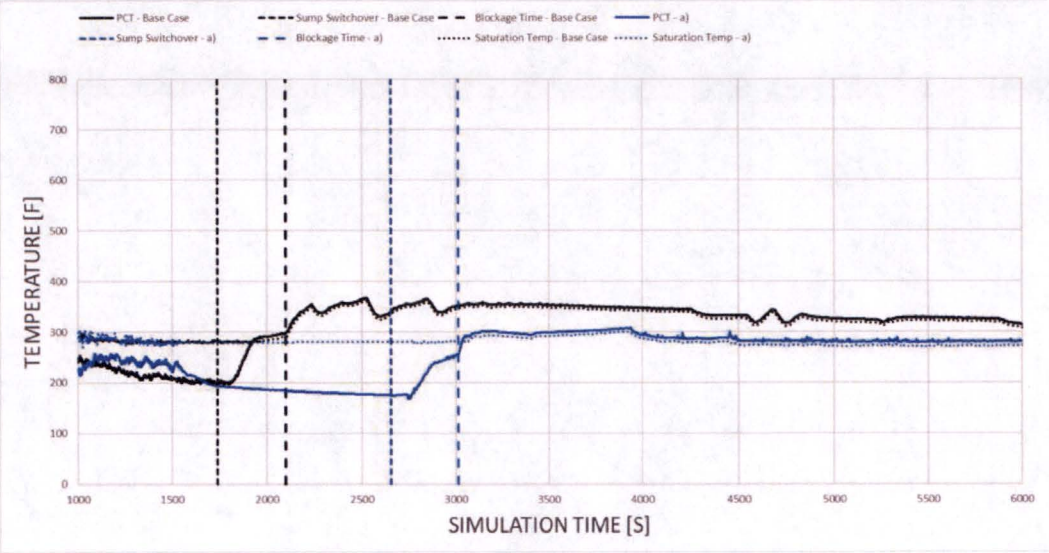

Figure 1. PCT (Sensitivity a)

The phenomena simulated in this sensitivity are similar to the ones observed in the LTCC EM Base Case. PCT is maintained slightly above the saturation temperature of the coolant in the core. Due to the lower injection flow rate for the sensitivity, the primary pressure is slightly lower than the one simulated with the base case. This results in a lower saturation temperature and, subsequently, in a lower PCT.

[1]. NUREG/CR-6770 LA-UR-015561, "GSI-191: Thermal-Hydraulic Response of PWR Reactor Coolant System and Containments to Selected Accident Sequences", August 2012.

SENSITIVITY b) - Axial power shape.

Boundary Conditions and other Assumptions

This sensitivity is performed to study the effect of the core axial power profile on the post-core blockage LTCC PCT. The LTCC EM assumes the core axial power distribution to follow the "chopped" cosine shape. Two axial power shapes are investigated in this sensitivity as described below.

Sensitivity b1) – Top Skewed.

The axial power profile is chosen to represent the STP relative axial power distribution at hot full power (HFP), beginning of life (BOL) and equilibrium Xenon.

Sensitivity b2) – Bottom Skewed.

The axial power profile is chosen to represent the STP relative axial power distribution at hot full power (HFP), end of life (EOL) and equilibrium Xenon.
All other boundary conditions for the sensitivities b1) and b2) are the same of the ones imposed in the LTCC EM Base Case.

Simulation Results

The accident scenario progression is summarized in Table 2. As expected, the accident progression simulated in these sensitivity (Case b1 and b2) are aligned with the event timing of the LTCC EM- Base Case during all phases. No appreciable difference in the event timing is observed. SSO time and core blockage time occurs approximately at the same time.

Table 2. Accident Progression Time Table (Sensitivity b)

Phase	Event	Simulation Time (s)		
		Base Case	B1	B2
Blowdown	Break Opening	300	300	300
	Low PZR pressure Signal	306	306	306
	MFW isolation	308	308	308
	Reactor Trip	308	308	308
	Reactor Fully Scrammed	311	311	311
	HPSI Pumps Activation	312	312	312
	RCP Trip	314	314	314
	LPSI Pumps Activation	316	316	316
Refill/Reflood	AFW Actuation	338	338	338
	Accumulator Actuation	383	383	383
	Minimum Core Collapsed Liquid Level	417	396	396
	Core Full	434	438	440
LTCC	SSO	1740	1738	1739
	Core Blockage	2100	2098	2099

Figure 2 shows the comparison of the PCT during the pre- and post-core blockage LTCC phases.

The PCT for the top and bottom skewed power profile cases shows peaks immediately after the core blockage time. This is related with the higher relative heat flux at the top and bottom of the core compared to the chopped cosine profile adopted in the base case (where heat flux is minimum at the core bottom and top regions).
These peaks are found to be recovered within a short time (< 100 s for the top skewed case, b1), and maintained well below the limit of 800 °F.

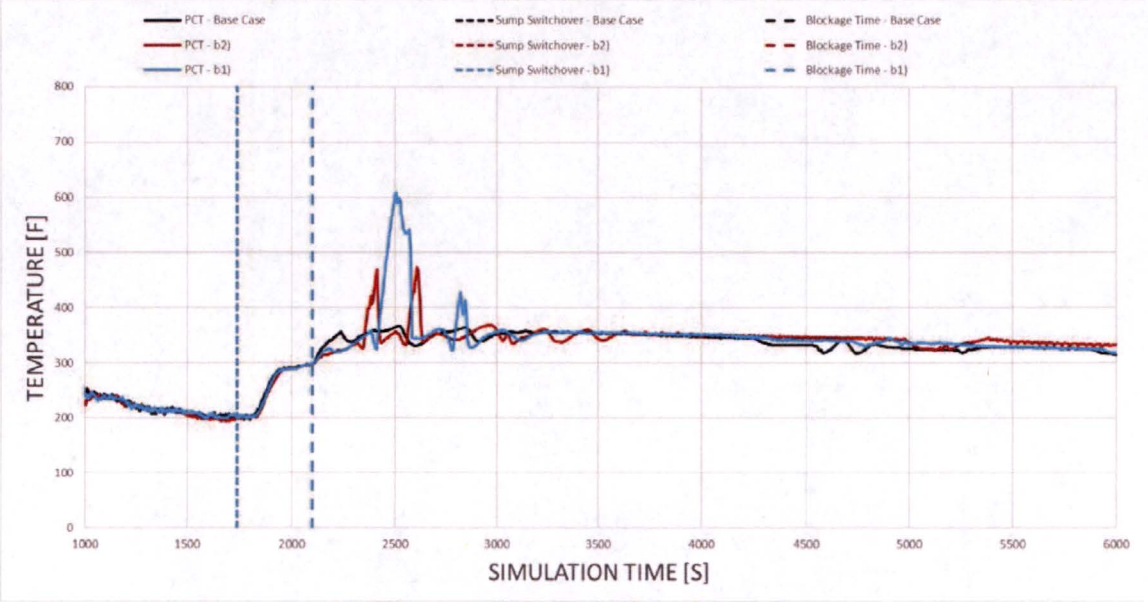

Figure 2. PCT (Sensitivity b1 and b2)

SENSITIVITY d) – Free Core Bypass

As stated in WCAP-17788, Volume 1, Section 6.4.1 (Last Paragraph) and again in WCAP-17788, Volume 6, Section 5.6 testing has shown, that Westinghouse upflow plant designs, like STP Units 1 and 2, have sufficiently large passages in the baffle-barrel (BB) bypass to pass fiber debris through that region. Also, as indicated in Volume 6, Section 3.55 of the WCAP, Westinghouse tested two hole sizes in order to address variations in the PWR fleet. Westinghouse has informed STPNOC that the STP hole size is in the range tested in the WCAP.

Based on the findings of the WCAP, STPNOC performed a sensitivity to show the effectiveness of the core barrel/baffle bypass as alternative flow path during a hypothetical full core blockage at the bottom of the core. The simulation conditions and the results are described below.

Boundary Conditions and other Assumptions
The boundary conditions applied to this sensitivity are the ones used in the LTCC EM Base Case. In particular:

- Usable RWST volume is set to its minimum of 360,000 gallons, as per STP design basis calculation MC-5037 Rev. 9.

- The RWST water temperature is set to 130 °F, as per STPNOC UFSAR
- The sump pool temperature is the one from the STP calculation NC-7032.
- No RHR HXs are simulated

In addition, the following boundary conditions from the sensitivity a) and combined:

- Appendix K decay heat (+20%)
- Maximum SG tube plugging of 10%
- Single worst ECCS train failure, assumed since the beginning of the accident in one of the intact loops.

Simulation Results

The accident scenario progression is summarized in Table 3.

No appreciable difference in the accident progression timing is shown, except for the SSO time and core blockage time, each occurring at a later time in the sensitivity case due to ECCS train unavailability. The STP LTCC EM model was used to perform a simulation to verify that flow through the BB bypass and the results showed adequate LTCC, as discussed below.

Based on the results, if the BB blockage testing described in the WCAP is confirmed, the current STP LTCC EM simulation and conclusions, in which credit for the bypass is not taken, are unaffected and represent a significant conservatism.

Table 3. Accident Progression Time Table (Sensitivity d)

Phase	Event	Simulation Time (s)	
		Base Case	D
Blowdown	Break Opening	300	300
	Low PZR pressure Signal	306	306
	MFW isolation	308	308
	Reactor Trip	308	308
	Reactor Fully Scrammed	311	311
	HPSI Pumps Activation	312	312
	RCP Trip	314	314
	LPSI Pumps Activation	316	316
Refill/Reflood	AFW Actuation	338	338
	Accumulator Actuation	383	381
	Minimum Core Collapsed Liquid Level	417	422
	Core Full	434	439
LTCC	SSO	1740	2167
	Core Blockage	2100	2527

The PCT is plotted with the core coolant saturation temperature in Figure 3. The PCT is maintained below 800 °F during the post-core blockage LTCC phase. Differences in the PCT between the cases are due to the slight difference in the primary pressure (saturation temperature).

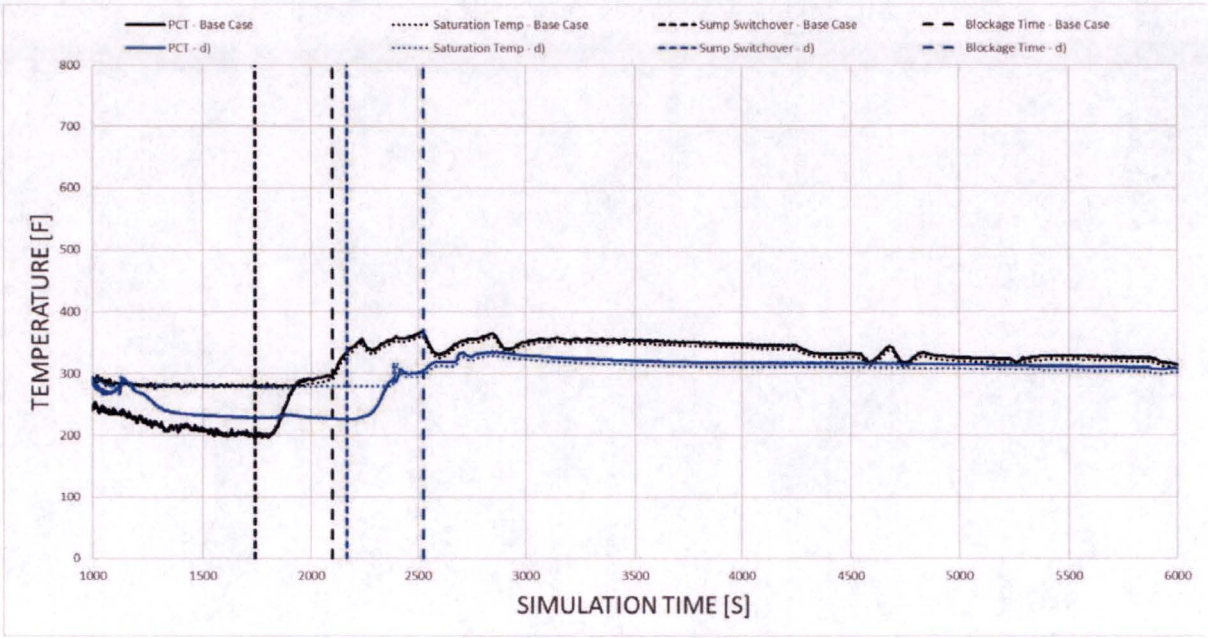

Figure 3. PCT (Sensitivity d)

Follow-up SNPB-3-22 Uncertainty and design margin

Initial RAI: *Provide a discussion on the impact of the uncertainties considered on the important figures of merit (e.g., PCT) for each of the accident scenarios and the margin to the design limit.*

Follow-up question:

In its response, STPNOC provided an overall summary of the uncertainties considered but did not provide sufficient details. Provide additional detail in the following areas:

- STPNOC makes the assertion that the 16-inch hot leg break would bound all smaller hot leg breaks, but does not justify this assertion.

STPNOC Response:
See response to RAI-SNPB-3-2 follow-up, bullet #4

- STPNOC discusses how the ECCS flow rate can impact the analysis, but did not discuss their choice for ECCS flow rate or its justification.

STPNOC Response

The STPNOC plant is equipped with three safety injection train. Each train contains one HHSI pump, one LHSI pump, one CS pump, and one accumulator.

In the LTCC EM, the volumetric flow rate of each component is determined as follows:

Assumptions on HHSI and LHSI pumps Flow Rate

The volumetric flow rate of these components is defined through tables as a function of the pressure of the primary system. In the LTCC EM these tables are imposed at their nominal value, calculated as the arithmetic average of the maximum and minimum ECCS flow safeguards specified in [1].

Assumptions on the CS pumps Flow Rate

The CS pumps volumetric flow rate withdrawn from the RWST is accounted in the LTCC EM when simulating the sump switchover time. The EM assumes two CS pumps running from the beginning of the LOCA event (from break opening time). This accounts for the LOCA EOP which guarantees the isolation of one CS pump. The volumetric flow rate of each pump is set to its nominal value, calculated as the arithmetic average of the maximum and minimum spray flow rates for two trains in operation [2].

Assumptions on the Accumulator's Flow Rate

The accumulators are modeled using the component "accumulator' available in RELAP5-3D. Being a passive component, the flow rate discharged by each accumulator results from the initial pressure of the accumulator and the pressure of the primary system. The initial conditions of the accumulators (liquid volume and thermodynamic conditions) are taken from the STPNOC UFSAR [3].

Considerations on Margin

The LTCC EM does not include conservatism in the HHSI, LHSI, and CS pumps volumetric flow rates. The expected effect on the sump switchover time (discussed in the original response to RAI-SNPB-3-22) is similar to the one of the RWST water volume, for which margin to the nominal value is already accounted for in the EM. Effects of the ECCS flow rate injected into the primary system on the post-core

blockage LTCC are accounted in the sensitivity described in the response to RAI-SNPB-3-20 a) *Appendix K decay heat load, with single worst failure and steam generator tube plugging.* In this sensitivity, the HPSI, LHSI, and accumulator of the SI train connected to one intact loop are disabled.

- STPNOC does not discuss its justification for the ECCS injection temperature or sump temperature.

STPNOC Response

Conservatism is accounted in the LTCC EM when defining the ECCS coolant injection temperature during the phases of the accident. Explanation of the assumptions made on the ECCS coolant temperature is provided below.

Safety Injection Phase:

This phase of the accident starts when the first SI pump is actuated and ends when the RWST low-low level alarm is reached. During this phase, water is withdrawn from the RWST. The nominal temperature of the water in the RWST is 85 °F. The RWST water temperature used in the LTCC EM is 130 °F as per STPNOC design criteria [4].

Recirculation Phase:

This phase of the accident starts when the ECCS injection sources switches to the containment sump and proceeds throughout the post-core blockage LTCC phase. The sump pool temperature profile adopted in the LTCC EM is taken from the STPNOC calculation NC-7032.

Qualitative comparison of the adopted profile, with best-estimate calculations available in literature for a typical PWR LBLOCA scenario [5], shows that the adopted profile exceeds the sump pool temperatures expected during such scenarios.

Considerations on Margin

The margin on the RWST temperature and sump pool temperature profile included in the EM are defined to:

- Minimize the level of sub-cooling of the water injected into the primary system at any time during the LOCA scenario,
- Maximize the enthalpy of the liquid injected into the primary system during the pre- and post-core blockage scenarios, and

- Minimize the total mass injected into the primary system (coolant at lower density).

- STPNOC alluded to sensitivity studies regarding the treatment of CCFL parameters but did not discuss them in sufficient detail for the NRC staff to understand how CCFL is treated.

STPNOC Response

See response to RAI-SNPB-3-13 follow-up – CCFL

References:

[1]. Title: TGX Minimum and Maximum Safeguards - Document NO: FRSS/CWBS-C-121 - Package NO: 5610H.
[2]. South Texas Project Risk-Informed GSI-191 Evaluation, Volume 3 CASA Grande Analysis, RI-GSI191-V03, Revision 2.
[3]. STPEGS UFSAR Revision 17.
[4]. EQ. Design Criteria 4E019NQ1009 Table 1, Section 5

SNPB-3-33

In response to SNPB RAI 10 and SSIB RAI 66 dated March 3, 2015 (ADAMS Accession No. ML 14357A171), STPNOC stated in its August 20, 2015, submittal that the current risk-over-deterministic (RoverD) analysis relies on the hot leg switchover (HLSO) timing of 5.5 hours as stated in STP UFSAR Section 15.6.5.2. As such, the NRC staff believes that changes to the HLSO timing would impact the RoverD analysis and thus the risk-informed resolution to GSI-191. In order to better understand the basis for the current HLSO timing, the NRC staff has audited STPNOC's current boric acid precipitation (BAP) control analysis on two occasions, in March 2015 and February 2016. During the February 2016 thermal-hydraulic audit at Westinghouse offices in Rockville, Maryland, the NRC staff were presented with testing data supporting STPNOC's contention that the barrel-baffle region mixes with the core under certain conditions. This region has not been previously credited in a BAP analysis. Given this, the NRC staff is not satisfied that a sufficient level of quantitative support has been provided for inclusion of any portion of the barrel-baffle region in the mixing volume. The NRC staff requests that STPNOC either:

a. Provide additional quantitative justification for the use of the barrel-baffle region in the mixing volume, including discussion of the applicability of test data to the STP plants (e.g., scaling of the tests used and the design of the test facilities relative to the design of STP), or
b. Perform a sensitivity analysis of the impact of omitting the barrel-baffle region from the mixing volume, to demonstrate that the current STP HLSO timing of 5.5 hours would be supported.

STPNOC Response

The requested analyses are attached and support the STP HLSO time.

In addition, the RoverD evaluation of debris for cold leg breaks (the breaks of interest for boric acid precipitation) shows that insufficient debris is present to significantly affect core cooling or circulation to the lower plenum. STPNOC believes there is sufficient information to demonstrate that there are no debris effects on boric acid precipitation or HLSO time.

Attachment 1

South Texas Units 1 and 2 Hot Leg Switchover Time Sensitivity Evaluation

1. Sensitivity Evaluation on the South Texas Units 1 and 2 Hot Leg Switchover Time Analysis

The hot leg switchover (HLSO) time analysis sensitivity evaluation is comprised of two elements. First, the bases for crediting mixing in the barrel-baffle region is discussed. Second, the results of several sensitivities are presented to quantify some of the margins in the South Texas HLSO time analysis.

2. Bases for Crediting Mixing in the Barrel-Baffle Region

The reactor internals design for South Texas Units 1 and 2 have an upflow barrel-baffle region design. Under normal operation, a small percentage of the reactor coolant flowing through the reactor vessel enters the barrel-baffle region at the bottom near the lower core support plate and exits this region just below the upper core plate. The baffle plates separate the barrel-baffle region from the active fuel region. Reactor internals that were originally designed for upflow in the barrel-baffle region have holes in the baffle plates at several elevations of the length of the fuel as well as flow gaps just above/below the lower/upper core plates. Under normal operation, there is little cross-flow between the barrel-baffle region and the active fuel region.

During two-phase natural circulation characteristic of the cold leg recirculation phase following a large, cold leg break loss-of-coolant accident (LOCA), several phenomena, as identified in WCAP-17047-NP [1], promote transport between the core region and the barrel-baffle region. With the presence of flow paths connecting the core and barrel-baffle regions, the density increase due to solute concentration that occurs in the core boiling region creates the instability needed across the baffle plates to drive circulation between the two regions. Also, as void moves and grows while traveling through the core, it displaces the borated liquid laterally. Particularly in the core periphery, this phenomenon will push liquid from the core to the barrel-baffle region through the holes in the baffle plates and the flow gap below the upper core plate.

The BACCHUS test facility described in WCAP-16317-P [2] was designed to investigate the phenomena and processes that influence the accumulation of boric acid in the reactor vessel under open-loop two-phase natural circulation conditions. The test facility includes the barrel-baffle region that can be opened to simulate the upflow plant design. The tests described in [2] were conducted with the barrel-baffle region opened to simulate the upflow reactor internals design like the South Texas units. The results of the two tests described in the report indicate that boric acid is being transported from the core to the barrel-baffle region as shown on Figure 2-11 in the report [2].

3. Sensitivity Evaluations on the Hot Leg Switchover Time

A series of sensitivity evaluations have been performed to quantify some of the margins in the South Texas Units 1 and 2 hot leg switchover time analysis. First, the relevant attributes of the analysis of record (AOR) are defined, then several sensitivity evaluations are described and the impacts quantified. The AOR results along with the results of the sensitivity evaluations are presented in Table 1.

Case 0: Analysis of Record

The AOR attributes relevant to the sensitivity evaluations are as follows:

1. Mixing in barrel-baffle region credited
2. ANS '71 decay heat for infinite irradiation plus 20%
3. Two-phase mixture level at the bottom of the hot leg
4. Maximum boric acid concentrations and minimum, 14.7 psia, containment backpressure

The AOR HLSO time is 6.05 hours.

Case 1: No Barrel-Baffle Region

This evaluation quantifies the effect of removing the credit for mixing in the barrel-baffle region. The AOR case is repeated but with the barrel-baffle volume removed. Note that the core region void fraction was applied to the barrel-baffle region in the AOR.

With the credit for barrel-baffle region mixing removed, the HLSO time reduces to 4.72 hours.

Case 2: No Barrel-Baffle Region and Nominal Decay Heat

This evaluation quantifies the effect of removing the credit for mixing in the barrel-baffle region; however, the decay heat standard is changed to the American Nuclear Society (ANS) 1971 standard for finite irradiation with no added uncertainty.

With the credit for barrel-baffle region mixing removed and nominal decay heat modeled, the HLSO time increases to 7.10 hours.

Case 3: No Barrel-Baffle Region, Nominal Decay Heat, and Increased Two-Phase Mixture Level

This evaluation quantifies the effect of removing the credit for mixing in the barrel-baffle region; however, the decay heat standard is changed to the American Nuclear Society (ANS) 1971 standard for finite irradiation with no added uncertainty and the a two-phase mixture level is credited within the upper plenum region to the top of the hot leg. No volume was credited in the reactor vessel outlet nozzles or in the hot legs

With the credit for barrel-baffle region mixing removed, and nominal decay heat, and the two-phase mixture level modeled in the upper plenum to the top of the hot legs, the HLSO time increases to 9.39 hours.

Case 4: No Barrel-Baffle Region, Nominal Decay Heat, Increased Two-Phase Mixture Level, Nominal RWST and Accumulator Boron Concentration, and Increased Containment Backpressure

This evaluation quantifies the effect of removing the credit for mixing in the barrel-baffle region; however, the decay heat standard is changed to the American Nuclear Society (ANS) 1971 standard for finite irradiation with no added uncertainty, the two-phase mixture level is credited within the upper plenum region to the top of the hot leg, average boric acid concentration in the refueling water storage tank (RWST) and accumulators are used, and a higher containment backpressure of 20.0 psia is modeled. At 20.0 psia, the saturation temperature is 228°F and corresponding boric acid solubility limit is 32 w/o (weight percent).

The potential benefits of recirculation coolant subcooling (decrease boil-off rate and lower void fraction) were not credited in this evaluation.

With the credit for barrel-baffle region mixing removed, nominal decay heat, the two-phase mixture level modeled in the upper plenum to the top of the hot legs, average boric acid concentrations, and increased containment backpressure, the HLSO time increases to 12.09 hours.

Table 1: Summary of HLSO Times

Case Number	Description	HLSO Time (hr)
0	AOR	6.05
1	AOR without the barrel baffle (B-B) region credit	4.72
2	Case 1 with nominal decay heat model	7.10
3	Case 2 with increased two-phase mixture level	9.39
4	Case 3 with average RWST and accumulator boron concentration and increased containment backpressure	12.09

4. Conclusions

Since there are phenomena that can drive transport between the core and barrel-baffle regions and test results from the BACCHUS test facility demonstrate that transport of boric acid occurs, there is sufficient justification to credit mixing in the barrel-baffle region in the hot leg switchover time analysis for South Texas Units 1 and 2.

The sensitivity evaluation results demonstrate that, even without credit for mixing in the barrel-baffle region, a hot leg switchover time of six hours is sufficient to preclude potential boric acid precipitation.

5. References

1. WCAP-17047-NP, "Phenomena Identification and Ranking Tables (PIRT) for Un-Buffered/Buffered Boric Acid Mixing/Transport and Precipitation Modes in a Reactor Vessel During Post-LOCA Conditions," May 2009.
2. WCAP-16317-P, "Review and Evaluation of MHI BACCHUS PWR Vessel Mixing Tests," November 2004.

SSIB

SSIB Round 3 Follow-up RAI 33

Original Follow-up RAI 33

In the December 23, 2009 RAIs, the NRC staff asked the licensee to provide the margin to flashing and the assumptions for the calculation. The licensee provided a calculation for the margin to flashing for large break loss of coolant accidents (LOCAs) at the start of recirculation as (in pounds per square inch [psi]):

Containment pressure + submergence – total strainer head loss – vapor pressure
= 43.1 + 0.3 - 1.5 - 39
= 2.9 psi

The licensee stated that post LOCA containment over pressure credit is needed to eliminate the potential for flashing. The licensee stated that the minimum strainer submergence was conservatively determined to be 0.5 inch for small break LOCA (SBLOCA), sump temperature and containment pressure would be lower for a SBLOCA than a large break LOCA (LBLOCA), strainer flow rate would also be lower, and debris transported to strainers would be much less such that there would be open strainer areas. Therefore, flashing is not expected to be an issue for SBLOCAs. The NRC guidance[1] is that sump temperature should be calculated conservatively high and containment pressure conservatively low to ensure no flashing will occur. It is acceptable to perform a time based calculation taking viscosity, chemical timing, and strainer submergence into account. Most design basis calculations maximize containment pressure, which is non conservative from a flashing perspective. Please explain in detail how sump temperature and containment pressure were calculated.

1 "Revised Content Guide for Generic Letter 2004-02 Supplemental Responses, November 2007" (ADAMS Accession No. ML073110278), and Regulatory Guide 1.82, "Water Sources for Long-Term Recirculation Cooling Following a Loss-of-Coolant Accident."

Staff Request for Further Clarification

An updated response to RAI 37 is required to justify that flashing will not occur for a SBLOCA. For the LBLOCA, STP should demonstrate that there is margin to flashing considering staff guidance that flashing evaluations that credit containment pressure should be performed using conservatively low containment pressure and conservatively high sump fluid temperature. Alternately, the licensee may demonstrate that there is adequate margin to flashing. Showing a large margin would negate the need to perform the conservative calculations for pressure and temperature. This would require that STP show that the margin to flashing is so large that any realistic plant conditions that might deviate from the analyzed conditions would not result in flashing.

Original Response

The response to the December 23, 2009 RAI included a sump temperature and containment pressure that were calculated as part of the LOCA containment pressure and

temperature response analysis. This was performed using the CONTEMPT computer code. The most recent LOCA containment pressure/temperature analysis was performed using the computer code GOTHIC. This resulted in a higher maximum sump temperature which was evaluated not to significantly impact the NPSH evaluation. An alternate analysis to change the design basis to maximize the sump temperature using COBRA/TRAC is an option but has not been fully evaluated to implement.

Addition to Response

Also see discussion in response to Follow-Up RAI 34 that addresses flashing and states that sump pool boiling does not occur and the discussion in the "SSIB Follow-up RAI 33, 34 Evaluation Support" that follows the Follow-Up RAI 34 response.

The maximum sump temperature determined for the initial submittals was from design basis calculations for containment analysis that yielded the maximum containment accident pressure for containment structural design for an RCS break, the maximum containment atmosphere temperature for environmental qualification for Main Steam line break, and the maximum containment sump temperature due to an RCS break for Low Head Safety Injection Pump, High Head Safety Injection Pump, and Containment Spray Pump NPSH evaluation.

The cases for containment pressure and sump temperature resulted in high containment accident pressures and coincident high sump temperatures. Use of the maximum sump temperature of 273.6°F and corresponding containment accident pressure of 44.9 psia resulted in acceptable evaluations for flashing, deaeration, and pump NPSH as further discussed below in RAI 34.

It is recognized that the NRC guidance in Reg. Guide 1.82 calls for the sump temperature to be calculated conservatively high and the containment pressure conservatively low in order to evaluate flashing, deaeration, and NPSH. Thus additional cases were used for the response to this RAI #33 and also for RAI #34. These cases were based on sensitivity runs using RELAP5-3D/MELCOR runs as described in the section below. These cases with a relatively high containment sump temperatures and low containment pressures were evaluated and found to yield acceptable results as described below and also in RAI#34.

SSIB Round 3 Follow-up RAI 34

The NRC has several questions regarding this RAI response.

- An updated response to RAI 37 is required to justify that debris head loss for the SBLOCA is zero (see below).
- The staff could not determine whether the plenum head loss should be accounted for in the deaeration evaluation. It is possible that there is adequate head above the plenum to negate the need for this. It appears that the plenum head loss is subtracted from the clean strainer head loss value for these calculations.
- The staff could not confirm that the use of the centerline elevation of the strainer provides a good approximation for the actual deaeration compared to a calculation that integrates deaeration over the strainer height. This issue was identified because deaeration is dependent on the submergence level at which the head loss (due to the debris bed and) occurs. An integrated solution is not necessary, but it should be demonstrated that an average taken at a few elevations of the strainer approximate the single centerline calculation.
- The RAI response stated that pressure credit was applied to ensure that the void fraction remained below 2%. The staff could not determine what actions regarding NPSH margin were taken for cases that have more than zero, but less than 2% void fraction. Reg Guide 1.82 imposes a penalty on NPSH required (NPSHR) where a positive void fraction is calculated. Were the NPSHR penalties applied to the NPSH margin calculation? Was it shown that void fraction would be zero so that no penalty is required? Alternately, does STP have plant specific information that justifies that their pumps are capable of operation with the calculated void fractions for the required time periods during which voids will be present?
- Please clarify how P_{Loss} is calculated. Is it: Corrected debris HL + (Corrected CSHL – Plenum HL)?
- Similar to the issue identified in the discussion of RAI 33 above, is the containment pressure credit conservative?

STPNOC Response

This supplemental response was written to provide further clarification and analysis to support follow up to RAI-34 response (2016). Follow-up to RAI-34 provided analysis of degasification for bounding temperature conditions from STP's design basis accident analysis [1]. For all analyzed temperatures above 212° F, overpressure was credited to prevent boiling in the pool or to evaluate for calculated void fraction cases that result in a void fraction of more than 2% when considering only saturation pressure. This overpressure credit was intended to be applied in accordance with RG 1.82 [2], which states that additional pressure credit should not be taken above what is needed to prevent a failing NPSH value and where boiling conditions and a void fraction >2% were treated as NPSH failure. This previous degasification analysis in the follow-up RAI-34 response, however, did not directly analyze the effect of the calculated void fraction on net positive suction head required (NPSHR) and calculated net positive suction head margin (NPSHM). This supplemental response provides NPSHM, as well as comparison to strainer head loss, analysis to support the follow-up RAI-34 analysis.

Additionally, this supplement provides results for best estimate LBLOCA temperature cases including cases for nominal LBLOCA temperature response and combined worst case LBLOCA response for 15" LBLOCA. As stated in the RAI-33 supplement, differences in results for

containment pool temperature and containment pressure response are negligible between the largest DEGB and 15" breaks.

Three 15" break scenarios were considered in this analysis with conditions provided in the following numbered list. Note that the case numbering used here does not relate to the degasification cases presented in the rest of the analysis and was adopted from case descriptions from the thermal-hydraulic (TH) calculations.

1. Case 1 – All trains operating (3-trains), all containment cooling fans (6-CFCs) operating, and nominal component cooling water system (CCW) temperatures
2. Case 22a – Two of three trains operating, 4/6-CFCs, and nominal CCW conditions
3. Case 43 – One of three trains operating, 6 CFCs, and nominal CCW conditions

The temperature and pressure results from the three cases described above is presented in Figure 1 and Figure 2.

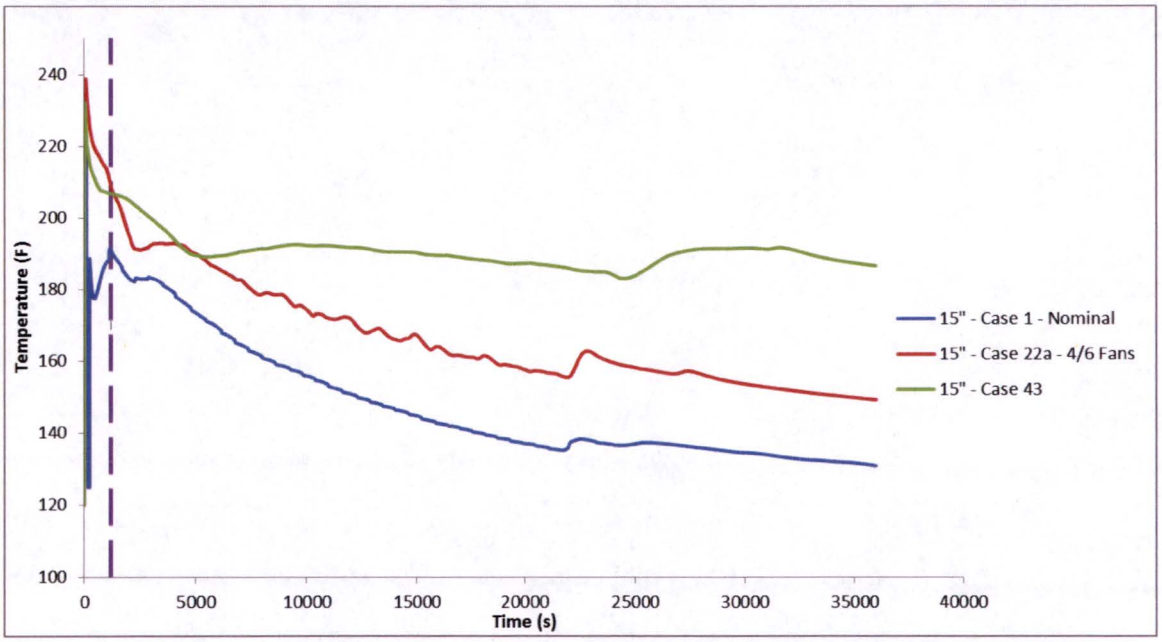

Figure 1 : Temperature response for analyzed best estimate break scenarios

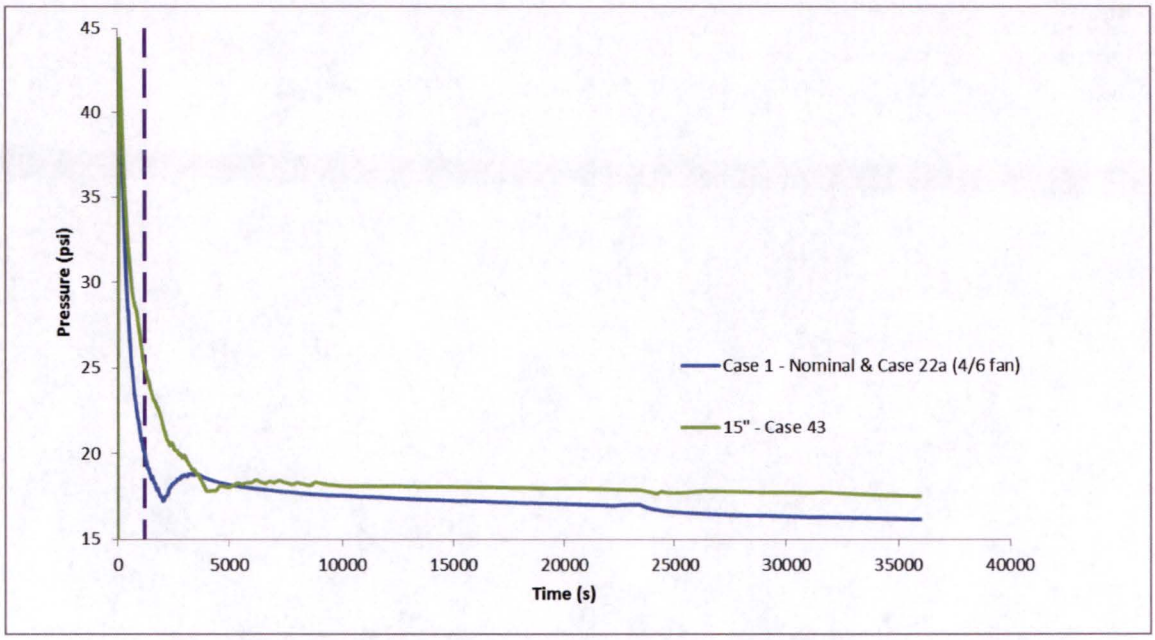

Figure 2: Pressure response for best estimate analyzed break scenarios

Of the numbered TH cases above Case 43 results in the highest long-term temperature/ pressure conditions while the nominal Case 1 response results in the lowest. Short-term max temperatures are similar for Case 43 and Case 22a, and were taken at 1200s (dashed vertical line in Figure 1) which is an assumed conservative switchover time for these cases; actual switchover times are estimated to be double this time or more, especially Case 43 which only has one train in operation.

In this evaluation, in addition to cases performed in RAI-34 analysis, combination degasification and NPSH margin will be evaluated for temperature and pressure combinations taken from TH analysis described above. Case C1 describes the worst combination, highest temperature (from Figure 1) and lowest pressure (from Figure 2) at the assumed 1200 second switchover time from the three cases. Case C2 describes the worst combination, highest temperature (from Figure 1) and lowest pressure (from Figure 2) long term at 36000 seconds (10-hours). Results from the follow-up to RAI-34 analysis are provided below for convenience in Table 1; which includes initial conditions and void fraction results for the additional combination case C1 and C2.

Table 1: Results from 2016 Follow-Up to RAI-34 Analysis

Case #	Temperature at Sump (°F)	Strainer Head Loss (ft)	Accident Analysis Containment Pressure (psia)	$P_{Containment}$ Analyzed Pressure (psia)			
				Pressure value used to yield non-boiling pool conditions / unchallenged conditions		Pressure value used to yield passing void fraction (<=0.02)	
				$P_{Containment}$ (psia)	Void Fraction	$P_{Containment}$ (psia)	Void Fraction
**1	269.8	0.497	43.3	*41.9	0.000		
**2	273.6	0.488	44.9	*44.5	0.000		
3	266.9	3.757	45.6			*41.3	0.020
4	213.6	4.946	29.0			*17.5	0.019
5	144.0	7.994	18.3	14.7	0.004		
6	144.0	1.071	18.3	14.7	0.000		
7	121.0	9.8780	16.9	14.7	0.006		
C1	209.1	5.078	20.1			*16.3	0.019
C2	186.6	5.844	16.2	14.7	0.006		

*Smallest pressure above saturation pressure credited to achieve passing degasification scenarios
**Debris bed head loss is not used for these cases; only clean strainer head loss is considered. These cases occur less than 5 minutes after the start of recirculation so there will be less than a third of a full sump pool volume turnover. Chemical debris is not expected at this early time post-LOCA. Thus, there will not be sufficient debris accumulated on the strainer to have an impact on head loss at the time of this case.

Per RG 1.82, NPSHM is defined as the margin without strainer head loss and this document implements the same nomenclature. NPSHM for a given pump can be calculated by taking the difference between the available head of water (NPSHA), adjusted by major and minor flow losses in system piping, and the NPSHR; defined by the pump manufacturer with testing corresponding to the centerline of the pump first stage impeller or calculated with flow rate and geometry at the pump inlet nozzle depending on which case is limiting. The vertical pumps installed at STP are limited by NPSHM calculated at the pump inlet nozzle in the design basis NPSH calculation [3]. However, adjustments of NPSHR for air ingestion, following RG 1.82, are made to the NPSHR value defined by the impeller centerline test. Therefore, calculation of adjusted NPSHR, and resultant NPSHM in this supplemental evaluation will be based on the test specified NPSHR value at the pump first stage impeller centerline.

The use of NPSHR found from the empirical examination of pump performance at the impeller centerline should not be confused with the calculation vertical datum. Because design basis analysis used a vertical datum at the pump inlet nozzles, all hydraulic head values in this supplemental evaluation will also be referenced from the elevation at the pump inlet nozzle. The equation for NPSHM is provided below for reference.

$$NPSHM = NPSHA - NPSHR \qquad \text{Equation 1}$$

Values of NPSHA and NPSHR from the NPSHM design basis [3] evaluation were used as inputs for this evaluation and are provided below in Table 2 below.

Table 2: NPSHR and NPSHA Values from Design Basis Calculation

Pump	NPSHR Pump Impeller (ft).	NPSHA 2015 Calc (ft) T>212 F	NPSHA 2015 Calc (ft) T=190 F	NPSHA 2015 Calc (ft) T<171 F
LHSI	13	7.5	20.1	27.9
HHSI	11	7.4	20.2	28
CS	12	7.2	19.8	27.6

To perform the NPSHM (without strainer head loss) and NPSHM with strainer head loss evaluation, first NPSHR from Table 2 was adjusted by the calculated void fraction (Table 1 above) from the follow-up to RAI-34 response utilizing the adjustment provided in RG 1.82 Rev. 4 [2] shown in the equation below; where α is the void fraction applied as the percentage value and not as a fractional value.

$$NPSHR_{Adj} = NPSHR * (1 + 0.5 * \alpha) \qquad \text{Equation 2}$$

Adjusted (RG 1.82) NPSHR values utilizing the void fractions calculated in follow-up RAI-34 are given in Table 3 below.

Table 3: Void Fraction Adjusted NPSH Values

Case #	Void Fraction	LHSI NPSHR Pump CL (ft)	HHSI NPSHR Pump CL (ft)	CS NPSHR Pump CL (ft)	LHSI $NPSHR_{Adj}$ @ Pump CL (ft)	HHSI $NPSHR_{Adj}$ @ Pump CL (ft)	CS $NPSHR_{Adj}$ @ Pump CL(ft)
1	0.000	13	11	12	13.00	11.00	12.00
2	0.000	13	11	12	13.00	11.00	12.00
3	0.020	13	11	12	26.00	22.00	24.00
4	0.019	13	11	12	25.35	21.45	23.40
5	0.004	13	11	12	15.60	13.20	14.67
*6	0.000	13	11	12	13.00	11.00	12.00
7	0.006	13	11	12	16.90	14.30	15.40
C1	0.019	13	11	12	25.16	21.29	23.22
C2	0.006	13	11	12	16.77	14.19	15.48

* Case 6 is a half full flow condition however full flow NPHSR values were used in this evaluation.

Next, void-adjusted NPSHR values, representing tested values adjusted to the centerline of the pump impeller, were related to the vertical pump inlet datum, which is 15 feet above the centerline of the pump impeller. This relation subtracts 15 feet from the adjusted NPSHR value to account for the 15 feet of water head gained by relating values to the pump inlet datum. In addition to this

adjustment to account for the 15-feet of static head, 0.3-feet must be subtracted from the NPSHM to account for the minor losses between the impeller and the pump suction inlet [3]. Results of this NPSHR relation as well as NPSHM calculated using Equation 1 are provided below in Table 4; noting that NPSHA is related to case temperatures using the rules in Table 2.

Table 4: Follow-Up to RAI-34 Void Adjusted NPSHM

Case #	Void Fraction	LHSI $NPSHR_{Adj}$ @ Pump Inlet (ft)	HHSI $NPSHR_{Adj}$ @ Pump Inlet (ft)	CS $NPSHR_{Adj}$ @ Pump Inlet (ft)	Void Adjusted NPSHM LHSI (ft)	Void Adjusted NPSHM HHSI (ft)	Void Adjusted NPSHM CS (ft)
1	0.000	-1.70	-3.70	-2.70	9.2	11.1	9.9
2	0.000	-1.70	-3.70	-2.70	9.2	11.1	9.9
3	0.020	11.30	7.30	9.30	-3.8	0.1	-2.1
4	0.019	10.65	6.75	8.70	-3.2	0.7	-1.5
5	0.004	0.90	-1.50	-0.30	27.0	29.5	27.9
6	0.000	-1.70	-3.70	-2.70	29.6	31.7	30.3
7	0.006	2.20	-0.40	0.90	25.7	28.4	26.7
C1	0.019	10.46	6.585	8.52	9.6	13.6	11.3
C2	0.006	2.07	-0.51	0.78	18.0	20.7	19.0

Utilizing the void adjusted NPSHM (Table 4) values, NPSHM with strainer head loss (Table 1) is now evaluated.

Table 5: NPSHM with Strainer Head Loss for Follow-up tor RAI-34 Cases

Case #	Temp (F)	Head Loss (ft)	Void Adjusted NPSHM LHSI (ft)	Void Adjusted NPSHM HHSI (ft)	Void Adjusted NPSHM CS (ft)	LHSI NPSHM with Strainer Head Loss (ft)	HHSI NPSH with Strainer Head Loss (ft)	CS NPSHM with Strainer Head Loss (ft)
1	269.8	0.497	9.2	11.1	9.9	8.7	10.6	9.4
2	273.6	0.488	9.2	11.1	9.9	8.7	10.6	9.4
3	266.9	3.757	-3.8	0.1	-2.1	-7.6	-3.7	-5.9
4	213.6	4.946	-3.2	0.7	-1.5	-8.1	-4.3	-6.4
5	144	7.994	27.0	29.5	27.9	19.0	21.5	19.9
6	144	1.071	29.6	31.7	30.3	28.5	30.6	29.2
7	121	9.878	25.7	28.4	26.7	15.8	18.5	16.8
C1	209.1	5.078	9.6	13.6	11.3	4.6	8.5	6.2
C2	186.6	5.844	18.0	20.7	19.0	12.2	14.9	13.2

Of the NPSHM with strainer head loss values calculated above, further analysis is only needed for cases 3 and 4 which yielded negative margins with strainer head loss when considering the void fractions calculated in follow-up RAI-34. For these cases (3 and 4) the void fraction was decreased in 0.001 increments, while updating NPSHR adjustments as performed in Table 3 and Table 4, until positive NPSH with strainer head loss was realized. This iteration yielded void

fractions of 0.008 and 0.006 for Case 3 and 4, respectively, which were the first void fraction values found by decreasing in 0.001 increments to yield a positive NPSHM with strainer head loss value. Results of this iteration are shown in Table 6 which follows the same calculation methodology used for Table 3 through Table 5.

Table 6: Results of Incremental Void Fraction Iteration for Positive Head Loss Difference

Case #	Temp (F)	Head Loss (ft)	Analyzed Pressure (psia)	Void Fraction	LHSI NPSH with Strainer Head Loss (ft)	HHSI NPSH with Strainer Head Loss (ft)	CS NPSH with Strainer Head Loss (ft)
3	266.9	3.757	*??	0.0080	0.2	2.9	1.3
4	213.6	4.946	*??	0.0060	0.4	2.9	1.4

* ?? denotes that this iteration was performed to find a void fraction that would yield a positive head loss difference. Analyzed pressure is found in the next step.

Table 6 shows the calculated NPSHM with strainer head loss values including NPSHR adjustment. Increasing the Column 5 void fraction by 0.001 and redoing calculations would yield a negative number for the NPSHM with strainer head loss; i.e., this is the first positive head loss difference value found with the void fraction incremental iteration. To complete the evaluation, the void fraction values for Case 3 and 4 in Table 6 were used as targets, and the CASA Grande degasification model was run by incrementally increasing containment pressure by 0.1 psia until void fraction values equal to or smaller than the respective fractions in Table 6 were found. This process will determine the lowest containment pressure needed to guarantee positive NPSHM with strainer head loss utilizing RG 1.82 adjustments for voiding. Note that all degasification inputs except for the containment pressure and the void fraction found in Table 6 were held constant to their assignments defined in the follow-up to RAI-34 response. Results of this incremental pressure iteration analysis are provided below in Table 7.

Table 7: Results for Lowest Containment Pressure to Satisfy Positive Head Loss Difference

Case #	Temp (F)	Head Loss (ft)	Analyzed Pressure (psia)	Void Fraction	LHSI NPSHM with Strainer Head Loss (ft)	HHSI NPSHM with Strainer Head Loss (ft)	CS NPSHM with Strainer Head Loss (ft)
3	266.9	3.757	42.4	0.0077	0.7	3.4	1.8
4	213.6	4.946	19.8	0.0059	0.7	3.2	1.7

The results of Table 7 were substituted for the original Follow-up to RAI-34 results in Table 5 to form the updated final results (Table 8).

Table 8: Updated Final Results - Degasification Implications on NPSHM with Strainer Head Loss

Case #	Temp (F)	Head Loss (ft)	Design Basis Calc Pressure (psia)	Analyzed Pressure (psia)	Pressure Difference [DBA-Analyzed] (psia)	Void Fraction	LHSI NPSH with Strainer Head Loss (ft)	HHSI NPSH with Strainer Head Loss (ft)	CS NPSH with Strainer Head Loss (ft)
1	269.8	0.497	43.3	41.9	1.4	0.000	8.7	10.6	9.4
2	273.6	0.488	44.9	44.5	0.4	0.000	8.7	10.6	9.4
3	266.9	3.757	45.62	42.4	3.22	0.008	0.7	3.4	1.8
4	213.6	4.946	29	19.8	9.2	0.006	0.7	3.2	1.7
5	144	7.994	18.3	14.7	3.6	0.004	19.0	21.5	19.9
6	144	1.071	18.3	14.7	3.6	0.000	28.5	30.6	29.2
7	121	9.878	16.9	14.7	2.2	0.006	15.8	18.5	16.8
C1	209.1	5.078	20.1	16.3	3.8	0.019	4.6	8.5	6.2
C2	186.6	5.844	16.2	14.7	1.5	0.006	12.2	14.9	13.2

The results in Table 8 show that positive head loss difference has been achieved for all cases while analyzed pressure remained below DBA accident calculated pressures. In accordance with RG 1.82 only over pressure needed in excess of vapor pressure was credited, and the difference between DBA calculated pressure and analyzed pressure has been tabulated.

References

[1] NC-07032 Rev. 19.

[2] Regulatory Guide 1.82 Rev. 4, "Water Sources for Long-Term Recirculation Cooling Following a Loss-of-Coolant Accident," March, 2012.

[3] MC06220 Rev. 6 , "SI & CS Pumps NPSH," 2016.

SSIB Follow-up RAI 33, 34 Evaluation Support

Summary

Four Cases are reviewed for subcooling following Sump Switch Over (SSO) with various combinations of Emergency Core Cooling System (ECCS), Containment Spray System (CSS), and Reactor Containment Fan Coolers (RCFC) operating as summarized in Table 1. The saturation pressure for a “worst case”, that is, Beyond Design Basis (BDB) Reactor Containment Building (RCB) floor pool temperature is compared to a best-estimate minimum pressure RCB case (Case 15-Case1-Nom) to obtain a conservative estimate of the margin to loss of subcooling.

The pressure comparisons indicate substantial margin to subcooling. Only in an extreme case of loss of all ECCS core cooling in which both the Residual Heat Removal System (RHR) heat exchangers are failed with loss of all CSS and BDB RCFC loss (two trains) is subcooling lost. Even in this case, there are about two to three hours available for recovery of vital systems prior to loss of subcooling.

Table 1: Summary of cases reviewed for subcooling following SSO at the assumed time of 1200 sec.

Case ID	ECCS	CSS	RCFC	Subcooling	Comment
Case 15-Case1-Nom	3	3	3	Yes	Minimum Pressure
Case 15-22a-4Fans	2	2	2	Yes	Best estimate single failure
Case 15-43	1	1	3	Yes[a]	Beyond Design Basis[b]
Case 15-Case1-Max	3[c]	0	1[d]	No	Beyond Design Basis[b]

Table notes.
[a]This case is core damage for Cold Leg Break (CLB) if the break is on the same loop as the operating ECCS train.
[b]Although core damage may (or will) occur, the RCB is intact.
[c]Assumes failed RHR heat exchanger in all Low Head Safety Injection (LHSI) trains; guarantees core damage (no core cooling).
[d]Assumes 150 degrees F Component Cooling Water System (CCW) temperature.

Analysis: Coupled RELAP5-3D/MELCOR evaluations

In 2013, Loss of Coolant Accident (LOCA) calculations were performed for 15 inch CLBs using the STP RELAP5-3D best estimate model (Felli et al., 2011) and (Hassan et al., 2011) coupled with the South Texas Project (STP) MELCOR model (Beeny et al., 2013; Vaghetto et al., 2013a). Based on results for Double Ended Guillotine Break (DEGB) sensitivities, it was found that the difference in RCB floor pool temperature (the summary of temperature analyses is shown in Figure 1) (STP MELCOR Model node CVH-TLIQ_5) and RCB pressure during the Long Term Core Cooling (LTCC) phase is negligible between DEGBs and 15 inch CLB (see Vaghetto et al., 2013b, or ML13323A190 Figure 2.2.1 for best estimate DEGB cases). Figure 1a compares the 15 inch break RCB pressure to the DEGB pressure for the same model (only break size changed).

Various plant configurations at 15 inch CLB size were analyzed to support studies of sump temperature effects on overall system responses. Four Cases from those analyses are evaluated in here as enumerated below.

1. Case 15-Case1-Nom: 3 Trains of ECCS, CSS, and RCFC (6 Fan Coolers) with nominal CCW temperature (85 degrees F) – Expected (3 trains, nominal conditions)
2. Case 15-Case1-Max: 3 Trains of ECCS, no CSS, and one train of RCFC (2 Fan Coolers) with summer CCW temperature (150 degrees F) to RCFC and no RHR heat exchangers – BDB.
3. Case 15-22a-4Fans: 2 Trains of ECCS, CSS, and RCFC (4 Fan Coolers) with nominal CCW temperature (85 degrees F) – best estimate design basis.
4. Case 15-43: 1 Train of ECCS, CSS, and 3 trains of RCFC (6 Fan Coolers) with nominal CCW temperature (85 degrees F) – BDB

For all the Cases, the Case 15-Case1-Nom RCB pressure is assumed Figure 1a. That is, this Case would represent the minimum pressure that could be obtained. The SSO time is noted on fig. 1a which is about 1200 seconds. This is a minimum time (due to maximum flow out of the Refueling Water Storage Tank (RWST) for the Case with all ECCS and CSS). Because the RCB pool floor fluid temperature decreases after SSO, it is conservative with regard to that temperature to assume minimum SSO time (highest temperature) with the exception of the BDB Cases (Case 15-Case1-Max and 15 Case1-43) shown in Figures 1b and 1c. For the exception Case 15 Case1-Max after several hours, RHR or more RCFCs would need to be restored in order to maintain subcooling. For the exception Case 15 Case1-43, although the floor pool temperature increases after SSO, substantial subcooling (referring to the 220 degrees F level in fig. 1b where subcooling is lost) would be maintained for the BDB Case.

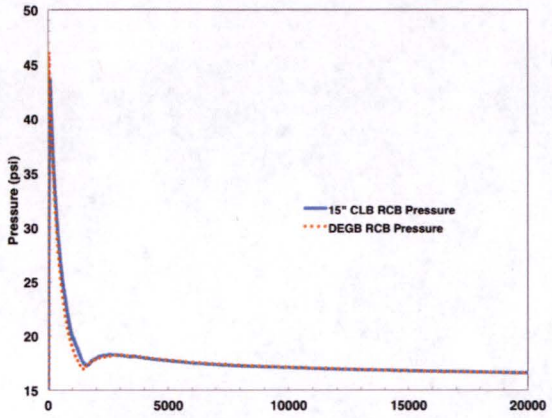

(a) Best estimate minimum RCB pressure (Case 15-Case1-Nom) compared to a DEGBin the same model (only break size changed).

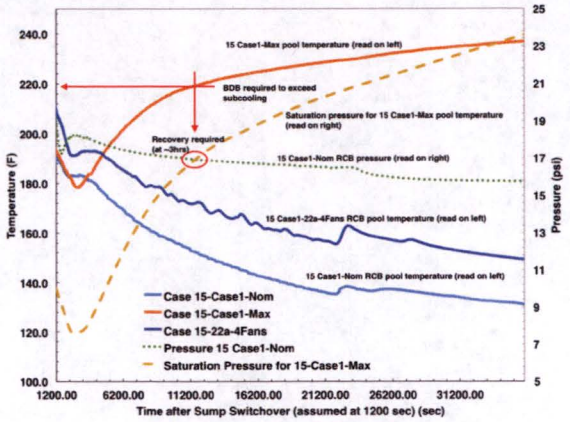

(b) Temperatures and pressures for Cases 15 Case1-Nom, 15 Case1-Max, and 15 Case1-22a-4Fans. Pressures are the 15 Case1-Nom and saturation pressure for the pool

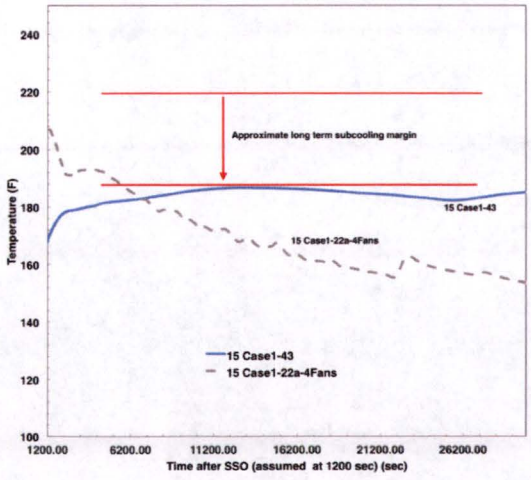

(c) Temperature for the 15 Case1-22a-4Fans compared to 15 Case 1-43 evaluated

Figure 1

References

Beeny, B., A. Franklin, R. Vaghetto, K. Vierow, and Y. Hassan (2013, January). MELCOR Input Deck Certification South Texas Project Large Dry Containment. TAMU GSI-002, Rev.2, STI33647084, Texas A&M University, College Station, Texas.

Felli, F., S. Kang, O. Rodriguez, and R. Vaghetto (2011, July). RELAP5 MODEL INPUT DECK CERTIFICATION. Technical Report Revision 3.0, STI 33647085, Texas A&M University, College Station, Texas.

Hassan, Y., S. Kang, and R. Vaghetto (2011, November). RELAP5 LOCA INPUT CERTIFICATION. Technical Report Revision 1.0, Texas A&M University, College Station, Texas.

Vaghetto, R., B. Beeny, Y. A. Hassan, and K. Vierow (2013a, January). 15-inch Cold Leg Break Scenario 30-Day Containment Response. TAMU GSI-003, Rev. 2 STI33647098, Texas A&M University, College Station, Texas.

Vaghetto, R., B. Beeny, Y. A. Hassan, and K. Vierow (2013b, January). Sump Temperature Sensitivity Analysis. TAMU GSI-005, STI 33647111, Texas A&M University, College Station, Texas.

SSIB Round 3 Follow-up RAI 37

RAI 37 – For RAI 37, STP needs to show that the debris head loss at the SBLOCA load is zero. This also needs to be shown to support RAIs 33 and 34. This issue was discussed during the 6/22/16 public meeting. The staff was unsure of the inputs used to calculate the debris loading in the RAI response. Please provide a justification for the SBLOCA case incurring zero head loss.

STPNOC Response

This response supplements the SSIB Follow-up to RAI-37 response with additional insights about transported fiber and maximum expected bed thickness. The sole intent of the original response to RAI-37 provided in the August 2015 submittal (Reference 1 in the cover letter) was to say that NPSH margin and head loss are bounded by LBLOCA analysis; meaning LBLOCAs represent the worst cases for STP resulting in smaller calculated NPSH margin and higher head losses. All two-train SBLOCA cases (<2") result in a max debris bed thickness smaller than 1/16". Note that pipe sizes with an inner diameter smaller than 2-inches were analyzed with a DEGB spherical ZOI, while those pipes with an inner diameter larger than 2-inches were analyzed with a hemispherical break in the direction of max fibrous debris generation. The maximum transported SBLOCA debris volumes and bed thickness support the assertion that head loss for these scenarios is very small and that NPSH margin and calculated head loss are bounded by evaluation of LBLOCA scenarios. This assertion is also supported for one-train cases. Evaluation of one-train scenarios yields ~1/16" debris beds for all cases.

Round 3 SSIB-3-6

Additional STPNOC RESPONSE

EPOXY COATINGS IN THE REACTOR CAVITY

Quantity of Coatings

Epoxy coatings within the Unit 1 reactor cavity include 1,570 lbs. on ceilings and walls and 74.9 lbs. on platform supports and decking. The epoxy amount in Unit 1 is bounding when considering recorded amounts for Units 1 and 2.

Unit 1 has a larger quantity since the Unit 2 walls are not epoxy coated all the way up to the ceiling and also since the ceilings in Unit 2 are not epoxy coated. The sump performance evaluation is based on the higher quantity for Unit 1.

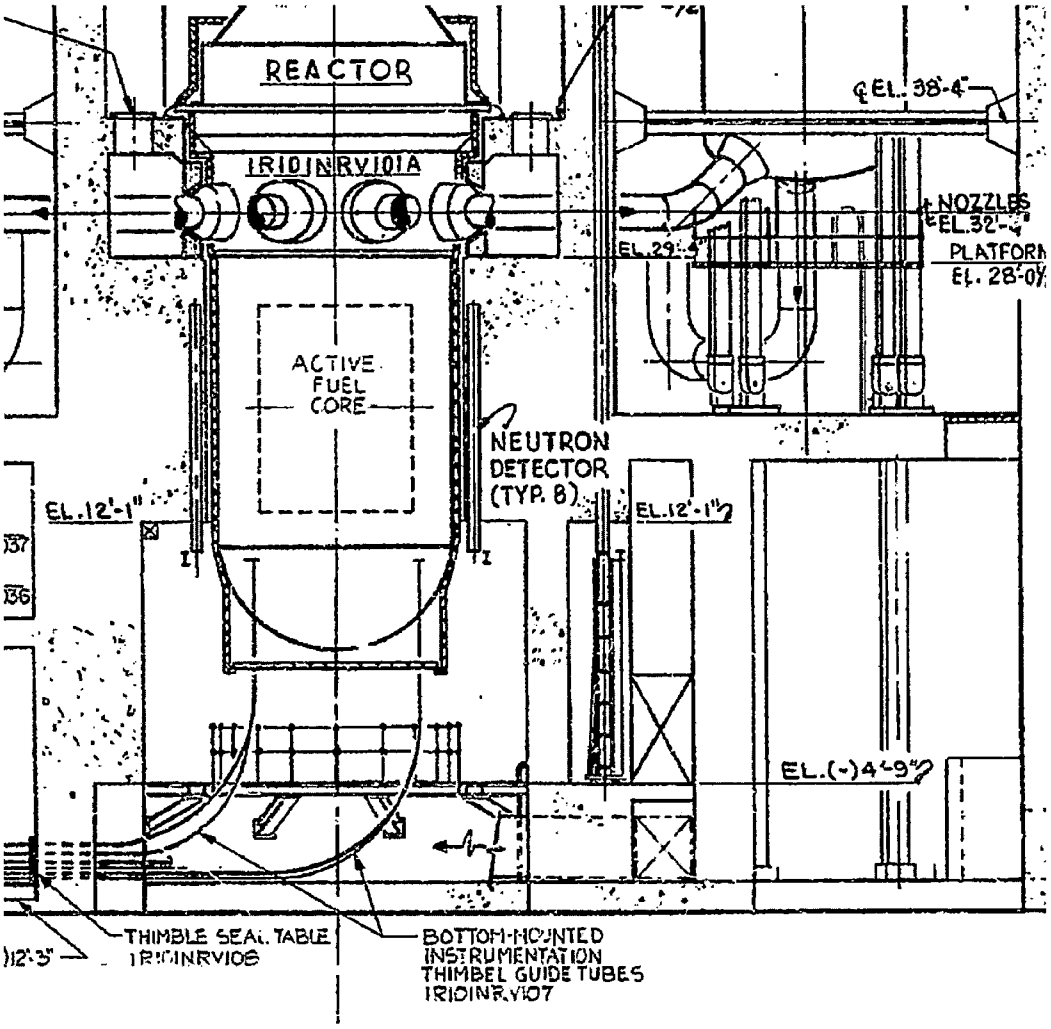

The Reactor Cavity is designated as Reactor Containment Building Room 001.

Type of Coatings

Brown and Root Technical Reference Document 5A810WQ005-A "Painting Schedule for Service Level I, II, and III Areas" from 1979 calls for the Reactor Cavity walls to be coated using the following Level I concrete coating system defined in HL&P Specification #7A810XS002-A-HL:

- Nutec 10 Primer/Sealer
- Nutec #11S Concrete Masonry/Surfacer
- Nutec #11 Concrete Masonry/Surfacer
- Reactic (Nutec) #1201 Epoxy Topcoat

The coatings data base for Unit 1 calls for the platform steel in the Reactor Cavity to have a top coat of Ameron 90.

Service History

Just prior to the initial startup of Unit 1 in 1987 during hot functional testing, repairs were made to the concrete wall coating in the Reactor Cavity. Cracks in the originally installed coating were chased and the adjacent coating was removed. These areas were not top-coated due to the unavailability of that coating at the time. Instead the areas were left with only a base sealer. See Unit 1 photographs.

No other evidence has been found of any repairs since then in Unit 1. Also Unit 2 had no evidence found of any repairs since the startup of the Unit in 1989. A search of work order history and a search of condition reports did not yield any repair requests or coating conditions in either Unit. The maintenance work planner who has been dealing with coatings since startup was not aware of any coating issues in Room 001. Similar discussion with engineering personnel who perform Reactor Vessel inspections in Room 001 also did not yield any information concerning coating problems. Long time STP Health Physics Supervisors also had no knowledge of any coating issues.

As seen in the photographs, the current condition of the coatings in both Units appears to be intact with no obvious delamination or cracking.

Current Condition Based on Photographs of the Area
Unit 1 Photos

Unit 1 Photos

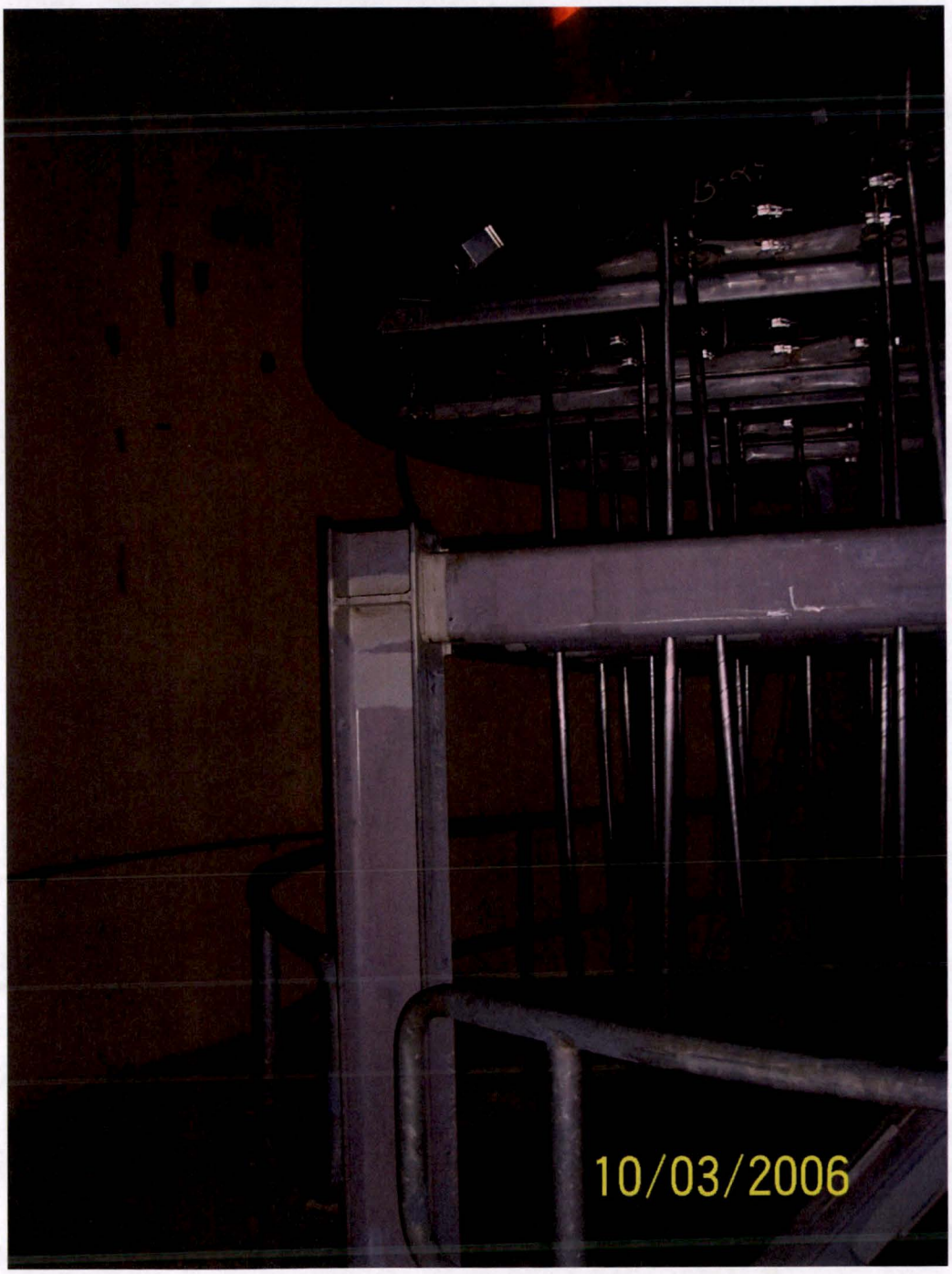

Unit 2 Photos from 2013


4/2/2013 9:31:27 AM 10.200.190.24

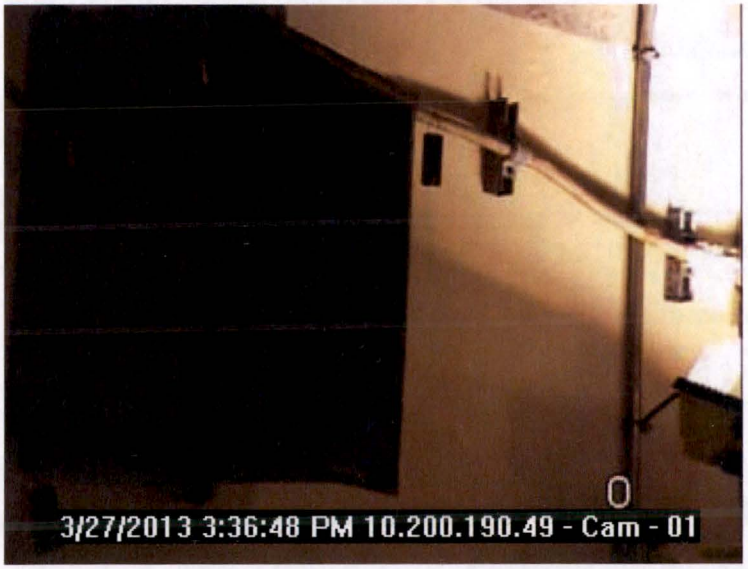
3/27/2013 3:36:48 PM 10.200.190.49 - Cam - 01

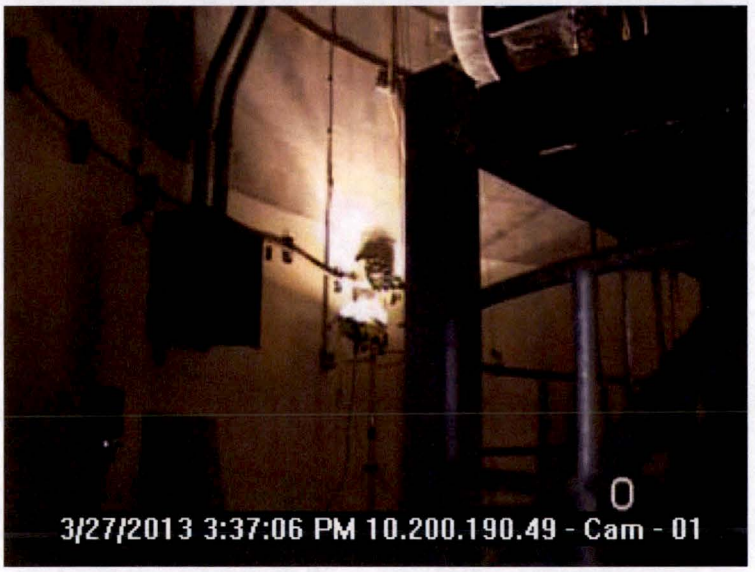

Manufacturer Qualification Data

The test document from Southern Imperial Coatings (filed as STI 525724) states that the Nutec 11/ 11S/ 1201 was qualified to 2E08 rads which is consistent with IEEE STD 323-1974 for normal plus LOCA dose.

However, the epoxy coating for the reactor cavity was deemed by Bechtel during the unqualified coating calculation rack up to be unqualified due to the excessive calculated cumulative radiation dose.

Cumulative Dose Received

The epoxy coating for the reactor cavity was deemed to be unqualified due to excessive radiation.

From design criteria document 4E019NQ1009:

The calculated cumulative design dose for the Reactor Cavity for 40 years is:

Neutron	2.5E10 Rads
Gamma	3.5E9 Rads

The accident dose is given as 1.5E8 Rads.

The calculated cumulative dose was determined considering the reactor operated at 100% power every day for 40 years.

The actual capacity factor for each Unit to date is:

Unit 1	83.7%	from initial operation in 1988 to March 2016 (28 years)
Unit 2	83.2%	from initial operation in 1989 to March 2016 (27 years)

Thus the actual cumulative dose to date is:

= capacity factor x (operating years / design life years) x calculated lifetime dose
= 0.8 x (28/40) x calculated lifetime dose
= 0.56 x calculated lifetime dose

Coatings Assessment

The epoxy coatings in the Reactor Cavity (RCB Room 001) in both Unit 1 and in Unit 2 were applied as Service Level I coatings during the construction phase of the plant. However, these epoxy coatings for the reactor cavity were subsequently deemed to be unqualified due to the excessive calculated cumulative radiation dose. They were not part of the qualified coatings inspection program and there was no continuity of inspections.

The epoxy coatings in the Reactor Cavity in both Unit 1 and in Unit 2 are now deemed as "Qualified But Degraded" based upon consideration of the following:

- Initial application was safety-related (Service Level I)
- No historical evidence of coating problem conditions requiring repairs since installation
- Recent visual observation (photos and personnel observations) shows no signs of degradation
- Estimated cumulative dose to date is over half of the calculated cumulative dose but no current signs of degradation
- Estimated cumulative dose to date exceeds the test qualification value but no current signs of degradation

EPRI Report 1014884 "Plant Support Engineering: Degradation Research for Nuclear Service Level I Coatings" concludes that the majority of coating failures and signs of degradation can be

attributed to undetected deficiencies that occurred at the time of coating application. These deficiencies are the major cause of coating deterioration during the coating systems' service life. The report also states that high radiation is not believed to be a significant cause of coating degradation in containment.

Since the epoxy coatings in the Reactor Cavity in both Units have been in service for over half of their design life with no signs of degradation, any degradation in the future is not expected.

Thus these coatings are considered "Qualified But Degraded".

Debris Characteristics

The Reactor Cavity epoxy coatings are considered as "Qualified But Degraded" and are assumed to fail as chips with the following debris characteristics:

Range (inches)	Weight Distribution (%)
1.0 – 2.0	32.0
0.5 - 1.0	9.04
0.25 – 0.50	4.41
0.125 – 0.25	5.02
< 0.125	37.1 as 15.6 mils chips; 12.3 as 6 mils particulate

Attachment 2

Requests for Exemptions for

STP Piloted Risk-Informed Approach to

Closure for GSI-191

Specific exemption requests, pertaining to requirements that concern Emergency Core Cooling System (ECCS) and Containment Spray System (CSS) system functions for core cooling, and containment heat removal and atmosphere cleanup following a postulated loss of cooling accident (LOCA), are provided as follows:

Request for Exemption from 10CFR50.46(a)(1)

Request for Exemption from GDC 35

Request for Exemption from GDC 38

Request for Exemption from GDC 41

These exemptions are described in detail in Reference 1 to the cover letter and are not repeated in this supplement. Reference 1 included a request for exemption to 10CFR50.46(d). That was superseded by a request for exemption to 10CFR50.46(a)(1) as described in a STPNOC letter to NRC dated April 13, 2016 (ML16111B204). That letter also tabulates the other parts of the STPNOC application that referenced the exemption to 10CFR50.46. Changing the specific paragraph for which exemption was requested had no effect on the technical basis for the exemption.

Attachment 3

License Amendment Request for

STP Piloted Risk-Informed Approach to

Closure for GSI-191

License Amendment Request for
STP Piloted Risk-Informed Approach to Closure for GSI-191

1. Summary Description – Methodology Change and Technical Specification Change

In accordance with 10CFR50.59(c)(2)(viii), STP Nuclear Operating Company requests an amendment to Operating Licenses NPF-79 and NPF-80 for South Texas Project Units 1 and 2 pursuant to 10CFR50.90. The proposed amendment will revise the licensing basis as described in the South Texas Project Electric Generating Station Updated Final Safety Analysis Report to allow the use of a risk-informed approach to address safety issues discussed in Generic Safety Issue -191, "Assessment of Debris Accumulation on Pressurized-Water Reactor Sump Performance". The risk-informed approach is consistent with the guidance of NRC Regulatory Guide 1.174, "An Approach for Using Probabilistic Risk Assessment in Risk-Informed Decisions on Plant-Specific Changes to the Licensing Basis". In addition to the overall methodology change to allow a risk-informed approach, the thermal-hydraulic analysis described in Sections 5 and 6 of Attachment 1-3 is included as part of the proposed methodology change as a method of long-term core cooling evaluation not described in the STP current licensing basis (CLB). The T-H analysis is part of the screening process for the risk-informed approach and shows that, even assuming full blockage of all flow into the core during HLB > 16 inches, there will be adequate cooling regardless of break size.

In addition, STPNOC proposes to amend the STP Unit 1 and Unit 2 Operating Licenses to revise the Technical Specifications (TS) for the Emergency Core Cooling System (ECCS) and the Containment Spray System (CSS). The changes proposed for these TS would add a required action and completion time specific to the effects of debris to TS 3/4.5.2, "ECCS Subsystems – Tavg Greater Than or Equal to 350°F" and TS 3/4.6.2, "Depressurization and Cooling Systems – Containment Spray System". The proposed TS changes will align the TS with the risk-informed methodology change.

The proposed changes will apply only for the effects of debris as described in GSI-191 and GL 2004-02.

The proposed change associated with the change in methodology is to use a risk-informed approach to determine the design requirements to address the effects of LOCA debris instead of a traditional deterministic approach. The details of the approach are provided in Attachment 1 to Reference 1 of the cover letter. The debris analysis covers a full spectrum of postulated LOCAs, including double-ended guillotine breaks, for all pipe sizes up to and including the design basis accident LOCA, to provide assurance that the most severe postulated loss-of-coolant accidents are evaluated. The deterministic current licensing basis (CLB) will continue to apply to LOCA break sizes that generate fine fiber debris that is bounded by STP plant-specific testing. The proposed methodology change will apply for LOCAs that can generate and transport fine fiber debris that is not bounded by the plant-specific testing. STP conservatively relegates to failure the LOCA break sizes that can generate and transport fine fiber debris that is not bounded by the STP plant-specific testing. STP applies NUREG 1829 to determine the break frequency for the smallest of those breaks to obtain the highest frequency, and uses that frequency as the ΔCDF for comparison to the criteria in RG 1.174. The results of the evaluation show that the risk from the proposed change is "very small" in

that it is in Region III of RG 1.174. These results meet the requirement in paragraph (e) of the proposed 10CFR50.46c rule change (ML15238A947) and associated RG 1.229 for the risk from debris to be small. The methodology includes conservatisms in the plant-specific testing and in the assumption that all the unbounded breaks are relegated to failure.

The proposed TS change associated with the change in methodology will create actions and completion times in the ECCS and CSS TS. ECCS and CSS are the only TS systems that depend on the containment emergency sumps as a support system and are therefore the only systems that are directly subject to the effects of debris. The purpose of the proposed changes is to establish actions that are associated with conditions that can potentially affect the effects of debris and provide a required action time that is commensurate with the very low risk associated with debris effects. The proposed action is based on the amount of debris tested in the STP plant-specific testing so that the determination of operability is performed without needing a risk assessment, which makes the process consistent with NRC guidance on operability determinations. The proposed completion time is 90 days.

The proposed change to the licensing basis implements a risk-informed rather than a deterministic method to demonstrate compliance. In conjunction with the proposed LAR, STPNOC is also requesting exemptions from 10CFR50.46(a)(1), GDC 35, GDC 38 and GDC 41 (see Attachment 2). The UFSAR markups are provided in Attachment 3-4.

2.1 Detailed Description – Methodology Change

Upon approval of the licensing basis changes, STPNOC will make the following changes to the STP UFSAR:

- Add Appendix 6A, "Risk-Informed Approach to Potential Impact of Debris Blockage on Emergency Recirculation during Design Basis Accidents". This appendix will describe the evaluations performed using a risk-informed approach to address GSI-191 concerns including the effects on long-term cooling due to debris accumulation on containment sump strainers for ECCS and CSS in recirculation mode, as well as core flow blockage due to in-vessel effects, following loss of coolant accidents (LOCAs).
    - STPNOC requests NRC approval of Section 2.0 of Appendix 6A since it includes criteria for changes that would require prior NRC approval.
- Make conforming changes to UFSAR Chapter 3 descriptions of evaluations against GDC 35, GDC 38 and GDC 41
- Make conforming changes to UFSAR Chapter 6
- Make conforming changes to UFSAR Chapter 15.

Modifications Previously Implemented to Address GSI-191

The current licensing basis for the sumps is based on a deterministic methodology that was used to analyze susceptibility of the ECCS and CSS recirculation functions for adverse effects of post-accident debris. The methodology was largely in accordance with Nuclear Energy Institute report NEI 04-07 and the associated NRC Safety Evaluation Report (SER). In addition, evaluations were performed in accordance with WCAP-16406-P-A, "Evaluation of Downstream Sump Debris Effects in Support of GSI- 191," Revision 1 and WCAP-16793-NP," Evaluation of Long-Term Cooling Considering Particulate and Chemical Debris in the

Recirculating Fluid" to consider the effects that debris carried downstream of the containment sump screen and into the reactor vessel has on core cooling, including fuel and vessel blockage. STPNOC also evaluated the type and expected quantity of chemical products that would be expected to form in the recirculation fluid specifically for STP using the methodology developed in WCAP-16530-NP, "Evaluation of Post-Accident Chemical Effects in Containment Sump Fluids to Support GSI-191". To support the sump performance evaluation, STPNOC performed containment walkdowns using the guidance of NEI 02-01.

The UFSAR changes attached to this application include a description of ECCS sump performance evaluations performed to address GSI-191 and respond to GL 2004-02 prior to this risk-informed licensing application. Those evaluations account for previously implemented hardware modifications and plant procedures and processes to provide high confidence that the sump design supports long-term core cooling following a design basis loss of coolant accident. Those design modifications and procedure changes were implemented in accordance with 10CFR50.59. STP is not requesting approval for those prior changes as part of this license amendment request. The risk-informed evaluation used in the application appropriately accounts for those earlier design modification and procedure changes.

Installation of New Sump Strainer Assemblies

To address debris related concerns associated with GSI-191 and in response to the debris issues identified in GL 2004-02, new ECCS containment sump strainer assemblies were installed in STP Unit 1 in October 2006 and in STP Unit 2 in April 2007. The surface area of the strainers was increased from approximately 155 square feet per sump to approximately 1818 square feet per sump. The screen-hole size of the strainers was reduced from 0.25 inches diameter to 0.095 inches diameter. Small particles in water entering the suction pipe from the sump cannot clog the containment spray nozzles (3/8-inch orifice diameter). Installation of the new strainers did not affect the independence and redundancy of the sumps.

The sump strainer design implemented by these modifications meets the current design basis requirements with respect to net positive suction head and ECCS performance. The sumps are designed according to RG 1.82 proposed Revision 1, dated May 1983, which recommends a calculation of sump screen head loss due to debris blockage. Utilizing the current licensing basis methodology, the pump NPSH is sufficient to accommodate this head loss. The STP sumps meet the function to preclude passage of debris particles large enough to damage downstream components in the ECCS and CSS. The sump strainer design has been evaluated to meet the current design basis assumptions for analyzing the effects of post-accident debris blockage and for compliance with 10CFR50.46 for long term cooling, GDC 35 for emergency core cooling, GDC 36 for inspection of ECCS, GDC 38 for containment heat removal, GDC 39 for inspection of containment heat removal system, and GDC 41 for containment atmosphere cleanup.

The new strainer design is a safety improvement that contributed to meeting the RG 1.174 criteria for Region III, "Very Small Changes," for the results from the risk-informed methodology.

Following installation of the new sump strainers, protective gratings were installed in front of the strainers to preclude inadvertent damage to these components. The framing structure for

the protective gratings consists of vertical grating panels attached to metal columns that are welded to base plates that are anchored into the concrete floor, and is qualified for Seismic II/I loading to ensure the maximum stresses are below the allowable limits. The structure is made of carbon steel and has a qualified coating applied.

Replacement of Fiber Insulation

Per the original plant design, the reactor vessel nozzles were insulated with a non-crush insulation material composed of calcium silicate (brand name Marinite). Marinite insulation was identified as a significant contributor to the debris loading associated with one of the worst case LOCA scenarios for strainer head loss based on previous evaluations. As a result, all of the Marinite insulation was replaced with NUKON fiberglass insulation during the Fall 2009 refueling outage for STP Unit 1 and the Spring 2010 refueling outage for Unit 2. The presence of Marinite in the plant-specific testing conducted in July 2008 is a conservative element of the testing.

Plant-Specific Testing

STP conducted successful plant-specific testing in July 2008 using generally prototypical debris, conservative chemical effects, prototypical simulation of strainer approach flow conditions, and a STP strainer module. This plant-specific test is described in more detail in Attachment 1 and forms the basis for the deterministic scope of the proposed methodology change.

Use of a Risk-Informed Approach to Address GSI-191

The risk associated with GSI-191 issues has been quantified as described in Attachment 1-3 and is "very small" as defined by Region III in RG 1.174. The proposed UFSAR Appendix 6A describes the risk-informed approach used to confirm that the ECCS and CSS will operate with a high probability following a LOCA when considering the impacts and effects described by GSI-191. Therefore no further physical modifications to STP Units 1 and 2 are proposed as part of this license amendment request to implement the risk-informed approach.

Attachment 4 provides the Licensee Commitment to implement the proposed amendment following approval and to revise affected sections of the UFSAR identified in this Attachment. Upon approval of the proposed amendment, applicable UFSAR safety system and design bases descriptions that take credit for the evaluation described in Appendix 6A will be revised. In addition, conforming changes to the Technical Specification Bases are provided in Attachment 3 to this Attachment for information only, to be implemented following NRC approval of the LAR.

The performance evaluations for accidents requiring ECCS operation described in Chapters 6 and 15, based on the South Texas Project Units 1 and 2 Appendix K Large-Break Loss-of-Coolant Accident analysis, demonstrate that for breaks up to and including the double-ended guillotine break of a reactor coolant pipe, the ECCS will limit the clad temperature to below the limit specified in 10CFR50.46, and assure that the core will remain in place and substantially intact with its essential heat transfer geometry preserved.

System redundancy, independence, and diversity features are not changed for those safety systems credited in the accident analyses. No new programmatic compensatory activities or reliance on manual operator actions are required to implement this change.

2.2 Technical Evaluation – Methodology Change

2.2.1 Current System Descriptions

The methodology change affects the analysis of systems and functions that are susceptible to the effects of LOCA debris. The affected systems are those that are supported by the emergency strainers and sumps during the recirculation phase of LOCA mitigation, which are ECCS (LHSI and HHSI) and CSS. The associated functions and associated regulations are:

- ECCS: 10CFR50.46(a)(1), GDC 35
- Containment Heat Removal: GDC 38
- Containment Atmosphere Cleanup: GDC 41

Emergency Core Cooling System

The Emergency Core Cooling System is designed to cool the reactor core and provide shutdown capability subsequent to the following accident conditions:

1. Pipe breaks in the Reactor Coolant System which cause a discharge larger than that which can be made up by the normal makeup system, up to and including the instantaneous circumferential rupture of the largest pipe in the RCS.

2. Rupture of a control rod drive mechanism causing a rod cluster control assembly ejection accident.

3. Pipe breaks in the steam system, up to and including the instantaneous circumferential rupture of the largest pipe in the steam system.

4. A steam generator tube rupture.

The primary function of the ECCS is to remove the stored and fission product decay heat from the reactor core and to provide shutdown capability during accident conditions.

The ECCS provides shutdown capability for the accidents above by means of boron injection. It is designed to tolerate a single active failure in the short term or a single active or passive failure in the long term. The system meets its minimum required performance level with onsite or offsite electrical power.

The ECCS consists of the high head safety injection and low head safety injection pumps, Safety Injection System accumulators, residual heat removal heat exchangers, the refueling water storage tank along with the associated piping, valves, instrumentation, and other related equipment.

The design bases for selecting the functional requirements of the ECCS, such as peak fuel cladding temperature, etc., are derived from Appendix K limits as delineated in 10CFR50.46. The subsystem functional parameters are integrated so that the Appendix K requirements are met over the range of anticipated accidents and single failure assumptions.

Reliability of the ECCS has been considered in selection of the functional requirements, selections of the particular components, and location of components and connected piping. Redundant components are provided where the loss of one component would impair reliability. Valves are provided in series where isolation is desired. Redundant sources of the ECCS actuation signal are available so that the proper and timely operation of the ECCS is not inhibited. Sufficient instrumentation is available so that a failure of an instrument does not impair readiness of the system. The active components of the ECCS are powered from separate buses which are energized from offsite power supplies.

In addition, the standby diesel generators assure that adequate redundant sources of auxiliary onsite power are available to meet all ECCS power requirements. Each diesel is capable of driving all pumps, valves, and necessary instruments associated with one train of the ECCS.

The elevated temperature of the sump solution during recirculation is well within the design temperature of all ECCS components. In addition, consideration has been given to the potential for corrosion of various types of metals exposed to the fluid conditions prevalent immediately after the accident and during long-term recirculation operations.

10CFR50.46(b) provides the following criteria to judge the adequacy of the ECCS.

1. Peak clad temperature calculated shall not exceed 2,200°F.

2. The calculated total oxidation of the clad shall nowhere exceed 0.17 times the total clad thickness before oxidation.

3. The calculated total amount of hydrogen generated from the chemical reaction of the clad with water or steam shall not exceed 0.01 times the hypothetical amount that would be generated if all of the metal in the clad cylinders surrounding the fuel, excluding the clad around the plenum volume, were to react.

4. Calculated changes in core geometry shall be such that the core remains amenable to cooling.

5. After any calculated successful initial operation of the ECCS, the calculated core temperature shall be maintained at an acceptably low value and decay heat shall be removed for the extended period of time required by long-lived radioactivity remaining in the core.

10CFR50.46(a)(1) requires that the criteria set forth in paragraph (b), be demonstrated with ECCS cooling performance calculated in accordance with an acceptable evaluation model, and includes a requirement for "other properties" with regard to the methodology for showing those requirements are met. The methodology is governed by 10CFR50.46(a)(1) and is deterministic with no provision for a risk-informed approach. The LAR supports the

exemptions to 10CFR50.46(a)(1) and GDC 35 described in Attachments 2-1, 2-2, and 2-3 to Reference 1 of the cover letter, as revised by the change to the applicable part of 10CFR50.46 per ML16111B204 .

Containment Heat Removal System

The CHRS is designed to meet the requirements of GDC 38. The CHRS consists of the Reactor Containment Fan Cooler Subsystem, which is a part of the Reactor Containment HVAC System, the RHR heat exchangers, and the Containment Spray System. The ECCS assists the CHRS by transferring heat from the reactor core to the Containment sump. The Residual Heat Removal heat exchangers, in conjunction with the ECCS low-head Safety Injection pumps, are used to transfer heat from the Containment sumps to the Component Cooling Water System. The RCFCs are also cooled by the CCWS following an SI signal. The CCWS rejects this heat to the ultimate heat sink via the Essential Cooling Water System.

The CHRS meets the following design bases:

1. The CHRS is capable of removing sufficient energy to limit the peak Containment pressure and to limit the Containment pressure to a low value at the end of 24 hours after a DBA.

2. In order to ensure the satisfactory operation of the systems after a DBA, each active component is testable during reactor power operation.

3. The system is divided into three trains, with each train receiving power from a separate Emergency Safety Features power supply.

As discussed in Attachment 2-1 and 2-4 to Reference 1 of the cover letter, GDC 38 requires use of deterministic methodology. The LAR complements the proposed exemption by proposing an amendment to the license to allow a risk-informed methodology.

Containment Atmosphere Cleanup System

Containment Atmosphere Cleanup System is designed to meet the requirements of GDC 41. The CSS is provided to reduce the concentration and quantity of fission products in the Containment atmosphere following a LOCA. Per 10CFR50.44, hydrogen recombiners are no longer required for design basis accidents.

The equilibrium sump pH is maintained by trisodium phosphate contained in baskets on the containment floor. The initial CSS water and spilled RCS water dissolves the TSP into the containment sump allowing recirculation of the alkaline fluid. Each unit is equipped with three 50-percent spray trains taking suction from the Containment sump. Each Containment spray train is supplied power from a separate bus. Each bus is connected to both the Offsite and the Standby Power Supply Systems. This assures that for Onsite or for Offsite Electrical Power System failure, their safety function can be accomplished, assuming a single failure.

The CSS is:

1. Designed such that it will tolerate a single active failure.

2. Designed to accommodate the operating basis earthquake within stress limits of applicable codes and to withstand the safe shutdown earthquake without loss of function.

3. Designed to assist in reducing offsite exposures resulting from a design basis accident (DBA) to less than the limits of 10CFR50.67 by rapidly reducing the airborne elemental iodine and particulate concentrations in the Containment following a DBA.

As discussed in Attachment 2-1 and 2-5 to Reference 1 of the cover letter, GDC 41 requires use of deterministic methodology. The LAR complements the proposed exemption by proposing an amendment to the license to allow a risk-informed methodology.

Containment Emergency Sump

The Containment emergency sump meets the following design bases:

1. Sufficient capacity and redundancy to satisfy the single-failure criteria. To achieve this, each CSS/ECCS train draws water from a separate Containment emergency sump.

2. Capable of satisfying the flow and net positive suction head requirements of the ECCS and the CSS under the most adverse combination of credible occurrences. This includes minimizing the possibility of vortexing in the sump.

3. Minimizes entry of high-density particles (specific gravity of 1.05 or more) or floating debris into the sump and recirculating lines.

4. Sumps are designed in accordance with RG 1.82, proposed revision 1, May 1983.

Three independent sumps serve as reservoirs to the ECCS and CSS pumps during the recirculation phase post-DBA. Each sump is stainless steel lined, contains a Vortex Suppressor, and is provided with four stainless steel strainer assemblies. The strainer assemblies for each sump consist of two 5-module assemblies, one 4-module assembly, and one 6-module assembly with each module made up of eleven strainer discs. The strainer screen consists of perforated plate with nominal 0.095 inch diameter openings. Flow leaving the strainer enters a four inlet plenum box (one inlet for each strainer assembly). The plenum box collects the flow from the strainer assemblies and directs the flow vertically downward directly into the sump pit. An access cover is provided on the plenum box for internal inspections of the sump structures, vortex suppressor, and the strainer assemblies.

The sumps are located at the -11 feet-3 inch level of Reactor Containment Building (RCB). The sumps are physically separated from each other. The floor around the emergency sumps slopes away from them and toward normal sumps located in the area. The drains from the upper levels of the RCB do not terminate in the immediate area of the sumps.

The sump structures are designed to withstand the SSE without loss of structural integrity. Water entering the suction pipe from the sump may contain a small amount of particulate and fiber debris (less than 0.095-inch in diameter). This debris cannot clog the spray nozzles (3/8-in. orifice diameter) which are the limiting restrictions in the CSS system served by the sump.

At the beginning of the recirculation phase, the minimum water level above the RCB floor is adequate to provide the required NPSH for the ECCS and CSS pumps.

The sumps are designed to NRC RG 1.82, proposed revision 1, May 1983. The sump structures are designed to limit approach flow velocities to less than 0.009 feet/second permitting high-density particles to settle out on the floor and minimize the possibility of clogging the strainers. The sump structures are designed to withstand the maximum expected differential pressure imposed by the accumulation of debris.

Most potential sources of debris are remote from the emergency sumps and are separated by shield walls or other partitions. Expected debris constituents are pieces of insulation and paint. The possibility of paint chips peeling off has been reduced by requiring proper surface preparation and by painting large surface components (such as: the Containment liner, RCS supports, floors, and structural steel) with coatings which have been qualified under DBA conditions.

The stainless steel reflective insulation is used exclusively on the Reactor Vessel including the head. The blanket fiberglass type is used on the hot piping, valves, and other equipment including the Steam Generators, the Pressurizer, and the Reactor Coolant Pumps. Cellular glass insulation is used on cold piping for antisweat purposes. Microtherm is also used for piping in the wall penetrations.

Containment emergency sumps are inspected periodically as delineated in the Technical Specifications.

2.3 Background

GSI-191 concerns the possibility that debris generated during a LOCA could clog the containment sump strainers in pressurized-water reactors and result in loss of net positive suction head for the ECCS and CSS pumps, impeding the flow of water from the sump. GL 2004-02 requested licensees to address GSI-191 issues, focused on demonstrating compliance with the ECCS acceptance criteria in 10CFR50.46. GL 2004-02 requested licensees to perform new, more realistic analyses using an NRC-approved methodology and to confirm the functionality of the ECCS and CSS during design basis accidents that require containment sump recirculation.

The current design for the containment sumps and strainers was assessed in response to NRC Generic Letter 2004-02. STPNOC provided specific information regarding the deterministic methodology for demonstrating compliance by applying industry and NRC guidance. However, since this methodology has not been demonstrated to fully address GSI-191 without the need for additional changes to the plant design, such as extensive

modifications to insulation in the containment, a risk-informed approach is applied to evaluate effects of LOCA debris using the guidance in RG 1.174.

Larger containment sump strainers have been installed that greatly reduce the potential for loss of net positive suction head. Problematic insulation was removed; reactor coolant system pipe welds where a break could generate large amounts of insulation debris and which were subject to PWSCC were mitigated.

The STP piloted risk-informed approach maintains the defense-in-depth measures as described in Attachment 1-4 to Reference 1 to the cover letter. These measures include those identified in response to NRC Bulletin 2003-01 and GL 2004-02 to address the potential for sump strainer clogging and other concerns associated with GSI-191.

The Commission issued Staff Requirements Memorandum (SRM)-SECY-10-0113, "Closure Options for Generic Safety Issue (GSI) - 191, Assessment of Debris Accumulation on Pressurized Water Reactor Sump Performance," directing the staff to consider alternative options for resolving GSI-191 that are innovative and creative, as well as risk-informed and safety conscious. Subsequently, STPNOC, through interactions with the staff, developed a risk-informed approach to address GSI-191 based on the guidance in RG 1.174. STPNOC submitted to the NRC the preliminary results showing that the risks, Core Damage Frequency and Large Early Release Frequency, associated with GSI-191 concerns are less than the threshold for Region III, "Very Small Changes," of RG 1.174, and notified the NRC of the intent to seek exemption from certain requirements of 10CFR50.46 (ML11354A386). SECY-12-0093, "Closure Options for Generic Safety Issue - 191, Assessment of Debris Accumulation on Pressurized-Water Reactor Sump Performance," described the staff plans to use STPNOC as a pilot for other licensees choosing to use this approach. The exemption request from certain requirements of 10CFR50.46 including impacted General Design Criteria of Appendix A of 10CFR50 is provided in Attachment 2 to this letter.

2.4 Engineering Analysis Evaluation Overview

The design and licensing basis descriptions of accidents requiring ECCS and CSS operation, including analysis methods, assumptions, and results provided in UFSAR Chapters 6 and 15 remain unchanged. This is based on the functionality of the ECCS and CSS during design basis accidents being confirmed by demonstrating that safety margin and defense-in-depth are maintained with high probability (Region III RG 1.174).

The performance evaluations for accidents requiring ECCS operation described in Chapters 6 and 15, based on the South Texas Project Units 1 and 2 Appendix K Large-Break Loss-of-Coolant Accident analysis, demonstrate that for breaks up to and including the double-ended guillotine break of a reactor coolant pipe, the ECCS will limit the clad temperature to below the limit specified in 10CFR50.46, and assure that the core will remain in place and substantially intact with its essential heat transfer geometry preserved.

The methodology for calculating the risk associated with GSI-191 concerns evaluates a full spectrum of breaks up to and including double-ended guillotine breaks, for all RCS pipe sizes. The results show the risk associated with GSI-191 concerns for STP Units 1 and 2 is "very small" as defined by Region III in RG 1.174. Based on evaluation of defense-in-depth, safety

margin, and a high probability of successful performance, the functionality of the ECCS and CSS is confirmed. The detailed technical evaluation is presented in Attachment 1.

The LAR is requested for the scope of breaks that can generate fiber debris on the ECCS sump strainer that exceeds the amount of fiber debris bounded by the plant-specific testing. In Attachment 1-2 and 1-3, STPNOC determined that only large breaks were in this scope and has identified 53 break locations (listed in Attachment 1-3). STPNOC is requesting an amendment to the license for this scope of breaks to allow evaluation of the debris effects using a risk-informed methodology because there is no practical deterministic methodology currently available. The amendment is requested to apply to the methodology and not to the specific set of break locations. Section 5 of Attachment 1-3, RoverD includes a thermal-hydraulic analysis that confirms that there is adequate core cooling for the entire spectrum of breaks. The thermal-hydraulics analysis is part of a risk-informed evaluation for downstream effects (see Section 2 of Attachment 1-3) and applies an 800°F success criteria for PCT. The detailed technical description of the risk-informed screening process is presented in Section 5 of Attachment 1-3.

The RELAP5-3D thermal-hydraulic analysis used to evaluate the down-stream effects for the deterministic scope of breaks to assure LTCC does not replace the ECCS evaluation methodology in the STP UFSAR Chapter 15.6. The current Chapter 15.6 LOCA thermal-hydraulic analysis applies only through the LOCA reflood phase and is not used for the assessment of long-term cooling required by the risk-informed assessment of debris effects.

2.5 Technical Specification Changes

STPNOC is proposing to change the TS for ECCS and CSS to specifically address the potential effects of debris. The ECCS and CSS are the only systems potentially affected by debris effects because they are the only systems that are supported by the containment emergency sumps and strainers.

The description of the Technical Specification change has been revised to incorporate STPNOC's response to STSB RAI 3-1 (Attachment 3 to ML16209A226). The changes include revising the basis for the 90-day required completion time to have a more deterministic rationale instead of the risk-informed basis proposed in Reference 1 to the cover letter, and making the discussion of the Required Action and Bases for the applicability of the TS more definitive with respect to limits on the conditions where the debris-specific action is to be used.

2.5.1 TS 3/4.5.2, "ECCS Subsystems – Tavg Greater Than or Equal to 350°F"

System Description – see Section 2.2.1, above

The change to the ECCS TS is proposed only for TS 3.5.2, which applies in MODE 1, 2, and 3. The risk-informed debris evaluation is performed with the plant assumed to be at-power when the initiating event LOCA occurs. Consequently, the debris generation and transport is initiated from normal operating temperature and pressure conditions. Those conditions maximize the break zones of influence (ZOI) and initial decay heat. STPNOC considered application of a debris-

specific TS requirement to TS 3.5.3, which applies in MODE 4 and determined that application of the current licensing basis for debris is adequate for the following reasons:

- STPNOC believes the deterministic testing is adequate for any MODE 4 LOCA because MODE 4 plant conditions do not support generation or transport of comparable quantities of debris.
    - RCS conditions with temperature less than 350° and pressure below the cold overpressure mitigation system setpoint would not be expected to result in ZOIs comparable to MODE 3 and higher
    - Cooling requirements are reduced because decay heat is much lower in MODE 4
    - Pipe break likelihood would be significantly lower based on lower operating stresses and much shorter lengths of time in MODE 4 compared to MODE 3 and higher.

Debris Related Required Action

STPNOC proposes the required action below.

c. With less than the required flow paths OPERABLE solely due to potential effects of LOCA generated and transported debris that exceeds analyzed amounts, perform the following:

1. Immediately initiate action to implement compensatory actions,

AND

2. Within 90 days restore the affected subsystems to OPERABLE status,

OR

Be in at least HOT STANDBY within the next 6 hours and in HOT SHUTDOWN within the following 6 hours

The proposed required action applies to the LCO 3.5.2.d requirement to have an operable flow path through the containment sump. It applies only for the potential effects of LOCA generated and transported debris that exceeds the amount that has been analyzed. It does not apply to non-conforming or degraded conditions that are not associated with the LOCA generated and transported debris, such as a strainer obstructed by a tarp (a condition that makes the strainer non-functional regardless of debris) or a strainer with large gaps that would pass debris fragments which would make non-applicable the risk evaluation based on fine fiber debris. The TS Bases address the limits of the applicability of the Required Action. The operability with respect to debris is based on a quantity of debris; therefore, emergent nonconforming or degraded conditions can be evaluated in a deterministic process based on analyzed debris conditions. No quantitative risk assessment is necessary, so the evaluation process is consistent with the guidance in NRC Inspection Manual Chapter 0326 that does not allow the use of risk in an operability determination.

The required action to implement compensatory action is based on the very low contribution of LOCA generated debris to the risk of core damage and the margins in the deterministic testing, and is a reasonable response to minimize the potential increase in risk from the debris source. Typical compensatory action would include actions such as:

- Remove the debris or source of debris or take action that would prevent transport of the debris to the emergency sump
- Defer maintenance that would affect availability of the affected systems and strainers
- Defer maintenance that would affect availability of primary defense in depth systems such as RCFCs
- Increase frequency of RCS leak detection monitoring
- Brief operators on LOCA debris management actions

The requirement to be in at least HOT STANDBY within the next 6 hours and in HOT SHUTDOWN within the following 6 hours is consistent with the existing end-state in the required actions in the ECCS TS. (Note that this is corrected from the "COLD SHUTDOWN in the following 30-days" end-state proposed in Reference 1 to the cover letter.)

Existing action c will be administratively redesignated as action d, and the ECCS TS pages will be renumbered to accommodate the new action statement.

Debris Related Required Completion Time

The action applies only for the potential effects of debris. Under the current TS, STPNOC would likely apply the Risk Managed Technical Specification (RMTS) PRA Functional allowance in NEI 06-09 Section 2.3.1 since the ECCS would still be functional for small and medium break LOCAs. Based on the risk evaluation in RoverD, STPNOC expects the 30-day "backstop" RMTS completion time would apply. Under current TS, STPNOC would monitor and manage risk based on plant configuration until operability was restored or the 1E-05 ICDP limit is reached.

Unlike RMTS, the proposed required completion time of 90 days is a set time and not subject to the risk management requirements of RMTS. Also, because the required completion time is longer than the 30-day RMTS backstop time, RMTS will not apply for the proposed action.

A 90-day completion time is reasonable for emergent conditions that involve debris that could be generated and transported under LOCA conditions. The likelihood of an initiating event in the 90-day completion time is very small (1/4 of the LOCA annual frequency). There are margins in the debris generation and transport analyses and in the downstream and in-core effects analyses. Ninety days is a reasonable time to identify and implement mitigating or compensatory action, such as removing the debris, securing or containing the debris so that it is not transportable, performing additional analysis, or obtaining regulatory relief (e.g., Enforcement Discretion and/or Emergency or Exigent TS change). The compensatory actions required by proposed Required Action c.1 provide additional assurance that the potential debris effects of the emergent condition would be mitigated. In addition to the actions directly addressing the debris just mentioned, plant system configuration can be managed by application of the CRMP to maximize availability of

mitigating systems (e.g., ECCS, AFW, SDGs) and defense in depth (e.g., containment isolation, RCFC, CCW, ECW) by limiting activities that remove them from service.

NRC approval of TSTF-448 under the Consolidated Line Item Improvement Process (ML063460558), which revised the TS required action and completion times for Control Room Envelope Ventilation and Filtration System (CREVFS), is precedence for a 90-day completion time with compensatory actions supporting the extended completion time.

The advantages of the 90-day completion time are:

1. It provides clarity for the operators with regard to application of the TS for degraded or nonconforming conditions associated with the potential effects of LOCA debris.
2. It eliminates the need to apply the "PRA Functional" feature of RMTS, which simplifies application of the TS.
3. It improves the usefulness of the STP pilot application as a precedent for other licensees.

2.5.2 TS 3/4.6.2.1, "Depressurization and Cooling Systems – Containment Spray System"

System Description – see Section 2.2.1, above

CSS applies in MODE 1, 2, 3, and 4. New Action c is added to address effects of debris in MODE 1, 2, and 3. As for the ECCS TS, the deterministic testing is considered to bound the LOCA debris for any LOCA in MODE 4. STPNOC is incorporating wording in the CSS TS Bases to clarify the difference between the debris related requirements for MODE 1, 2, and 3 and MODE 4.

Debris Related Required Action

The proposed required action for CSS is essentially the same as that for ECCS:

c. With one or more Containment Spray Systems inoperable in MODE 1, 2, or 3 solely due to potential effects of LOCA generated and transported debris that exceeds analyzed amounts, perform the following:

    1. Immediately initiate action to implement compensatory actions,

    AND

    2. Within 90 days restore the affected system(s) to OPERABLE status,

OR

Be in at least HOT STANDBY within the next 6 hours and in COLD SHUTDOWN within the following 30 hours

Debris Related Required Completion Time

As with ECCS, STPNOC is proposing a 90-day required completion time. Also, similar to ECCS, RMTS applies to CSS, so the same elements of the ECCS discussion above apply for CSS. The basis for the CSS completion time is the same as the basis for the ECCS completion time.

The CSS TS pages will be renumbered to accommodate the new action statement.

3.0 Evaluation of Defense-in Depth (DID) and Safety Margin

Detailed evaluations of DID and Safety Margin are presented in Attachment 1-4 to Reference 1 of the cover letter and can be applied to both the methodology change and the TS change.

4.0 Implementation and Monitoring Program

Design modifications addressing GSI-191 concerns, including installation of new sump strainers and replacement of problematic insulation, have been previously implemented using the STP design change process.

STPNOC has implemented procedures and programs for monitoring, controlling and assessing changes to the plant that have a potential impact on plant performance related to GSI-191 concerns. These provide the capability to monitor the performance of the sump strainers and the ability to assess impacts to the inputs and assumptions used in the PRA and the associated engineering analysis that support the proposed change. Programmatic requirements ensure that the potential for debris loading on the sump does not materially increase. These include:

- Programs and procedures have been implemented to evaluate and control potential sources of debris in containment:
    - Technical Specification Surveillance Requirements implemented by STP procedures require visual inspections of all accessible areas of the containment to check for loose debris, and each containment sump to check for debris, as described in Section 4.1.3.
    - The STP Design Change Package procedure includes provisions for managing potential debris sources such as insulation, qualified coatings, addition of aluminum or zinc, and potential effects of post-LOCA debris on recirculation flow paths and downstream components. The procedure has been augmented to explicitly require changes that involve any work or activity inside the containment be evaluated for the potential to affect the following:
        - Reactor coolant pressure boundary integrity
        - Accident or post-accident equipment inside containment
        - Quantity of metal inside containment

- Quantity or type of coatings inside containment
- Thermal insulation changed or added
- Post-LOCA recirculation flow paths to the emergency sumps
- Post-LOCA recirculation debris impact on internals of fluid components
- Addition or deletion of cable

- A 10CFR50.59 screening or evaluation is required to be completed for all design changes. This process ensures that new insulation material that may differ from the initial design is evaluated for GSI-191 concerns.

- Programs to ensure that Service Level 1 protective coatings used inside containment are procured, applied, and maintained in compliance with applicable regulatory requirements. Procedures have been implemented to govern the use of signs and labels inside containment.

- As part of the STP Condition Reporting Process, condition reports are written due to adverse conditions identified during the containment inspections or containment emergency sumps and strainers surveillances.
- The STP Maintenance Rule program includes performance monitoring of functions associated with ECCS and CSS. The inclusion of the ECCS and CSS into the Maintenance Rule program and the assessment of acceptable system performance provide continued assurance of the availability for performance of the required functions.
- The STP QA program is implemented and controlled in accordance with the Operations Quality Assurance Plan and is applicable to SSCs to an extent consistent with their importance to safety, and complies with the requirements of 10CFR50, Appendix B and other program commitments as appropriate.

  The QA Program is implemented with documented instructions, procedures, and drawings which include appropriate quantitative and qualitative acceptance criteria for determining that prescribed activities have been satisfactorily accomplished. Procedures control the sequence of required inspections, tests, and other operations when important to quality. To change these controls, the individual procedure must be changed and a similar level of review and approval given to the original procedure is required. Such instructions, procedures, and drawings are reviewed and approved for compliance with requirements appropriate to their safety significance.

  QA program controls are applied to safety-related SSCs to provide a high degree of confidence that they perform safely and activities are performed as expected. The rigorous controls imposed by the QA program provide adequate quality control elements to ensure system component reliability for the required functions.

The proposed change does not involve any changes to ASME Section XI inspection programs or mitigation strategies that have been shown effective in early detection and mitigation of weld and material degradation in Class I piping applications.

5.0 Technical Evaluation Conclusion

The technical evaluation shows that the functionality of the ECCS and CSS during design basis accidents is confirmed by demonstrating that safety margin and defense-in-depth are maintained with high probability (Region III RG 1.174).

6.0 Regulatory Evaluation

6.1 Regulatory Requirements

The following regulations apply to the proposed amendment. Approval of the proposed amendment is contingent upon approval of the requests for exemptions from these regulations as provided and justified in Attachments 2-1 through 2-5 of Reference 1 in the cover letter, as revised by the change to the applicable part of 10CFR50.46 per ML16111B204.

- 10CFR50.46(a)(1)
- GDC 35, "Emergency core cooling"
- GDC 38, "Containment heat removal,"
- GDC 41, "Containment atmosphere cleanup,"

6.2 Regulatory Guidance

NRC Regulatory Guide 1.174, "An Approach for using Probabilistic Risk Assessment in Risk-Informed Decisions on Plant-Specific Changes to the Licensing Basis," provides the NRC staff's recommendations for using risk information in support of licensee-initiated Licensing Basis changes to a nuclear power plant that require NRC review and approval. This regulatory guide describes an acceptable approach for assessing the nature and impact of proposed Licensing Basis changes by considering engineering issues and applying risk insights.

In implementing risk-informed decision making, Licensing Basis changes are expected to meet a set of key principles. These principles include the following:

1. *The proposed change meets the current regulations unless it is explicitly related to a requested exemption (i.e., a specific exemption under 10CFR50.12, "Specific Exemptions").*

   The exemptions requested in Attachment 2 to this letter implement this requirement.

2. *The proposed change is consistent with a defense-in-depth philosophy.*

   Defense-in-depth is presented in detail in Attachment 1-4. The proposed change is consistent with the defense-in-depth philosophy in that the following aspects of the facility design and operation are unaffected:

   - Functional requirements and the design configuration of systems
   - Existing plant barriers to the release of fission products
   - Design provisions for redundancy, diversity, and independence
   - Plant's response to transients or other initiating events
   - Preventive and mitigative capabilities of plant design features

   The STP risk-informed approach analyzes a full spectrum of LOCAs, including double-ended guillotine breaks for all piping sizes up to and including the largest pipe in the reactor coolant system. By requiring that mitigative capability be maintained in a realistic and risk-informed evaluation of GSI-191 for a full spectrum of LOCAs, the approach ensures that defense-in-depth is maintained.

3. *The proposed change maintains sufficient safety margins.*

   As described in Attachment 1-4, sufficient safety margins associated with the design will be maintained by the proposed change.

4. *When proposed changes result in an increase in CDF or risk, the increases should be small and consistent with the intent of the Commission's Safety Goal Policy Statement.*

   The proposed change is defined as the risk associated with effects of LOCA debris. Using engineering analysis and the PRA, this risk has been calculated and shown to be "very small" as defined by Region III in RG 1.174 and is therefore consistent with the Commission's Safety Goal Policy Statement.

5. *The impact of the proposed change should be monitored using performance measurement strategies.*

   Performance monitoring is discussed in Section 4.0 above.

NRC Regulatory Guide 1.200, "An Approach for Determining the Technical Adequacy of Probabilistic Risk Assessment Results for Risk-Informed Activities," describes one acceptable approach for determining whether the quality of the PRA, in total or the parts that are used to support an application, is sufficient to provide confidence in the results, such that the PRA can be used in regulatory decision-making for light-water reactors. The STPNOC PRA model used for the risk-informed approach for addressing GSI-191 concerns is in compliance with Revision 1 of RG 1.200 (ML13323A183, Enclosure 4-2; ML14178A481, Attachment 1, pg. 2).

6.3 Precedents

As discussed above, TSTF-448 under the Consolidated Line Item Improvement Process (ML063460558), which revised the TS required action and completion times for Control Room Envelope Ventilation and Filtration System (CREVFS), is precedence for a 90-day completion time with compensatory actions supporting the extended completion time.

6.4 No Significant Hazards Consideration Determination (unchanged from previous submittal)

STPNOC has evaluated whether or not a significant hazards consideration is involved with the proposed amendment by focusing on the three standards set forth in 10CFR50.92, "Issuance of amendment," as discussed below:

1. Does the proposed change involve a significant increase in the probability or consequences of an accident previously evaluated?

Response: No.

The proposed changes are a methodology change for assessment of debris effects that adds the results of a risk-informed evaluation to the STP licensing basis, changes to the ECCS and CSS TS to extend the required completion time for potential LOCA debris related effects and associated administrative TS changes. The methodology change concludes that the ECCS and CSS will have sufficient defense-in-depth and safety margin and will operate with high probability following a LOCA when considering the impacts and effects of debris accumulation on containment emergency sump strainers in recirculation mode, as well as core flow blockage due to in-vessel effects, following loss of coolant accidents. The methodology change also supports the changes to the TS.

There is no significant increase in the probability of an accident previously evaluated. The proposed changes address mitigation of loss of coolant accidents and have no effect on the probability of the occurrence of a loss of coolant accident. The proposed methodology and TS changes do not implement any physical changes to the facility or any SSCs, and do not implement any changes in plant operation that could lead to a different kind of accident.

The proposed changes do not involve a significant increase in the consequences of an accident previously evaluated. The methodology change confirms that required SSCs supported by the containment sumps will perform their safety functions with a high probability, as required, and does not alter or prevent the ability of SSCs to perform their intended function to mitigate the consequences of an accident previously evaluated within the acceptance limits. The safety analysis acceptance criteria in the UFSAR continue to be met for the proposed methodology change. The evaluation of the changes determined that containment integrity will be maintained. The dose consequences were considered in the assessment and quantitative evaluation of the effects on dose using input from the risk-informed approach shows the increase in dose consequences is small.

Therefore, the proposed change does not involve a significant increase in the probability or consequences of any the accident previously evaluated in the UFSAR.

2. **Does the proposed change create the possibility of a new or different kind of accident from any accident previously evaluated?**

   Response: No.

   The proposed changes are a methodology change for assessment of debris effects from LOCAs that are already evaluated in the STP UFSAR, an extension of TS required completion time for potential LOCA debris related effects on ECCS and CSS, and associated administrative changes to the TS. No new or different kind accident is being evaluated. None of the changes install or remove any plant equipment, or alter the design, physical configuration, or mode of operation of any plant structure, system or component. The proposed changes do not introduce any new failure mechanisms or malfunctions that can initiate an accident. The proposed changes do not introduce failure modes, accident initiators, or equipment malfunctions that would cause a new or different kind of accident. Therefore, the proposed changes do not create the possibility for a new or different kind of accident from any previously evaluated.

3. **Does the proposed change involve a significant reduction in a margin of safety?**

   Response: No.

   The proposed changes are a methodology change for assessment of debris effects from LOCAs that are already evaluated in the STP UFSAR, an extension of TS required completion time for potential LOCA debris related effects on ECCS and CSS, and associated administrative changes to the TS. The effects from a full spectrum of LOCAs, including double-ended guillotine breaks for all piping sizes up to and including the largest pipe in the reactor coolant system, are analyzed. Appropriate redundancy and consideration of loss of offsite power and worst case single failure are retained, such that defense-in-depth is maintained.

   Application of the risk-informed methodology showed that the increase in risk from the contribution of debris effects is very small as defined by RG 1.174 and that there is adequate defense in depth and safety margin. Consequently, STP determined that the risk-informed method demonstrates the containment sumps will continue to support the ability of safety related components to perform their design functions when the effects of debris are considered. The proposed change does not alter the manner in which safety limits are determined or acceptance criteria associated with a safety limit. The proposed change does not implement any changes to plant operation, and does not significantly affect SSCs that respond to safely shutdown the plant and to maintain the plant in a safe shutdown condition. The proposed change does not significantly affect the existing safety margins in the barriers for the release of radioactivity. There are no changes to any of the safety analyses in the UFSAR.

Defense in depth and safety margin was extensively evaluated for the methodology change and the associated TS changes. The evaluation determined that there is substantial defense in depth and safety margin that provide a high level of confidence that the calculated risk for the methodology and TS changes is conservative and that the actual risk is likely much lower.

Therefore, the proposed change does not involve a significant reduction in a margin of safety.

Based on the above, STPNOC concludes that the proposed amendments do not involve a significant hazards consideration under the standards set forth in 10CFR50.92(c), and accordingly, a finding of "no significant hazards consideration" is justified.

6.5 Conclusion

Based on the considerations discussed above, (1) there is reasonable assurance that the health and safety of the public will not be endangered by operation in the proposed manner, (2) such activities will be conducted in compliance with the Commission's regulations contingent upon approval of the exemption requested in Attachment 2 to this letter, and (3) the issuance of the amendment will not be inimical to the common defense and security or to the health and safety of the public.

7.0 Environmental Consideration

A review has determined that the proposed amendment would change a requirement with respect to installation or use of a facility component located within the restricted area, as defined in 10 CFR 20. However, the proposed amendment does not involve (i) a significant hazards consideration, (ii) a significant change in the types or a significant increase in the amounts of any effluents that may be released offsite, or (iii) a significant increase in individual or cumulative occupational radiation exposure. Accordingly, the proposed amendment meets the eligibility criterion for categorical exclusion set forth in 10CFR51.22(c)(9). Therefore, pursuant to 10CFR51.22(b), no environmental impact statement or environmental assessment need be prepared in connection with the proposed amendment.

Attachment 3-1

Technical Specification Page Markups

EMERGENCY CORE COOLING SYSTEMS

3/4.5.2 ECCS SUBSYSTEMS - T_{AVG} GREATER THAN OR EQUAL TO 350°F

LIMITING CONDITION FOR OPERATION

3.5.2 Three independent Emergency Core Cooling System (ECCS) subsystems shall be OPERABLE with each subsystem comprised of:

a. One OPERABLE High Head Safety Injection pump,

b. One OPERABLE Low Head Safety Injection pump,

c. One OPERABLE RHR heat exchanger, and

d. An OPERABLE flow path capable of taking suction from the refueling water storage tank on a Safety Injection signal and automatically transferring suction to the containment sump during the recirculation phase of operation through a High Head Safety Injection pump and into the Reactor Coolant System and through a Low Head Safety Injection pump and its respective RHR heat exchanger into the Reactor Coolant System.

APPLICABILITY: MODES 1, 2, and 3.*

ACTION:

a. With less than the above subsystems OPERABLE, but with at least two High Head Safety Injection pumps in an OPERABLE status, two Low Head Safety Injection pumps and associated RHR heat exchangers in an OPERABLE status, and sufficient flow paths to accommodate these OPERABLE Safety Injection pumps and RHR heat exchangers,** within 7 days restore the inoperable subsystem(s) to OPERABLE status or apply the requirements of the CRMP, or be in at least HOT STANDBY within the next 6 hours and in HOT SHUTDOWN within the following 6 hours.

b. With less than two of the required subsystems OPERABLE, within 1 hour restore at least two subsystems to OPERABLE status or apply the requirements of the CRMP, or be in at least HOT STANDBY within the next 6 hours and in HOT SHUTDOWN within the following 6 hours.

EMERGENCY CORE COOLING SYSTEMS

3/4.5.2 ECCS SUBSYSTEMS - T_{AVG} GREATER THAN OR EQUAL TO 350°F

LIMITING CONDITION FOR OPERATION

c. With less than the required flow paths OPERABLE solely due to potential effects of LOCA generated and transported debris that exceeds analyzed amounts, perform the following:

1. Immediately initiate action to implement compensatory actions,
AND
2. Within 90 days restore the affected flowpath(s) to OPERABLE status,

OR

Be in at least HOT STANDBY within the next 6 hours and in HOT SHUTDOWN within the following 6 hours.

d. In the event the ECCS is actuated and injects water into the Reactor Coolant System, a Special Report shall be submitted within 90 days describing the circumstances of the actuation and the total accumulated actuation cycles to date. The current value of the usage factor for each affected Safety Injection nozzle shall be provided in this Special Report whenever its value exceeds 0.70.

---

* Entry into MODE 3 is permitted for the Safety Injection pumps declared inoperable pursuant to Specification 4.5.3.1.2 provided that the Safety Injection pumps are restored to OPERABLE status within 4 hours or prior to the temperature of one or more of the RCS cold legs exceeding 375°F, whichever comes first.

** Verify required pumps, heat exchangers and flow paths OPERABLE every 48 hours.

CONTAINMENT SYSTEMS

3/4.6.2 DEPRESSURIZATION AND COOLING SYSTEMS

CONTAINMENT SPRAY SYSTEM

LIMITING CONDITION FOR OPERATION

3.6.2.1

Three independent Containment Spray Systems shall be OPERABLE with each Spray system capable of taking suction from the RWST and transferring suction to the containment sump.

APPLICABILITY: MODES 1, 2, 3, and 4

ACTION:

a. With one Containment Spray System inoperable, within 7 days restore the inoperable Spray System to OPERABLE status or apply the requirements of the CRMP, or be in at least HOT STANDBY within the next 6 hours; restore the inoperable Spray System to OPERABLE status within the next 48 hours or be in COLD SHUTDOWN within the following 30 hours.

b. With more than one Containment Spray System inoperable, within 1 hour restore at least two Spray Systems to OPERABLE status or apply the requirements of the CRMP, or be in at least HOT STANDBY within the next 6 hours and in COLD SHUTDOWN within the following 30 hours.

c. With one or more Containment Spray Systems inoperable in MODE 1, 2, or 3 solely due to potential effects of LOCA generated and transported debris that exceeds analyzed amounts, perform the following:

1. immediately initiate action to implement compensatory actions,

AND

2. within 90 days restore the affected system(s) to OPERABLE status,

OR

Be in at least HOT STANDBY within the next 6 hours and in COLD SHUTDOWN within the following 30 hours.

CONTAINMENT SPRAY SYSTEM
SURVEILLANCE REQUIREMENTS

4.6.2.1 Each Containment Spray System shall be demonstrated OPERABLE:

a. At a frequency in accordance with the Surveillance Frequency Control Program by verifying that each valve (manual, power-operated, or automatic) in the flow path that is not locked, sealed, or otherwise secured in position, is in its correct position;

b. By verifying on a STAGGERED TEST BASIS, that on recirculation flow, each pump develops a differential pressure of greater than or equal to 283 psid when tested pursuant to Specification 4.0.5;

c. At a frequency in accordance with the Surveillance Frequency Control Program during shutdown, by:

1) Verifying that each automatic valve in the flow path actuates to its correct position on a Containment Pressure High 3 test signal, and

2) Verifying that each spray pump starts automatically on a Containment Pressure High 3 test signal coincident with a sequencer start signal.

d. By verifying each spray nozzle is unobstructed following maintenance activities that could result in spray nozzle blockage.

Attachment 3-2

"Clean" Technical Specification Pages

EMERGENCY CORE COOLING SYSTEMS

3/4.5.2 ECCS SUBSYSTEMS - T_{AVG} GREATER THAN OR EQUAL TO 350°F

LIMITING CONDITION FOR OPERATION

3.5.2 Three independent Emergency Core Cooling System (ECCS) subsystems shall be OPERABLE with each subsystem comprised of:

a. One OPERABLE High Head Safety Injection pump,

b. One OPERABLE Low Head Safety Injection pump,

c. One OPERABLE RHR heat exchanger, and

d. An OPERABLE flow path capable of taking suction from the refueling water storage tank on a Safety Injection signal and automatically transferring suction to the containment sump during the recirculation phase of operation through a High Head Safety Injection pump and into the Reactor Coolant System and through a Low Head Safety Injection pump and its respective RHR heat exchanger into the Reactor Coolant System.

APPLICABILITY: MODES 1, 2, and 3.*

ACTION:

a. With less than the above subsystems OPERABLE, but with at least two High Head Safety Injection pumps in an OPERABLE status, two Low Head Safety Injection pumps and associated RHR heat exchangers in an OPERABLE status, and sufficient flow paths to accommodate these OPERABLE Safety Injection pumps and RHR heat exchangers,** within 7 days restore the inoperable subsystem(s) to OPERABLE status or apply the requirements of the CRMP, or be in at least HOT STANDBY within the next 6 hours and in HOT SHUTDOWN within the following 6 hours.

b. With less than two of the required subsystems OPERABLE, within 1 hour restore at least two subsystems to OPERABLE status or apply the requirements of the CRMP, or be in at least HOT STANDBY within the next 6 hours and in HOT SHUTDOWN within the following 6 hours.

3/4.5.2 ECCS SUBSYSTEMS - T_{AVG} GREATER THAN OR EQUAL TO 350°F

LIMITING CONDITION FOR OPERATION

c. With less than the required flow paths OPERABLE solely due to potential effects of LOCA generated and transported debris that exceeds analyzed amounts, perform the following:

1. Immediately initiate action to implement compensatory actions,
AND
2. Within 90 days restore the affected flowpath(s) to OPERABLE status,

OR

Be in at least HOT STANDBY within the next 6 hours and in HOT SHUTDOWN within the following 6 hours.

d. In the event the ECCS is actuated and injects water into the Reactor Coolant System, a Special Report shall be submitted within 90 days describing the circumstances of the actuation and the total accumulated actuation cycles to date. The current value of the usage factor for each affected Safety Injection nozzle shall be provided in this Special Report whenever its value exceeds 0.70.

---

* Entry into MODE 3 is permitted for the Safety Injection pumps declared inoperable pursuant to Specification 4.5.3.1.2 provided that the Safety Injection pumps are restored to OPERABLE status within 4 hours or prior to the temperature of one or more of the RCS cold legs exceeding 375°F, whichever comes first.

** Verify required pumps, heat exchangers and flow paths OPERABLE every 48 hours.

CONTAINMENT SYSTEMS

3/4.6.2 DEPRESSURIZATION AND COOLING SYSTEMS

CONTAINMENT SPRAY SYSTEM

LIMITING CONDITION FOR OPERATION

3.6.2.1

Three independent Containment Spray Systems shall be OPERABLE with each Spray system capable of taking suction from the RWST and transferring suction to the containment sump.

APPLICABILITY: MODES 1, 2, 3, and 4

ACTION:

a. With one Containment Spray System inoperable, within 7 days restore the inoperable Spray System to OPERABLE status or apply the requirements of the CRMP, or be in at least HOT STANDBY within the next 6 hours; restore the inoperable Spray System to OPERABLE status within the next 48 hours or be in COLD SHUTDOWN within the following 30 hours.

b. With more than one Containment Spray System inoperable, within 1 hour restore at least two Spray Systems to OPERABLE status or apply the requirements of the CRMP, or be in at least HOT STANDBY within the next 6 hours and in COLD SHUTDOWN within the following 30 hours.

c. With one or more Containment Spray Systems inoperable in MODE 1, 2, or 3 solely due to potential effects of LOCA generated and transported debris that exceeds analyzed amounts, perform the following:

1. immediately initiate action to implement compensatory actions,

AND

2. within 90 days restore the affected system(s) to OPERABLE status,

OR

Be in at least HOT STANDBY within the next 6 hours and in COLD SHUTDOWN within the following 30 hours.

SURVEILLANCE
REQUIREMENTS

4.6.2.1 Each Containment Spray System shall be demonstrated OPERABLE:

a. At a frequency in accordance with the Surveillance Frequency Control Program by verifying that each valve (manual, power-operated, or automatic) in the flow path that is not locked, sealed, or otherwise secured in position, is in its correct position;

b. By verifying on a STAGGERED TEST BASIS, that on recirculation flow, each pump develops a differential pressure of greater than or equal to 283 psid when tested pursuant to Specification 4.0.5;

c. At a frequency in accordance with the Surveillance Frequency Control Program during shutdown, by:

1) Verifying that each automatic valve in the flow path actuates to its correct position on a Containment Pressure High 3 test signal, and

2) Verifying that each spray pump starts automatically on a Containment Pressure High 3 test signal coincident with a sequencer start signal.

d. By verifying each spray nozzle is unobstructed following maintenance activities that could result in spray nozzle blockage.

Attachment 3-3

Technical Specifications Bases
Page Markups

(Information Only)

Technical Specifications Bases Page Markups (Information Only)

Add the following to the Bases Section for 3/4.5.2 ECCS Subsystems:

The OPERABILITY of the ECCS Subsystems is assured by the capability of the containment emergency sump strainers to limit entry of debris into the sump and recirculating lines. This capability ensures that the flow and net positive suction head requirements of ECCS are satisfied. Assurance that containment debris will not block the sump strainers and render the ECCS Subsystem inoperable on emergency recirculation during design basis accidents is provided by inspection and engineering evaluation. UFSAR Appendix 6A provides a risk-informed approach that addresses the potential of debris blockage concluding that long-term core cooling following a design basis loss of coolant accident is assured with high probability. UFSAR Appendix 6A also provides guidance for assessing the potential impact on Operability due to unexpected material such as loose debris discovered in containment that may contribute to debris loading on the strainers.

Technical Basis:

The Licensing Basis with regard to effects of debris is that there is a high probability that ECCS and CSS can perform their design basis functions based on successful plant-specific prototypical testing using deterministic NRC-approved assumptions, and that the risk from breaks that could generate debris that is not bounded by the testing is very small and acceptable in accordance with the criteria of RG 1.174.

STP evaluated the risk associated with the effects on long-term cooling due to debris accumulation on Emergency Core Cooling System (ECCS) and Containment Spray System (CSS) sump strainers in recirculation mode, as well as core flow blockage due to in-vessel effects of debris that penetrates the strainers. A full spectrum of postulated LOCAs is analyzed, including double-ended guillotine breaks (DEGBs) for all pipe sizes up to the largest pipe in the reactor coolant system. The changes to CDF and LERF associated with the effects of debris are quantified by applying the LOCA frequencies published in NUREG-1829, and then compared to RG 1.174 acceptance guidelines. The STP analysis shows that the contribution to risk from the breaks that are not deterministically mitigated is within RG 1.174 Region III.

Strainer Operability:

The affected ECCS and CSS are OPERABLE with respect to the effects of debris when the expected effects of the debris on the emergency sump strainers are consistent with the analysis. This operability requirement is based on quantity and characteristics and location of the debris in the RCB being consistent with the debris analysis assumptions. The types of debris considered in the analysis included insulation and latent debris fiber fines, particulate from coatings and latent debris, and chemical precipitates (primarily from aluminum corrosion).

Strainer operability evaluation is fundamentally deterministic and the intent is to not require a risk assessment to make the operability determination. The criterion recognizes that there is margin

and conservatism in the debris assumptions used for the deterministic testing and in the debris generation and transport analyses that can be applied to account for previously unidentified debris.

Guidance for evaluating potential debris is provided in 0PSP03-XC-0002A.

Applicability:

This required action applies only for the potential effects of debris on emergency sump strainer operability or on in-core debris effects. It does not apply for effects other than those caused by debris. Debris effects are conditions caused by transportable debris that could impact the net positive suction head or otherwise degrade pump performance, or cause strainer structural failure by excess accumulation on one of more of the emergency sump strainers. Obstructions or covers on the strainers such as tarps, gaps or other conditions that are a physical degraded or nonconforming condition of the strainer (e.g., gaps, deformations) are to be addressed by the system train-specific, non-debris TS actions a and b.

The requirements apply in MODE 1, 2, and 3. In these MODEs, the plant is in normal operating pressure and temperature where generation of design basis quantities of debris can reasonably be postulated. For lower MODEs of operation, there is less energy in the RCS and reduced capability to generate the zones of influence associated with pipe breaks, and the core is at generally lower levels of decay heat generation. Consequently, effects of debris are less likely to cause a condition where ECCS or CSS is inoperable.

Technical Specifications require that all applicable actions must be entered. If concurrent maintenance requirements or a non-debris related degraded or nonconforming condition occurs that would make any system(s) or subsystem(s) inoperable, the non-debris required action for the system(s) or subsystem(s) must be applied. The action from the debris related condition will continue to apply from the time it was initially entered.

Required Action:

The required action to implement compensatory action is based on the very low contribution by LOCA generated debris to the risk of core damage, and is a reasonable response to minimize the potential increase in risk from the debris source. Typical compensatory action would include actions such as:

- Remove the debris or source of debris or take action that would prevent transport of the debris to the emergency sump
- Defer maintenance that would affect availability of the affected systems and strainers
- Defer maintenance that would affect availability of primary defense in depth systems such as RCFCs
- Increase frequency of RCS leak detection monitoring
- Brief operators on LOCA debris management actions

Completion Time:

The 90 day completion time is based on the very low contribution to risk from LOCA generated debris. It provides sufficient time to more thoroughly assess the condition and to take corrective action. Operability can be restored by mitigation of the debris such as by removal or making it non-transportable, or by performing an evaluation that demonstrates that the Licensing Basis is maintained.

Add the following to the Bases Section 3/4.6.2.1 Containment Spray System:

The OPERABILITY of the ECCS Subsystems is assured by the capability of the containment emergency sump strainers to limit entry of debris into the sump and recirculating lines. This capability ensures that the flow and net positive suction head requirements of ECCS are satisfied. Assurance that containment debris will not block the sump strainers and render the ECCS Subsystem inoperable on emergency recirculation during design basis accidents is provided by inspection and engineering evaluation. UFSAR Appendix 6A provides a risk-informed approach that addresses the potential of debris blockage concluding that long-term core cooling following a design basis loss of coolant accident is assured with high probability. UFSAR Appendix 6A also provides guidance for assessing the potential impact on Operability due to unexpected material such as loose debris discovered in containment that may contribute to debris loading on the strainers.

Technical Basis:

The Licensing Basis with regard to effects of debris is that there is a high probability that ECCS and CSS can perform their design basis functions based on successful plant-specific prototypical testing using deterministic NRC-approved assumptions, and that the risk from breaks that could generate debris that is not bounded by the testing is very small and acceptable in accordance with the criteria of RG 1.174.

STP evaluated the risk associated with the effects on long-term cooling due to debris accumulation on Emergency Core Cooling System (ECCS) and Containment Spray System (CSS) sump strainers in recirculation mode, as well as core flow blockage due to in-vessel effects of debris that penetrates the strainers. A full spectrum of postulated LOCAs is analyzed, including double-ended guillotine breaks (DEGBs) for all pipe sizes up to the largest pipe in the reactor coolant system. The changes to CDF and LERF associated with the effects of debris are quantified by applying the LOCA frequencies published in NUREG-1829, and then compared to RG 1.174 acceptance guidelines. The STP analysis shows that the contribution to risk from the breaks that are not deterministically mitigated is within RG 1.174 Region III.

Strainer Operability:

The affected ECCS and CSS are OPERABLE with respect to the effects of debris when the expected effects of the debris on the emergency sump strainers are consistent with the analysis.

This operability requirement is based on quantity and characteristics and location of the debris in the RCB being consistent with the debris analysis assumptions. The types of debris considered in the analysis included insulation and latent debris fiber fines, particulate from coatings and latent debris, and chemical precipitates (primarily from aluminum corrosion).

Strainer operability evaluation is fundamentally deterministic and the intent is to not require a risk assessment to make the operability determination. The criterion recognizes that there is margin and conservatism in the debris assumptions used for the deterministic testing and in the debris generation and transport analyses that can be applied to account for previously unidentified debris.

Guidance for evaluating potential debris is provided in 0PSP03-XC-0002A.

Applicability:

This required action applies only for the potential effects of debris on emergency sump strainer operability or on in-core debris effects. It does not apply for effects other than those caused by debris for which the testing and analysis apply. Debris effects are conditions caused by transportable debris that could impact the net positive suction head or otherwise degrade pump performance, or cause strainer structural failure by excess accumulation on one of more of the emergency sump strainers. Obstructions or covers on the strainers such as tarps, gaps or other conditions that are a physical degraded or nonconforming condition of the strainer (e.g., gaps, deformations) are to be addressed by the system train-specific, non-debris TS actions a and b.

The requirements apply in MODE 1, 2, and 3. In these MODEs, the plant is in normal operating pressure and temperature where generation of design basis quantities of debris can reasonably be postulated. For lower MODEs of operation, there is less energy in the RCS and reduced capability to generate the zones of influence associated with pipe breaks, and the core is at generally lower levels of decay heat generation. Consequently, effects of debris are less likely to cause a condition where ECCS or CSS is inoperable.

Technical Specifications require that all applicable actions must be entered. If concurrent maintenance requirements or a non-debris related degraded or nonconforming condition occurs that would make any system(s) or subsystem(s) inoperable, the non-debris required action for the system(s) or subsystem(s) must be applied. The action from the debris related condition will continue to apply from the time it was initially entered.

Required Action:

The required action to implement compensatory action is based on the very low contribution by LOCA generated debris to the risk of core damage, and is a reasonable response to minimize the potential increase in risk from the debris source. Typical compensatory action would include actions such as:

- Remove the debris or source of debris or take action that would prevent transport of the debris to the emergency sump
- Defer maintenance that would affect availability of the affected systems and strainers
- Increase frequency of RCS leak detection monitoring

- Brief operators on LOCA debris management actions

Completion Time:

The 90 day completion time is based on the very low contribution to risk from LOCA generated debris. It provides sufficient time to more thoroughly assess the condition and to take corrective action. Operability can be restored by mitigation of the debris such as by removal or making it non-transportable, or by performing an evaluation that demonstrates that the Licensing Basis is maintained.

Attachment 3-4

UFSAR Markups

STPEGS UFSAR Page Markups

Section 2.0 of UFSAR Appendix 6A describes change control requirements, monitoring requirements and reporting requirements which require prior NRC approval for changes and NRC approval of Section 2.0 is requested as part of this application. The remainder of Appendix 6A and complementary changes to other parts of the UFSAR were provided for the staff's information in Reference 1 to the cover letter.

APPENDIX 6A

Resolution of NRC Generic Letter 2004-02, "Potential Impact of Debris Blockage on Emergency Recirculation During Design Basis Accidents at Pressurized-Water Reactors," Including Application of a Risk-Informed Approach to Potential Impact Of Debris Blockage on Emergency Recirculation During Design Basis Accidents

2.0 Change Control and Reporting

This section describes the parts of the methodology change for Appendix 6A which have additional regulatory requirements for prior NRC approval or notification. The requirements in this section may not be changed without prior NRC approval.

2.1 Change Control

2.1.1 Changes to key methods and approaches of the risk-informed methodology set forth in [final NRC-approved RoverD description] are to be evaluated as a potential "departure from a method of evaluation described in the FSAR (as updated) used in establishing the design bases or in the safety analyses" analogous to 10CFR50.59(c)(2)(viii).

2.1.1.1 The key aspects of the RoverD methodology subject to Section 2.1.1 are the following:

1. The methodology for quantifying the pipe break frequencies used to calculate the change in CDF and LERF.
   a. The pipe break frequency source (NUREG 1829)
   b. The methodology for calculation of D_i(small)
   c. The methodology to identify break locations. This requirement applies to the criteria, but not to the tool or program used to identify the locations; i.e., programs other than CASA Grande may be used.
   d. The methodology to interpolate the pipe break frequencies to quantify the ΔCDF associated with pipe breaks
   e. The methodology for assigning the RPV HL breaks to failure
   f. The methodology used to calculate ΔLERF for effects of debris
2. The assumption that fine fiber is to be applied as the governing debris source
   a. The methodology used to quantify the amount of fiber generated at each break location, including assumed ZOI. This requirement applies to the criteria, but not to the tool or program used; i.e., programs other than CASA Grande may be used.
   b. The use of the July 2008 STP-specific test to establish the deterministic baseline for the quantity of fine fiber.
3. The assumptions and methods in the thermal-hydraulic analyses
   a. The use of 800°F as the acceptance criterion for long-term core cooling

b. Assumptions regarding core blockage

4. The availability of key sources of defense in depth.
   a. Capability for containment heat removal unaffected by debris on ECCS strainers (RCFCs)
   b. Capability to refill the RWST

2.1.1.2 Plant Design Changes

In addition to the controls of Section 2.1.1.1, changes to plant design shall be subject to the following requirements:

1. Procedural controls establish limits on the introduction of new debris sources into containment, particularly fine fiber or particulate sources, to assure the deterministic licensing basis testing and calculations performed for the RoverD methodology remain bounding.

2.2 Reporting

Nonconforming conditions that make the strainer(s) inoperable for longer than required TS completion time will meet the 10CFR50.73 reporting criteria for a condition prohibited by TS. Conditions that cause the emergency sump strainers to be inoperable and result in the debris-related ΔCDF or ΔLERF to be greater than the RG 1.174 Region II acceptance guidance are to be reported in accordance with 10CFR50.72 or 10CFR 50.73.

Attachment 4

List of Commitments

List of Commitments

The following table identifies the actions to which STP Nuclear Operating Company (STPNOC) has committed. Statements in the submittal with the exception of those in the table below are provided for information purposes and are not considered regulatory commitments.

Commitment	Tracking Numbers	Scheduled Completion Date
The document changes required to implement the LAR (approved UFSAR Change Notice, TS, and TS Bases) will be done within 90 days of NRC approval.	CR 11-4249-9 (UFSAR CN) CR 11-4249-10 (TS/TSB)	90 days following approval of LAR

Attachment 5

Definitions and Acronyms

Definitions and Acronyms

AFW
Auxiliary Feed Water.
BAP
Boric Acid Precipitation.
BB
Baffle Barrel.
BDB
Beyond Design Basis.
BOL
Beginning of Life.
BTU
British Thermal Units.
CCFL
Counter-Current Flow Limit.
CCW
Component Cooling Water.
CDF
Core Damage Frequency.
CFC
Containment Fan Cooler, also Reactor CFC (RCFC).
CHF
Critical Heat Flux.
CHRS
Containment Heat Removal System.
CLB
Cold Leg Break or Current Licensing Basis.
CPU
Central Processing Unit.
CREVFS
Control Room Envelope Ventilation and Filtration System.
CSS
Containment Spray System (also CS).
DBA
Design Basis Accident.
DEGB
Double-ended Guillotine Break.
ECCS
Essential Core Cooling System.
EM
Evaluation Model.
EOL
End of Life.
EOP
Emergency Operating Procedure.
EPRI
Electric Power Research Institute.
EQ
Equipment Qualification.
FA
Fuel Assembly.
FiDOE
Fiber Diffusion Operations Engine.
GDC
General Design Criterion(ia).
GSI
Generic Safety Issue.
HFP
Hot Full Power.
HHSI
High Head Safety Injection.
HL
Head Loss.
HLB
Hot Leg Break.
HLSO
Hot Leg Switchover.
HX
Heat Exchanger.
ICDP
Incremental Core Damage Probability.
INL
Idaho Nuclear Laboratory (also INEL).
LAR
License Amendment Request.
LBLOCA
Large Break LOCA (also LLOCA).
LCO
Limiting Condition for Operation.
LERF
Large Early Release Frequency.
LHSI
Low Head Safety Injection.
LOCA
Loss of Coolant Accident.
LTCC
Long-term core cooling.
MFW
Main Feed Water.
MSIV
Main Steam Isolation Valve.

Definitions and Acronyms

MWe
Megawatt electric.
NPSH
Net Positive Suction Head.
NPSHA
NPSH Available.
NPSHM
NPSH Margin.
NPSHR
NPSH Required.
PRA
Probabilistic Risk Assessment (or Analysis).
PWR
Pressurized Water Reactor.
PWSCC
Primary Water Stress Corrosion Cracking.
RAI
Request for Additional Information.
RCB
Reactor Containment Building.
RCFC
Reactor Containment Fan Cooler (same as CFC).
RCS
Reactor Coolant System.
RHR
Residual Heat Removal.
RMTS
Risk Managed Technical Specifications.
RoverD
Risk over Deterministic.
RTE
Run Time Environment.
RWST
Refueling Water Storage Tank.
SBLOCA
Small Break LOCA (also Small LOCA - SLOCA).
SDG
Standby Diesel Generator.
SER
Safety Evaluation Report.
SG
Steam Generator.
SSC
System, Structures and Components.
SSO
Sump Switch-over.
STP
South Texas Project.
STPNOC
STP Nuclear Operating Company.
TH
Thermal-Hydraulic.
TS
Technical Specification(s).
TSB
Technical Specification Bases.
TSP
Tri-sodium Phosphate.
TSTF
Technical Specification Task Force.
UFSAR
Updated Final Safety Analysis Report.
UPTF
Upper Plenum Test Facility.
WCAP
Westinghouse Commercial Atomic Power.
ZOI
Zone of Influence.